Thèse de Doctorat de l'Université de Strasbourg

Discipline : Sciences du Vivant

Spécialité : Aspects Moléculaires et Cellulaires de la Biologie

Tissue-specific expression of the human Glycyl-tRNA synthetase: connection with the Charcot-Marie-Tooth disease

Présentée par

Jana Alexandrova

pour l'obtention du grade de Docteur de l'Université de Strasbourg

Soutenue le 19 septembre 2014 devant la commission d'examen :

Dr. Magali Frugier	Directeur de thèse *(Directeur de Recherche CNRS, Strasbourg)*
Dr. Albena Jordanova	Rapporteur externe *(Associate professor, University of Antwerp, Belgique)*
Dr. Tamara Hendrickson	Rapporteur externe *(Associate professor, Wayne State University, USA)*
Dr. Gilbert Eriani	Examinateur interne *(Directeur de Recherche CNRS, Strasbourg)*

ACKNOWLEDGEMENTS

First, I would like to thank all the members of the thesis committee, Dr. Albena Jordanova, Associate Professor in Molecular Neurosciences at the University of Antwerp (Belgium), Dr. Tamara Hendrickson, Associate Professor in Biochemistry at Wayne State University (USA) and Dr. Gilbert Eriani, Research Director at CNRS (Strasbourg) for accepting to judge my work.

Je remercie le Professeur Eric WESTHOF, de m'avoir accueillie au sein de l'UPR 9002 du CNRS.

Un très très très grand Merci à Magali ! Je ne pourrais jamais te remercier assez pour tout ce que tu as fait pour moi ces six dernières années… bien sûr pour tout ce que tu m'as appris en tant que scientifique mais aussi pour ton soutien, tes encouragements et la confiance que tu m'as accordée et celle que tu as réussi à me donner en moi. Même quand j'étais désespérée, tu as toujours trouvé les bons mots pour repartir avec encore plus d'enthousiasme et de motivation. Je te remercie pour tous les superbes moments qu'on a passés ensemble… dommage qu'on ne puisse pas rester en thèse toute sa vie…

Un très grand Merci aussi à tous les gens de notre équipe sans qui la vie au labo n'aurait pas été si agréable ! Merci Caro pour tout ce que tu m'as appris, pour nos belles pauses Icetea avec les plantes carnivores de l'IBMC et l'expérience photos sous la chaleur accablante. Merci à Joëlle et Anne pour tous nos moments de rigolade mais aussi pour tous vos conseils. Merci Nassira pour tes encouragements, tes conseils, les grandes discussions scientifiques et pas seulement et pour tous les super moments qu'on a partagés. Merci Pupuce (Delphine) d'avoir apporté plein de joie et de bonne humeur au quotidien mais aussi dans les moments de déprime, pour les innombrables et inoubliables « soirées et week-end labo » et surtout celles en dehors du labo…

Merci Alain pour tous tes conseils et discussions scientifiques du soir, pour m'avoir montré comment détecter de jolies cellules fluos et que c'est pas du bruit de fond…

Un très grand Merci à tous les amis du labo pour tout ce qu'on a partagé ces dernières années : les pauses café, soirées, sorties ski, montagne… Merci Micka, Pierre, Patryk, Hagen, Anne So, Mélo, Delphine, Franzi et tous les autres que j'ai oubliés…

Un énorme Merci à Micka, Pierre, Delphine[2] et Paola : sans vous les derniers mois auraient été très éprouvants… merci pour les barbecues, sorties escalade qui m'ont presque fait apprécier l'écriture de la thèse.

Un très très très grand Merci à mes parents qui m'ont toujours encouragée et soutenue, et enfin mais pas en dernier à Yannick avec qui on a traversé tout le chemin de la Fac et la thèse ensemble.

CONTENT

I. mRNA AND THE ROAD LEADING TO TRANSLATION

Messenger RNAs (mRNA) are the key link between DNA and proteins. After several steps of processing such as splicing, polyadenylation and cap attachment, the mature mRNA is exported to the cytosol where it can be degraded or loaded to the ribosome and translated. All cellular processes depend on protein synthesis: on one hand a constant level of protein translation is maintained in the cell, on the other hand local and quick translation is needed to regulate particular events such as secretion of hormones or conduction of neuronal signals. Indeed, to maintain cellular homeostasis it is important to coordinate the translation of all mRNAs. A huge network of regulatory mechanisms is responsible for monitoring this translation, which takes place in different cell types, at different cellular localizations and at different moments of the cell's "life" (Sonenberg and Hinnebusch, 2009).

1. Translation initiation of eukaryotic mRNAs

Translation is a four-step process comprising initiation, elongation, termination and recycling of the ribosomes. In eukaryotic translation, initiation is the limiting step and is a highly coordinated and regulated process, involving at least 12 eukaryotic initiation factors (eIFs) (Jackson *et al.,* 2010; Hinnebusch, 2011). The main eIFs involved in these regulatory processes will be described in this chapter. In agreement with my phD work, I will focus on conventional and unconventional translation initiation mechanisms in mammalian cells.

1.1. Cap-dependent initiation

Cap-dependent translation initiation is the classical mechanism that eukaryotic cells use to synthetize proteins. Most cellular mRNAs contain a methyl-7-guanosine triphosphate (m7Gppp), the so-called cap, on their 5'-termini. This cap structure, along with the 3'-end polyA tail bind several translation initiation factors allowing circularization of the mRNA molecule and subsequent ribosome loading.

1.1.1. Ternary complex formation

The first step of translation initiation is the formation of the ternary complex (TC) (Figure 1). This complex comprises Met-tRNAi, eIF2 initiation factor and a GTP molecule: eIF2*GTP binds Met-tRNAi with higher affinity than does eIF2*GDP. This factor is a heterotrimer (α, β and γ); while the γ subunit binds GTP and recognizes the Met-tRNAi, the α and β subunits stabilize this interaction (Naveau *et al.,* 2010). The rate of translation initiation is regulated upon the availability of this ternary complex. Indeed, under stress conditions, eIF2 is phosphorylated and forms an unproductive eIF2B-eIF2*GDP complex (eIF2B being the

GTP*GDP exchange factor), which inhibits translation initiation. Once the ternary complex is formed, it joins the 40S ribosomal subunit to make the pre-initiation complex (PIC).

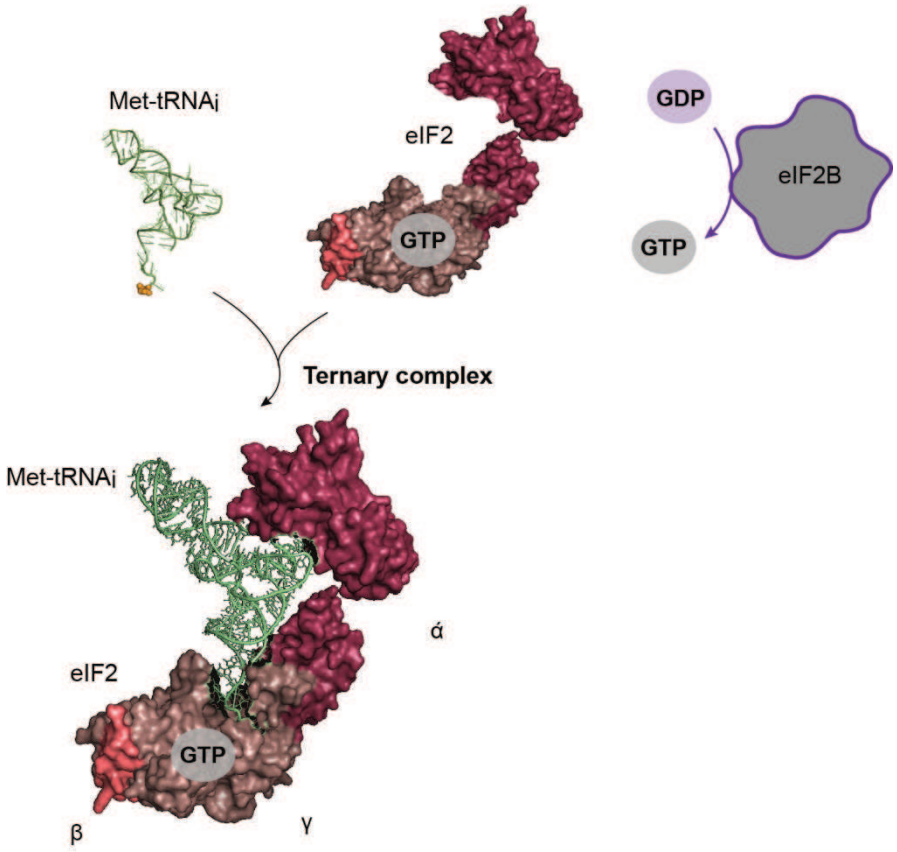

Figure 1. Ternary complex formation
eIF2B (grey) converts eIF2*GDP to active eIF2*GTP. Met-tRNAi (green) is recognized by eIF2*GTP, composed of 3 subunits (α, β and γ) to form the ternary complex.

1.1.2. The open pre-initiation complex

Initiation factors eIF1, eIF1A, eIF3 and eIF5 bind the 40S ribosomal subunit and promote the recruitment of the ternary complex to form the 43S pre-initiation complex (Figure 2). Both eIF1 and eIF1A cooperatively bind to the small ribosomal subunit near the peptidyl (P) site and the aminoacyl (A) site respectively, stabilizing the open conformation of the complex. Both factors are important for mRNA loading and scanning. Then eIF3, the largest factor (almost as large as the 40S subunit) binds on the solvent exposed surface of the 40S subunit, stabilizes the open conformation of the PIC and promotes mRNA recruitment. In this complex, the position of eIF1 obstructs the P site and the Met-tRNAi stays in a metastable conformation (P_{out} state).

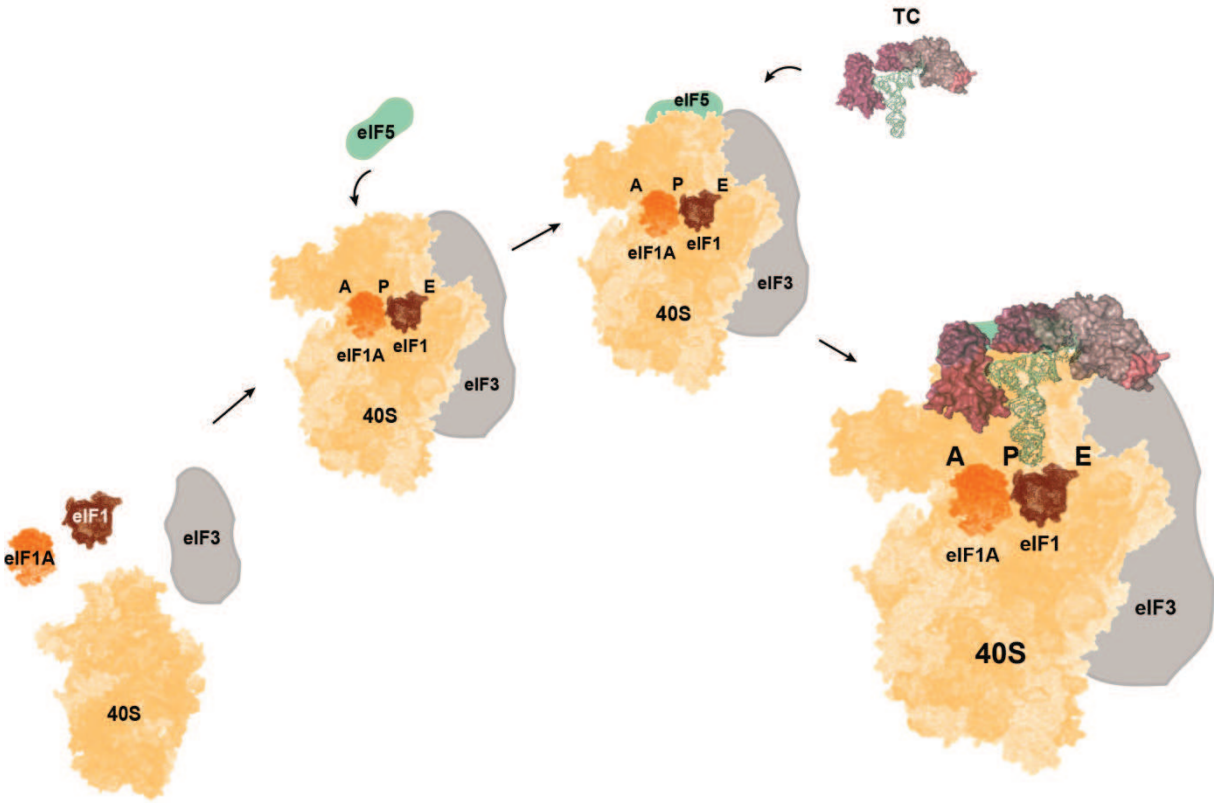

Figure 2. Open pre-initiation complex (PIC)
The 40S ribosomal subunit (in yellow) associates with eIF1 (brown), eIF1A (orange), eIF3 (grey) and eIF5 (green). Upon binding of the TC, an "open" PIC is formed.

1.1.3. PIC and mRNA recruitment

Before loading on the PIC, the mRNA is recognized by several factors allowing the formation of a "closed loop mRNP" (Figure 3). Once the mature mRNA, with poly(A) binding protein (PABP) attached to its polyA tail, is exported in the cytoplasm eIF4E binds the 5'-cap structure. eIF4G recognizes both eIF4E and PABP, thus connecting the 5' and 3' extremities of the messenger. This assembly enables the loading of eIF4A and eIF4B factors. eIF4A is a DEAD box ATP-dependent helicase that disrupts RNA duplexes and unwinds mRNA 5'-UTRs. This helicase is important for clearing out parts of the RNA where the ribosome would bind. However, further unwinding of long and structured 5'-UTRs is achieved by other helicases. The mRNA is then recruited to the PIC thanks to the interactions between eIF4G and eIF3.

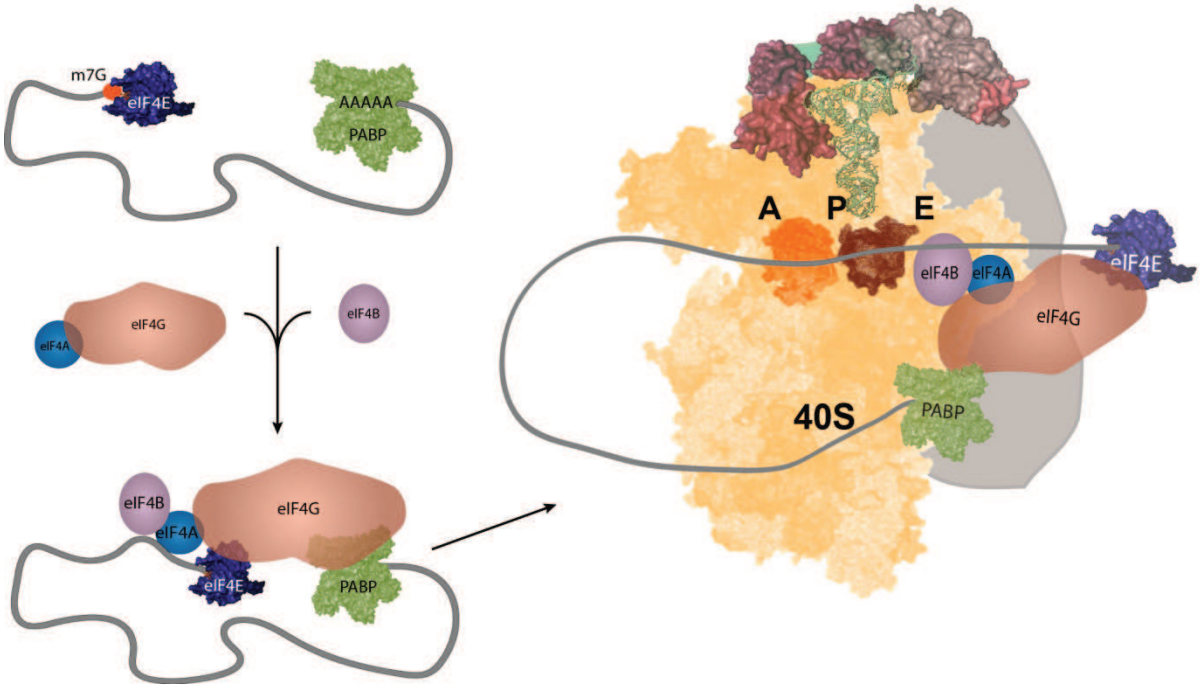

Figure 3. mRNA activation and recruitment
The mRNA m7G cap (red) is recognized by eIF4E (dark blue). The polyA tail with the PABP (green) and eIF4E are recognized by eIF4G (light brown), eIF4A (blue), and eIF4B (pink) to trigger mRNA circularization. Thus, the activated mRNA is loaded on the 43S complex.

1.1.4. mRNA scanning and start codon recognition

Once the mRNA is recruited to the 43S pre-initiation complex, ribosome scanning starts seeking for the initiation codon. According to Kozak, the sequence surrounding the initiation codon is of particular importance for its efficient recognition. An optimal context would correspond to the following sequence: –GCC(**A/G**)CC**AUGG**–, where a purine at position -3 and a G at position +4 play a leading part (Kozak, 1987). When the initiator codon is loaded in the P site of the 40S subunit, several conformational changes occur. Upon codon-anticodon pairing, the Met-tRNAi is fully engaged in the P site, leading to a steric clash and the clearance of eIF1. The ejection of eIF1 is promoted by eIF5, probably by competition for the same binding site on the pre-initiation complex. Ejection of eIF1 also triggers Pi release from eIF2 and the scanning process stops. The eIF5 factor interacts with eIF1A and stabilizes the PIC in a closed conformation state, which is then ready to recruit the 60S subunit to form the 80S initiation complex (IC).

1.1.5. 80S initiation complex formation

Upon removal of eIF2*GDP and eIF5, eIF1A is free to interact and recruit the GTPase eIF5B, which promotes joining of the 60S subunit into the complex. After GTP hydrolysis, eIF5B*GDP dissociates from the 80S IC. Finally, eIF1 is the last factor to leave the IC, which is now ready to elongate. Sometimes, eIF3 remains bound on the elongating 40S subunit and participates in further reinitiation steps.

1.2. 5'- and 3'-UTR regulatory elements

Every single step of gene expression, from chromatin to a functional protein, is precisely regulated to avoid dysfunction in cellular homeostasis. Thus, the presence of alternative untranslated regions for a given mRNA is an important source of regulation. Between 15 and 21% of genes contain alternative 5'- or 3'-UTRs, generated either by alternative transcriptional promoters (5'-UTR), splicing (5'- and 3'-UTRs), or polyadenylation sites (3'-UTR) (Hughes, 2006). This diversity provides the possibility to express the same protein differentially in different development stages, tissues, physiological conditions, or cell compartments.

During my thesis I was particularly interested in post-transcriptional events regulating the expression of the human glycyl-tRNA synthetase (GRS). Thus, in this introduction, I will describe some general mechanisms of post-transcriptional regulation involving mRNA untranslated regions (5'- and 3'-UTRs) that take place in eukaryotic cells. When describing the role of 5'-UTRs, I will especially focus on mechanisms that control translational initiation. To illustrate each mechanism, I have chosen a few examples from the literature that concern preferentially the questions I addressed during my PhD work: neuronal protein translation, aminoacyl-tRNA synthetase regulation, etc.

1.2.1. mRNA localization

Sequences or structural motifs commonly named zip codes are present in 5'- and 3'-UTRs. They are recognized by different RNA binding proteins, which target these mRNAs to specific sub-cellular localizations.

Well known examples correspond to proteins expressed in neurons, where translation occurs not only in the cellular body but also in neuronal projections. This local synthesis of proteins is important for a quick response to a neuronal signal and more precisely for synaptic plasticity. For example, a 21 nt sequence in the 3'-UTR of MBP (myelin basic protein) is recognized by the hnRNP A2 protein (Heterogeneous nuclear ribonucleoprotein A2) and then located to the myelin compartment of oligodendrocytes (Ainger *et al.,* 1997) (Figure 4,

top). A similar nucleotide sequence named "RNA transport signal-like" was also identified in the 5'-UTR of neurogranin (Kiebler and DesGroseillers, 2000), in the 3'-UTR of the GABA receptor α subunit and in the 5'-UTR of nitric oxide synthase, which are all dendritically localized in growth cones (Crino and Eberwine, 1996). Another important motif is the G-quadruplex structure found in the 3'-UTR of at least 30% of dendritically localized mRNA (Subramanian *et al.,* 2011). The trans-acting factor Fragile-X mental retardation protein (FMRP) specifically recognizes this G-quadruplex structure and localizes at least two key proteins, PSD-95 (postsynaptic density protein 95) and CaMKIIa (Calcium/calmodulin-dependent protein kinase II), in post-synaptic terminations (Figure 4), (Subramanian *et al.,* 2011).

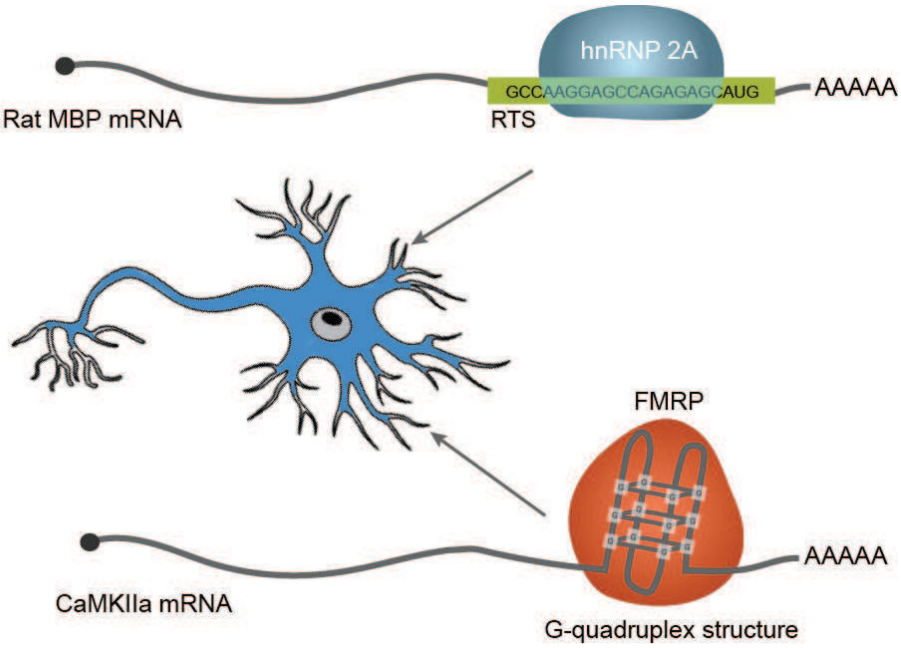

Figure 4. Neuronal localization guided by 3'-UTR motifs
The mRNA of MBP, containing a 21 nt RNA transport signal (RTS) sequence (green) is recognized by the hnRNP 2A protein and is located in the myelin compartment of oligodendrocytes. FMRP binds specifically to a G-quadruplex structural element in the 3'-UTR of CaMKIIa mRNA and triggers its localization to dendrites.

In other cell types, zip codes allow the localization of mRNAs in specific cellular compartments: This is the case for vimentin, c-myc and metalloprotein-I mRNAs that are targeted to the perinuclear cytoplasm (reviewed in Hervé *et al.,* 2004). In some cases, mRNA translated by ribosomes coupled to the mitochondria or to the endoplasmic reticulum (ER) are localized in these structures prior their translation. For example the 3'-UTR of yeast PMP1 (plasma membrane protein 1) mRNA contains a UG rich region that mediates its

association with the ER membrane (Loya *et al.,* 2008). Likewise, the 3'-UTR of the yeast ATM1 (ATP-binding cassette transporter mitochondrial) contains a zip code, which leads to its mitochondrial localization in a translation-independent manner (Corral-Debrinski *et al.,* 2000).

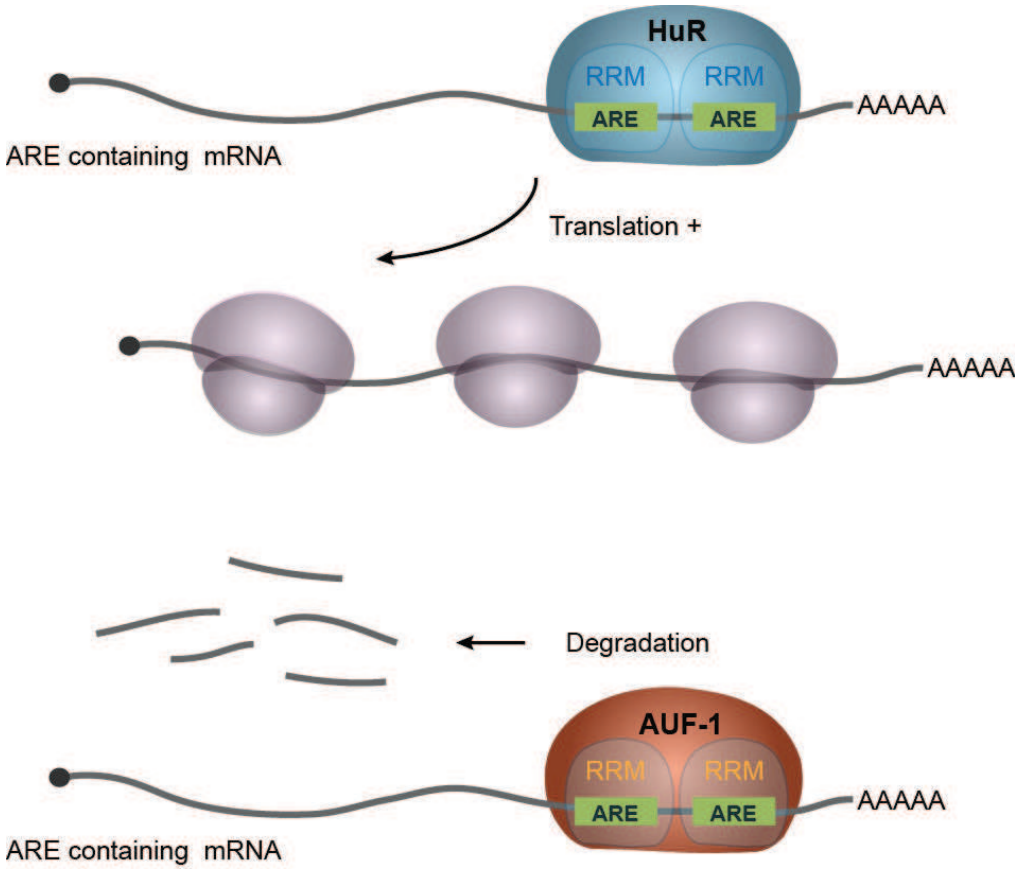

Figure 5. ARE (AU rich elements) mediated regulations
ARE are usually located in the 3'-UTR of mRNAs and are recognized by two types of proteins. While the binding of HuR (blue) and other members of the Hu family stabilizes the target mRNA and stimulates translation, the binding of AUF-1 (dark orange) promotes mRNA degradation and translation inhibition.

1.2.2. Regulatory elements in 3'-UTRs

The 3'-UTR usually contains information about mRNA stability. Independent of the length of the PolyA tail, which is a major stability determinant for cellular mRNAs, at least three well-characterized motifs inducing either mRNA degradation or translation repression have been identified in 3'-UTRs (reviewed in Knapinska *et al.,* 2005). For example, mRNAs coding for oncogenes, cytokines and growth factors such as c-myc, c-jun, interleukin 3 and TNF α (tumor necrosis factor alpha) contain AU rich elements (ARE). These AREs are targeted by different RNA binding factors characterized by two RNA binding domains (RRM: RNA recognition motif). Amongst these factors, the Hu (Human antigen R) proteins

are stabilizing factors and promote mRNA translation. In contrast, AUF-1 (AU-rich element RNA-binding protein 1), TTP (Tristetraprolin), and KSRP (KH-type splicing regulatory protein) are destabilizing factors and lead to mRNA deadenylation and its subsequent decay (Figure 5) (Lal *et al.,* 2004). Interestingly, HuR and AUF-1 recognize exactly the same ARE element (Barker *et al.,* 2012), however the corresponding regulatory mechanisms are still

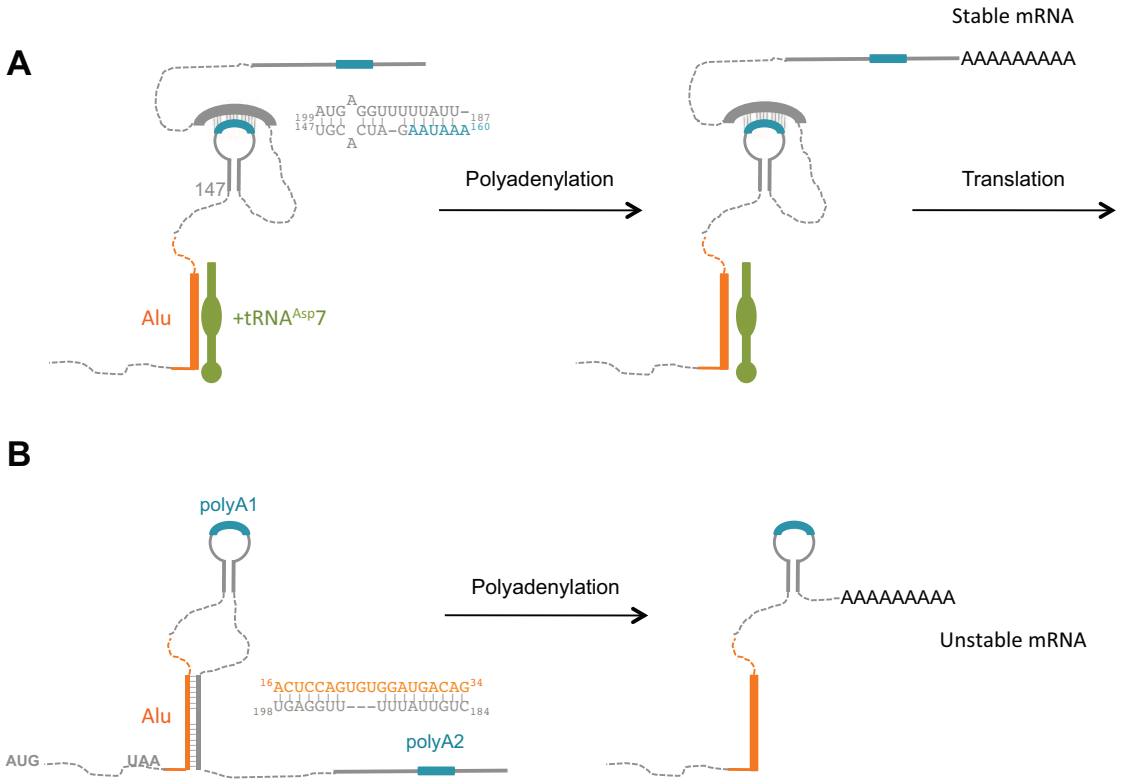

unclear.

Figure 6. Regulation of human DRS expression
(A) tRNA^{Asp} 7 (green) recognizes a partial Alu sequence (orange) and induces conformational changes of the DRS 3'-UTR. It exposes the second polyadenylation signal, thus generating a stable mRNA. **(B)** In the absence of tRNA^{Asp} 7, the proximal PolyA (PolyA1) is recognized and induces the synthesis of a shorter and unstable mRNA.

Another intricate regulation involves the human aspartyl-tRNA synthetase (DRS) 3'-UTR. In our laboratory, Rudinger and collaborators have shown that the 3'-UTR of DRS mRNA contains two alternative polyadenylation sites and a partial Alu element that regulate DRS expression (Figure 6). This partial Alu element is recognized by one specific human tRNA^{Asp} isodecoder sequence. This regulatory tRNA sequence adopts a peculiar structure. Upon tRNA^{Asp} binding, the folding of the 3'-UTR reorganizes and the distal polyadenylation signal is recognized, thus triggering normal expression of DRS. In the absence of this tRNA^{Asp}, the Alu sequence forms a 16 bp duplex with part of the 3'-UTR unmasking the proximal

polyadenylation site. The resulting short 3'-UTR destabilizes the mRNA and prevents protein expression (Rudinger-Thirion *et al.,* 2011).

3'-UTRs are also targets for micro RNAs (miRNA). miRNAs are small endogenous RNA regulatory molecules that usually bind a specific sequence in the 3'-UTR and either inhibit translation or induce mRNA degradation. This kind of regulation is essential in various stages of cell development and differentiation such as neurogenesis, myogenesis, angiogenesis, and hematopoiesis (Song and Tuan, 2006), but will not be detailed here.

1.2.3. Regulatory elements in 5'-UTRs

mRNAs encoding house-keeping proteins are generally expressed constitutively and contain relatively short 5'-UTRs. Such 5'-UTRs are deprived of stable structures and display a unique start codon in a suitable context. On the contrary, genes encoding regulatory proteins are characterized by more complex 5'-UTRs (Davuluri *et al.,* 2000). Regulatory elements located in mRNA 5'-UTRs are mostly implicated in translation initiation. Indeed, even in absence of particular regulatory motifs, the length and the structure complexity of this region are sufficient to influence translation initiation efficiency. They may display several initiation codons, sites of internal translation initiation, upstream open reading frames, or sequence and structural motifs. Stable secondary structures are often located at the very 5'-end, next to the cap structure, preventing 43S complex fixation, or further away, rendering ribosomal scanning difficult.

1.2.4. Structural regulatory elements

The Iron Response Element (IRE) is a well characterized 5'-structural element. It contains a highly conserved stem loop structure, which controls the expression of proteins involved in iron metabolism and storage. When the cellular iron level is low, iron regulatory proteins (IRP1 and IRP2) bind the IRE element and inhibit mRNA translation (Figure 7 A). If this stem loop element is close to the cap, then 43S recruitment is impeded. Alternatively, the position of this structural element distant to the cap will block scanning of the ribosome (reviewed in Araujo *et al.,* 2012).

Another particular structural element is the JRE (c-Jun amino terminal kinase Response Element) that regulates expression of the Transforming Growth Factor beta (TGFβ) (Kim *et al.,* 1992). The RNA binding protein YB-1 (Y box protein-1) recognizes the JRE motif (a stem loop domain embedded in a GC rich sequence) in the 5'-UTR of the TGFβ mRNA and inhibits translation initiation (Figure 7 B). Likewise, YB-1 along with nucleolin bind the JRE

element present in the 5'-UTR of the Interleukin 2 (IL-2) mRNA (Chen *et al.,* 2000). However, in this case, they stabilize and avoid degradation of the mRNA (Jenkins *et al.,* 2010).

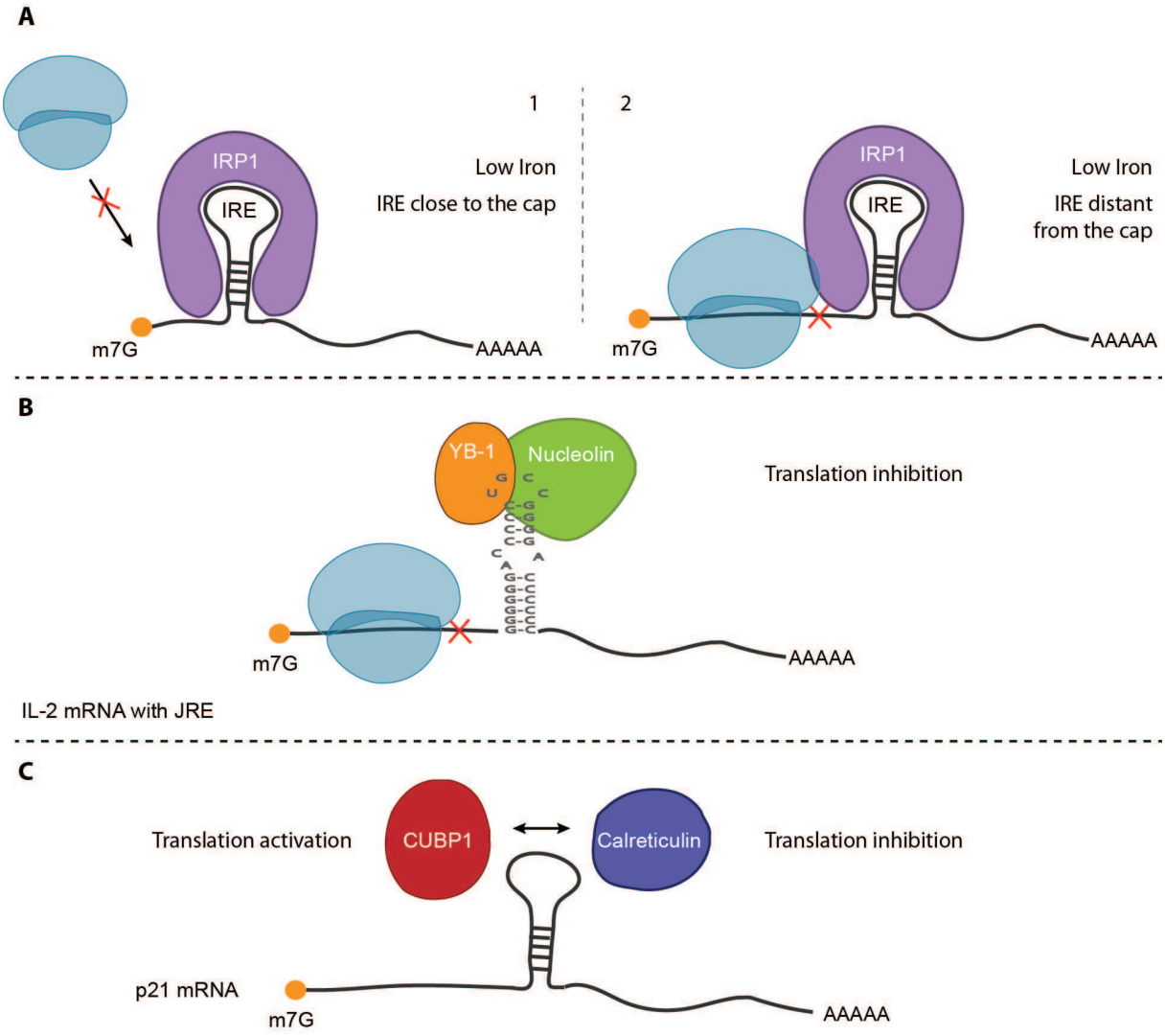

Figure 7. Structural regulatory elements
(A) IRE element regulates expression of iron storage proteins: Upon low iron concentration IRP1 binds an IRE element in the 5'-UTR of ferritin mRNA. It inhibits translation by hindering (1) 43S loading (light blue) or (2) 43S scanning.
(B) Isoleucine 2 (Il-2) mRNA contains a JRE stem loop structure recognized by YB-1 (orange) along with nucleolin (green) which inhibit translation.
(C) Regulation of p21 mRNA expression by a conserved stem loop structure: CUBP1 (red) competes with Calreticulin (blue) for the same binding site (the stem loop) to activate or inhibit translation.

An interesting example also is the regulation of p21 (cyclin-dependent kinase inhibitor) during cellular senescence (Figure 7 C). The same type of structural element (a stable stem loop) in the 5'-UTR is recognized by two different proteins CUGBP1 (CUG triplet repeat

RNA-binding protein 1) and calreticulin, which are competing for the same binding site and have antagonistic roles. While CUGBP1 is responsible for the activation of p21 expression, calreticulin binding induces its translation inhibition (Iakova *et al.,* 2004).
These examples show the complexity of such regulatory mechanisms where different RNA binding proteins recognize the same RNA motifs and control mRNA fate in different ways.

1.2.5. uORFs

Upstream open reading frames (uORF) are amongst the major regulatory elements in 5'-UTRs. An exhaustive analysis of human 5'-UTRs from 5962 validated mRNAs shows that 44% of the human mRNAs contain an upstream AUG (uAUG) or uORF (Iacono *et al.,* 2005). Usually uORFs are inhibitory regulators that reduce protein expression (up to 80%) (Calvo *et al.,* 2009). They regulate gene expression using several complex mechanisms (reviewed in Somers *et al.,* 2013). Often, 5'-UTRs containing one or several uORFs are long, and their length increases with the number of uORFs they contain (Iacono *et al.,* 2005). These uORFs can be distant, can overlap each other or can even overlap with the main ORF (Figure 8). Translation initiation depends on the presence of secondary structures, the distance of the uORF from the cap structure and from the main ORF, as well as the context of the uAUG. Moreover, the presence of particular stress conditions can influence the efficiency of uAUG recognition and the rate of translation initiation. As for subsequent translation initiation at the main ORF, it occurs either by leaky scanning, reinitiation, or an internal ribosome entry site.

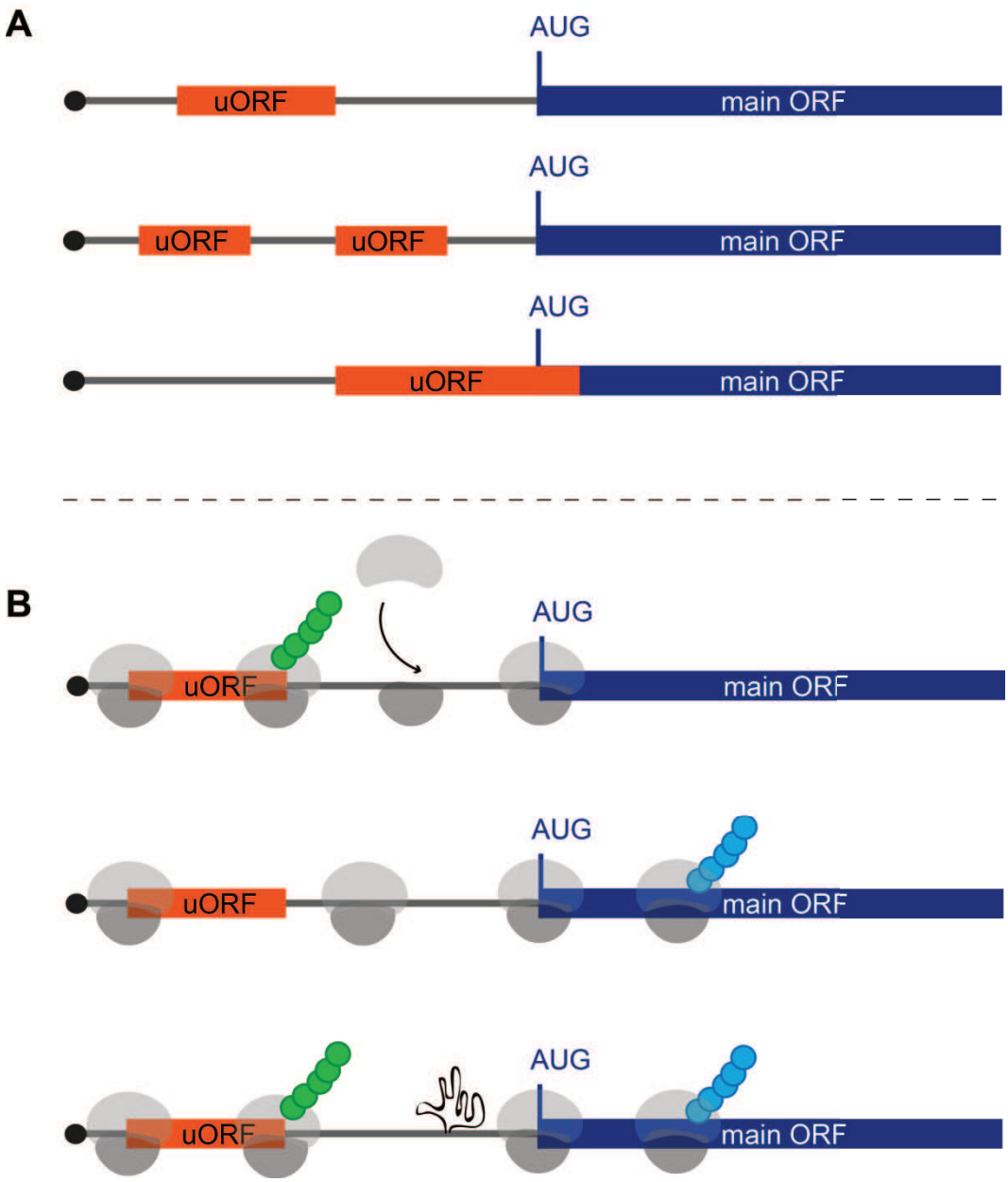

Figure 8. uORF translational control

(A) uORFs regulate gene expression by different mechanisms depending on the number of uORFs and their location compared to the main ORF (mORF). **(B)** After translation of the uORF, if the distance is suitable, the 40S ribosome remains on the mRNA and reinitiates translation at the mORF. Or else, the scanning ribosome bypasses (leaky-scan) the uORF and initiates directly at the mORF. In some cases, when an internal ribosome entry sequence (IRES) is present, after translation the uORF, ribosomes reenter at the mORF start codon.

* "Canonical" uORFs

Expression of the C/EBP Homologous Protein (CHOP) is enhanced under endoplasmic reticulum (ER) stress (Palam *et al.,* 2011). The 5'-UTR of CHOP is characterized by the presence of an inhibitory uORF. This uORF is efficiently translated under normal conditions, despite the unfavourable "Kozak" context of its uAUG and thus inhibits translation of the downstream CHOP ORF (Jousse *et al.,* 2001) (Figure 9).

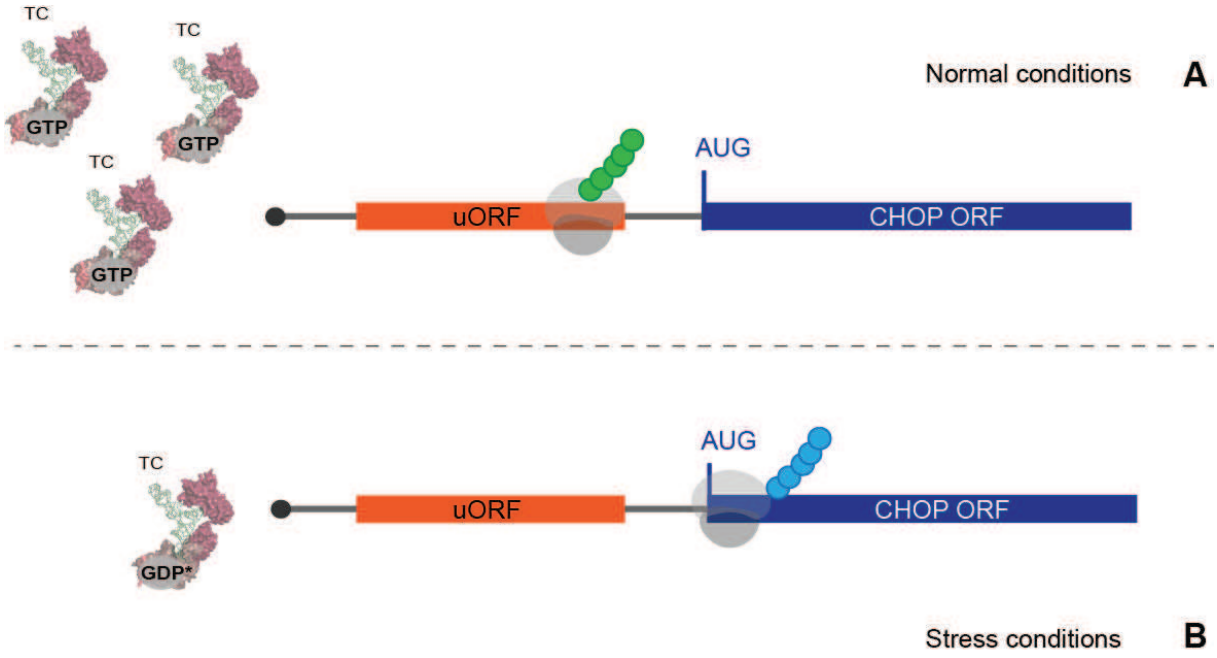

Figure 9. CHOP expression regulation by uORF

(A) Under normal conditions, the uORF present in the CHOP mRNA 5'-UTR is translated and inhibits downstream initiation at CHOP's main ORF AUG. **(B)** Under stress conditions, the ternary complex is limited and scanning ribosomes bypass the uORF to initiate CHOP translation.

In contrast, under ER stress, phosphorylation of eIF2α reduces initiation, especially at codons in less optimal contexts (the availability of active ternary complex decreases and global translation is inhibited). This allows scanning ribosomes to bypass the uORF and initiate directly at the main ORF (Palam *et al.,* 2011).

Another well-studied example is the mammalian ATF4 (activating transcription factor 4) gene encoding a stress dependent transcriptional activator of stress-related genes (Harding *et al.,* 2003). The 5'-UTR of ATF4 mRNA contains 2 uORFs: Under normal conditions, the translation initiation at the uAUG1 is efficient and allows further reinitiation at uAUG2. Since uORF2 overlaps the main coding frame, its translation inhibits ATF4 production (Figure 10). However, cellular stress increases the concentration of inactive phosphorylated

eIF2α, and active eIF2α becomes limiting in the cell, so that the 43S initiation complex resumes scanning, bypasses uAUG2 and reinitiates only at the main ATF4 ORF (Lu *et al.,* 2004).

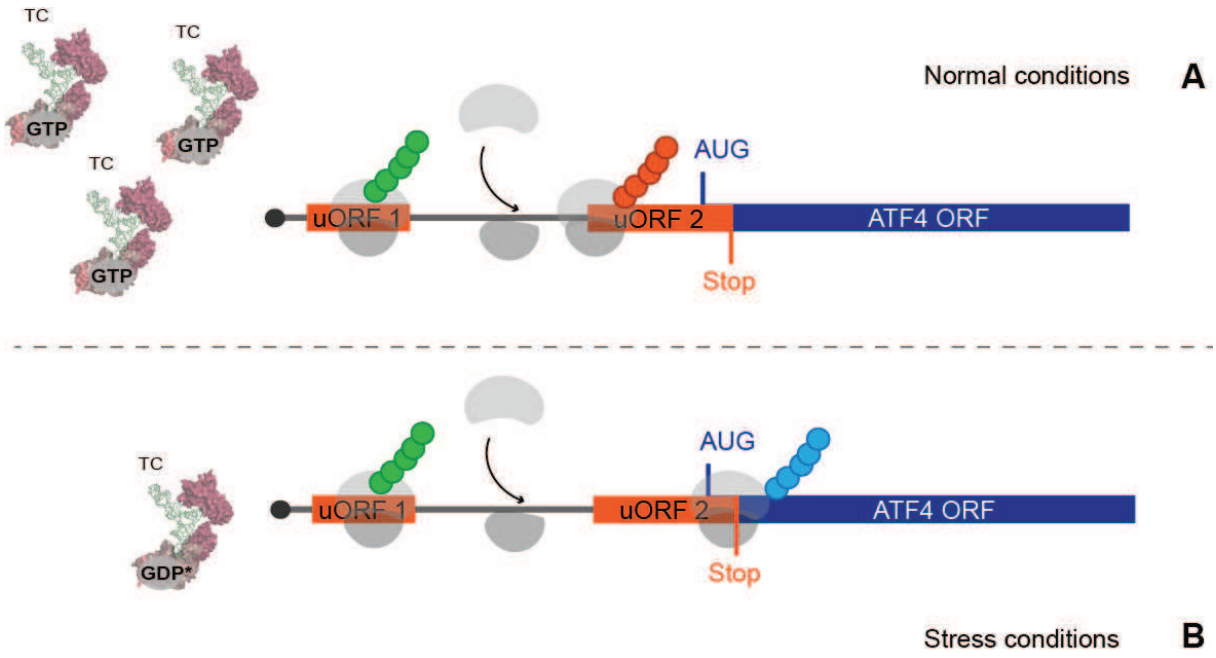

Figure 10. ATF4 expression regulation by two uORFs
ATF4 mRNA contains 2 uORFs: the first one is efficiently translated and under normal conditions **(A)** allows reinitiation at the second inhibitory uORF overlapping the ATF4 ORF. Upon cellular stress **(B)**, when the ternary complex carrying the Met-tRNAi is less available, the 43S complex resumes scanning after translation of uORF1 and reinitiates at the main ATF4 ORF.

* uORF/IRES combinations

The 5'-UTR of some highly regulated genes are characterized by the simultaneous presence of uORFs and IRES structures. This arrangement creates a further level of complexity in the regulatory mechanism. A particularly complex example is the expression of the VEGF (Vascular Endothelial Growth Factor) gene, which is regulated at several levels from its transcription to its cellular localization. This gene produces several mRNA isoforms (Akiri *et al.,* 1998), containing different poly(A) sites and regulatory elements in both the 3'- and 5'-UTRs (reviewed in Arcondéguy *et al.,* 2013). Among these mRNA isoforms, one is characterized by a long and complex 5'-UTR. It contains 2 IRES structures (Huez *et al.,* 1998) and one uORF embedded within the second IRES (Bastide *et al.,* 2008). The first IRES (IRES-B) induces cap-independent initiation from a non-canonical CUG codon (Huez *et al.,* 2001; Touriol *et al.,* 2003), and generates a long L-VEGF, which is further maturated. The second IRES (IRES-A) initiates translation at the AUG canonical initiation codon and in

turn allows direct expression of the shorter secreted form of VEGF (Figure 11). However, the recognition of this downstream AUG codon is hindered by the presence of a uAUG within the IRES-A structure. In this case, uORF translation is cap-independent. Specific trans-acting factors are certainly involved but the exact mechanism remains unclear (Bastide *et al.,* 2008).

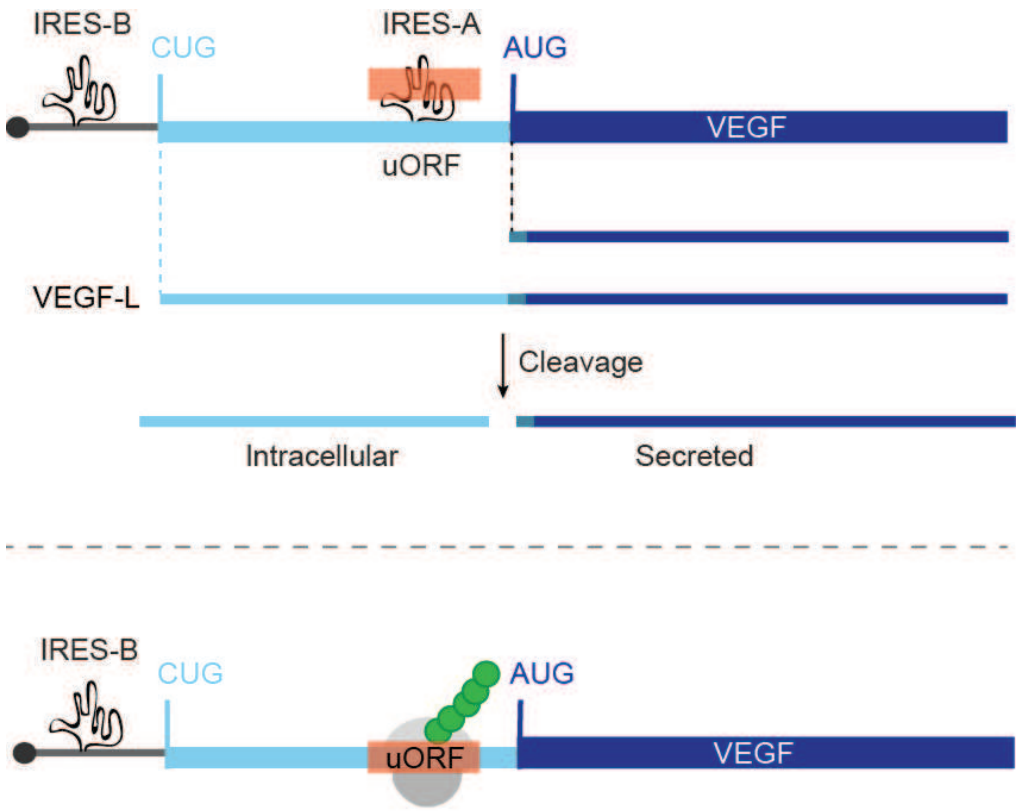

Figure 11. VEGF expression is regulated by uORF and two IRESs
One VEGF mRNA isoform contains 2 IRES and a uORF to synthetize 2 proteins: L-VEGF and a shorter secreted VEGF version. The L-VEGF protein is generated *via* the IRES-B sequence from a non-canonical CUG initiation codon. The proximal IRES-A directly allows the synthesis of the secreted form of VEGF from the AUG start codon. However, this IRES-A encloses a uORF, which inhibits translation of the main ORF. The exact mechanism is still not clear.

* The role of uORF peptides

Although for most of the uORFs the coding sequence is not important for regulation, there are a few examples where the uORF inhibitory activity is mediated by the amino acid sequence of the nascent peptide. In fact, little is known about the outcome of upstream peptides, since only a few peptides have been detected (Oyama *et al.,* 2004 and 2007; Slavoff *et al.,* 2013). They are either quickly degraded or current techniques are not sensitive enough to detect them. One of the best-known examples is S-adenosyl-methionine decarboxylase (ADOMetDC) mRNA, whose expression is dependent on polyamine cellular concentrations

(Figure 12) (Ruan *et al.,* 1996). The mRNA 5'-UTR contains an inhibitory uORF coding for a 6 amino acid peptide -MAGDIS- (Hill and Morris, 1992). In the presence of an elevated polyamine concentration, this small peptide interacts with the translation machinery, induces ribosomal stalling, and thus blocks ribosome access to the main ORF (Law *et al.,* 2001). In contrast, when the level of polyamines is low, there is no ribosomal pausing and the main ORF is efficiently translated.

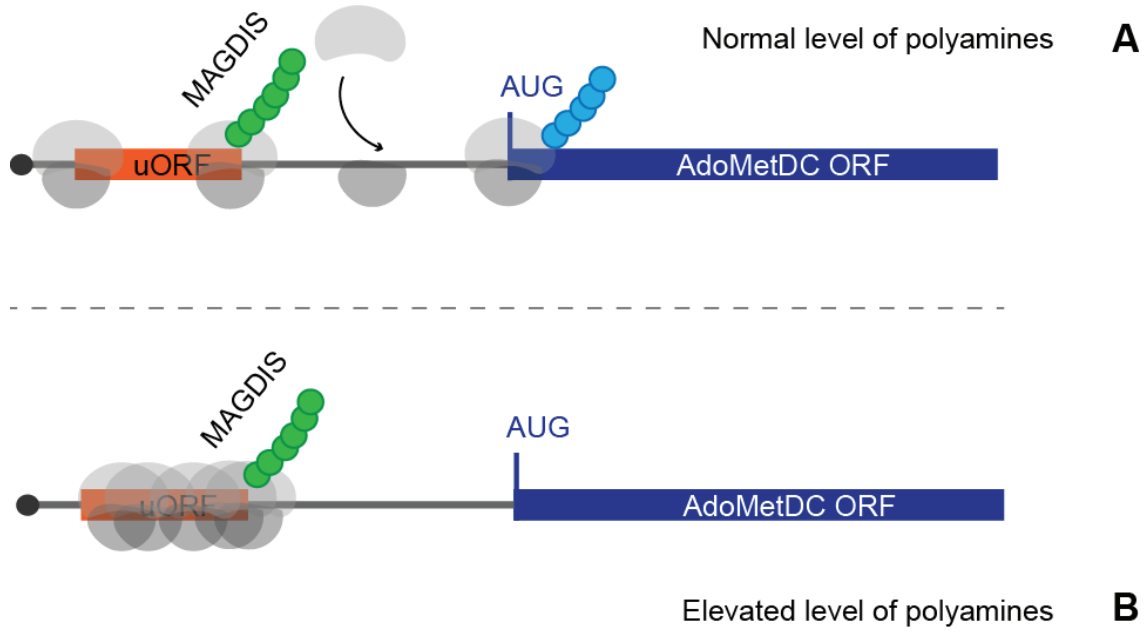

Figure 12. Polyamine dependent expression of AdoMetDC
AdoMetDC expression is regulated by a uORF peptide. **(A)** When cellular levels of polyamines are low, the 43S reinitiates at the main ORF. **(B)** When polyamines are elevated, the small peptide interacts with the translation machinery and induces ribosomal stalling, blocking reinitiation at the main ORF.

1.2.6. Alternative Non-AUG initiation codons

Non-AUG codons are quite rare in eukaryotes and are tipically present in genes encoding regulatory proteins such as proto-oncogenes, transcription factors, kinases, or growth factors. Usually the first initiation codon is a near cognate initiation codon (one nucleotide is different from the AUG codon) and the second one is a classical AUG initiation codon. Efficient initiation at a non-AUG codon depends on its environment: (i) its positioning in an optimal "Kosak" context that permits leaky scanning of the ribosome, (ii) the involvement of translation initiation factors such as eIF1, eIF5 and eIF2 or (iii) the presence of an IRES directed initiation. These mechanisms allow the translation of longer protein isoforms,

generally displaying localization signals for specific cellular compartments (Touriol *et al.,* 2003).

Interestingly, this is the case in the 5'-UTR of the yeast glycyl-tRNA synthetase (GRS) mRNA. In *S. cerevisiae*, two distinct nuclear GRS genes were identified. The first one, *GRS1* codes for the housekeeping enzyme that possesses both cytosolic and mitochondrial glycylation activities, while the second one, *GRS2*, codes only for a stress-induced cytosolic GRS. *GRS1* encodes two distinct protein isoforms through alternative use of two in-frame initiator codons. The longer mitochondrial form (with the mitochondrial localization signal) is synthetized using a UUG initiation codon and the shorter cytosolic form uses a canonical AUG initiation codon (Figure 13). Both codons are in the same suitable, but not optimal, Kozak context (Chang and Wang, 2004). Different UUG/AUG mutants showed that the UUG start codon is less efficient than the AUG, indicating that the cytosolic GRS is simply generated by leaky-scanning (Chen *et al.,* 2008).

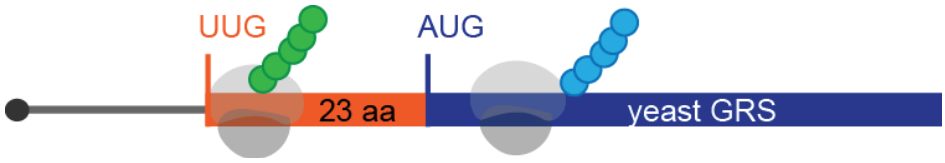

Figure 13. Yeast GRS1 organization

The *GRS1* gene encodes both cytosolic and mitochondrial GRS in *S. cerevisiae*. Translation initiation at UUG generates mitochondrial GRS (green peptide) with N-terminal 23 amino acids targeting signal and translation initiation of the cytosolic GRS (blue peptide) starts at AUG by leaky-scanning.

1.3. Cap-independent initiation

The majority of eukaryotic mRNAs are translated using the classical model of scanning. This mechanism implies the presence of a cap structure (m7G) at the 5'-end of the mRNA. This cap structure is recognized by eIF4E and allows mRNA circularization *via* PABP and eIF4G. This complex then recruits the 43S preinitiation complex that scans the 5'-UTR until it recognizes the AUG initiator codon. However, another mechanism of translation initiation was discovered in 1988. Two groups showed independently that the poliovirus and the encephalomyocarditis virus RNAs use cap-independent translation initiation (Jang *et al.,* 1988; Pelletier and Sonenberg, 1988). In the case of poliovirus mRNA, they observed that the 5'-UTR was particularly GC rich, contained several AUG codons and had no cap structure. Despite this hostile context, the mRNA was efficiently translated and once inserted in a bicistronic reporter, it was able to promote internal translation initiation (Pelletier and

Sonenberg, 1988). This internal translation initiation was triggered by a specific region of the viral RNA called the Internal Ribosome Entry Site (IRES). Indeed the structured RNA domain drives direct recruitment of the 43S ribosomal complex next to the AUG start codon. Over the following years, many other viral IRESs were discovered, mainly divided in 4 groups depending on their structure and the corresponding initiation mechanism (reviewed in Balvay *et al.,* 2009). Globally, type 1 and 2 IRESs are characteristic for picornaviruses. Translation initiation is triggered by the 43S complex, eIF4G and eIF4GA, but do not involve eIF4E. Type 3 or HCV-like (hepatitis C virus) viral IRESs attach the 43S complex containing only eIF3 and eIF5. Finally, type 4 IRESs (cricket paralysis virus) directly recruit the 40S ribosomal subunit and initiate translation without any additional initiation factor and even without the Met-tRNAi. In this case, the first coding codon (CUG) is directly positioned into the A site of the ribosome (Schüler et al, 2006). In addition to being able to initiate translation in a cap-independent manner, these viruses often reduce cellular mRNA cap-dependent translation by inhibiting the cap recognition mechanism: eIF4G is cleaved (Pelletier and Sonenberg, 1988) or eIF4E is sequestered by 4E-BP (eIF4E binding protein) (Beretta *et al.,* 1996, Gingras *et al.,* 1996).

However, during this period of cap-dependent translation inhibition, certain cellular mRNAs (3-5%) were still translated (Johannes and Sarnow, 1998) and thus the first evidence that cellular mRNAs may also undergo cap-independent translation initiation emerged. Later on, more evidence was collected to demonstrate that cellular mRNAs indeed also contain functional IRES structures (Yang *et al.,* 2006; Schepens *et al.,* 2005; Fox *et al.,* 2009; Riley *et al.,* 2010; Marash *et al.,* 2008; Dobbyn *et al.,* 2008).

1.3.1. Cellular IRES

Despite scepticism concerning the existence of cellular IRESs, several eukaryotic mRNAs containing such structures were identified during the last 20 years. Most of them concern highly regulated proteins such as i) proto-oncogenes: c-myc (Nanbru *et al.,* 1997; Stoneley, 1998), n-myc (Jopling and Willis, 2001), l-myc (Jopling *et al.,* 2004) and p53 (Ray *et al.,* 2006); ii) growth factors like IGF-2 (Teerink *et al.,* 1995), VEGF (Huez *et al.,* 1998; Stein *et al.,* 1998), FGF-2 (Vagner *et al.,* 1995) and iii) stress responsive genes such as Hif-1a (Lang *et al.,* 2002), cat-1 (Fernandez *et al.,* 2001) and Apaf-1 (Coldwell *et al.,* 2000). Cellular IRESs vary in length, structure and sequence. They are found in GC rich 5'-UTRs containing highly structured regions often characterized by the presence of several start codons and uORFs, these features being incompatible with the classical scanning model of translation initiation. Cellular mRNAs containing IRES structures are not or poorly translated during cap-

dependent initiation under normal cellular conditions (Spriggs *et al.,* 2005). However, their expression is boosted under particular physiological conditions where cap-dependent translation is inhibited (reviewed in Komar and Hatzoglou 2011). There are only a few examples of proteins expressed by both cap-dependent and cap-independent translation like neurogranin and neuronal calmodulin binding protein (Pinkstaff *et al.,* 2001).

The exact mechanisms of internal initiation for most of these cellular IRESs remain unclear and more mechanistic studies are needed. Only a few structural models are available: c-myc, cat-1, FGF-2, Apaf-1 and FGF1-A (Le Quesne *et al.,* 2001; Yaman *et al.,* 2003; Bonnal *et al.,* 2003; Mitchell *et al.,* 2003; Martineau *et al.,* 2004). The highly structured domains that render experimental approaches difficult explain it. A comparison of the existing models as well as sequence analysis did not reveal any specific structural or sequence motif (Baird *et al.,* 2007). Usually the structure of viral IRESs is highly conserved and small deletions or mutations disrupt their functionality. On the contrary, cellular IRES appear to be a combination of several segments working independently or together to promote internal initiation (Chappell *et al.,* 2000) and deletions decrease their capacity to initiate translation without abolishing it completely (Huez *et al.,* 1998; Stoneley, 1998; Chappell *et al.,* 2000).

An interesting example of such an IRESs, is the IRES present in the cat-1 (Amino acid transporter cationic 1) mRNA 5'-UTR. This IRES is not functional under normal physiological conditions. The 5'-UTR of this mRNA also contains a normally expressed uORF. Because of the sequence of the nascent peptide, upon amino acid starvation, the rate of translation is slowed down and induces ribosomes stalling (Figure 14) (Fernandez *et al.,* 2005). This event triggers structural changes in the mRNA and induces the formation of a functional IRES sequence responsible for translation of the main ORF.

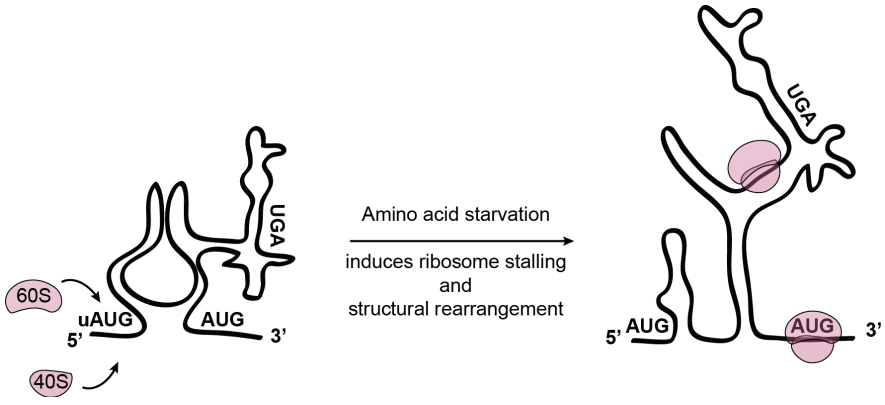

Figure 14. Cat-1 IRES formation

Upon amino acid starvation, ribosomes translating the cat-1 uORF sequence stall and induce conformational modifications in the 5'-UTR that shape an IRES structure, thus targeting internal initiation at the main ORF AUG.

1.3.2. Canonical initiation factors and IRES recognition

Several factors are important for cap-independent initiation; they correspond to a selection of canonical initiation factors or to IRES-specific *trans*-acting factors (ITAFs). As mentioned above little is known about the mechanism that cellular IRESs use to recruit the initiation complex directly at the start codon. For most of the cellular mRNAs, the IRES sequence is located upstream of the initiation codon and can promote landing and then scanning of the ribosome, as was proposed for c-myc, L-myc and N-myc (Spriggs *et al.,* 2009). None of c-myc or N-myc IRESs require the eIF4E and eIF4G to initiate translation, instead they use eIF4A and eIF3 probably to induce conformational changes at the landing site. On the contrary L-myc IRES activity is dependent on the presence of the eIF4F complex and the association of PABP and eIF3 with eIF4G (Spriggs *et al.,* 2009).

Surprisingly, the c-Src (Proto-oncogene tyrosine-protein kinase Src) IRES seems to directly bind the 40S subunit without the requirement of any canonical initiation factor, comparable to hepatitis C virus-like IRES, which recruit the small subunit *via* multiple direct contacts (Allam and Ali, 2010). Many cellular IRESs such as cat-1, c-Src and N-myc IRESs are not sensitive to eIF2 phosphorylation. They probably use other still unknown factors to position the Met-tRNAi in the P-site of the 40S ribosomal subunit (reviewed in Komar and Hatzoglou 2011).

It is worth noting that the smallest identified IRES is only a 9 nt sequence found in the mRNA of the human homodomain protein Gtx. This short sequence is complementary to nucleotides 1132–1124 in the 18S rRNA (Chappell *et al.,* 2000) and is sufficient to efficiently recruit the ribosome small subunit.

1.3.3. IRES trans-acting factors and cellular stress

IRES mediated translation initiation also requires some IRES specific *trans*-acting factors (ITAF). It was proposed that these factors sense changes in the physiological state of the cell and thus regulate IRES-dependent expression. Many ITAFs are part of heterogeneous nuclear ribonucleoproteins (HnRNP), such as HnRNP A1, C1/C2, E1/E2, I, K and L (reviewed in Komar and Hatzoglou, 2005) or other RNA binding proteins with nuclear and cytoplasmic localization: p54nrb, PSF (p54nrb–protein-associated splicing factor) and YB-1 (Cobbold *et al.,* 2008; Spriggs *et al.,* 2009).

Even if the exact mechanism is still unknown, there are two theories about how these proteins regulate cap-independent translation (Figure 15) (Lewis and Holcik, 2007). According to the first hypothesis, after mRNA synthesis in the nucleus, ITAFs would bind IRES-containing mRNAs and retain them in the nucleus. Then, only a specific cell signal

would promote their release into the cytosol where they will be translated. In the second hypothesis, ITAFs would be confined to the nucleus and released into the cytoplasm upon a specific cell signal and would bind there to cytosolic IRES-containing mRNAs and activate or inhibit their translation (Lewis and Holcik 2007).

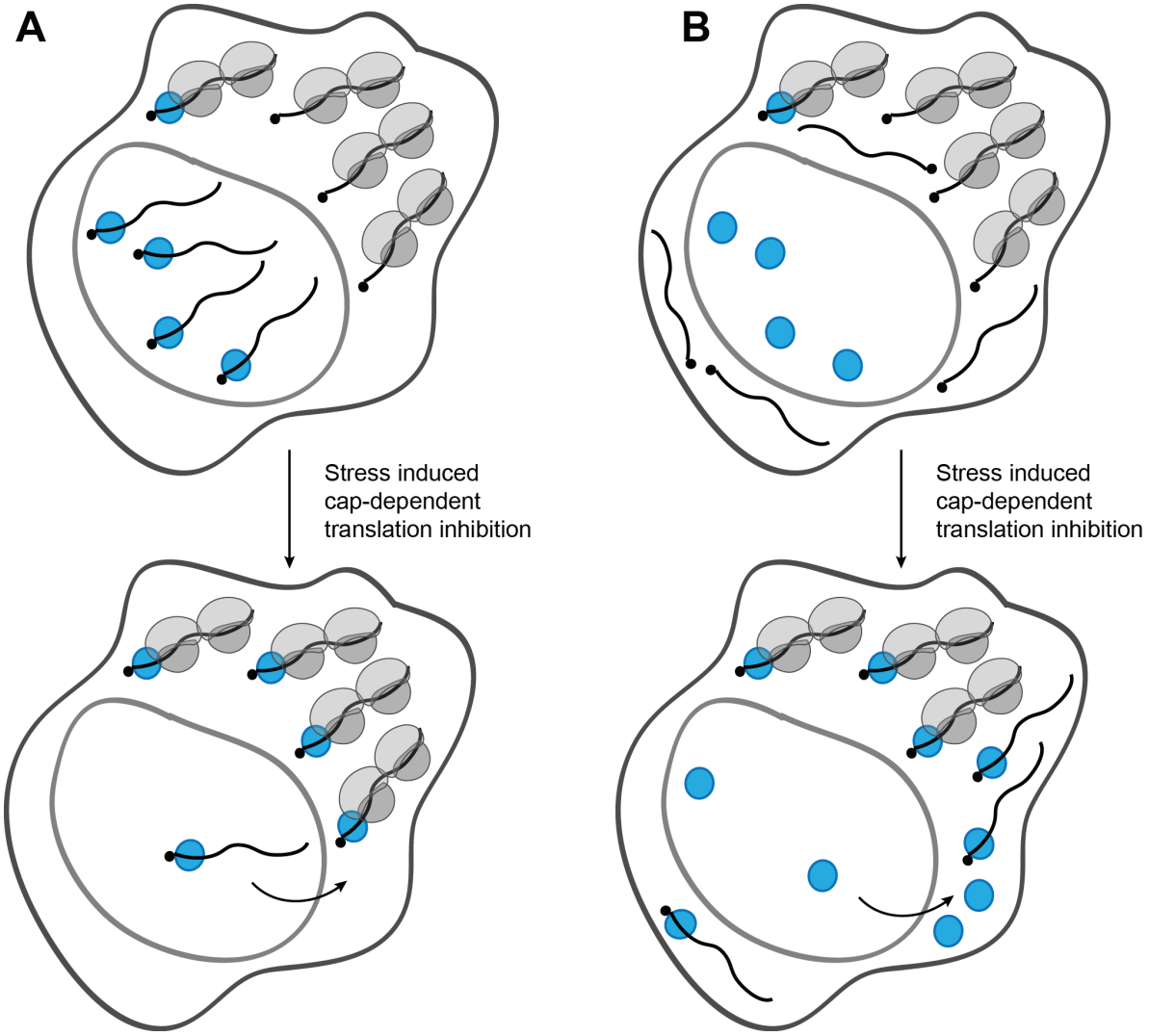

Figure 15. Two alternative mechanisms for ITAFs in cap-independent translation initiation

(A) ITAFs (blue) bind directly to IRES containing-mRNAs in the nucleus and are exported together into the cytosol to induce IRES-dependent translation. **(B)** Upon particular stress signals, ITAFs leave the nucleus and bind cytosolic IRES-containing mRNAs and modulate their translation.

Actually, the same ITAF can have opposite effects, depending on the targeted IRES. Indeed, hnRNP A1, when located in the cytosol activates IRES-dependent translation of FGF-2 (Fibroblast Growth Factor 2) (Bonnal *et al.,* 2005) but can also inhibit IRES-dependent translation of XIAP (X-linked inhibitor of apoptosis protein) (Lewis *et al.,* 2007). Likewise, PTB (Polypyrimidine tract-binding protein), which is one of the commonly used ITAFs,

promotes Apaf-1 (Apoptotic peptidase activating factor 1) expression (Mitchell *et al.,* 2001) or represses IRES-mediated translation initiation of Bip (Binding immunoglobulin protein) (Kim *et al.,* 2000). Usually ITAFs cooperate to perform their activity. For example the unr (N-ras upstream gene protein) ITAF binds to the Apaf-1 IRES and induces structural conformation changes, allowing the binding of PTB, which subsequently allows 43S landing (Mitchell *et al.,* 2001).

As seen above, ITAFs can influence IRES dependent translation depending on the physiological state of the cell or in response to particular stimuli. Yet, some ITAFs are also cell- or tissue-specific. This is the case for PTB, which has a neuronal enhanced paralog called nPTB. Apaf-1, normally activated by PTB, is highly expressed in neurons because nPTB binds its IRES and induces even more efficient expression (Mitchell *et al.,* 2003).

1.4. Cap-assisted internal initiation

Recent studies revealed another intricate mechanism of translation initiation, different from the cap-dependent scanning mode and cap-independent IRES initiation. This mechanism was discovered by Eriani and colleagues in 2011. They characterized the particular case of cap-assisted internal initiation of translation of the mouse Histone H4 (Martin *et al.,* 2011). Histone mRNAs are unique because they don't have PolyA tails and contain short 5'-UTRs (only 9 nt in H4 mRNA) (Meier *et al.,* 1989). Thus the usual mechanism involving the formation of a closed mRNA to recruit the initiation complex does not apply. Instead, H4 mRNA contains a double stem-loop structure similar to the 4E-sensistive element (4E-SE) in its coding sequence, which binds eIF4E in a cap-independent manner. Moreover, another structure, located 19 nt downstream the 5' end, forms a three-way helix junction shaping a cap-binding pocket which sequesters the cap structure. The 43S initiation complex is thus recruited using a tethering mechanism involving both the 4E-SE element and the three-way helix junction. Finally, the release of the cap facilitates the positioning of the ribosome at the AUG start codon.

All these examples of non canonical translation initiation mechanisms emphasise the plasticity of regulation processes and illustrate the ingenious mechanisms eukaryotic cells use to maintain homeostasis and to quickly adapt to different stresses. In particular, IRES mediated translation initiation presents a complex network of regulations that is far from being completely understood. More mechanisms have to be elucidated before elaborating a complete picture of interacting cellular factors and cellular conditions that are required in these processes.

II. Aminoacyl-tRNA synthetases: translation and beyond

Translation of genetic information is crucial for the assembly and survival of each whole organism. It implies the decoding of mRNAs into proteins, which is a highly specific and regulated process. In eukaryotes, translation can take place in the cytosol or the mitochondria and occurs on ribosomes with the cooperation of numerous other proteins. Aminoacyl-tRNA synthetases (aaRS) are important housekeeping proteins that play a key role in this mechanism. They catalyse the covalent attachment of a specific amino acid to their cognate tRNAs, thus supplying aminoacylated tRNAs to the translation machinery. Each eukaryotic cell contains a set of 20 canonical aminoacylation systems, composed of one specific aminoacy-tRNA synthetase and one or more cognate tRNAs for each amino acid (Ibba and Soll, 2000). Surprisingly, over the last 10 years a palette of alternative functions outside the realm of aminocylation, as well as their implication in several diseases, have been discovered for these enzymes (Guo and Schimmel, 2013; Yao and Fox, 2013). In this chapter, I will briefly describe the canonical function of aaRSs and then go more deeply into the alternative functions of mammalian aaRSs, emphasizing glycyl-tRNA sythetase's (GRS) moonlighting functions in cellular processes such as Ap4A synthesis, its implications in cancer, and in Poliovirus infection.

1. Aminoacylation: catalysis and specificity

Protein synthesis is one of the most complex biosynthetic process, involving a huge number of proteins and RNA molecules: ribosomal RNAs and proteins, translation initiation, elongation and termination factors, tRNAs, aminoacyl-tRNA synthetases and several auxiliary proteins. The fidelity of the translation reaction relies on two main mechanisms. The first one is aminoacylation of tRNAs and the second one is based on ribosome-directed codon/anticodon recognition and the correct decoding of the mRNA by tRNA molecules.

1.1. Aminoacylation reaction

Aminoacylation is a two–step reaction. The first step (1) consists of the activation of the amino acid (aa), by the formation of a high-energy aminoacyl-adenylate (aa~AMP) in the

$$(1)\quad aa + ATP + aaRS \overset{Mg^{2+}}{\rightleftharpoons} aaRS.aa\sim AMP + PPi$$

$$(2)\quad aaRS.aa\sim AMP + tRNA \longrightarrow aaRS + aa\text{-}tRNA + AMP$$

aminoacyl-tRNA synthetase catalytic site. This reaction requires Mg^{2+} ions and releases PPi. This step occurs usually in the absence of tRNA, except for activation of glutamate, glutamine and arginine by the glutamyl-, glutaminyl- and arginyl-tRNA synthetases, respectively. During the second step of the reaction (2), the activated amino acid is transferred by esterification to the 2'- or 3'-OH on the 3'-terminal adenosine of the cognate tRNA. The fidelity of the aminoacylation reaction is particularly important to avoid incorporation of the wrong amino acids in the peptide sequence. It involves the specific recognition of tRNA identity elements (reviewed in Giegé *et al.,* 1998). Indeed, the tRNA molecule is characterized by the presence of several identity elements (specific nucleotides), usually located in the acceptor stem and/or in the anticodon regions that interact with the catalytic and the anticodon domains in the aaRS, respectively. This specificity is often further improved thanks to the presence of editing domains in certain aaRSs. These domains increase aa selectivity by a "double sieve" mechanism and insure the accuracy of aa activation and/or transfer (Fersht and Kaethner, 1976; Schmidt and Schimmel, 1994). The first filter sits in the catalytic site and discriminates against most non-cognate aas based on their size. The second filter is an additional hydrolytic editing domain present in selected aaRSs (Table 1), which releases any misactivated or mischarged aa.

Correctly aminoacylated tRNAs are then recognized by the eukaryotic elongation factor EF-1α and loaded in the A-site of the ribosome, where their anticodon interacts with the corresponding codon in the mRNA sequence.

1.2. Structure and characterisation of eukaryotic aaRSs

AaRSs are modular proteins characterized by the presence of conserved domains (Wolf *et al.,* 1999). The central domain is the catalytic domain, where the aminoacylation reaction occurs. AaRSs are divided in two classes based on the structure of their catalytic domains and each class presents three sub-classes (Table 1) (Cusack *et al.,* 1990; Eriani *et al.,* 1990; Arnez and Cavarelli, 1997).

Class I Aminoacyl-tRNA synthetases are almost exclusively monomeric with a Rossman ATP-binding fold in the catalytic core as well as two well conserved motifs KMSKS and HIGH sequences, both of which important for amino acid stabilization and activation. Class I aaRSs catalyse the attachment of the aa on the 2'-OH of the 3'-end adenosine of the tRNA (Ibba et Soll, 2000).

Table 1. AaRSs classification

Class I	Oligomeric state	**Class II**	Oligomeric state
Ia		**IIa**	
VRS*	α	SRS	α_2
IRS*	α	TRS*	α_2
LRS*	α	PRS*	α_2
MRS	α_2	GRS	α_2
CRS	α	HRS	α_2
RRS	α	ARS*	α_4
Ib		**IIb**	
ERS	α	DRS	α_2
QRS	α	NRS	α_2
		KRS	α_2
Ic		**IIc**	
WRS	α_2	FRS*	$\alpha_2\beta_2$
YRS	α_2		

The 20 eukaryotic canonical aaRSs are organized in two classes according to their catalytic site structural characteristics, aminoacylation mechanism and oligomery. AaRSs containing an editing domain are indicated with an asterisk.

Class II aaRSs are all multimeric (dimeric or tetrameric), the catalytic core is composed of 7 antiparallel β-sheets flanked by α-helices, containing three relatively well conserved motifs (I, II and III). In these cases, the aa is attached on the 3'-OH group of the terminal adenosine.
The second important module is the anticodon-binding domain that provides an additional level of selectivity. It allows the specific recognition of the cognate tRNA by interacting with the anticodon region of the aaRS.
During evolution aminoacyl-tRNA synthetases have acquired additional modules. Some of which increase the strength of the aaRS-tRNA interaction. This is the case for N-terminal extension domains present in lysyl-, aspartyl- and asparaginyl-tRNA synthetases (KRS, DRS and NRS). In mammals, other appended domains involved in protein-protein interactions appeared to facilitate the formation of the multisynthetase complex (MSC). The MSC contains 9 of the 20 cytosolic aaRSs (RRS, KRS, LRS, IRS, QRS, MRS, DRS and EPRS) and 3 non-catalytic factors (AIMP1, 2 and 3). The reason why these 9 aaRSs assemble in a complex in the cell is still not elucidated. Two mutually non-exclusive hypotheses have been

proposed: (i) this complex allows efficient channelling of aminoacylated tRNAs to the translational machinery and/or (ii) the MSC serves to keep sequestered the aaRSs away from their non-canonical functions, waiting to be released to the cytosol upon a specific cellular signal.

2. Non-canonical functions of mammalian cytosolic aminoacyl-tRNA synthetases

As mentioned above, during the last 10 years, a myriad of non-canonical functions have been uncovered for aaRSs, often in connection with a particular disease. AaRSs are involved in various processes such as transcription and translation regulation, apoptosis, immune responses, angiogenesis, inflammatory pathways and the mTOR signalling pathway (Figure 16) (reviewed in Guo and Schimmel, 2013). AaRSs are important housekeeping proteins that are ubiquitously expressed and required for cell survival. It is particularly difficult to study their non-canonical functions, since their deletion or overexpression leads to lethality or causes important cellular dysfunctions. However, several molecular and cellular mechanisms involving aaRS alternative functions are well described. Moreover, future development of high throughput proteomic and interactome analyses in different cellular compartments, tissues and pathological cases should allow even more moonlighting functions to be uncovered and establish connections between aaRSs and additional biological processes.

2.1. AaRSs and post-transcriptional regulations

In order to ensure accurate aminoacylation and alternative functions it is important to maintain a stable and regulated expression of aaRSs in the cell. AaRSs are able to regulate expression of their own genes, acting at the transcriptional or translational level. These mechanisms are not conserved, they are different from one aaRS to the other and from one cell type to the other (bacteria or eukaryotes). A large variety of mechanisms are well described in bacteria, almost all of them involve amino acid or tRNA availability or tRNA structural mimics to activate or inhibit either transcription or translation. (reviewed in Ryckelynck *et al.,* 2005). However only a few mechanisms concerning such regulations have been studied in eukaryotes and one can imagine that many more remain undiscovered. Nevertheless, six eukaryotic multifunctional aaRSs (DRS, QRS, MRS, EPRS, KRS and GRS) are involved in transcriptional and translational regulations, not only for their own but also for other proteins' expression.

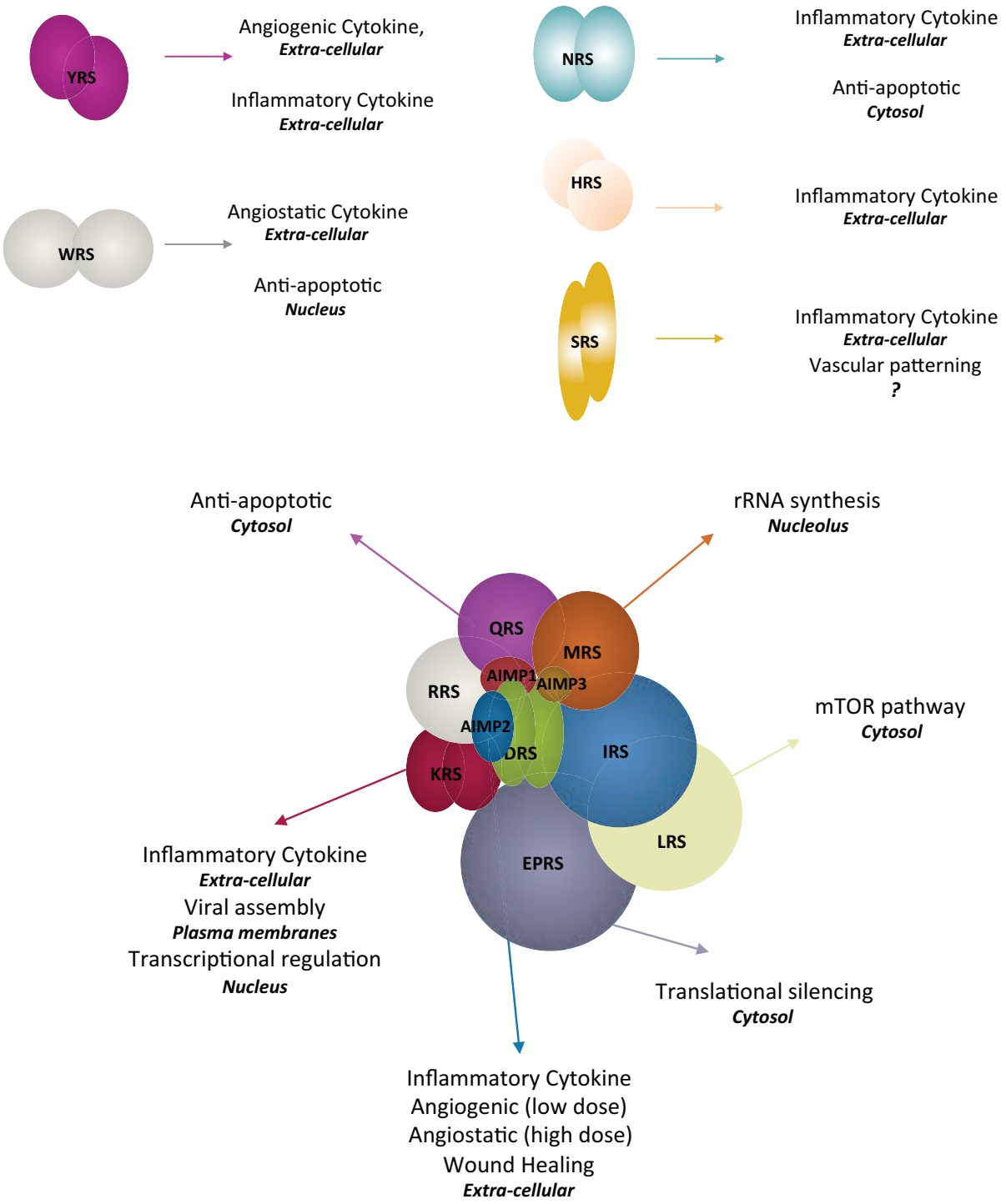

Figure 16. aaRS non-canonical functions

At least 11 human aaRS are associated with various alternative functions. Tyrosyl-, tryptophanyl-seryl-, histidyl- and asparaginyl-tRNA synthetases (YRS, WR, SRS, HRS, NRS) are free cytoplasmic aaRSs. The case of glycyl-tRNA synetase (GRS) is not presented in this figure because it will be detailed later on. Glutaminyl-, methionyl-, leucyl-, glutamyl-, prolyl-, arginyl-, lysyl- and aspartyl-tRNA synthetases (QRS, MRS, LRS, EPRS, RRS, KRS and DRS) are components of the MSC and are released from it to accomplish their non-canonical functions.

2.1.1. Yeast DRS regulates its own expression

In yeast, aspartyl-tRNA synthetase (DRS) expression is regulated *via* a feedback mechanism (Figure 17). In the cytosol, DRS attaches aspartic acid to its cognate tRNAs, which is then delivered to the ribosome. However, when a surplus of free DRS (unbound to its cognate tRNA) accumulates, the synthetase is imported into the nucleus, where it binds its own mRNA and inhibits its expression (Frugier *et al.,* 2005). Yeast DRS contains an N-terminal appendage of 70 amino acid residues that protrudes from the anticodon-binding domain. It is able to bind a domain in the DRS mRNA covering the 5'-UTR and the beginning of the coding sequence (Ryckelynck *et al.,* 2005). Several levels of regulation can be considered to explain this regulatory mechanism: mRNA transcription, mRNA degradation or impeded export from the nucleus.

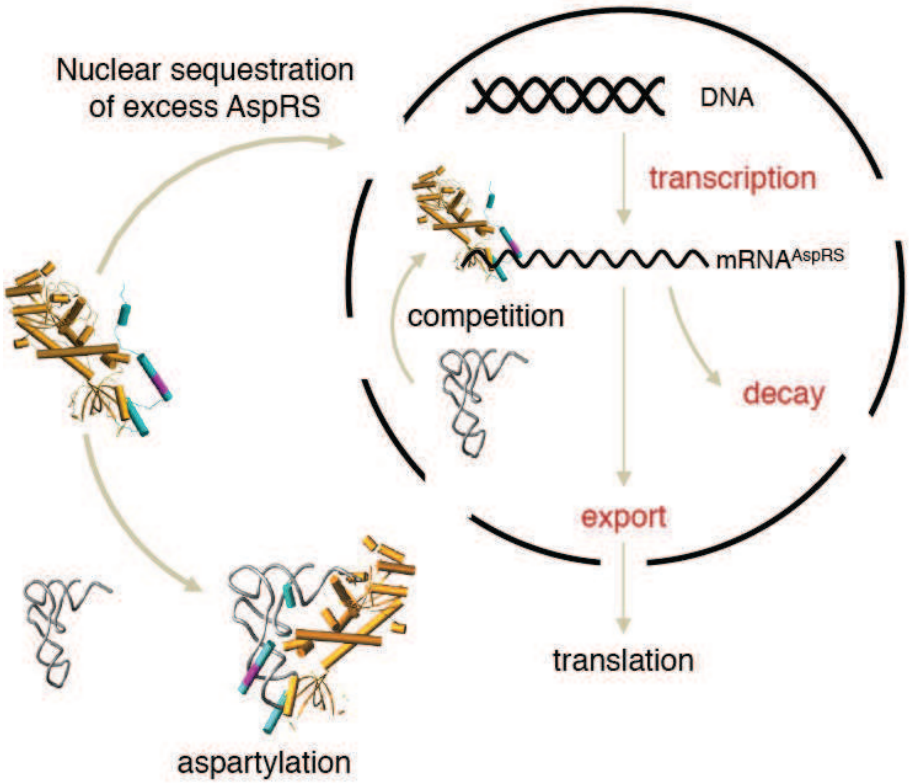

Figure 17. DRS expression regulation

In the cytosol, DRS aspartylates $tRNA^{Asp}$. When there is not enough $tRNA^{Asp}$ available compared to the DRS cellular concentration, the enzyme translocates to the nucleus and binds its own mRNA 5'-end. This interaction hinders further synthesis of DRS (from Frugier *et al.,* 2005).

2.1.2. Human MRS regulates ribosomal RNA biogenesis

Aminoacyl-tRNA synthetases are also able to regulate expression of other proteins or RNAs. For instance, methionyl-tRNA synthetase (MRS), one of the nine synthetases of the MSC is involved in ribosomal RNA biogenesis. In proliferating cells, human MRS translocates to the nucleolus and activates ribosomal RNA synthesis (Ko *et al.,* 2000). Indeed, specific MRS antibodies block rRNA synthesis. MRS nucleolar localization is triggered by different growth factors, such as insulin, platelet-derived growth factor (PDGF) and epidermal growth factor (EGF). However, yet again, the exact regulatory mechanism remains unclear.

2.1.3. Human EPRS and the GAIT system

The GAIT (IFN-γ–activated inhibitor of translation) system is a multiprotein complex, which inhibits expression of a family of inflammatory genes. The GAIT complex is composed of the bifunctional glutamyl-prolyl-tRNA synthetase (EPRS), the NS1-associated protein 1 (NSAP1), the glyceraldehyde-3-phosphate dehydrogenase (GAPDH) and the ribosomal protein L13a. In myeloid cells and monocytes, IFN-γ induces the formation of this complex, which binds to a specific stem loop structure, the GAIT element. The GAIT element is present in the 3'-UTR of several mRNAs, including those of ceruloplasmin (Cp) (Mazumder and Fox, 1999; Sampath *et al.,* 2003), VEGF-A (Ray and Fox, 2007), death-associated protein kinase (DAPK), zipper-interacting protein kinase (ZIPK) (Mukhopadhyay *et al.,* 2008), and a group of chemokine ligand and receptors (CCL22, CCR3, CCR4, CCR6 and apolipoprotein L2) (Vyas *et al.,* 2009).

The bifunctional EPRS displays two catalytic cores joined by a linker region containing three WHEP (helix-turn-helix) domains (R1, R2 and R3) (Jeong *et al.,* 2000), which are involved in several processes that allow the EPRS to switch from its canonical aminoacylation function in the MSC to its regulatory function outside the MSC. During the first hours after IFN-γ induction, serine^{886} and serine^{999}, surrounding WHEP R3, are phosphorylated (cyclin-dependent kinase 5, 1, ERK and AGC kinases) (Arif *et al.,* 2011). Phosphorylation promotes EPRS release from the MSC and NSAP1 can then bind R2 and R3 in the modified EPRS (Jia *et al.,* 2008). Twelve to sixteen hours post IFN-γ induction, the L13a ribosomal protein is in turn phosphorylated and released from the 60S ribosomal subunit (Mazumder *et al.,* 2003). Phosphorylated L13a, together with GAPDH, bind EPRS and promote a conformational shift, which liberates R1 and R2. Both L13a and EPRS become available to bind the GAIT element of the targeted mRNA 3'-UTR (Figure 18) (Jia *et al.,* 2008). Finally, L13a binds the translation factor eiF4G and inhibits mRNA translation initiation by preventing the recruitment of the eIF3-containing 43S ribosomal complex (Kapasi *et al.,* 2007).

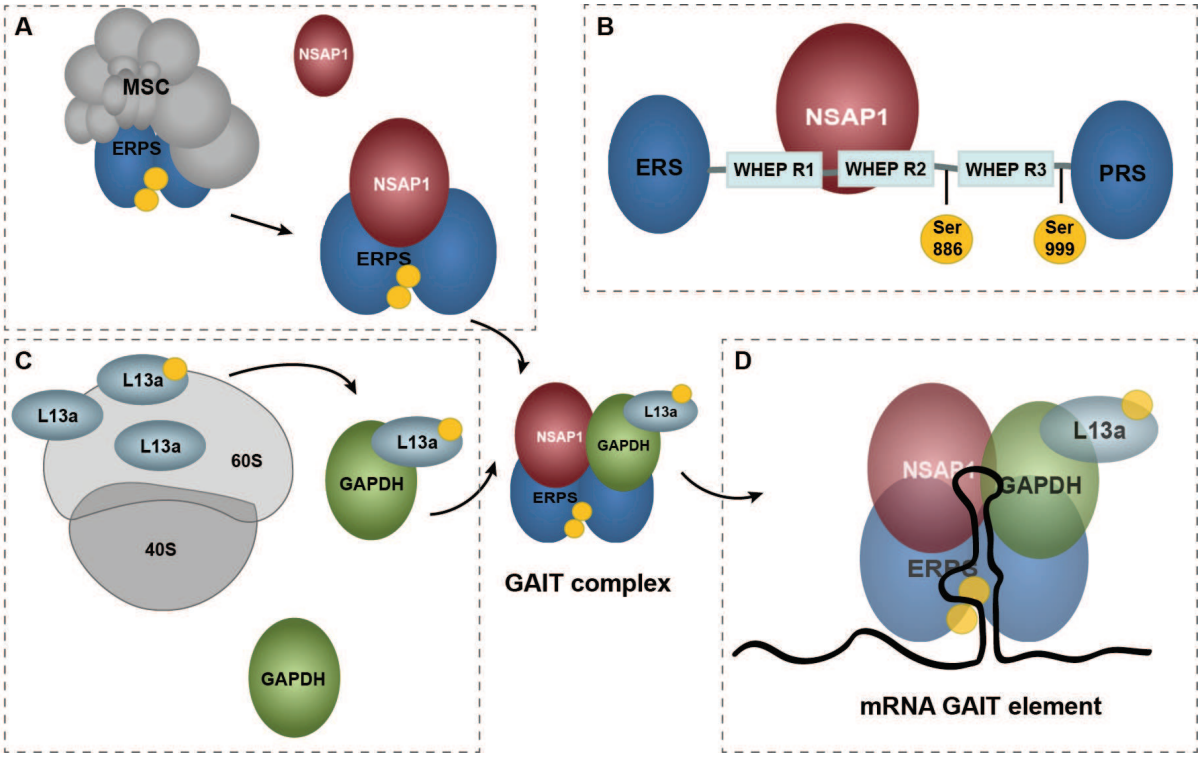

Figure 18. EPRS and the GAIT complex formation

(A) Upon IFN-γ stimulation, EPRS (blue) is phosphorylated (yellow) and released from the MSC (grey). **(B) The** NSAP1 protein (red) binds R1 and R2 of the WHEP domain, hindering further mRNA binding. **(C)** Later on, phosphorylation of the L13a (light blue) ribosomal protein induces its release from the 60S ribosomal subunit and facilitates its interaction with GAPDH (green). **(D)** Once the GAIT complex is assembled, it can bind mRNAs containing GAIT elements and inhibit binding of the 43S initiation complex. (According to the mechanisms described in Arif *et al.,* 2011; Jia *et al.,* 2008; Mazumder *et al.,* 2003).

2.1.4. Human KRS regulates transcription

The lysyl-tRNA synthetase (KRS) stimulates transcription by activating the microphthalmia transcription factor (MITF) and the upstream transcription factor 2 (USF2) (Lee *et al.,* 2004; Lee and Razin, 2005). This moonlighting activity is triggered by the synthesis of diadenosine tetraphosphate (Ap_4A). Several aaRSs (KRS, FRS, SRS and GRS) are able to synthesize diadenosine polyphosphates (from 2 to 7 phosphates) (Goerlich *et al.,* 1982), which are well known secondary messenger molecules involved in different cellular processes. KRS is the major contributor to this production (reviewed in Yannay-Cohen and Razin, 2006).

In mast cells, upon IgE–antigen binding to the FcεRI receptor, KRS is phosphorylated at serine^{207} *via* the MAP kinase (MAPK) pathway (Yannay-Cohen *et al.,* 2009) (Figure 19). This phosphorylation triggers KRS dissociation from the MSC and its translocation to the nucleus. It also induces a conformational change in the enzyme and promotes a switch from

aminoacylation to Ap_4A synthesis (Ofir-Birin *et al.,* 2013). In the nucleus, the subsequent increased concentration of Ap_4A leads to the release of MITF and USF2 from the histidine triad nucleotide-binding protein 1 (Hint-1), allowing both factors to recover their specific transcription activities (Lee *et al.,* 2004; Lee and Razin, 2005).

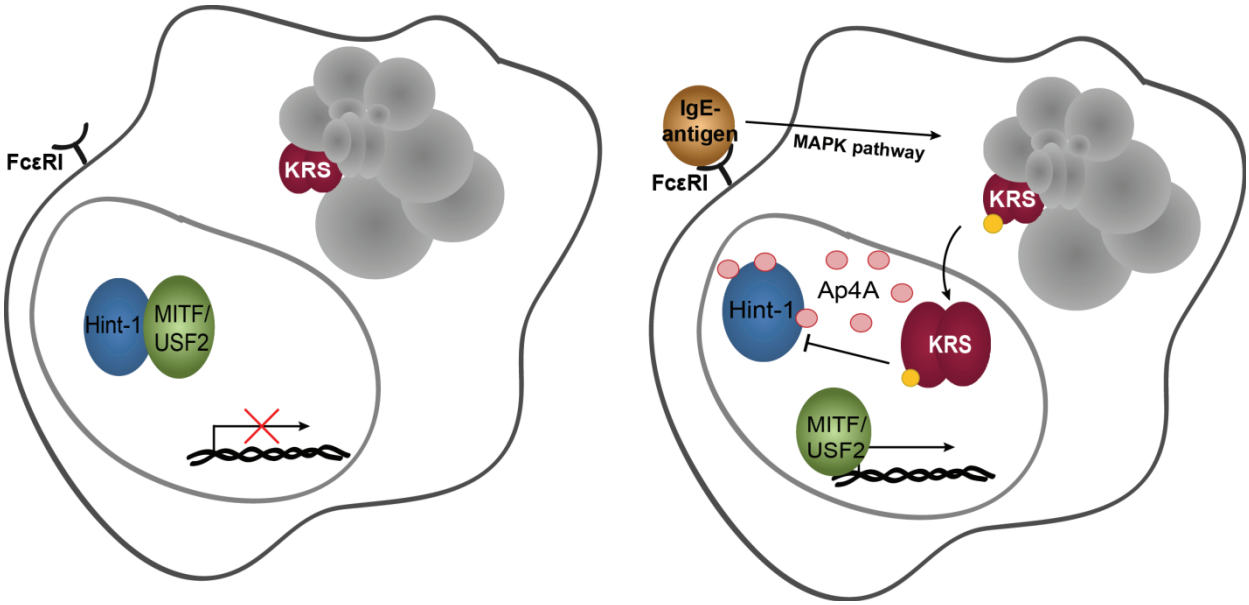

Figure 19. KRS regulates transctiption
In mast cells, Hint-1 (blue) binds the MITF and USF2 transcription factors (green) and prevents their fixation to their target genes. When the IgE antigen (orange) binds on mast cells, the MAPK pathway is activated and triggers KRS (red) phosphorylation (yellow circle). KRS is then released from the MSC (grey) and translocates to the nucleus where it produces Ap4A (pink circles). Finally, Ap4A binds Hint-1, and releases MITF/USF2 to allow transcription to occur (adapted from Motzik *et al.,* 2013).

2.2. Alternative functions related to signalling pathways

2.2.1. Human aaRSs as cytokines

Several aaRSs were identified as secreted proteins and act as cytokines; fragments of YRS and WRS, as well as full length KRS, GRS, QRS and NRS are involved in inflammatory and apoptotic pathways.

Human tyrosyl-tRNA synthetase (YRS) is characterized by the presence of an appended domain at its C-terminus: the endothelial and monocyte-activating polypeptide II-like (EMAP II-like) protein. The full-length YRS is dedicated to aminoacylation and is inactive in cell signalling. However, two fragments are generated by endoproteolysis, each with their own cytokine activities. On the one hand, the C-terminal YRS fragment contains the EMAP II-like domain and is an immune cell stimulating factor, which induces production of tumor necrosis factor-α (TNF-α) and tissue factor (TF) (Wakasugi and Schimmel, 1999). On the

other hand, the N-terminal fragment, also called mini-YRS, acts as a pro-angiogenic cytokine. After TNF-α stimulation mini-YRS is secreted from endothelial cells and activates angiogenesis through transactivation of the vascular endothelial growth factor receptor-2 (VEGFR2) (Greenberg *et al.,* 2008).

Human tryptophanyl-tRNA synthetase (WRS) is also involved in angiogenesis but in contrast to YRS, WRS inhibits neovascularization. This mechanism is triggered by a WRS fragment (mini-WRS). Mini-WRS lacks its N-terminal moiety and is generated either by alternative splicing or by proteolytic cleavage (Wakasugi *et al.,* 2002; Otani *et al.,* 2002). Upon IFN-γ stimulation, mini-WRS binds and inhibits the vascular endothelial (VE)-cadherin, a key player in promoting angiogenesis. Inhibition is achieved by the fixation of two tryptophan residues from VE-cadherin in the mini-WRS catalytic domain (the native WRS, with its N-terminal domain does not bind VE-cadherin) (Tzima and Schimmel, 2006). It was also shown that IFN-γ stimulation triggers WRS translocation into the nucleus. There, it forms a complex with the catalytic subunit of the DNA-dependent protein kinase (DNA-PKcs) and the poly(ADP-ribose) polymerase 1 (PARP-1). This association further activates the major apoptotic factor p53 (Sajish *et al.,* 2012).

The human lysyl-tRNA synthetase (KRS) was shown to trigger a proinflammatory response upon TNF-α induction. In contrast to YRS and WRS, it is the full-length KRS that is secreted from several cancer cell lines. KRS binds to macrophages and peripheral mononuclear blood cells and activates the p38 mitogen-activated kinase (MAPK), the extracellular signal-regulated kinase (ERK), and G-proteins to promote cell migration and TNF-α production (Park *et al.,* 2005).

In addition, two other aminoacyl-tRNA synthetases: histidyl- (HRS), and asparaginyl- (NRS) tRNA synthetases were also described as cytokines (Howard *et al.,* 2002). They stimulate immune cells and mediate inflammatory response, however their mechanisms of action are still not clear.

2.2.2. AaRS as amino acid sensors

The level of amino acids in the cell is an important indicator of nutrition status and controls homeostasis. The mTOR (mammalian Target Of Rapamycin) pathway, a major regulator of cell growth, proliferation, motility and survival, is regulated by two complexes: mammalian TORC1 and TORC2. Recently, two studies in yeast and mammalian cells showed that leucyl-tRNA synthetase (LRS) acts as a leucine sensor and activates the mTOR pathway (Han *et al.,* 2012; Segev and Hay, 2012) *via* mTORC1. Upon amino acid stimulation, LRS is translocated to the lysosomal membrane, where its C-terminal domain interacts with the

RagD-GTPase. It induces the recruitment of mTORC1 to the lysosome and its activation. Mutations in LRS, inactivating leucine binding, renders the mTORC1 pathway insensitive to amino acids (Han *et al.,* 2012).

Likewise, glutaminyl-tRNA synthetase (QRS) responds to increased levels of glutamine in the cell and acts as an anti-apoptotic factor. Elevated glutamine specifically induces QRS interaction with the apoptosis signal-regulating kinase 1 (ASK1) and in turn inhibits cell death (Ko *et al.,* 2001).

These examples of aaRS alternative functions highlight their importance in several crucial processes, such as cell signalling, death and survival, and the existence of complex regulated networks. Noteworthily, cells have developed various strategies to dissociate aminoacylation from non-canonical functions, employing mechanisms such as alternative splicing, protein cleavage, post-translational modifications and differential cellular localizations.

3. Human cytosolic aaRSs involved in diseases

Several aaRSs are associated with various human diseases, ranging from cancer to autoimmune and neuronal pathologies (Figure 20).

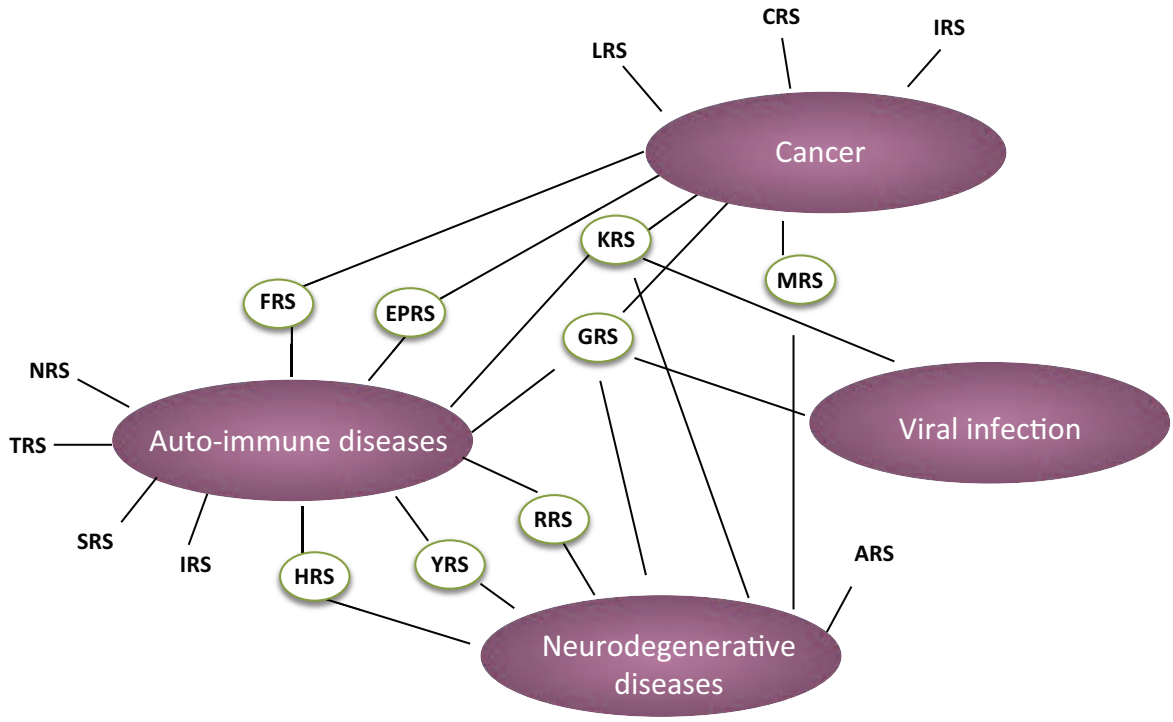

Figure 20. aaRS are implicated in different diseases

At least 16 of the 20 aaRSs are involved in different diseases, including antisynthetase syndrome, neurodegenerative diseases, viral infections and cancers. Note that GRS and KRS are implicated in all of them (adapted from Park *et al.,* 2008).

Although these diseases may be related to the non-canonical functions of aaRSs involved in the control of inflammation, angiogenesis, tumorigenesis and other important physiopathologic processes, mutations or misregulation of aaRS expression could also affect aminoacylation and thus affect cellular homeostasis and cellular development.

3.1. Antisynthetase syndrome

The first uncovered disease associated with human aaRSs was the antisynthetase syndrome. In 1983, Mathews and Bernstein identified autoantibodies targeting histidyl-tRNA sythetase (HRS) in serum from a patient with myositis (Mathews and Bernstein, 1983). This autoimmune disease is characterized by weakness and muscle loss. Since then, seven other synthetases have been identified as autoantibody targets: tryptophanyl- (TRS) (Mathews *et al.,* 1984), alanyl- (ARS) (Bunn *et al.,* 1986), isoleucyl- (IRS) (Targoff, 1990), glycyl- (GRS) (Targoff, 1990), asparaginyl- (NRS) (Hirakata *et al.,* 1999), tyrosyl- (YRS) (Targoff, 2006) and phenylalanyl- (FRS) (Betteridge *et al.,* 2007) tRNA synthetases. Clinical manifestations vary and do not clearly associate with a specific type of pathology. Nevertheless, the antisynthetase syndrome includes idiopathic inflammatory myopathies, interstitial lung diseases, arthritis, and Reynaud's phenomenon. The exact mechanism for generating these autoantibodies is still unclear. Yet, it was shown that most of the autoantigen fragments targeted in systemic autoimmune diseases are generated by the cellular protease granzyme B (Casciola-Rosen *et al.,* 1999). Since IRS, HRS and ARS are cleaved by granzyme B *in vitro*, it was proposed that aaRS autoantigenic fragments can be produced and presented on the surface of mononuclear cells to initiate the primary immune response against these self-antigens (Howard *et al.,* 2002).

3.2. Cancer

Numerous studies and experimental evidence have shown that aaRS expression and functional versatility are tightly linked with tumorigenesis (reviewed in Park *et al.,* 2008; Kim *et al.,* 2011;Yao and Fox, 2013). Because of their function as key players in protein synthesis, aaRSs are indirectly implicated in cell growth or arrest. One can imagine that unbalanced expression of a specific component of the protein synthesis machinery could lead to anarchic translation or to reduced protein synthesis. Similarly, increased aaRS concentrations could lead to tRNA mischarging, promote production of mutated proteins and, thus, contribute to cancer development. Moreover, secreted “cytokine” aaRSs are directly related to

angiogenesis and cancer cell signalling cascades, which in turn regulate cellular survival and death (Kim *et al.,* 2011).

For instance, several aaRSs show cancer related overexpression, yet the molecular processes involved in these connections are is not clear. This is the case for KRS in breast cancer (Park *et al.,* 2005), and the FRS alpha-subunit in solid lung tumors and acute phase chronic myeloid leukemia (Rodova *et al.,* 1999). The methionylation system is often involved in development of malignant cells. It was shown that: (i) overexpression of Met-tRNAi promotes oncogenic transformation (Marshall *et al.,* 2008); (ii) The catalytic activity of MRS is increased in human colorectal cancer (Kushner *et al.,* 1976); and, (iii) MRS itself is overexpressed in different other types of cancers, such as glioblastomas, malignant gliomas, sarcomas and malignant fibrous histiocytomas (Won Lee *et al.,* 2006). MRS promotes tumor progression upon C/EBP homologous protein (CHOP) overexpression. Indeed, a sequence in the MRS mRNA 3'-UTR is complementary to the CHOP mRNA 3'-UTR. Since, the CHOP 3'-UTR also contains an AU-rich element, which normally induces mRNA degradation, the association between MRS and CHOP mRNAs stabilizes the mRNA and leads to CHOP accumulation in the cell (Ubeda *et al.,* 1999). Moreover, a recent study has demonstrated that a frameshift mutation in exon 3 of the MRS mRNA leads to a premature stop codon in gastric and colorectal cancer. Again the molecular mechanism that leads to tumorigenesis is not known (Park *et al.,* 2010).

Some aaRSs act on other proteins and promote indirect tumor development. For example, KRS activates the MITF transcription factor *(see Ch.II-2.1.4)*, which is a well-known melanoma oncogene (Levy and Fisher, 2011), and QRS binds ASK-1 and suppresses its pro-apoptotic activity *(see Ch.II-2.2.2)* (Ko *et al.,* 2001). This is also the case for aaRS fragments that are secreted from different cell types to induce or inhibit angiogenesis or apoptosis. As described above *(see Ch.II-2.2.1)*, the N-terminal domain of YRS (mini-YRS) stimulates angiogenesis at low doses through transactivation of vascular endothelial growth factor receptor-2 (VEGFR2) (Greenberg *et al.,* 2008). In contrast, mini-WRS, lacking the N-terminal domain, inhibits neovascularization (Tzima and Schimmel, 2006), that is of prime necessity for tumor development and growth.

3.3. Viral infection

Eukaryotic aaRSs are also key elements of viral infection. GRS, as shown below in *Ch.II-4.2.*, binds region V of the poliovirus IRES to induce cap-independent translation (Andreev *et al.,* 2012). Another virus taking advantage of the cellular machinery to undergo its infectious cycle is HIV-1. This retrovirus uses the human $tRNA^{Lys3}$ as a primer to reverse transcribe its

RNA genome into cDNA, which is then integrated into the host cell DNA (Jiang *et al.,* 1993). The newly synthetized viral RNA genome is packaged into a nucleoprotein complex comprising the viral precursor proteins, but also the host $tRNA^{Lys3}$ (and two other isodecoders, $tRNA^{Lys1\ and\ 2}$) and KRS (Kleiman *et al.,* 2010). Guo and collaborators have shown that HIV-1 infectivity depends on the relative levels of packaged $tRNA^{Lys3}$ and that, in turn, the concentration of $tRNA^{Lys3}$ correlates with the level of packaged KRS. Indeed, knocking down cytoplasmic KRS expression proportionally reduced the amount of encapsidated $tRNA^{Lys3}$ and, subsequently, virus infectivity. In contrast, KRS overexpression in the host cell boosts HIV-1 infectivity (Guo *et al.,* 2005). Selective incorporation of $tRNA^{Lys3}$ is achieved by specific interaction between the viral Gag protein and KRS. Interestingly, a $tRNA^{Lys}$ anticodon-like element was uncovered in the viral RNA, it is located close to the primer-binding site, and is specifically recognized by KRS. It was proposed that HIV-1 uses this molecular mimicry of the $tRNA^{Lys}$ anticodon to increase efficient annealing of $tRNA^{Lys3}$to viral RNA during retrotranscription initiation (Jones *et al.,* 2013).

4. GRS alternative functions and roles in diseases

The human glycyl-tRNA synthetase that I studied during my PhD (Figure 21) is a member of the class II aaRSs. Mitochondrial and cytosolic GRS are encoded by the same gene and differ only in their N-termini by a 54 amino acid mitochondrial localization signal, which is cleaved upon GRS translocation into the mitochondria. GRS is present in the cell as a homodimer and does not belong to the MSC. Each monomer is composed of: i) the catalytic domain, with the characteristic motifs I, II and III; this domains performs glycine activation and transfer on to $tRNA^{Gly}$; and, ii) the anticodon binding domain, which specifically recognizes the $tRNA^{Gly}$ anticodon. Human GRS also contains appended modules, which could participate in cellular processes other than aminoacylation. The N-terminal WHEP domain (Figure 21) is a particular helix-turn-helix domain that appeared in metazoan GRS (as well as WRS, HRS, EPRS, TRS and MRS) and is usually involved in protein-protein interactions. The role of this WHEP domain in GRS is still unknown and further co-immunoprecipitation experiments would allow the identification of putative binding partners. Insertions I, II and III in the catalytic domain are specific to all eukaryotic GRSs. Insertion I is implicated in Ap4A synthesis (Guo *et al.,* 2009) and glycylation (along with insertion III) (Qin *et al.,* 2014). Interestingly, when analysing a multiple alignment of eukaryotic GRSs, we noticed that the last 12 C-terminal residues are present and conserved only in vertebrates.

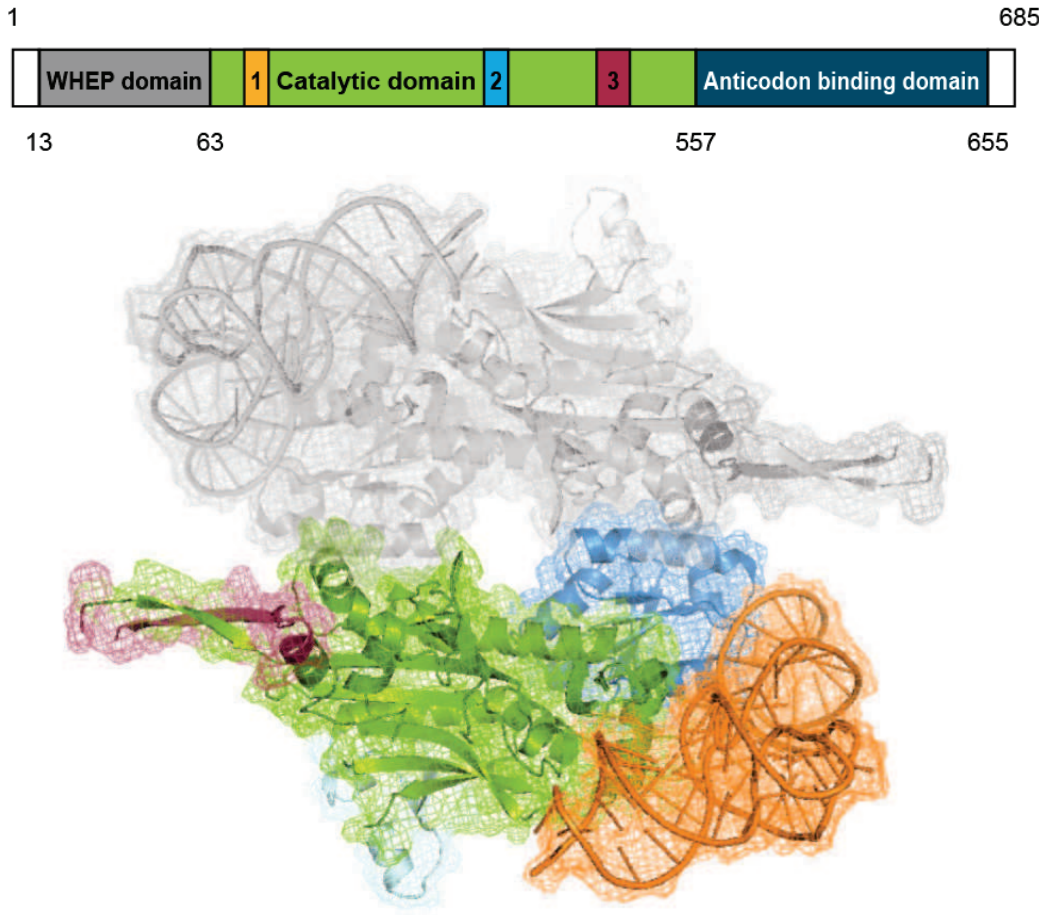

Figure 21. Human GRS organization
GRS is an homodimer. Each monomer displays an N-terminal WHEP domain (grey), a central catalytic domain (green) with insertions 1 (yellow), 2 (light blue), 3 (red), and a C-terminal anticodon-binding domain (blue). The GRS homodimer (4KR2 Protein Data Bank structure) is presented with its cognate $tRNA^{Gly}$ (orange). Note that the WHEP domain, insertion 1, part of insertion 3 and the last 10 amino acids from the C-terminus are not present on the crystal structure).

Amongst aaRSs, GRS is one of the best examples of highly regulated housekeeping proteins with several moonlighting functions. Moreover, GRS is also implicated in various diseases, such as peripheral neuropathies, cancer, and the antisynthetase syndrome. This particular aaRS was the subject of my phD work, thus I will present its roles in signalling functions and in diseases in detail. As for the particular case of GRS involvement in Charcot-Marie-Tooth disease, I will present the related data in the third part of this introduction.

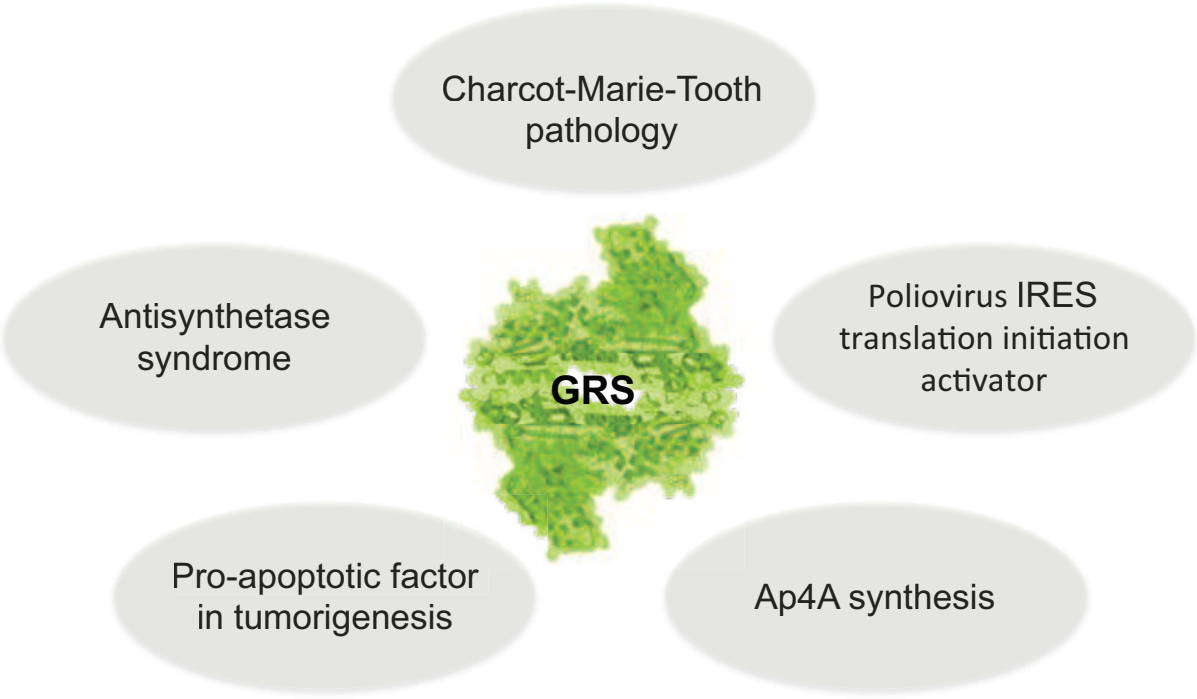

Figure 22. Non-canonical functions of GRS and its connections to in diseases
GRS is a multifunctional protein. In the cytosol it aminoacylates its cognate tRNA, synthetizes the Ap4A signalling molecule, and promotes IRES-mediated translation initiation of the poliovirus mRNA. Autoantibodies against GRS were discovered in sera of patients diagnosed with antisynthetase syndrome and breast cancer. GRS is also secreted from different tumor cells and promotes tumor suppression. Moreover, several mutations in the GRS gene lead to Charcot-Marie-Tooth peripheral neuropathy.

4.1. Ap4A synthesis

Like several other aaRSs, GRS synthesizes the extra- and intracellular signalling molecule Ap4A (Goerlich *et al.,* 1982). In general, in the absence of cognate tRNA, the aaRS.aa~AMP complex binds a second ATP molecule and generates Ap4A. However, GRS uses a different and unique mechanism, which is glycine-independent and consists of the direct condensation of two ATP molecules to generate Ap4A (Guo *et al.,* 2009) (Figure 23). This particular way of synthesizing Ap4A is uncoupled from aminoacylation and is important for cell signalling processes involving GRS. Indeed, Ap4A and other diadenosine polyphosphates were shown to trigger synaptic release in a calcium dependent manner in different neuronal types (Miras-Portugal *et al.,* 2003).

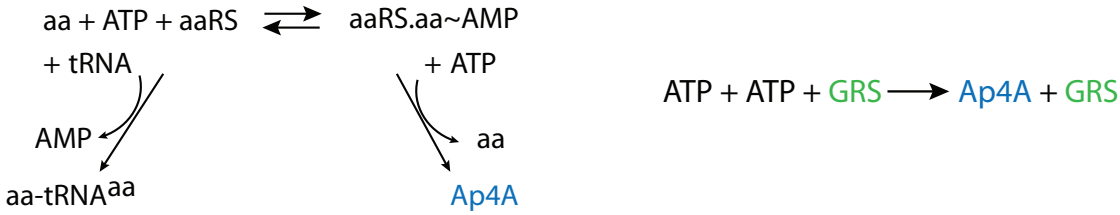

Figure 23. Ap4A synthesis
In the absence of tRNA, the aminoacyl-adenylate in the catalytic site of almost all aminacyl-tRNA synthetases is converted into Ap4A *via* an additional ATP. GRS is the only synthetase able to generate Ap4A directly from direct condensation of two ATP molecules without previous formation of a glycyl-adenylate.

4.2. IRES mediated translation activation of Poliovirus

Recently it was shown that GRS promotes IRES-dependent translation initiation of poliovirus mRNA. A particular structure in domain V of this viral IRES region displays a $tRNA^{Gly}$ anticodon stem–loop mimic. This structure recruits GRS (Figure 24), which facilitates the accommodation of the IRES domain into the ribosomal mRNA entry site and thus enhances the efficiency of translation initiation. When a mutation is introduced in the anticodon mimic, it abolishes GRS binding and decreases translation initiation drastically. Thus GRS also acts as an ITAF for group I viral IRES translation (Andreev *et al.,* 2012).

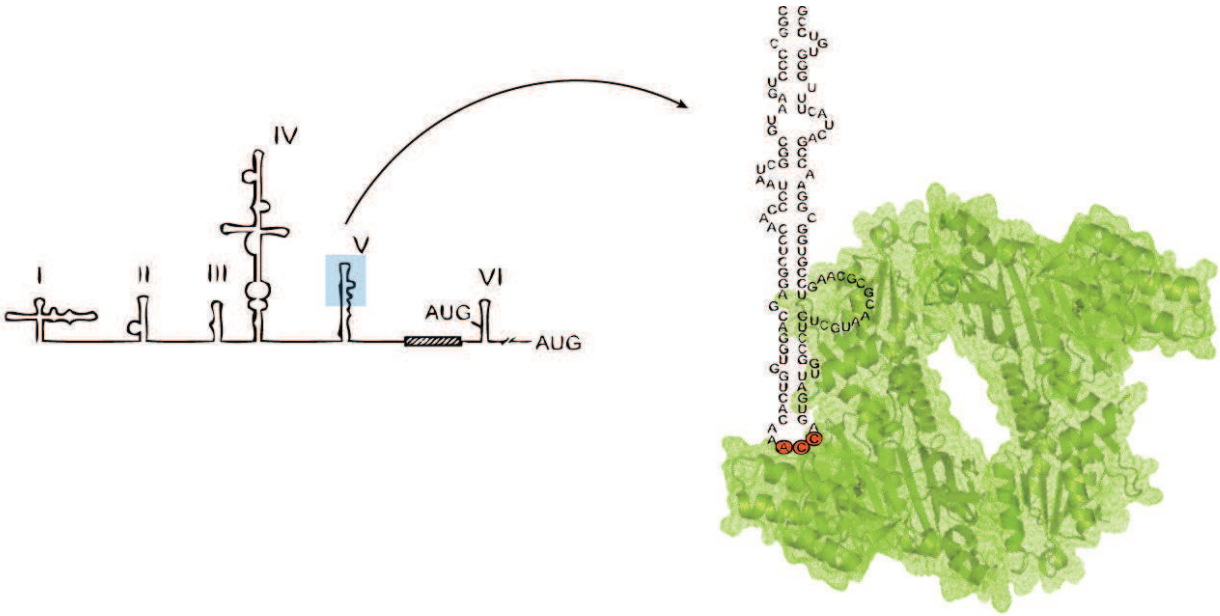

Figure 24. GRS binding to poliovirus IRES
GRS (green) recognizes and binds a $tRNA^{Gly}$ anticodon stem–loop mimic in region V of the Poliovirus IRES and stimulates its translation.

4.3. Anti-GRS syndrome

Antibodies against GRS were identified for the first time in the serum (Anti-EJ) of a patient with antisynthetase syndrome autoimmune disease (Targoff, 1990). Patients with anti-GRS antibodies present signs of inflammatory myopathy, interstitial lung disease and dermatomyositis, associated with arthritis and Raynaud's phenomenon (Targoff *et al.,* 1992; Mahler *et al.,* 2014). The reason for the generation of autoantibodies against GRS is still not clear. Indeed, extracellular GRS is also found in the sera of normal human subjects and patients with cancer and do not induce immunogenic effects (Park *et al.,* 2012).

4.4. GRS and cancer

While other aaRSs are hijacked by tumor cells to induce growth, angiogenesis or immune escape, GRS protects cells against cancer development. Indeed, recently, GRS was shown to play a role as a natural defender against tumor growth (Park *et al.,* 2012). Because autoantibodies against GRS were discovered in patients with breast cancer (Mun *et al.,* 2010), GRS was categorized as a cancer-associated autoantigen. Further investigations showed that upon serum starvation, glucose deprivation, DNA damage, or TNF-α stimulation, GRS is secreted from different types of macrophage cell lines (human U937 and mouse RAW264.7). This secretion was specifically triggered by the Fas-ligand that is released from tumor cells. Extracellular GRS binds cadherin CDH 6 on tumor cells (Figure 25), leading to the release of phosphatase 2A (PP2A), which in turn inhibits ERK kinase activated tumorigenesis. When the complex between GRS and CDH6 is hindered (antibodies against CDH 6), ERK is no longer inhibited and tumor cells develop as usual. GRS antitumor activity was also tested *in vivo* by injecting GRS into mice developing HTC116 cell-induced tumors. After a 21 day treatment, the volume of the tumors was significantly reduced. Even more strikingly, when nude mice were simultaneously injected with HTC116 tumor cells and GRS, tumors failed to grow. When considering those recent findings, modifying GRS expression or activity appears to be a promising therapeutic strategy against cancers involving highly expressed CDH6 and active ERK pathway (Park *et al.,* 2012).

How can cells coordinate the expression of the same protein, encoded by the same gene, and localize it in different cellular compartments such as the cytosol, mitochondria, neuronal projections, extracellular medium and probably endoplasmic reticulum? How can a ubiquitously expressed housekeeping protein with a key role in translation manage at the same time to: i) aminoacylate tRNAs, ii) synthetize the signalling molecule Ap4A, iii) be a cytokine, iv) be a ITAF, v) induce the synthesis of autoantibodies, and vi) when mutated,

provoke neurodegeneration? During the 4 years of my PhD work, I tried to answer some of these questions by exploring the regulation of human GRS expression.

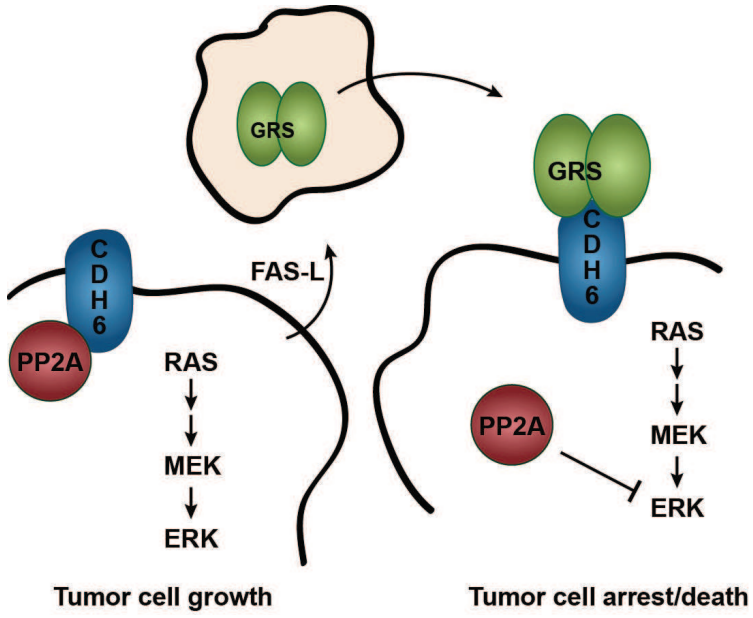

Figure 25. GRS against ERK-activated tumorigenesis
Fas-ligand induces GRS secretion from macrophage cells, triggering its binding to cadherin CDH6 on tumor cells. Upon GRS binding, phosphatase 2A (PP2A) is released and blocks ERK mediated tumor cell growth (adapted from Park *et al.,* 2012).

III. GRS AND CHARCOT-MARIE-TOOTH DISEASE

1. Charcot-Marie-Tooth

The Charcot-Marie-Tooth (CMT) disease constitutes a heterogeneous group of peripheral neuropathies, first described by Jean Charcot, Pierre Marie, and Howard Henry Tooth in 1886. CMT, also described as a hereditary motor and sensory neuropathy (HMSN), is the most common inherited neuromuscular disorder, estimated to affect 1 in 2500 individuals (Skre, 1974). The disease usually begins in childhood or adolescence and progress slowly. However, age of onset, disease course, rate of progression, and severity depend on the CMT form, the causative gene, and the mutation type. Clinical manifestations include muscular weakness and atrophy in the distal extremities, hammer toes, steppage gait, pes carvus, foot drop, absent or diminished deep-tendon reflexes and impaired sensations. It first affects the lower limbs and then extends to the upper limbs (Pareyson and Marchesi, 2009) (Figure 26).

Figure 26. Phenotypic manifestations in patients with Charcot-Marie-Tooth disease
Major CMT symptoms include muscle wasting in lower limbs (left), foot deformation (center) and atrophy of hand muscles (right) (Adapted from Pareyson and Marchesi, 2009).

No effective drug treatment for CMT disease is currently available. Treatments are only symptomatic for non-neuropathic and neuropathic pains and supportive treatments are based on rehabilitation and surgical corrections of skeletal deformities. Previous studies on CMT1A showed that high doses of ascorbic acid (vitamin C) reduced the neuropathy severity in a mouse model but unfortunately had no effect on humans (Pareyson *et al.,* 2011).

The CMT disease pathology is genetically heterogeneous. Most forms of CMT are inherited as autosomal dominant traits, however X-linked and autosomal recessive inheritances also occur. The number of CMT causing gene mutations has expanded over the past few decades, so that more than 40 CMT-associated genes have now been described (Siskind *et al.,* 2013; Rossor *et al.,* 2013). They include genes coding for proteins involved in myelin formation, compaction and maintenance, cytoskeleton formation, axonal transport, mitochondrial metabolism and, unexpectedly, six aaRS (Siskind *et al.,* 2013; Wallen and Antonellis, 2013;

Table 2. CMT classification

	Inheritance	Phenotype	Mutated genes
CMT1	AD	Usually typical clinical phenotype	*PMP22* duplication
		Uniform and diffuse motor and sensory NCV slowing (<38 m/s in upper-limb motor nerves)	*MPZ*
		Nerve biopsy: onion bulbs or other myelin abnormalities; secondary axonal degeneration	*PMP22* point mutations
			EGR2
			SIMPLE/LITAF
			NEFL
CMT2	AD or AR	Usually typical phenotype	*MFN2*
		Normal or slightly reduced NCV (>38 m/s in upper-limb motor nerves) and decreased amplitudes	*MPZ*
		Nerve biopsy: chronic axonal neuropathy usually without any specific diagnostic features	*NEFL*
			HSPB1 (HSP27)
			HSPB8 (HSP22)
			RAB7
			GARS
			GDAP1 (AD/AR)
			LMNA (AD/AR)
			MED25 (AR)
CMTX	X-linked	CMTX1: men more affected than women; motor NCV commonly intermediate in men (30–45 m/s) and in the lower range of CMT2 in women; NCV slowing can be non-uniform and asymmetrical; nerve biopsy: axonal loss and some demyelination, few onion bulbs; occasional CNS involvement	*GJB1/Cx32* *PRPS1*
		Other CMTX types: only males affected	
Intermediate CMT	AD	Mild to moderate severity	*MPZ*
		NCVs intermediate between CMT1 and CMT2 (25–45 m/s)	*DNM2*
		Pathological features of both CMT1 and CMT2	***YARS*** *(NEFL)*
dHMN	AD or AR X-linked	Pure motor involvement on clinical, electrophysiological, and morphological basis	*HSBP1*
		Preserved or mildly slowed NCVs; >38 m/s in upper-limb motor nerves; normal sensory action potential	*HSBP8*
		Sural nerve biopsy normal or near-normal	***GARS***
			BSCL2
			DCTN1 *(IGHMBP2)*

Classification of Charcot-Marie-Tooth neuropathy subtypes, based on electrophysiological manifestations and mode of inheritance. **CMT1** and **CMT2**=Charcot-Marie-Tooth type 1 and 2; **dHMN**=distal hereditary motor neuronopathy; **AD**=autosomal dominant; **AR**=autosomal recessive; **NCV**=nerve-conduction velocity; **CNS**=central nervous system. Genes: **PMP22**=peripheral myelin protein 22; **MPZ**=myelin protein zero; **EGR2**=early-growth-response 2; **SIMPLE/LITAF**=small integral membrane protein of lysosome/late endosome; lipopolysaccharide-induced tumor necrosis factor-alpha factor; **NEFL**=neurofilament light chain; **MFN2**=mitofusin 2; **HSPB1**/HSP27=heat shock 27-kDa protein 1; **HSPB8**/HSP22=heat shock 22-kDa protein 8; **RAB7**=small GTPase late endosomal protein 7; **GARS**=glycyl-tRNA synthetase; **GDAP1**=ganglioside-induced differentiation-associated protein 1; **LMNA**=lamin A/C nuclear envelope protein; **MED25**=mediator of RNA polymerase II transcription, subunit 25; **GJB1**/Cx32=gap junction B1/connexin 32; **PRPS1**=phosphoribosylpyrophosphate synthetase 1; **DNM2**=dynamin 2; **YARS**=tyrosyl-tRNA synthetase; **BSCL2**=Berardinelli-Seip congenital lipodystrophy type 2; **DCTN1**=dynactin motor neuronopathy. (Adapted from Pareyson and Marchesi, 2009).

Gonzalez *et al.,* 2013), (Table 2). In addition, CMT associated mutant proteins are expressed in different cellular types, such as developing and myelinating Schwann cells or neuronal axons.

Despite their genetic heterogeneities, Charcot-Marie-Tooth peripheral neuropathies share a common clinical phenotype: they are characterized by the progressive impairment of peripheral nerves, muscle and touch sensation loss. The classification of CMT is based on nerve pathology and nerve-conduction studies (Table 2). In CMT type 1, patients exhibit decreased motor nerve conductance velocities (MNCVs) (less than 35 m/s) with demyelinating axons. On the contrary, CMT type 2 patients exhibit normal MNCVs (more than 45 m/s) and no demyelination but have decreased amplitudes of motor and sensory nerve responses and axonal loss. Some intermediate forms of CMT (with MNCVs raging from 35 to 45 m/s) have been also described, (Skre, 1974; Siskind *et al.,* 2013; Pareyson and Marchesi, 2009).

In 2003, Antonellis and colleagues described for the first time mutations in the gene encoding GRS *(GARS)* as the cause of the neurodegenerative disorders Charcot-Marie-Tooth type 2D (CMT2D) and distal spinal muscular atrophy type V (dSMA-V) (Antonellis *et al.,* 2003). Later, Jordanova and collaborators identified mutations in the tyrosyl-tRNA synthetase (YRS) gene *(YARS)* causing Dominant Intermediate CMT neuropathy (DI-CMTC) (Jordanova *et al.,* 2006). Since then, more CMT inducing mutations have been identified in 4 other genes coding aaRSs: alanyl- (*AARS*; CMT type 2N) (Latour *et al.,* 2010), lysyl- (*KARS*; CMT intermediate recessive type B) (McLaughlin *et al.,* 2010), hytidyl- (*HARS*) (Vester *et al.,* 2013) and methionyl- (*MARS*) (Gonzalez *et al.,* 2013) tRNA synthetases. These findings suggest that these aaRSs could play specific roles in axon development and function. Numerous studies, most of them concerning GRS and YRS, have been performed to assign the importance of these CMT inducing mutations. They include structural and functional studies, as well as development of animal models. In this chapter, I will describe GRS mutations implicated in the CMT pathology and, when possible, discuss these data in light of other mutated aaRSs inducing CMT, especially YRS mutants.

2. GRS mutants in CMT2D and dSMA-V

As previously described (*see Ch.II-4.*), human GRS is a homodimer, where each monomer is composed of an N-terminal WHEP domain, a catalytic domain and a C-terminal anticodon-binding domain. The 13 reported CMT-causing mutations are all dominant mutations. They introduce single amino acid changes that are spread throughout the GRS primary sequence

(Figure 27) (Motley at al., 2010). In general, mutations are classified as gain of function or loss of function. Gain of function means that the mutant protein has acquired a new function that is "toxic" to the cell (such as the capacity to interact with new partners (proteins, RNA or DNA)), and induces or disturbs associated cellular processes. In contrast, loss-of-function implies that the mutant protein is no longer active, or cannot interact anymore with its usual partner(s). As higher eukaryotes are heterozygous, the presence of mutations on one allele only partially impairs the functionality of the protein, since the second allele can still produce a functional protein. However, the production of only 50% functional protein is not necessarily sufficient to properly accomplish its roles in the cell. In this case, the mutation leads to haploinsufficiency. In some cases, the mutated protein can interfere with the wild-type protein and provoke a dominant negative effect (see below).

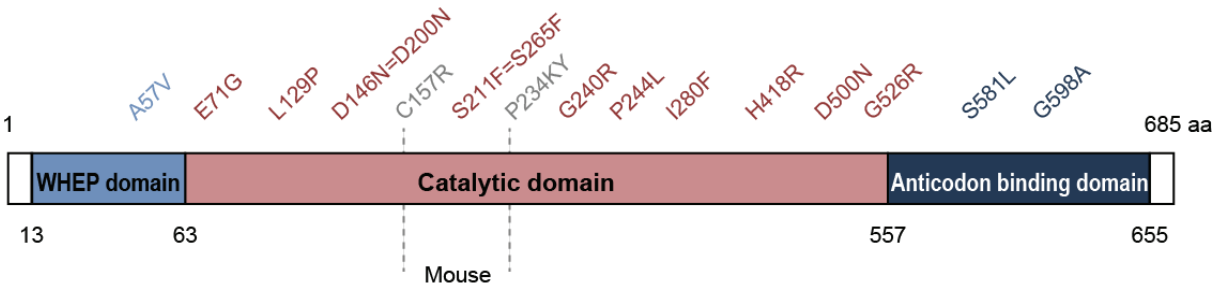

Figure 27. Domain localization of CMT mutations in GRS
The cytosolic GRS monomer (685 aa) displays a WHEP domain, a catalytic domain and an anticodon-binding domain. The thirteen known GRS mutations present in human CMT patients are indicated in blue, brow or grey (depending on their domain localization). Two mutations that were characterized in mouse models (C157R and P234KY) are indicated in grey. Notice that mutants D200N and S265F (identified by Lee *et al.,* 2012a) were initially mapped to mitochondrial GRS; the corresponding residues on the shorter cytosolic enzyme are D146N and S211F, respectively (Adapted from Motley *et al.,* 2010).

2.1. Effect of CMT mutations on GRS aminoacylation activity

Several *in vitro* and *in vivo* studies were performed to characterize GRS CMT mutants aiming to uncover a common molecular mechanism responsible for the CMT pathology. As the canonical function of this housekeeping enzyme is the charging of glycine onto its cognate $tRNA^{Gly}$, it was proposed that GRS CMT causing mutations would affect glycylation and thus impair protein synthesis. Aminoacylation activities of mutant GRSs were thus tested *in vitro* and compared to the activity of the wild-type GRS. Three of the tested mutants, L129P, G240R, G526R, were inactive (Table 3), probably because the mutations affect highly concerved residues in the catalytic domain (Nangle *et al.,* 2007). However, E71G, P234KY,

D500N and S581L GRS mutants were still able to aminoacylate $tRNA^{Gly}$ with the same catalytic constant as the wild-type enzyme.

Table 3. Structural and functional data on aminacyl-tRNA synthetase mutants in CMT

Mutants	AARS domains	Aminoacy-lation	Yeast comple-mentation essay	Dimeri-zation	Conforma-tional opening
GRS					
A57V	N-terminal WHEP	NA	NA	NA	NA
E71G	Catalytic	wt	normal	NA	NA
L129P	Catalytic	inactive	reduced	-	Yes
D146N	Catalytic	NA	NA	NA	NA
S211F	Catalytic	NA	NA	NA	NA
P234KY	Catalytic	wt	NA	wt	NA
G240R	Catalytic	inactive	normal	-	Yes
I280F	Catalytic	NA	NA	NA	NA
H418R	Catalytic	NA	reduced	wt	NA
D500N	Catalytic	wt	NA	+++	NA
G526R	Catalytic	inactive	reduced	+++	Yes
S581L	Anticodon Binding	wt	NA	+++	Yes
G598A	Anticodon Binding	NA	normal	NA	Yes
YRS					
G41R	Catalytic	residual	reduced	wt	NA
153 -156 ΔVKQV	Catalytic	inactive	NA	NA	NA
E196K	Catalytic	normal	normal	wt	NA
ARS					
N71Y	Catalytic	inactive	not viable	NA	NA
R329H	Anticodon Binding	inactive	not viable	NA	NA
D893N	Editing	NA	NA	NA	NA
KRS					
L137H	Anticodon Binding	inactive	normal	NA	NA
Y173SerfsX7.	Anticodon Binding	NA	NA	NA	NA
HRS					
R137Q	Catalytic	NA	not vial	NA	NA

Peripheral neuropathy causing mutations in 5 aminoacyl-tRNA syntetases: GRS, YRS, ARS, KRS and HRS. Distribution of each mutation in the corresponding aaRS domain is indicated. Notice that mutation Y173SerfsX7 is a frame-shift mutation hindering the synthesis of KRS. Y173SerfsX7 and L137H were found simultaneously in the same patient. *In vitro* aminoacylation assays, yeast complementation, dimer formation, structural conformation opening and localization in neurons were evaluated compared to the wild type of the corresponding synthetase. NA=Not Assigned. (Adapted from Wallen and Antonellis, 2013 and based on experimental data from: **(GRS)** Antonellis *et al.,* 2006; Nangle *et al.,* 2007; Stum *et al.,* 2011; He *et al.,* 2011; Chihara *et al.,* 2007; **(YRS)** Jordanova *et al.,* 2006; Storkebaum rt al., 2009; Froelich and First, 2011; **(ARS)** Latour *et al.,* 2010; McLaughlin *et al.,* 2012; **(KRS)** McLaughlin *et al.,* 2012; **(HRS)**; Vester *et al.,* 2013)

Based on these data, general loss of aminoacylation activity cannot be responsible for the CMT pathology, since most of the GRS mutants are fully active.

Evaluation of GRS activity was also performed in yeast complementation assays (Table 3). In these experiments, yeast viability was evaluated when the gene coding for the endogenous GRS was deleted and replaced by a selection of mutated yeast GRSs carrying the corresponding human CMT mutations. Yeast expressing human E71G, G598A and the mouse P234KY GRS mutants did not show any growth defect compared to the wild-type GRS (Stum *et al.,* 2011). Logically, the L129P and G526R mutants, with impaired aminoacylation activities *in vitro*, caused growth defects *in vivo*. However, G240R, which was also inactive in *in vitro* aminoacylation assays, did not affect yeast viability or growth (Antonellis *et al.,* 2006), indicating that *in vitro* assays and yeast complementation experiments can lead to divergent results.

This was also the case for YRS mutations causing DI-CMTC, where similar discrepancies between both approaches were observed (Jordanova *et al.,* 2006; Storkebaum *et al.,* 2009; Froelich and First, 2011) (Table 3).

Only the CMT causing mutants N71Y and R329H in ARS showed coherent results where complete loss of aminoacylation led to unviability in yeast complementation assays (McLaughlin *et al.,* 2012).

Even if aaRSs are expressed ubiquitously, only peripheral nerves are affected in CMT patients. Thus, one cannot completely exclude that, in the particular context of the neuronal environment and especially in long axons, GRS and YRS aminoacylation activities would behave differently than in *in vitro* assays. Likewise, the yeast model does not match the complexity of neuron's biology and the data obtained in these experiment may not be relevant.

2.2. Effect of CMT mutations on GRS dimerization

Another possible way to induce CMT pathologies is in a dominant negative manner, meaning that a mutant enzyme can modify the behavior of the WT enzyme. Because all aaRSs causing CMT are dimers (GRS, YRS, KRS and HRS) or tetramers (ARS), the association of one mutated monomer with a wild-type monomer could change the polymer "performance" (activity, localization, interactions, etc.). Moreover, mapping of CMT causing mutations on the human GRS crystal structure (Nangle *et al.,* 2007; Lee *et al.,* 2012a) showed that most of the mutations are located close to or directly at the dimer formation interface (Figure 28).

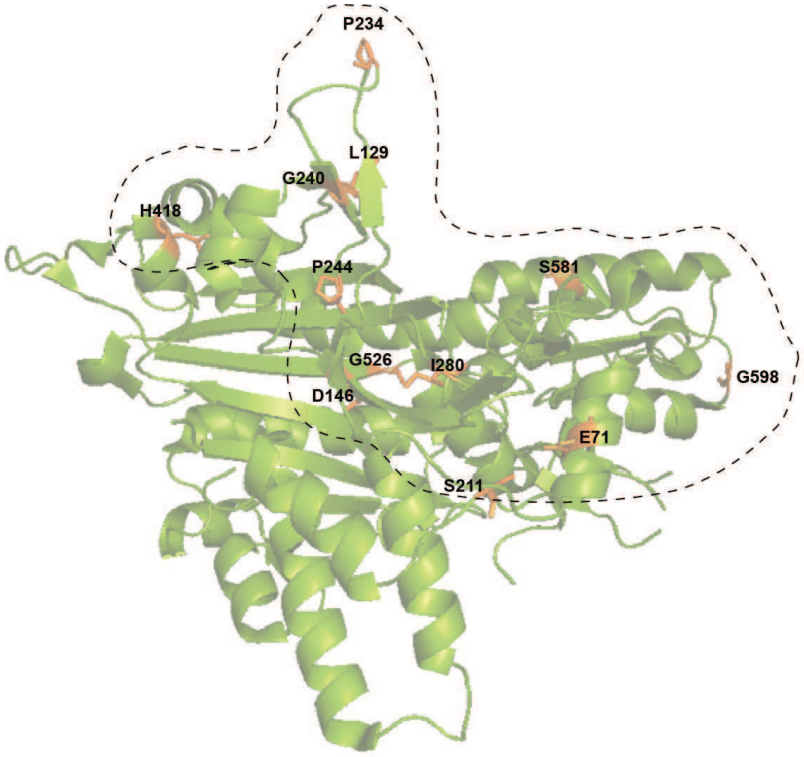

Figure 28. Mapping of GRS CMT causing mutations
Twelve GRS mutations are displayed on the crystal structure (Protein Data Banck 2PME) of the monomeric GRS. The upper face of the monomer displays the dimer interface (dashed line) (Adapted from Nangle *et al.,* 2007; Lee *et al.,* 2012a).

In order to evaluate dimer formation, Nangle and collaborators expressed 7 GRS mutants in transfected mouse neuroblastoma N2a cells and performed pull down assays (Table 3). In these experiments, they examined the capacity of the mutated GRS monomer to dimerize with the endogenous wild-type GRS monomer (Nangle *et al.,* 2007). The mouse P234KY GRS was the only mutant for which neither dimerization capacity nor aminoacylation activity were affected. Two other mutants, D500N and S581L, exhibited stronger capacities to dimerize than WT GRS, a situation that does not affect their respective aminoacylation activities *in vitro*. Likewise, the absence of any evidence for dimer formation for the L129P and G240R mutants would, somehow, explain why these mutants are inactive *in vitro*. However, these data showed again some contradictions. Indeed, H418R conserved its WT ability to dimerize, but did not support efficient yeast growth. Similarly, G526R has enhanced dimerization ability but does not perform glycylation *in vitro*. Though the crystal structure of this GRS mutant was solved, it didn't show any significant structural differences compared to the wild-type enzyme (Xie *et al.,* 2007). As well, the crystal structure of the S581L mutant confirmed that the ability to form more stable dimers did not lead to a different interaction pattern between monomers (Cader *et al.,* 2007) than in the WT enzyme.

A complementary approach used the capacity of proteins to incorporate deuterium (H/D exchange) in their exposed regions. When coupled with mass spectrometry, this technique allowed comparing the flexibility of WT and CMT causing mutant (L129P, G240R, G526R, S581L, G598A) GRSs. In all 5 mutants, 8 regions located predominantly at the dimer interface were identified as hotspot for conformational changes (He *et al.,* 2011). It was suggested that conformational opening of the mutant GRS structure could promote CMT-associated pathological interactions.

Although loss-of-function mechanisms could possibly explain the pathogenesis of CMT, it seems that the "lost function" is still unidentified. Indeed, altogether, *in vitro* aminoacylation, yeast complementation assays and structural studies showed that there is no strict correlation between CMT mutations and GRS canonical functionality (Table 3). However, it has been proposed that CMT-causing mutations in GRS may affect Ap4A synthesis (Guo *et al.,* 2009). It is interesting to notice that even if KRS was described as the major contributor to Ap4A synthesis in the cell, GRS, ARS, HRS and MRS are also able to synthetize this molecule. Ap4A is an important signaling molecule, which has been detected in neurons and acts to trigger the release of neurotransmitters such as glutamate, GABA or acetylcholine (Klishin *et al.,* 1994; Miller, 1998). Yet, none of the aaRS CMT causing mutants were evaluated in their ability to generate Ap4A *in vitro* or *in vivo*.

2.3. Neuronal expression of GRS CMT causing mutants

2.3.1. Granules or not granules: that is the question?

As loss of aminoacylation activity *in vitro* failed to explain peripheral nerve axonal degeneration caused by GRS mutations, several independent studies have also investigated the localization of mutated GRSs in neuronal cells. A first investigation in normal human tissues showed that GRS is expressed not only in the cellular body but also in neuronal projections of the spinal cord and sural neurons (a sensory nerve located in the leg) (Antonellis *et al.,* 2006). Moreover, GRS showed a granular distribution in axons of the ventral horn, dorsal horn, ventral root, dorsal root, and sural nerve, indicating that this particular distribution is characteristic for both sensory and motoneurons (Figure 29).

Granule formation was also observed in cultured cells with (i) endogenous GRS in human SH-SY5Y neuroblastoma cells and (ii) GFP-tagged GRSs in mouse motoneuron cells (MN-1) (Antonellis *et al.,* 2006). These GRS granules do not match any known cellular structure, such as the mitochondria, Golgi apparatus or cytoskeleton. Interestingly, some of them were localized in the nucleolus, suggesting either an artifact from antibody staining or a new differentiated mouse motoneuron cells, they were still localized in neuronal projections but

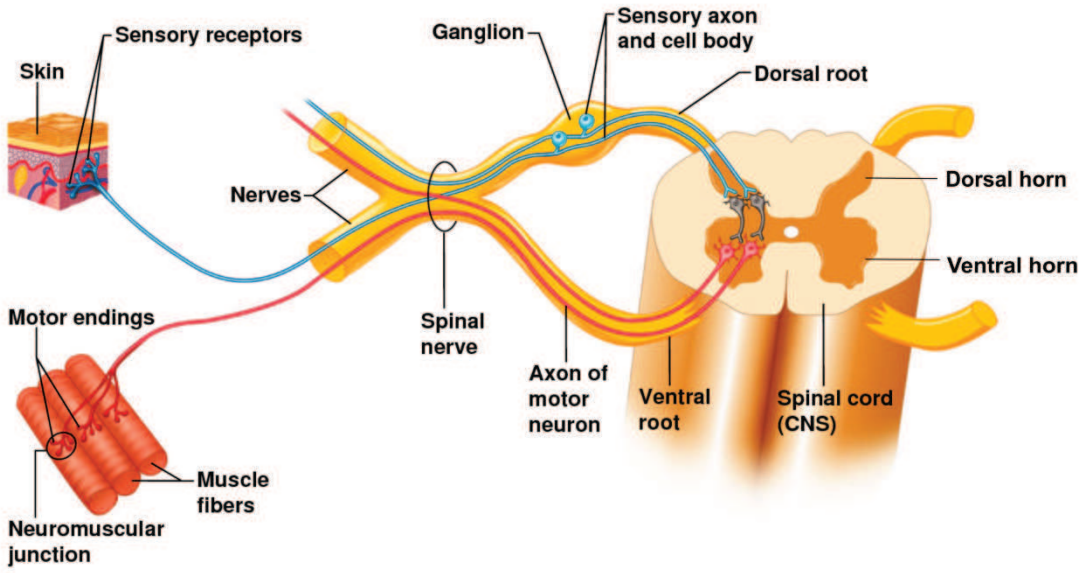

Figure 29. Spinal cord and peripheral neuron organization
The dorsal part of the spinal cord conveys sensory information from the body to the brain. Cell bodies of sensory neurons are located in the dorsal ganglion and their axons are in the dorsal root, with synaptic signals arriving in the dorsal horn. The ventral part of the spinal cord transmits signals from the brain to the muscles. Motoneuron cell bodies are located in the ventral horn with projecting axons in the ventral root. (Adapted from Quick Books Docstoc)

exhibited a diffused localization (Antonellis *et al.,* 2006). It was proposed that proper localization of GRS within granules and subsequent transport of these granules to the cell periphery are essential for maintaining axonal health and would reveal a special requirement for GRS in peripheral nerve cell axons (Table 4).

In a second study, 7 GRS mutants (L129P, P234KY, G240R, H418R, D500N, G526R and S581L) were transfected into differentiated mouse neuroblastoma cells (N2a) and their respective localizations were investigated (Table 4) (Nangle *et al.,* 2007). In this study, WT and mutated GRSs were fused to a C-terminal V5-tag in order to differentiate transfected enzymes from the endogenous GRS. While the WT GRS localized to the cell body and neurite projections, all the mutants were defective in their localization to sprouting neurites. The authors stated that significant variability accured from cell to cell and from mutant to mutant, indicating that, different mutations have different reasons for protein mislocalization. However, in this study, neither endogenous GRS, nor transfected WT GRS presented the granular profile observed previously by Antonellis and collaborators (Antonellis *et al.,* 2006).

Table 4. Neuronal expression of aaRS CMT causing mutants

Mutants	Granule formation	Neurite projection localization	Cell type	Illustration	Ref
GRS					
WT	Yes	Yes	MN-1	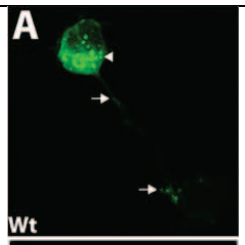	Antonellis *et al.*, 2006
WT	?	Yes	N2a	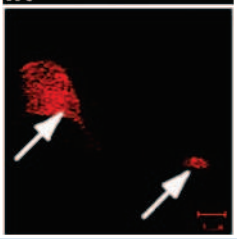	Nangle *et al.*, 2007
E71G	Yes	Not shown	MN-1	Not shown	Antonellis *et al.*, 2006
L129P	No	No	MN-1	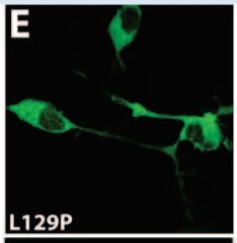	Antonellis *et al.*, 2006
L129P	?	No	N2a	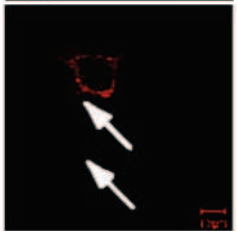	Nangle *et al.*, 2007
P234KY	?	No	N2a		Nangle *et al.*, 2007
G240R	No	No	MN-1	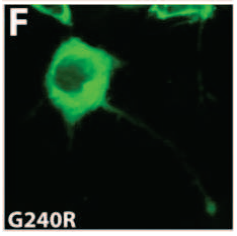	Antonellis *et al.*, 2006
G240R	?	No	N2a	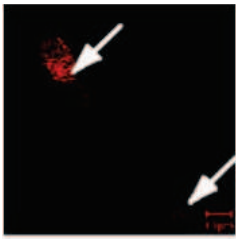	Nangle *et al.*, 2007

H418R	No	?	MN-1	Not shown	Antonellis *et al.,* 2006
H418R	?	No	N2a	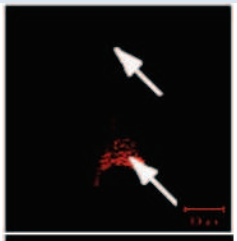	Nangle *et al.,* 2007
D500N	?	No	N2a	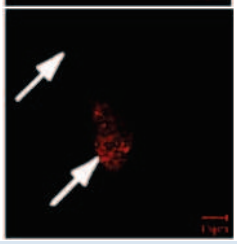	Nangle *et al.,* 2007
G526R	Yes	?	MN-1	Not shown	Antonellis *et al.,* 2006
G526R	?	No	N2a	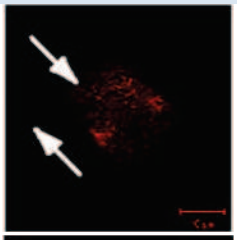	Nangle *et al.,* 2007
S581L	?	No	N2a	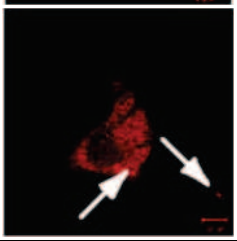	Nangle *et al.,* 2007
YRS					
WT	Yes	Yes	N2a	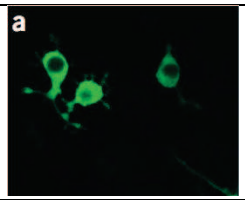	Jordanova *et al.,* 2006
G41R	No	No	N2a	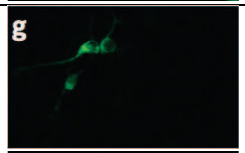	Jordanova *et al.,* 2006
E196K	No	No	N2a	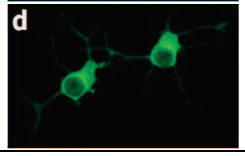	Jordanova *et al.,* 2006

Different GRS and YRS mutants were tested for their ability to localize in neurite projections and for granules formation (or tear drop effect for YRS). In Antonellis *et al.,* 2006, GRS was fused to a C-terminal GFP (green) and transfected in mouse motoneurons (MN-1). In Nangle *et al.,* 2007, GRS was fused to a C-terminal V5-tag (detected in red) and transfected in mouse neuroblastoma cells (N2a). In Jordanova *et al.,* 2006, YRS was fused to GFP (green) (N-terminal) and transfected in mouse neuroblastoma cells (N2a).

GRS is not the only aaRS that localizes in neurite projections. WT YRS also localizes in granular structures in the growth cone, branch points and the most distal part of projecting neurites in differentiated N2a and SH-SY5Y cell types (Jordanova *et al.,* 2006). This granular distribution called the 'teardrop effect' was specific to YRS and was not observed with arginyl-(RRS) or tryptophanyl- (WRS) tRNA synthetases. Moreover, when two YRS mutants (G41R and E196K) causing DI-CMTC were expressed in differentiated N2a cells, they exhibited diffuse localization and reduced teardrop effects (Table 4), as was observed with GRS CMT causing mutants. These findings suggest that both synthetases are involved in some non-canonical function(s) specific to neuronal endings and that this alternative function is certainly related to the protein specific sub-cellular localization.

2.3.2. Animal models for aaRSs and CMT

Since then several animal models expressing mutant GRSs that cause neuropathy were used to characterize GRS neuronal specificity *in vivo*.

2.3.2.1. Mouse models

* GRS point mutations

The first mouse model, $Gars^{Nmf249/+}$, presents a spontaneous mutation corresponding to the P234KY residues of human GARS gene. It showed that both sensory and motor neurons are affected, like in human CMT-2D, with abnormal neuromuscular junction morphology and impaired transmission, reduced nerve conduction velocities and a loss of large diameter peripheral axons, without defects in myelination (Seburn *et al.,* 2006, Stum *et al.,* 2011).

The second mutant GRS model, $GRS^{C201R/+}$, presented only signs of mild neuropathy. In this case, when histological examination didn't show any abnormality in the spinal cord, the diameter of large axons from the sciatic nerve was 50% decreased (Achilli *et al.,* 2009).

Further investigations into the role that mutant GRSs play in the mechanism leading to peripheral neurodegeneration revealed that $Gars^{Nmf249/+}$ and $GRS^{C201R/+}$ mice display a persistent defect in neuromuscular junction maturation that precedes the progressive, age-dependent degeneration. Denervation in mice was observed only in limb neurons and not in proximal abdominal nerves (Sleigh *et al.,* 2014). This observation is consistent with human CMT patients, where only distal nerves are affected.

* GRS deletion

A transgenic mouse, $Gars^{XM256/+}$, lacking a complete copy of the GARS gene (null allele) presented no loss-of-function and showed no evidence of peripheral neuron dysfunction. Since this mutant mouse still expressed 50% of GRS mRNAs, it indicates that a simple

reduction of aminoacylation or other GRS activity is not the cause of CMT (Seburn *et al.,* 2006).

* GRS overexpression

Another transgenic mouse overexpressing wild-type GRS was designed (Motley *et al.,* 2011). They crossed this mouse with either $Gars^{Nmf249/+}$ or $GRS^{C201R/+}$ mutants, but didn't observe any decrease in neuropathological symptoms. Indeed, despite WT GRS overexpression, these mice still exhibited motor and sensory axon loss as well as neuromuscular junction impairment. Moreover, the production of a heterozygous $Gars^{Nmf249/C201R}$ increased the severity of the neuropathy symptoms. These experiments led to two conclusions: GRS associated peripheral neuropathy (i) is not due to GRS loss-of-function and (ii) is caused by a dose-dependent gain of function that is not rescued by over-expression of the functional wild-type protein (at least in mutant mice).

* Tissue specific expression of GRS mutants

Recently, adenovirus expressing the human G240R mutated GRS was injected directly into the sciatic nerve of wild-type mice (Seo *et al.,* 2014). Seven days after injection, the mutant GRS was found in sensory and motoneuron cellular bodies, but not in axons (contrary to WT GRS). Even if the mechanism is not yet elucidated, it is clear that the G240R mutation in human GRS is sufficient to hinder GRS localization in mouse peripheral axons. Unfortunately, due to restrictive experimental timing, it was not possible to observe if this impaired distribution could lead to axonal degeneration, or determine if the mutant GRS had to be already present at the early development stages to induce neuropathy.

2.3.2.2. Drosophila models

Several *Drosophila melanogaster* models were designed to characterize YRS mutants inducing DI-CMTC neuropathy and GRS mutants inducing CMT2D (Storkebaum *et al.,* 2009; Ermanoska *et al.,* 2014). Mutated YRSs (G41R, E196K and ΔVKQV) were expressed ubiquitously or specifically in neurons, and in both cases, they impaired motoneuron performance progressively in an age-dependent manner.

In contrast, mutated GRSs, G240R and P234KY, were toxic when expressed ubiquitously and induced lethality at early stages of *Drosophila* development. In the same way, when overexpression of these mutants was specifically induced in neurons, they showed neurotoxicity. These data matched the results observed in the corresponding mouse models, with a more severe phenotype associated with the P234KY mutation (Ermanoska *et al.,* 2014).

Despite progress made in characterizing aaRSs mutants, so far the reason why these mutations affect only distal neurons remains to be elucidated. Especially, the role of both GRS and YRS in the pathological mechanism leading to related peripheral neuropathies remain puzzling. Further experiments aiming to characterize the specific role that these multifunctional proteins play in neurons and particularly in axons should help to find a common molecular mechanism. Interestingly, a recent study revealed the existence of two common genetic modifiers for GRS and YRS mutants in *Drosophila*. These genes specifically enhance the rough eye phenotype that YRS E196K and GRS P234KY induce when expressed in *Drosophila* retina. However, the associated molecular function is still unknown (Ermanoska *et al.,* 2014). These new data lead the way towards the necessity to determine GRS and YRS neuronal interactomes. This will be helpful to explore aaRS interactions with specific neuronal partners and understand potential gain or loss of pathological functions of mutated enzymes either in patients or animal models.

IV. GOALS OF THE THESIS

During the last decade, numerous non-translational functions have been assigned to different aminoacyl-tRNA synthetases involved in several cellular pathways, regulatory mechanisms and diseases. The human glycyl-tRNA synthetase GRS is a perfect example of such a multifunctional protein. In addition to aminoacylation, GRS synthesizes the Ap4A signaling molecule (Guo *et al.,* 2009), participates in the defense against ERK-induced tumorigenesis (Park *et al.,* 2012), and stimulates translation initiation of the poliovirus genome by binding its IRES sequence (Andreev *et al.,* 2012). In addition, at least 13 mutations in the GRS gene have been reported to cause a dominant axonal form of the Charcot-Marie-Tooth (CMT) type 2D as well as spinal muscular atrophy type V (SMA-V) (Antonellis et al, 2003; Antonellis et al, 2006 rev: Motley *et al.,* 2010; Wallen and Antonellis 2013; Yao and Fox 2013, Lee *et al.,* 2012 a).

Though GRS activity is required in all cells, the CMT-associated mutations affect only the peripheral nervous system (Antonellis et al, 2006). These findings suggest that this tRNA charging enzyme, in addition to its canonical role in translation, may have another particular function in neurons and plays a key role in maintaining peripheral axons. However, the links between GRS mutations, tissue-specificity, and the pathological mechanism remain unclear.

Most of the research devoted to human GRS concerns the cytosolic enzyme and particularly its structural and functional characterization in the context of the CMT pathological mutations. We decided to use a different and complementary approach to explore GRS through its coding mRNA. Indeed, the goal of my project was to understand the particular expression of the human GRS in neurons, and to try to identify a possible neuron-specific non-canonical function affected by GRS CMT2D causing mutations.

First, we concentrated our research on the basic expression of the human GRS and tried to answer the following questions:

- How are the mitochondrial and cytosolic enzymes generated from the same gene?
- How is this expression regulated?

We brought answers to these questions in the article: **Elaborate uORF/IRES features control expression and localization of human glycyl-tRNA synthetase.**

Then we tried to further explore the specific expression and accumulation of GRS in neuronal granules and to find a connection with the CMT pathology.

I. REGULATION OF HUMAN GLYCYL-tRNA SYNTHETASE EXPRESSION

1. Approach and main findings

In order to understand how the two human GRSs are expressed and regulated, we first used RACE PCR to identify the corresponding mRNA. We discovered two isoforms that differed in their 5'-UTR but had no difference in the main coding sequence or the 3'-UTR.

The longer mRNA (mRNA1) displays three initiation codons that we named AUG_0, AUG_{mito} and AUG_{cyto}. AUG_0 is not in frame with the GRS ORF and would initiate the translation of an upstream reading frame encoding a 32 amino-acid peptide. AUG_{mito} and AUG_{cyto} initiate translation of the mitochondrial GRS precursor and the cytosolic form of GRS, respectively. Immunolocalization and *in vitro* translation studies showed that mRNA1 expresses essentially the cytosolic GRS, while the translation of the small uORF (whose stop codon is located between AUG_{mito} and AUG_{cyto}) hinders the synthesis of the mitochondrial enzyme.

The shorter mRNA (mRNA2) contains only the AUG_{mito} and AUG_{cyto} start codons. Even though AUG_{mito} is only 20 nt away from the very 5'-end of the mRNA, this isoform allows efficient synthesis of both cytosolic and mitochondrial GRSs.

Moreover, mRNA1 contains an Internal Ribosome Entry Site (IRES) and can be expressed in a cap-independent manner. We showed that this GRS IRES is functional under normal cellular conditions as well as during different cell stresses such as starvation, glucose deprivation, hypoxia, or inhibition of the mTOR pathway.

Interestingly, we also observed a particular GRS localization pattern when it was expressed from mRNA1: GRS organizes in a network structure. After removal of free cytosolic proteins, we found that GRS colocalizes with the endoplasmic reticulum (ER) bound ribosomes. Even if there is no evident N-terminal ER localization signal, we propose that this localization is guided either by some zip code motif in the mRNA1 5'-UTR sequence or by the 32 amino acid peptide encoded by the uORF.

Taken together our findings show that mitochondrial, cytosolic, but also ER-bound, GRS expression are highly regulated processes, involving two mRNA isoforms, three initiation codons, an uORF as well as an IRES. This complex regulation could potentially explain the moonlighting activities of GRS, like its secreted protective anti-tumor cytokine action, its peculiar expression in peripheral neurons, and its implication in CMT disease.

2. Elaborate uORF/IRES features control expression and localization of human glycyl-tRNA synthetase

Running head: Control of human glycyl-tRNA synthetase expression

Jana Alexandrova, Caroline Paulus, Joëlle Rudinger-Thirion, Fabrice Jossinet and Magali Frugier*

Architecture et Réactivité de l'ARN, Université de Strasbourg, CNRS, IBMC, 15 rue René Descartes, 67084 Strasbourg Cedex, France

* To whom correspondence should be addressed. E-mail: M.Frugier@ibmc-cnrs.unistra.fr

Abstract

The canonical activity of Glycyl-tRNA synthetase (GRS) is to charge glycine onto its cognate tRNAs. However, outside translation, GRS was also shown to participate in many other functions, amongst which its involvement in peripheral axonal degeneration (Charcot-Marie Tooth disease) is still not understood. A single gene encodes both the cytosolic and mitochondrial forms of GRS but we identified two mRNA isoforms. Using immunolocalization assays, *in vitro* translation assays, and bicistronic constructs, we provide experimental evidence that one of these mRNAs tightly controls expression and localization of human GRS. An intricate regulatory domain was found in its 5'-UTR which displays a functional IRES and a uORF. Together, both elements hinder the synthesis of the mitochondrial GRS and target the translation of the cytosolic enzyme to ER-bound ribosomes. This post-transcriptional regulatory mechanism is conserved in mammals. This finding reveals a complex picture of GRS translation and localization. In this context, we discuss how human GRS expression could influence its moonlighting activities of GRS and its involvement in diseases.

Endoplasmic reticulum localization/Glycyl-tRNA synthetase/IRES/post-transcriptional regulation /uORF

INTRODUCTION

Human Glycyl-tRNA synthetase (GRS) is an essential component of the translation apparatus. GRS is ubiquitously expressed and plays a central role in protein synthesis by catalyzing the attachment of glycine to cognate transfer RNAs (tRNAs). However, GRS, like other mammalian aminoacyl-tRNA synthetases (aaRS) [1-3] is involved in functions beyond translation [4]. These alternative functions were identified mainly through the discovery of several diseases linked to mutations in the corresponding gene or to the presence of antibodies against extracellular GRS. In human, at least 13 dominant mutations in the GRS gene cause motor and sensory axon loss in the peripheral nervous system and lead to clinical phenotypes ranging from Charcot-Marie-Tooth (CMT) type 2D neuropathy to a severe infantile form of spinal muscular atrophy type V [5-10]. Though GRS activity is required in all cells, the CMT-associated mutations affect only the peripheral nervous system. These findings suggest that this tRNA charging enzyme may also play a key role in maintaining peripheral axons. However, the links between GRS mutations, tissue-specificity, and the pathological mechanism remain unclear (reviewed in [7]). Several studies identified autoantibodies to 8 different aaRSs; amongst them, anti-GRS antibodies (anti-EJ) are mainly found in patients with inflammatory myopathy, polymyositis and dermatomyositis (reviewed in [11]). Yet information on their clinical impact is still limited. Interestingly, GRS autoantibodies were also detected in sera of patients with breast cancer [12]. Further reports suggested that GRS is indeed secreted by macrophages and acts as a cytokine with a distinct role against specific tumor cells [13]. Moreover, that GRS binds the Internal Ribosome Entry Site (IRES) located at the 5'-end of the poliovirus RNA genome and promotes its cap-independent translation initiation [14]. Together these observations suggest that, in mammals, GRS expression may be regulated in response to many different stimuli.

Three independent reports indicated that a single gene encodes both the cytoplasmic and mitochondrial forms of human GRS [15-17]. This is in contrast to other aaRSs for which cytoplasmic and mitochondrial tRNA aminoacylations are achieved by two separate genes (the only other exception being lysyl-tRNA synthetase). The GRS gene was predicted to produce both cytoplasmic and mitochondrial enzymes *via* alternative translational start sites [15]. Analysis of fetal liver cDNA encoding human GRS [16], as well as primer extension experiments on transfected cells [17], identified a single mRNA characterized by a long 5'-UTR with 5 putative initiation codons. Based on these observations, it was anticipated that the more distal codons relative to the transcriptional start site would initiate translation of the cytosolic GRS, while one or more proximal codons would initiate the mitochondrial enzyme.

In addition, the presence of three other upstream initiation codons could indicate the existence of some regulatory mechanism(s); for instance one of these codons would lead to the synthesis of a short Upstream Open Reading Frame (uORF), encoding 47 amino acids and potentially controlling GRS expression [16].

We focused our study on the control of human GRS expression, especially because the progress of other teams in investigating the novel functions of GRS adds further complexity to these regulatory mechanisms. Indeed, many aspects of the regulation of this enzyme remain unclear, especially its tissue specific expression and the control of both mitochondrial and cytosolic forms of the enzyme. Therefore, in this study, we used different human tissues to further characterize the 5'-UTR of the human GRS mRNA that may lead to the understanding of the molecular mechanisms governing such regulations. Contrary to previous studies, we identified two mRNA isoforms different from the mRNA previously isolated. These two GRS mRNAs were present in all tissues and vary only by the length of their 5'-UTRs. They were tested for their respective capacity to support translation of the mitochondrial and the cytosolic GRS, *in vitro* and in transfected cells. We noticed that the two 5'-UTRs behave differently. Interestingly, the longer 5'-UTR contains not only an uORF but also a functional IRES and an endoplasmic reticulum localization signal, strengthening our prediction of a complex regulatory mechanism.

RESULTS

Identification of two mRNA isoforms:

Both the human mitochondrial and cytosolic glycyl-tRNA synthetase (GRS) enzymes are encoded by the same gene, located on chromosome 7 and using two alternative initiation codons. One mRNA isoform was previously identified from fetal liver cDNA, showing the presence of a long 5'-UTR (357 nucleotides upstream the putative initiator codon for mitochondrial GRS synthesis) containing three other potential initiation codons [17] (Figure 1A). To further explore the presence of alternative mRNA isoforms in other human tissues, we performed 5'- and 3'-RLM-RACE PCR (RNA Ligase Mediated Rapid Amplification of cDNA Ends PCR, Supplementary Figure 1A) on total RNA from six different tissues: liver, brain, spinal cord, muscle, heart and spleen. We identified two populations of mRNAs (mRNA1 and mRNA2), present in brain, spinal cord, muscle, heart and spleen tissues and only one (mRNA2) was found in the liver tissue (Supplementary Figure 1B). These two mRNA isoforms contained both the initiator codons corresponding to the predicted translation start sites of the mitochondrial GRS (AUG_{mito}, at position +1) and of the cytosolic GRS (AUG_{cyto}, at position +163); mRNA1 and mRNA2 shared the same 3'-UTR sequence (166 nts; data not shown) and differed only by the length of their 5'-UTR (Figure 1A). The longest mRNA (mRNA1) was characterized by a 85 nt long 5'UTR (+/- 6 nts) and contained one extra AUG initiation codon (AUG_0) close to the 5'-end (position -69). Unlike AUG_{mito} and AUG_{cyto}, AUG_0 was not in frame with the GRS Open Reading Frame (ORF) and codeed for a small upstream ORF (uORF). This uORF would potentially initiate the synthesis of a 32 amino acids long peptide that ends at a stop codon (UAG) located 26 nt downstream AUG_{mito}. The shortest mRNA, mRNA2, had a very short 5'-UTR (between 21 and 29 nt) and displayed only AUG_{mito} and AUG_{cyto} (Figure 1A).

5'-RLM-RACE PCR was done again, in the same conditions, but without removing the 5'-cap from mRNAs before ligation of the 5'-adaptor (Supplementary Figure 1A). No PCR fragments were retrieved, indicating that both GRS mRNA1 and mRNA2 are capped in the cell.

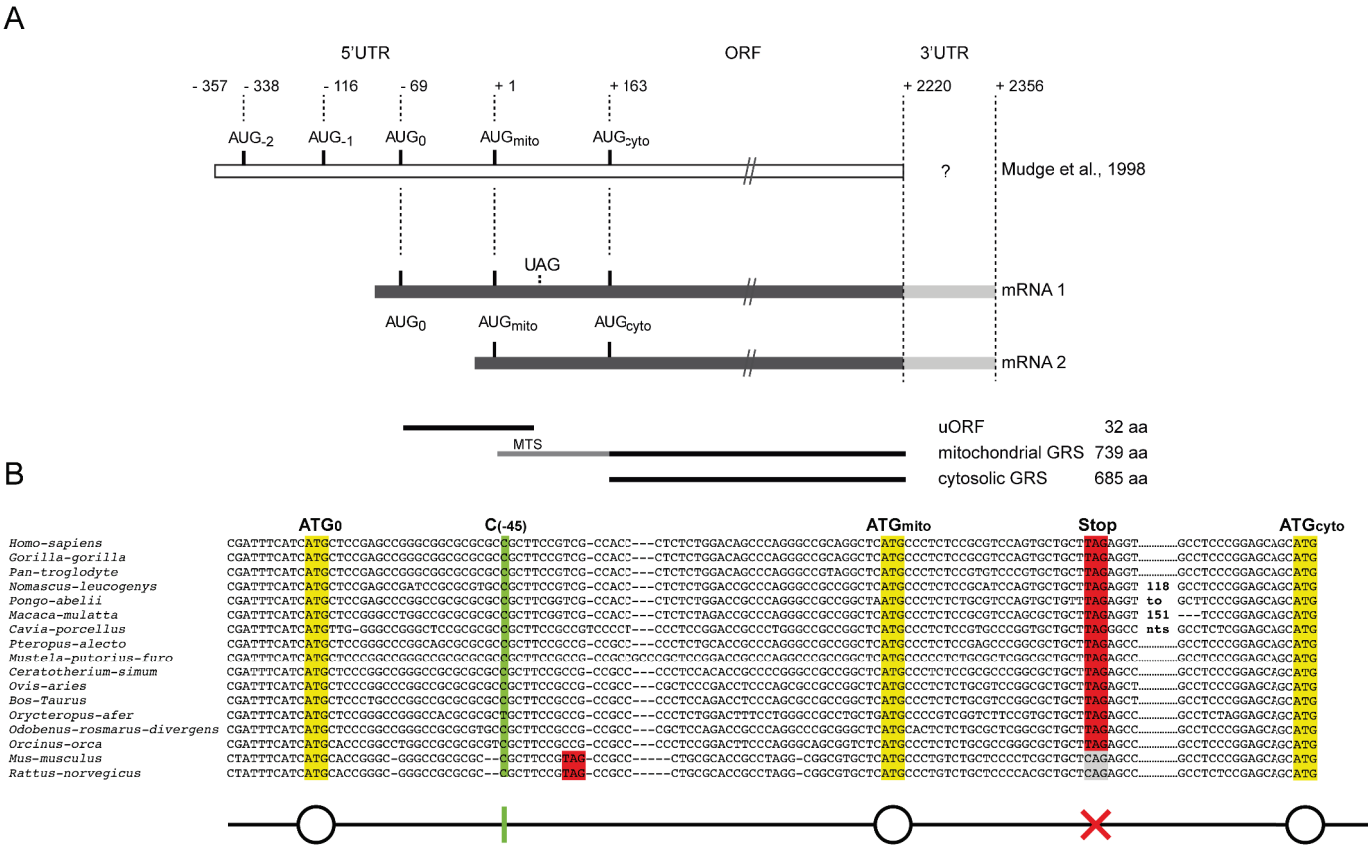

FIGURE 1: Organization of human GRS mRNAs. (A) Schematic representation of the 2 isoforms of the human GRS mRNA revealed in this study. The sequence identified by Mudge and collaborators in 1998 in fetal liver cells was used as a reference. The long mRNA1 contains three initiation codons, AUG_0 (initiates the synthesis of an uORF), AUG_{mito} (initiates translation of the mitochondrial targeting signal -MTS- fused to GRS), AUG_{cyto} (initiates translation of the cytosolic GRS) and a UAG stop codon (ends translation of the uORF). The shorter mRNA2 contains only AUG_{mito} and AUG_{cyto}. (B) Multiple alignment of mammalian mRNA1 5'UTR: blasting the nucleotide sequence of *Homo sapiens* GRS mRNA1 (NC_018918.2) against all NCBI nucleotide databases (http://blast.ncbi.nlm.nih.gov/Blast) retrieved 43 sequences only from other mammalian genomes. Among them, 14 GRS sequences were from primates. Here, we chose to show only a representative selection of the retrieved sequences: *Homo-sapiens* (NC_018918.2), *Gorilla-gorilla* (NC_018431.1), *Pan-troglodyte* (NC_006474.3), *Nomascus-leucogenys* (NC_019832.1), *Pongo-abelii* (NC_012598.1), *Macaca-mulatta* (NC_007860.1), *Cavia-porcellus* (XM_003467957.2), *Pteropus-alecto* (XM_006912040.1), *Mustela-putorius-furo* (XM_004762573.1), *Ceratotherium-simum* (XM_004418866.1), *Ovis-aries* (XM_004007927.1), *Bos-Taurus* (NM_001097566.1), *Orycteropus-afer* (XM_007945456.1), *Odobenus-rosmarus-divergens* (XM_004413949.1), *Orcinus-orca* (XM_004269943.1), *Mus-musculus* (NC_000072.6), *Rattus-norvegicus* (NC_005103.3) GRS sequences. Sequence alignments were computed with Tcoffee software (http://igs-server.cnrs-mrs.fr/Tcoffee/tcoffee_cgi/index.cgi). The three AUG codons, AUG_0, AUG_{mito} and AUG_{cyto}, are boxed in yellow, the stop codon in red. However, in the case of mouse and rat genomes, which are reliable, GRS DNA sequences differ by the position of the stop codon, found before the AUG_{mito}. Absence of these specific codons is indicated in grey on the alignment. Moreover, there are other few exceptions in the translation potential of some sequences (not shown on the alignment): pika (*Ochotona princeps*), wild boar (*Sus scrofa*), elephant (*Loxodonta Africana*) and dog (*Canis lupus familiaris*) have the AUG_0 in the same open reading frame than AUG_{mito} and AUG_{cyto} and the dolphin (*Lipotes vexillifer*) sequence is missing AUG_0. All of these particularities could be the consequence of sequencing mistakes. The schematic representation of the 5'- end of mRNA1, used in this manuscript, is indicated: AUGs are signaled with circles, the uORF stop codon with a red cross and the frameshift deletion with a green bar.

Sequence comparison:

The 5'-end of GRS mRNA1 sequence was used to blast NCBI nucleotide databases. We retrieved 43 sequences, showing that this complex organization, with three ATG codons and one stop codon was found only among mammals (Figure 1B). Besides mammals, other eukaryotic GRS gene sequences did not align with the 250 nts found at the 5'-end of the GRS mRNA1 sequence.

Characterization of mRNA1 and mRNA2 in translation:

DNA constructs encoding mRNA1 and mRNA2 sequences fused to the V5-tag were transfected in COS-7 cells. In order to compare the capacity of each mRNA isoform to support GRS expression and determine its nature (mitochondrial or cytosolic), we performed Western Blot and immunolocalization experiments (Figure 2) on transfected cells. Western Blot analysis (Figure 2A) showed that both mRNAs produced a unique band corresponding to the theoretical size of the cytosolic GRS (approximately 90 kDa), yet with a slightly higher expression for mRNA2 compared to mRNA1. Because the mitochondrial targeting signal (MTS) (54 amino acids, 5.6 kDa) is removed when the mitochondrial GRS enzyme is targeted to its final destination, the resulting mature enzyme cannot be distinguished from the cytosolic GRS based only on its size. Thus, mRNA 1 and mRNA2 were tested *in vitro* in wheat germ extract translation assays (Figure 2A). In this system, proteins are not matured, thus it is possible to distinguish the mitochondrial from the cytosolic GRS based on their respective lengths. Indeed, in the test performed with mRNA2, we could distinguish the mitochondrial (long) from the cytosolic (short) GRS. However, mRNA1 led only to the synthesis of the cytosolic (short) GRS. Immunolocalization experiments (Figure 2B) allowed us to further characterize the products of the two mRNA translations. Based on the GRS-V5 subcellular localization, we determined that, in agreement with the results of *in vitro* translation experiments, mRNA2 construct led to the synthesis of both the mitochondrial and the cytosolic GRSs. This indicated that both AUG_{mito} and AUG_{cyto} codons present in this mRNA are used to initiate efficient translation. However, the longer mRNA1, which contains 3 potential initiation sites, coded essentially for the cytosolic form of the protein.

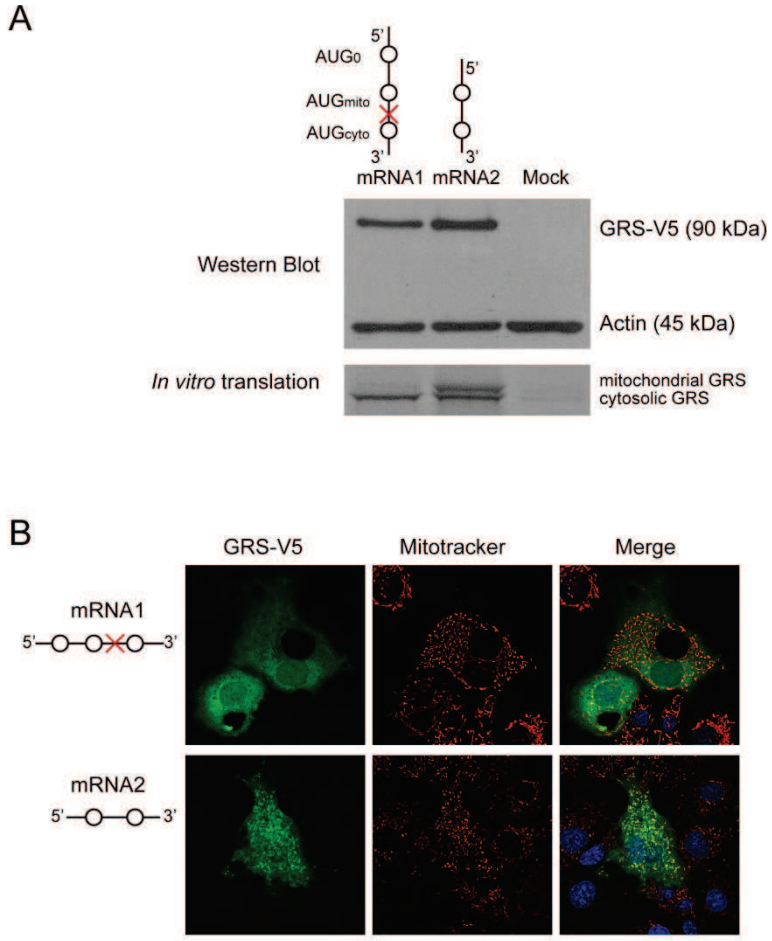

FIGURE 2: Translation of both mRNA isoforms *in vivo* and *in vitro*. (A) Western blot analysis of COS-7 cells transfected with pcDNA3.1 encoding mRNA1 or mRNA2 fused to a V5 epitope nucleotide sequence on their 3'-end. Translated GRS-V5 proteins are detected by anti-V5 antibodies. Detection of the 42 kDa ß-actin (anti-actin antibodies) was included as a loading control. Translation of radioactive GRSs from mRNA1 and mRNA2 *in vitro* was accomplished using wheat germ extracts. (B) GRS-V5 was detected by immunofluorescence, using anti-V5 antibodies coupled to FITC (green). Mitochondria were stained with Mitotracker Orange CMTMRos (red) and nuclei were stained with DAPI (blue). For mRNA1 scheme, please refer to the end of the Figure 1 legend.

Functional characterization of the three AUG codons present in mRNA1:

In order to assess if all 3 AUG codons in mRNA1 can initiate translation, they were mutated individually and in combination. The subcellular localizations of GRS translated from mRNA1 variants were determined by immunolocalization on transfected COS-7 cells (Figure 3A). When AUG_0 (mutant a), AUG_{mito} (mutant b) or AUG_{cyto} (mutant c) were the single initiation codons still available in mRNA1, we observed no synthesis, the synthesis of the mitochondrial GRS or the synthesis of the cytosolic GRS, respectively. The signal intensity for expressed proteins was significantly decreased compared to the wt mRNA1, however. Addition of AUG_0 upstream of AUG_{mito} (mutant d), prevented initiation at AUG_{mito}; yet, AUG_0 did not affect translation initiation at AUG_{cyto} (mutant e). These observations indicated

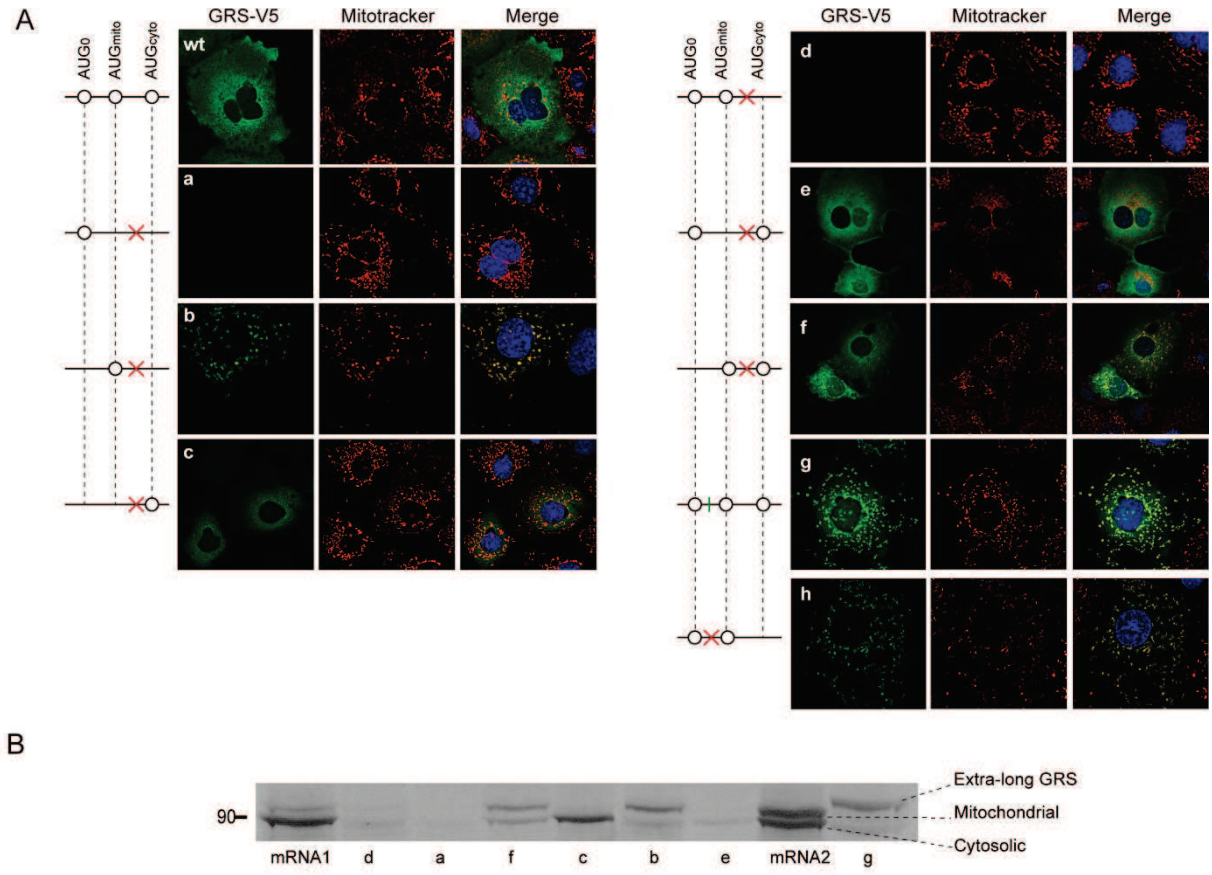

FIGURE 3: Immunolocalization of GRS expressed from mutated mRNA1. (A) Six mutants (a to h) were generated where the different AUG codons were tested for translation. GRS-V5, mitochondria and nuclei detection were performed as indicated in the legend of Figure 2 and mRNA1 scheme is described at the end of the Figure 1 legend. (B) The same mutants were used in *in vitro* translation experiments (rabbit reticulocyte extracts) in presence of ^{35}S methionine.

that AUG_0 selectively prevents translation of the mitochondrial GRS. On the contrary, mutation of AUG_0 (mutant f) restored translation initiation at AUG_{mito}. Finally, we deleted nt C at position -45 (Figure 1 B) so that AUG_0 was in the same reading frame as AUG_{mito} and AUG_{cyto} (mutant g). Interestingly, this frame-shift allowed the synthesis of a GRS that was mainly targeted to the mitochondria, suggesting that in this mutant, AUG_0 or AUG_{mito} might be used to initiate translation.

T7 RNA polymerase transcribed mRNA1 and mRNA2 as well as mRNA1 mutants (a to g) were tested for *in vitro* translation (Figure 3B). The results confirmed globally what was observed with immunolocalization experiments: AUG_0 alone or with AUG_{mito} did not allow GRS expression (mutants a and d), removing AUG_0 permitted the ribosomes to initiate at AUG_{mito} and AUG_{cyto} (mutant f), the presence of only AUG_{cyto} (mutant c) or AUG_{mito} (mutant b) led to the synthesis of the cytosolic or the mitochondrial GRS, respectively. Lastly, the frameshift mutation (mutant g) led to the synthesis of an "extra-long" GRS that corresponds to the addition of 23 extra amino acids at the N terminus of the MTS, indicating that initiation

takes place at AUG_0. This addition didn't affect the targeting sequence (Figure 3 A, mutant g). This clearly shows that despite its close proximity to the 5'-end of mRNA1 (3 to 20 nts, Supplementary Figure 1 B), AUG_0 is recognized as an efficient initiation codon and would thus promote the synthesis of the 32 residue peptide.

We observed two main differences between immunolocalization and *in vitro* translation results: the wild type mRNA1 product did not show any mitochondrial localization in Figure 3A, however *in vitro* we could detect a weak band that corresponded to the mitochondrial GRS. The other difference concerned mutant e, which was strongly expressed in the cell cytosol *in vivo* but was a poor substrate *in vitro*. Artifacts, such as mRNA alternative structures, due to *in vitro* T7 RNA polymerase production could explain these discrepancies.

The ribosome reinitiates at the AUG immediately downstream of the stop codon:

In order to test the possibility that the ribosome reinitiates after synthesis of the uORF, the stop codon initially present between AUG_{mito} and AUG_{cyto} (mutant d) was moved before AUG_{mito} (mutant h). We observed that, as expected for ribosome reinitiation, the mitochondrial GRS was translated instead of the cytosolic GRS (Figure 3A).

mRNA1 supports cap-independent translation initiation:

Taking into account the high percentage of GC (74%) and our unsuccessful attempts to solve the mRNA1 structure in solution using chemical and enzymatic methods, we considered that mRNA1 would encompass a stable fold. Together with its unique expression pattern, we hypothesized that the extra RNA sequence present at the 5'-end of mRNA1 would contain an Internal Ribosome Entry Site (IRES). In order to test this idea, we produced mRNA1 and mRNA2, each 5'-modified either with the natural m7G cap analog or with the non-functional Ap3G cap analog. These mRNA transcripts were subjected to *in vitro* translation in wheat germ extracts (Figure 4A). As expected, translation of m7G capped mRNA1 generated one major band corresponding to the cytosolic GRS (about 80%) and translation of m7G-capped mRNA2 lead to two bands of comparable intensities (55% cytosolic GRS and 45% mitochondrial GRS). On the contrary, when mRNAs were capped with the non-functional Ap3G cap analog, mRNA1 was still translated (>50%) while translation of mRNA2 was abolished.

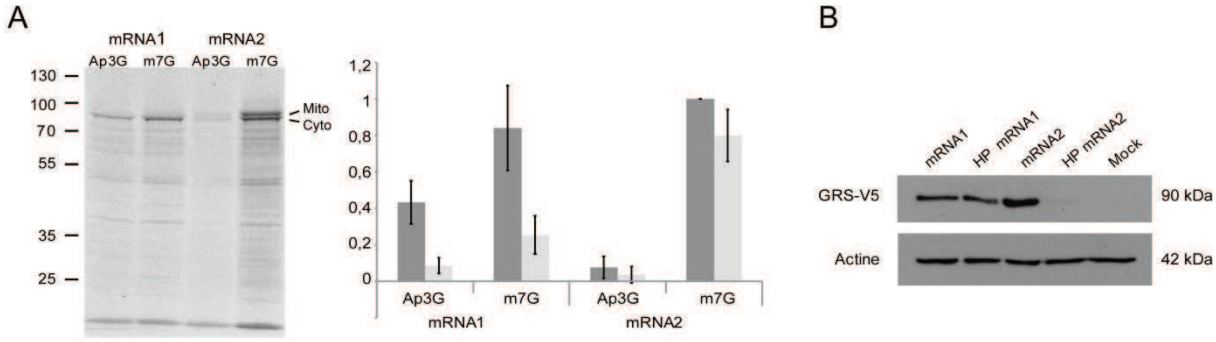

FIGURE 4: Cap-independent *versus* cap-dependent initiations. (A) *In vitro* translations of mRNA1 and mRNA2 were performed in wheat germ extracts. Both mRNAs were capped either with the natural m7G or the inhibitor cap analog Ap3G. Synthesized GRSs correspond to the mitochondrial (upper band) and cytosolic (lower band) enzymes. Expression levels of cytosolic (dark bars) and mitochondrial (light bars) GRSs were quantified relative to the cytosolic GRS translated from mRNA2. Error bars were calculated from 3 independent experiments. (B) Western blot analysis: Effect of a strong hairpin structure on GRS expression: COS-7 cells were transfected with pcDNA3.1 constructs containing a strong hairpin structure introduced at the 5'-end of mRNA1 and mRNA2 (HP mRNA1 and HP mRNA2, respectively).

To further confirm the ability of the mRNA1 to initiate the translation in a cap-independent manner, we inserted a stable hairpin structure [18] at the 5'-extremity of both mRNA1 and mRNA2 constructs. Such a structure is supposed to hinder ribosome scanning and in consequence cap-dependent initiation [19,20]. mRNAs without or with the stable hairpin structure were expressed for 24 hours in COS-7 cells. The corresponding Western Blot analysis (Figure 4B) clearly shows that the hairpin structure indeed inhibited mRNA2 but not mRNA1 translation, confirming the presence of a particular initiation in mRNA1.

mRNA1 contains a functional IRES:

To test the presence of a functional IRES in mRNA1, we used the bicistronic renilla/firefly luciferase system pRF. The pRF vector contains a SV40 promoter and generates long mRNAs with two consecutive cistrons: the first one is translated in a cap-dependent manner and codes for the renilla luciferase (R), whereas the second one codes for the firefly luciferase (F), which is expressed only if the inserted intercistronic region has an IRES activity [19].

Vectors pRF and $pR_{Vcip}F$ (containing the well-characterized cellular IRES) [21] were used as negative and positive controls, respectively. The extremity of mRNA1 (nt -78 to +163, including AUG_0, AUG_{mito} and AUG_{cyto}) was cloned in the intercistronic region (Figure 5A). COS-7 cells were then transiently transfected with the three constructs and both renilla and firefly luciferase activities were measured (Figure 5B). The relative firefly/renilla ratio shows a strong IRES activity for $pR_{mRNA1}F$, 150 fold higher than the negative control and comparable to $pR_{Vcip}F$ IRES activity (70%).

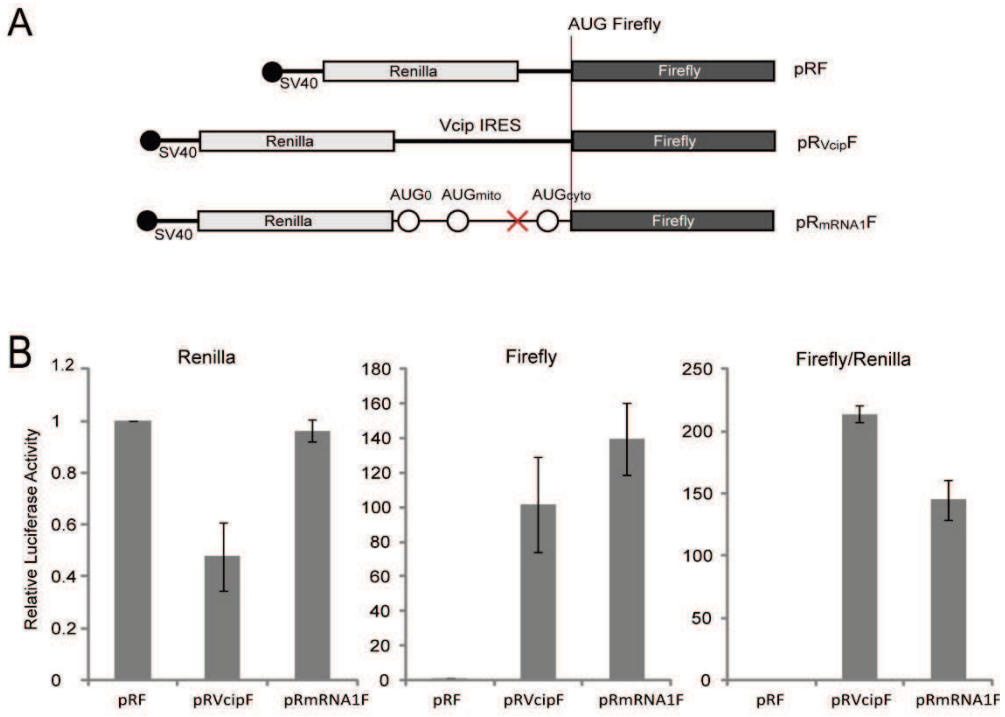

FIGURE 5: Comparison of mRNA1 and Vcip IRES elements for their ability to initiate translation. (A) Schematic representation of biscistronic pRF constructs: sequences corresponding to the Vcip IRES and mRNA1 5'-end (containing the three AUG codons) were inserted in the intercistronic region between the renilla and firefly ORFs ($pR_{Vcip}F$ and $pR_{mRNA1}F$). The cap structure at the 5'-end of the bicistronic mRNA is indicated with a black circle. (B) pRF, $pR_{Vcip}F$ and $pR_{mRNA1}F$ were transfected in COS-7 cells and renilla (cap dependent initiation) and firefly (IRES-mediated initiation) luciferases activities were measured. $pR_{Vcip}F$ and $pR_{mRNA1}F$ luciferases activities were represented relative to pRF activity. Error bars were calculated from 3 independent experiments. For mRNA1 scheme, please refer to the end of the Figure 1 legend.

Several controls were carried out to exclude any experimental artifacts (Supplementary Figure 2). To rule out the presence of cryptic promoters, the SV40 promoter was deleted from the bicistronic vectors, hindering the transcription of bicistronic mRNAs. As expected, both renilla and firefly activities were drastically decreased confirming the absence of strong cryptic promoters (Supplementary Figure 2A). However, for both $pR_{Vcip}F$ and $pR_{mRNA1}F$, a residual firefly luciferase activity (20% and 15%, respectively) can still be detected.

Because unwanted splicing could lead to the production of two monocystronic mRNAs instead of the bicistronic mRNA, the synthesis of the firefly luciferase could be the result of a cap-dependent initiation. Thus, we tested the presence of such putative splicing events; total RNAs, purified from transfected COS-7 cells, were subjected to reverse transcription and PCR amplification. Specific primers covering the promoter region and part of the firefly luciferase sequence were used (Supplementary Figure 2B). The results of this specific RT-PCR reaction showed that a unique product was amplified corresponding to each pRF construct (the size of amplified inserts were: 1245 nt, 1815 nt and 1498 nt for pRF, $pR_{Vcip}F$ and pR_{mRNA1}, respectively).

Finally, to eliminate the possibility of ribosome shunting or read-through of the renilla stop codon, we verified the length of the produced firefly luciferase protein by Western Blot (Supplementary Figure 2C). Whereas no protein is detected either for pRF or the mock transfections, a unique band of the expected size (62 kDa) is observed when $pR_{Vcip}F$ and $pR_{mRNA1}F$ constructs were transfected in COS-7 cells, showing that the synthesis of the firefly luciferase is indeed initiated at the expected AUG.

Looking for control of IRES-dependent expression:

Cellular IRESs are often expressed when cap-dependent translation is inhibited either by stress or under particular physiological conditions [22-24]. Therefore, we tested several conditions where mRNA1 IRES mediated expression could be affected.

First, different stress conditions were applied on cells transfected with bicistronic constructs: (i) starvation by omitting the serum in the medium; (ii) glucose deprivation using a low glucose medium; (iii) mTOR pathway inhibition in presence of 100 nM Rapamycin and (iv) hypoxia with addition of 150 μM $CoCl_2$. We didn't observe any particular stimulation either with Vcip, or GRS mRNA1.

Another consideration was the presence of a putative 5 base-pair sequence (5'-$_{152}$CGGAG$_{156}$-3') complementarity to the 3'-extremity of the 18S ribosomal RNA (5'-$_{1839}$UUCCG$_{1843}$-3'). By mutating this sequence in $pR_{mRNA1}F$, we tested if these nucleotides could stabilize the mRNA on the 40S subunit and facilitate AUG_0/AUG_{cyto} recognition by the ribosome. Again, in this context, the mutations did not lead to reduction of IRES activity (data not shown).

Finally, because it has been shown that GRS binds to and stimulate translation from the poliovirus IRES, we cotransfected GRS with the bicistronic constructs and tested whether GRS co-expression could modify firefly luciferase synthesis. Again, this did not alter mRNA1 IRES controlled expression of firefly luciferase (data not shown).

Insights in mRNA1 IRES structure:

We faced technical problems in studying the mRNA1 IRES structure in solution due to the intricate and stable IRES folding that hindered all our attempts to solve its structure. Thus, we used bioinformatics tools to build a structural model of the GRS IRES based on sequence alignments with mammalian 5'-UTRs (Supplementary Figure 3A). The two-dimensional model shows a three-way junction linking Watson-Crick helices: (i) the 5'- and 3'-ends interact together to form a double stranded domain (helix I) containing both AUG_0 and

AUG_{cyto}, (ii) the left arm (helix II) covers most of the uORF and displays AUG_{mito} and the uORF stop codon, (iii) the right arm (helix III) corresponds to the rest of the MTS coding sequence of the mitochondrial GRS. Such a structure presents strong potential for tertiary interactions as well as extensive major/minor groove contacts between helices [25]. Progressive shortening of mRNA1 at both the 5'- and 3'-ends led systematically to reduced IRES activity, indicating that the entire domain is involved in efficient translation initiation (Supplementary Figure 3B). Thus, any change in the sequence could destabilize this structure and affect the initiation mechanism. Indeed, this is what is observed in mRNA1 mutants missing AUG_0 (mutants b, c and f). In the case of an exclusive IRES initiation mechanism, these mutants should be completely inactive in translation. However, because AUG_0 is involved in the structure of helix I, its mutation could lead to a partial unfolding of this domain and introduce enough instability so that cap-dependent initiation and ribosome scanning can occur *in vivo* and *in vitro* (Figure 3).

mRNA1 GRS colocalizes with endoplasmic reticulum associated ribosomes:

Contrary to mRNA2, the GRS produced by mRNA1 showed some ambiguous localization (Figure 2B). Indeed, in our hands, the GRS produced from mRNA1 organizes in a network structure. We thus performed additional immunolocalization assays using digitonin, in order to extract the soluble cytoplasmic GRS and keep only GRS attached to cellular structures (Figure 6A). Colocalization assays between GRS-V5 and the Mitotracker label confirmed that the GRS translated from mRNA2 is indeed present in the mitochondria whereas most of the GRS translated *via* the mRNA1 IRES is clearly associated with some other cellular structures (compare panels a and b). To identify the nature of this cellular structure, mRNA1 and mRNA2 constructs were co-expressed with the Signal Recognition Particle (SRP) receptor B subunit which is an integral endoplasmic reticulum protein (ER) (coupled to DsRed: Srprb-DsRed) or with the endogenous ribosomal protein rm6S. We observed that mRNA2 does not show obvious colocalization with ER or with ribosomes (panels e and f), but mRNA1 behaves differently. Indeed, panel c shows that the GRS network was clearly confined in the close proximity of the ER. Besides, it superimposed clearly with ribosomes (panel e), suggesting that the mRNA1 product interacts with ER-associated translating ribosomes. Moreover, overexpression of mRNA1 increases considerably the ER-bound ribosomes density. Since mRNA2 product does not, it implies that

this specific localization is due to the 5'-end RNA domain containing the mRNA1 IRES structure.

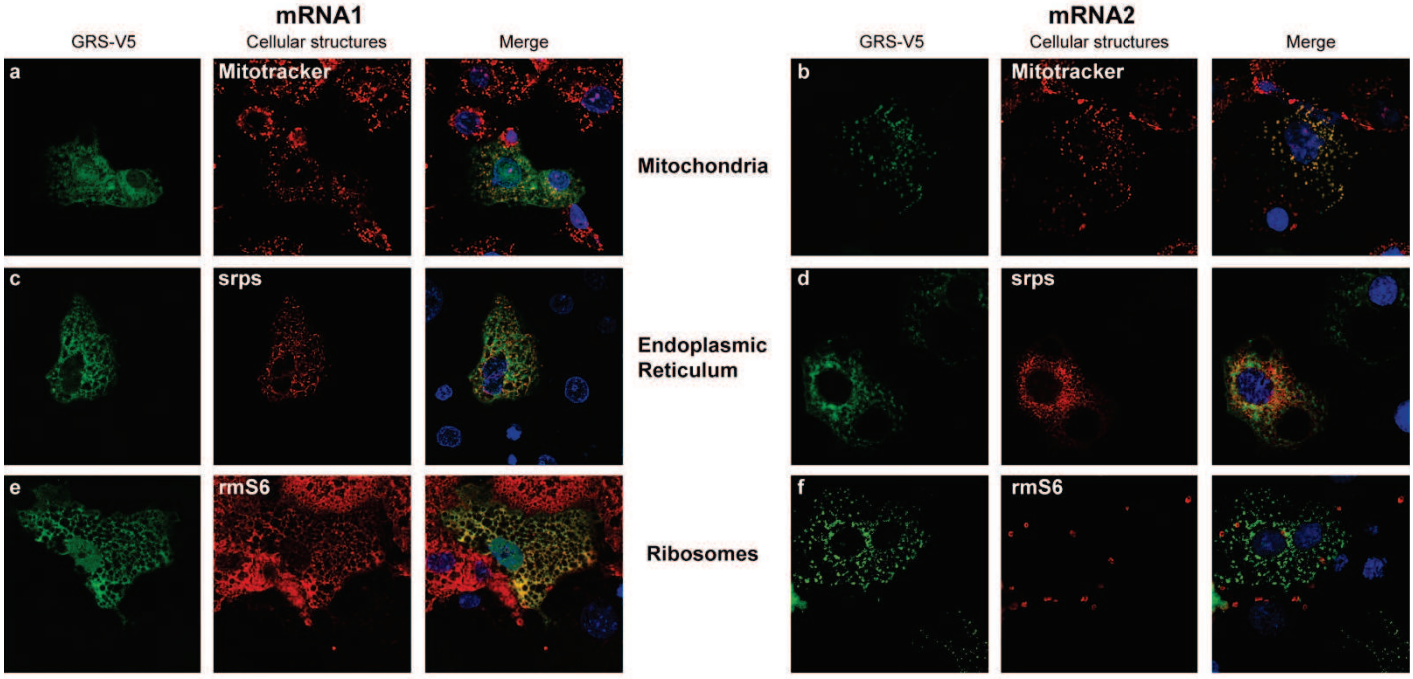

FIGURE 6: Differential colocalization of GRS with subcellular structures, depending on mRNA isoforms. (A) GRS-V5 was expressed from mRNA1 (left) or mRNA2 (right). GRS-V5 localizations (green) were compared with red markers for mitochondria (a and b, Mitotracker), ER protein (c and d, SRPs-DsRed) and endogenous ribosomal protein S6 (e and f, rmS6). In order to remove the background noise due to the cytosolic GRS, transfected COS-7 cells were first permeabilized with digitonin. This treatment strips the plasma membrane, such that cells lose most of their cytosolic content but retain intact mitochondria and ER. Nuclei were stained with DAPI (blue).

DISCUSSION

The previous study analyzing the fetal liver cDNA encoding human glycyl-tRNA synthetase (GRS) identified a single mRNA isoform by primer extension [16]. This mRNA encoded the two initiator codons dedicated to the mitochondrial (AUG_{mito}) and the cytosolic (AUG_{cyto}) forms of the enzyme. The 5'-UTR was 371 nucleotides long and contained 3 other AUG codons upstream of AUG_{mito}. However, despite repeated attempts, the authors were unable to confirm the mRNA transcription start site (TSS) by 5'-RACE or RNase protection assays [17]. Surprisingly, they also observed that an effective promoter activity was present 55 base pairs downstream of the TSS identified by primer extension, suggesting that this proximal promoter element may be important for GRS expression. In our study, we confirmed this assumption by identifying two shorter mRNA isoforms in 6 different adult tissues (heart, brain, bone marrow, muscle, spleen and liver). The two mRNA isoforms (mRNA1 and mRNA2) that we identified both contained AUG_{mito} and AUG_{cyto}, but the longer 5'-UTR (mRNA1) contained only 90 nucleotides upstream of AUG_{mito} and a unique additional AUG (AUG_0). The shorter mRNA2 encodes both the mitochondrial and the cytosolic GRS, suggesting a leaky scanning mechanism [26,27] whereas the longer mRNA1 codes essentially for the cytosolic GRS (Figure 2B).

Further analysis of mRNA1 identified the presence of an IRES structure. Indeed, although the mature mRNA1 (like other cellular IRESs) contains a 5'-cap structure, it drives cap-independent translation as expected for functional IRESs. It has been suggested that up to 10% of cellular mRNAs contain IRES elements [28] that would associate with many states where cap-dependent initiation is diminished, such as differentiation, mitosis, stress, and proliferation [22,23]. In this way IRES structures may respond to changing cellular conditions and control the localization and cellular concentration of the produced proteins. An alignment-based structural model of this IRES sequence combined with deletions in the mRNA sequence indicates that the 3 hairpin structures are involved in recruiting the ribosome. However, since cellular IRESs do not share any common structural motif [29], it is difficult from here to draw a model for translation initiation of mRNA1. Further studies to understand the dynamics of this IRES structure and to identify the proteins involved (initiation factors and IRES trans-acting factors) will be decisive to comprehend both how this IRES captures the translation machinery to initiate at AUG_0 and how it drives reinitiation at AUG_{cyto}.

The complexity of the initiation mechanism that characterizes mRNA1 is further increased by the presence of a short upstream Open Reading Frame (uORF) initiating at

AUG_0 and encoding a putative 32 residue peptide. Interestingly, this particular organization of the 5'-UTR is conserved in all the mammalian genes encoding GRS (Figure 1B). The introduction of a frameshift mutation between AUG_0 and AUG_{mito} showed that AUG_0 is the main initiator codon used to initiate mRNA1 translation and that the peptide is potentially produced (yet not detectable by mass spectrometry). The presence of such a uORF usually reduces the translation efficiency of the downstream ORF (reviewed in [30]). Indeed, in mRNA1, because the uORF sequence covers AUG_{mito}, translation of this peptide specifically hinders the production of the mitochondrial GRS.

On the contrary, uORF translation terminates before AUG_{cyto}, allowing translation of the cytosolic GRS by reinitiating at the AUG directly downstream of the stop codon [31]. Efficient reinitiation commonly occurs after translation of short ORFs and can be modulated in response to environmental changes [32]. Moreover, genome wide bioinformatic analyses show that >45% of mammalian mRNAs contain at least one uORF [30], and they are frequently translated [33]. We cannot exclude that mRNA1 sequence can also be used for cap-dependent initiation, even if the short 5'-UTR upstream of AUG_0 does not support this option.

Even more striking is the specific colocalization we observe for most of the mRNA1 GRS product and ER-bound ribosomes (Figure 6). Using proteomic technology, David and coworkers have shown that phenylalanine-tRNA synthetase and each of the nine aminoacyl-tRNA synthetases of the multi synthetase complex co-sediment with polysomes in sucrose gradients and interact with ER-bound ribosomes [34]. These results confirmed previous immunoelectron microscopy data [35] and provide additional evidence for the concept of channeled translation [36]. However, here GRS localization appears to be unique. Indeed, its targeting to ER-bound ribosomes does not involve direct interaction between the ribosome and the enzyme, but rather seems to be driven by the IRES domain of mRNA1. According to the classical Signal Recognition Particle (SRP) pathway, a specific translated signal peptide targets protein synthesis to the ER compartment. However, new data demonstrate that the mRNA itself might contain ER targeting information [37], although clear motifs have not yet been identified. Because mRNA2 does not show colocalization with ER bound ribosomes GRS localization could be driven by the additional RNA domain that specifies mRNA1.

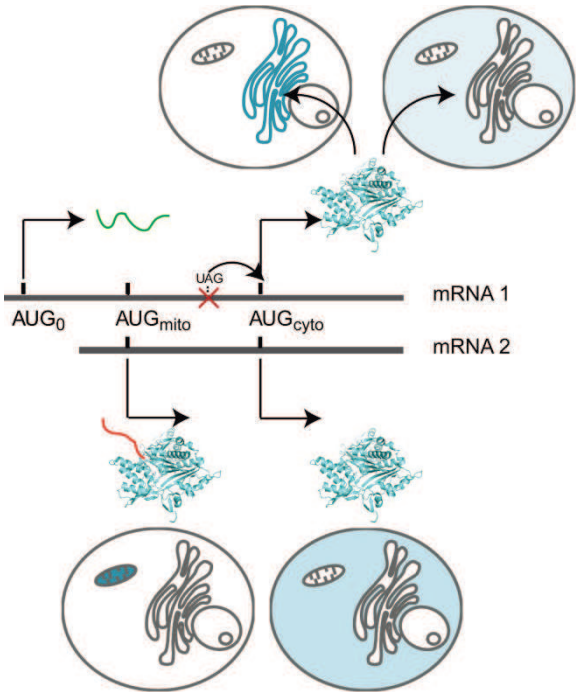

FIGURE 7: Suggested model. Summary of GRS expression from mRNA1 and mRNA2 isoforms: mRNA2 codes both the mitochondrial and the cytosolic GRSs using a leaky scanning mechanism. Only 2 initiation codons are recognized in mRNA1, due to a uORF containing IRES, which hinders the mitochondrial GRS synthesis. Translation initiation at AUG_0 leads (i) to the synthesis of a short peptide and (ii) to the subsequent reinitiation at AUG_{cyto}. The 5'-additional sequence in mRNA1 allows most of the GRS to be translated on ER-bound ribosomes.

This work shows that the 5'-extremity of GRS mRNA1 is the site of intricate regulatory mechanisms connecting cap-independent translational initiation and subcellular localization of human GRS (summarized in Figure 7B). Such complexity matches the range of uncovered moonlighting activities for mammalian GRS connected with tissue-specific expression or extracellular localization [4,13,14]. Indeed, the involvement of GRS in Charcot-Marie-Tooth disease suggests its peculiar expression and function in peripheral motor and sensory neurons [5-7,9,10]. GRS is active in translation in neurons, in the cell body and in the periphery of cells; local translation is essential for dendritic and axonal terminal arborization during development and maintenance of the nervous system. Could a disequilibrium between mRNA1 and mRNA2 transcriptions in "sick" neurons disturb GRS expression and activity? Could this imbalance affect the cytoplasmic, the mitochondrial or the ER-bound GRSs specifically in dendritic and axonal terminal arborizations and affect some alternative function? Likewise, macrophages secrete "cytokine GRS" [13] and GRS autoantibodies are present in the blood of polymyositis and dermatomyositis patients [39,40]. The localization of mRNA1-driven translation at the ER explains this "extracellular GRS" pool, even though no secretion signal was found in the sequence of this enzyme. There is increasing evidence

that mRNAs are zip-coded to specific regions in cells for localized translation [37,41,42]. Directing mRNAs to the ER for translation may function to modulate the relative protein expression [43]. Thus, by exploiting the differential translation activities of cytosolic and ER-bound ribosomes, the cell may control the level GRS synthesis through regulating the relative subcellular distribution of its mRNA isoforms. In this context, GRS mRNA1 colocalization with ER-bound ribosomes enables localized GRS synthesis and influences cellular responses distal to the cell cytosol.

MATERIALS AND METHODS

RNA ligase-mediated rapid amplification of cDNA ends (RLM-RACE): Identification of GRS mRNA 5'-and 3'UTRs was performed using the First Choice RLM-RACE kit (Ambion, Life Technologies) according to the manufacturer's instructions. Experiments were performed with 10 μg of highly pure total RNA from six different tissues (liver, spinal cord, brain, skeletal muscle, heart and spleen, purchased from Ambion).

For 5'-RLM-RACE, RNAs were first decapped (as appropriate), ligated to a 5'-adaptor and reverse transcribed using a specific reverse primer 5'-TTCCTCGATTGTCTCTTTTTT-ACCAGTCTCTTGC-3', hybridizing between nucleotides (nt) 2184 and 2216 at the very end of the predicted mitochondrial-GRS ORF sequence. The resulting cDNAs were then subjected to two nested PCRs in the presence of 5% DMSO. PCRs were performed with two primers complementary to the 5'-adaptor sequence and two nested primers hybridizing the mitochondrial GRS ORF sequence: outer primer 5'-CTCCATTTTTTACGTCTTTCA-CCATGAAGTCAGC-3' (nt 595 to 628), inner primer 5'-GGGCTGTAACGCCAGCTCCT-TTGCTTCCAGAACCCTC-3' (nt 306 to 342).

Alternatively the 3'-RLM-RACE was performed on complete cDNAs reverse transcribed using a primer hybridizing mRNA polyA tails and containing a 3'-adaptor sequence. PCRs were performed with two primers complementary to the 3'-adaptor sequence and two nested primers hybridizing the GRS ORF sequence: outer primer 5'-ACTTTGACACAGTGAACA-AGAC-3' (nt 2018-2039) and inner primer 5'-AGCATAGTCCAAGACCTAGCCAATGG-3' (nt 2110-2135).

PCR-amplified fragments were cloned into pDrive cloning vector (PCR cloning kit, Qiagen) and sequenced.

Construction of GRS mammalian expression vectors: GRS mRNA sequences were introduced into a modified pcDNA3.1 vector for expression. In order to transcribe mRNAs beginning with their exact 5'-extremity, the "extra" sequence present between the pcDNA3.1 transcription start site and the *Kpn*I restriction site was removed by mutagenesis (Phusion Site-Directed Mutagenesis Kit, Thermo Scientific). The sequence of the GRS ORF was generated by RT-PCR from HeLa cell total RNA, fused to a C-terminal V5 epitope sequence, and introduced in the modified pcDNA3.1 between *Kpn*I and *Xba*I restriction sites. Then both 5'-UTR sequences were PCR amplified from brain cDNA (Ambion) and introduced between the *Kpn*I restriction site and the unique internal *Nhe*I restriction site present at nt 205 in the mitochondrial GRS ORF. Mutants were generated by replacing each putative ATG initiator

codon by the ATA sequence (Phusion Site-Directed Mutagenesis Kit). A 5' stable hairpin structure [18] was introduced at the *Kpn*I site using two overlapping primers: 5'-AATTGGTACCTTTGCAAAAAGCTCCACCACGGCCCAAGCTTGGGC-3' and 5'- TTA-AGGTACCAAGCTCCACCACGGCCCAAGCTTGGG-3'.

Bicistronic vectors pRF and $pR_{Vcip}F$ were a kind gift from Catherine Schuster, described previously [19]. Briefly, pRF contains two ORFs, the first one coding for the Renilla luciferase and the second for the Firefly luciferase. Renilla luciferase is expressed constitutively (cap-dependant translation), while Firefly is expressed only if an IRES sequence is introduced in the intercistronic region. The mRNA1 5'-end sequence and different variants were inserted in the intercistronic region between *EcoR*I and *Nco*I to obtain the $pR_{mRNA1}F$ vector and the mRNA1 structure deletants. pRF, $pR_{Vcip}F$ and $pR_{mRNA1}F$ promotorless constructs were created by excision of the SV40 promoter (between *Sma*I and *EcoR*V sites).

Cell culture and transfection.

COS-7 cells were cultured in DMEM GlutaMAX growth medium (Life Technologies) containing 4,5 mg/L glucose, 50 U/mL penicillin, 50 µg/mL streptomycin and 10% fetal calf serum. Cells were grown at 37 °C with 5% CO_2.

Twenty-four hours prior to transfection COS-7 cells were seeded into 6 (or 12) well plates, at a density of 2.10^5 (or 10^5) cells per well and cells were then transfected with 100 (or 50 ng) of pcDNA3.1 (or pRF) constructs, using the Nanofectin transfection reagent according to the manufacturer's instructions (PAA labs). After 24 hours incubation, cells were washed with PBS (Life Technologies) and collected for further investigations.

Immunostaining.

For immunolocalization assays, cells were seeded directly on coverslips treated with 10 $\mu g/cm^2$ collagen type I (BD Bioscience). Twenty-four hours after transfection, mitochondria were labeled with 50 nM MitoTracker Orange CMTMRos (Mitochondrion Selective Probe from Life Technologies) for 30 min at 37 °C. When needed, extraction of free cytoplasmic proteins was performed in the presence of 25 μg/mL digitonin (Sigma-Aldrich) for 10 minutes on ice. Cells were then washed twice in PBS, fixed for 10 min with 4% paraformaldehyde (PFA) and permeabilized in ice-cold methanol for 5 minutes. Cells were washed with PBS and blocked in 3% BSA (Euromedex) for one hour.

Immunostaining of GRS was performed with FITC-conjugated mouse anti-V5 monoclonal antibody from Life Technologies (1:500) at 37 °C for two hours. Ribosomes were labeled first under the same conditions with rabbit monoclonal anti-S6 ribosomal protein antibody (Pierce) and further detected with TRITC-conjugated anti-rabbit antibody (40 min at 37 °C). Slides were counterstained with DAPI (Sigma-Aldrich), mounted in anti-fading solution and visualized under confocal laser scanning microscope (Zeiss LSM 780 Confocal system, Carl Zeiss, Göttingen, Germany). The resulting images were analyzed using Image J Software.

Western blot: Twenty-four hours after transfection, COS-7 cells were incubated in lysis buffer (Promega) for 15 min at RT and the protein concentration was measured using the Bradford protein assay reagent (Bio-Rad). Equal quantities of total protein were separated on 10% SDS-PAGE and transferred to PVDF membrane (Bio-Rad). The membrane was blocked for 1 hour in 1X TBS-0.5% Tween20, 3% non-fat dry milk and then incubated with (i) mouse anti-V5 monoclonal antibody HRP–conjugated (1:5000; Life Technologies) for 2 hours, (ii) rabbit anti-firefly luciferase polyclonal (1:5000; Pierce) for 1 hour, or (iii) mouse monoclonal anti-ßActin (1:10000; Sigma-Aldrich) for 1 hour. Secondary sheep anti-mouse antibody HRP–conjugated was from GE Healthcare and goat anti-rabbit HRP–conjugated from Bio-Rad. All the incubations were carried out at room temperature.

Luciferase activity: Assays were conducted as indicated in the dual luciferase reporter assay system manual (Promega, France) and error bars were calculated from 3 independent experiments.

***In vitro* transcription of GRS mRNA and *in vitro* translation:** The V5 epitope was replaced by the sequence corresponding to the 3'-UTR of the GRS mRNA, inserted immediately downstream of the GRS constructs (*Xba*I and *Xho*I). The T7 RNA polymerase promoter and a polyA tail (40 As) were then introduced by PCR at the 5'- and 3'-ends of each DNA template, respectively. *In vitro* transcription was performed in reaction mixtures containing 40 mM Tris-HCl pH 8.1 (37 °C), 22 mM $MgCl_2$, 5 mM dithiothreitol, 0.1 mM spermidine, 4 mM ATP, CTP, and UTP, 1 mM GTP, 2 mM 3'-O-Me-m7G(5')ppp(5')G [m7G] cap structure analog (BioLabs), 40 ng/μL DNA template and 5 μg/mL T7 RNA polymerase. Transcription mixtures were incubated for 2 h at 37 °C and reactions were stopped by acidic phenol/chloroform extraction. RNA transcripts were purified on Nap5

columns (GE-Healthcare) to remove non-incorporated ribonucleotides, ethanol precipitated, and quantified on a NanoDrop ND-1000 spectrophotometer. For cap-dependant/independant *in vitro* translation assays, mRNAs were synthetized in the presence of 10 mM 3'-O-Me-m7G(5')ppp(5')G [m7G] or G(5')ppp(5')A [Ap3G] cap structure analogs (BioLabs).

In vitro translation reactions were carried out with 5 nM mRNA and 10 μCi [^{35}S] methionine, in rabbit reticulocytes or wheat germ extract from Promega, according to the manufacturer's instructions, for 60 minutes at 30 °C or for two hours at 25 °C, respectively. Translated proteins were further analyzed by 10% SDS-PAGE, followed by autoradiography and quantification.

RT-PCR analysis of pRF constructs: Twenty-four hours after transfection, total RNA was extracted from transfected COS-7 cells using the TRI Reagent® Protocol (Sigma-Aldrich). Extracted RNA was treated with DNaseI: 10 μg of RNA were incubated in the presence of 5U of DNaseI (Sigma-Aldrich) for 40 minutes at 37 °C. DNaseI-treated RNA (0.5 μg) was reverse transcribed for 1 hour at 42 °C, using the first strand cDNA synthesis kit (GE Healthcare) following the manufacturer's protocol. PCR reactions were performed with the Phusion Taq polymerase (Thermo-Scientific) on 1 μL of reverse transcription product in the presence of 3% DMSO.

Multi-alignment-based structure:

Using the structural aligner LocARNA [44], we inferred a consensus structure from all mammalian sequences. This structure has was evaluated and curated with the last version of the graphical tool Assemble [45].

AKNOWLEDGMENTS:

We thank Alain Lescure and Catherine Schuster for support and discussions and Rebecca Wagner Alexander for comments on the manuscript. This work was supported by the CNRS, the Strasbourg University, and the French Association for Myopathies (AFM).

AUTHORS CONTRIBUTION

J.A., C.P., J.R.T., F.J. and M.F. performed research; J.A, and M.F. designed the research, analyzed the data and wrote the paper.

REFERENCES

1. Park SG, Ewalt KL, Kim S (2005) Functional expansion of aminoacyl-tRNA synthetases and their interacting factors: new perspectives on housekeepers. Trends Biochem Sci 30: 569-574.
2. Hausmann CD, Ibba M (2008) Aminoacyl-tRNA synthetase complexes: molecular multitasking revealed. FEMS Microbiol Rev 32: 705-721.
3. Kim S, You S, Hwang D (2011) Aminoacyl-tRNA synthetases and tumorigenesis: more than housekeeping. Nat Rev Cancer 11: 708-718.
4. Guo M, Schimmel P (2013) Essential nontranslational functions of tRNA synthetases. Nat Chem Biol 9: 145-153.
5. Antonellis A, Ellsworth RE, Sambuughin N, Puls I, Abel A, et al. (2003) Glycyl tRNA synthetase mutations in Charcot-Marie-Tooth disease type 2D and distal spinal muscular atrophy type V. Am J Hum Genet 72: 1293-1299.
6. Antonellis A, Lee-Lin SQ, Wasterlain A, Leo P, Quezado M, et al. (2006) Functional analyses of glycyl-tRNA synthetase mutations suggest a key role for tRNA-charging enzymes in peripheral axons. J Neurosci 26: 10397-10406.
7. Motley WW, Talbot K, Fischbeck KH (2010) GARS axonopathy: not every neuron's cup of tRNA. Trends in Neurosciences 33: 59-66.
8. Lee HJ, Park J, Nakhro K, Park JM, Hur Y-M, et al. (2012) Two novel mutations of GARS in Korean families with distal hereditary motor neuropathy type V. Journal of the Peripheral Nervous System 17: 418–421.
9. Yao P, Fox PL (2013) Aminoacyl-tRNA synthetases in medicine and disease. EMBO Mol Med 5: 332-343.
10. Wallen RC, Antonellis A (2013) To charge or not to charge: mechanistic insights into neuropathy-associated tRNA synthetase mutations. Curr Opin Genet Dev 23: 302-309.
11. Mahler M, Miller FW, Fritzler MJ (2014) Idiopathic inflammatory myopathies and the anti-synthetase syndrome: A comprehensive review. Autoimmunity Reviews 13: 367-371.
12. Mun J, Kim Y-H, Yu J, Bae J, Noh D-Y, et al. (2010) A proteomic approach based on multiple parallel separation for the unambiguous identification of an antibody cognate antigen. ELECTROPHORESIS 31: 3428-3436.
13. Park MC, Kang T, Jin D, Han JM, Kim SB, et al. (2012) Secreted human glycyl-tRNA synthetase implicated in defense against ERK-activated tumorigenesis. Proceedings of the National Academy of Sciences 109: E640-E647.
14. Andreev DE, Hirnet J, Terenin IM, Dmitriev SE, Niepmann M, et al. (2012) Glycyl-tRNA synthetase specifically binds to the poliovirus IRES to activate translation initiation. Nucleic Acids Research 40: 5602-5614.
15. Shiba K, Schimmel P, Motegi H, Noda T (1994) Human glycyl-tRNA synthetase. Wide divergence of primary structure from bacterial counterpart and species-specific aminoacylation. Journal of Biological Chemistry 269: 30049–30055.
16. Williams J, Osvath S, Khong TF, Pearse M, Power D (1995) Cloning, sequencing and bacterial expression of human glycine tRNA synthetase. Nucleic acids research 23: 1307-1310.
17. Mudge SJ, Williams JH, Eyre HJ, Sutherland GR, Cowan PJ, et al. (1998) Complex organisation of the 5′-end of the human glycine tRNA synthetase gene. Gene 209: 45–50.
18. Kozak M (1986) Influences of mRNA secondary structure on initiation by eukaryotic ribosomes. Proceedings of the National Academy of Sciences 83: 2850–2854.
19. Stoneley M (1998) C-Myc 5′ untranslated region contains an internal ribosome entry segment. , Published online: 21 January 1998; | doi:101038/sjonc1201763 16.

20. Coldwell MJ, Mitchell SA, Stoneley M, MacFarlane M, Willis AE (2000) Initiation of Apaf-1 translation by internal ribosome entry. Oncogene 19: 899-905.
21. Blais JD, Addison CL, Edge R, Falls T, Zhao H, et al. (2006) Perk-Dependent Translational Regulation Promotes Tumor Cell Adaptation and Angiogenesis in Response to Hypoxic Stress. Molecular and Cellular Biology 26: 9517-9532.
22. Spriggs KA, Bushell M, Willis AE (2010) Translational regulation of gene expression during conditions of cell stress. Mol Cell 40: 228-237.
23. Spriggs KA, Stoneley M, Bushell M, Willis AE (2008) Re-programming of translation following cell stress allows IRES-mediated translation to predominate. Biol Cell 100: 27-38.
24. Komar AA, Hatzoglou M (2011) Cellular IRES-mediated translation: The war of ITAFs in pathophysiological states. Cell Cycle 10: 229-240.
25. Lescoute A, Westhof E (2005) Riboswitch structures: purine ligands replace tertiary contacts. Chemistry & Biology 12: 10-13.
26. Kozak M (2002) Pushing the limits of the scanning mechanism for initiation of translation. Gene 299: 1–34.
27. Hinnebusch AG (2011) Molecular mechanism of scanning and start codon selection in eukaryotes. Microbiol Mol Biol Rev 75: 434-467, first page of table of contents.
28. Spriggs KA, Bushell M, Mitchell SA, Willis AE (2005) Internal ribosome entry segment-mediated translation during apoptosis: the role of IRES-trans-acting factors. Cell Death & Differentiation 12: 585-591.
29. Baird SD, Lewis SM, Turcotte M, Holcik M (2007) A search for structurally similar cellular internal ribosome entry sites. Nucleic Acids Research 35: 4664-4677.
30. Calvo SE, Pagliarini DJ, Mootha VK (2009) Upstream open reading frames cause widespread reduction of protein expression and are polymorphic among humans. Proceedings of the National Academy of Sciences 106: 7507–7512.
31. Jackson RJ, Hellen CU, Pestova TV (2010) The mechanism of eukaryotic translation initiation and principles of its regulation. Nat Rev Mol Cell Biol 11: 113-127.
32. Jackson RJ, Hellen CU, Pestova TV (2012) Termination and post-termination events in eukaryotic translation. Adv Protein Chem Struct Biol 86: 45-93.
33. Ingolia Nicholas T, Lareau Liana F, Weissman Jonathan S (2011) Ribosome Profiling of Mouse Embryonic Stem Cells Reveals the Complexity and Dynamics of Mammalian Proteomes. Cell 147: 789-802.
34. David A, Netzer N, Strader MB, Das SR, Chen CY, et al. (2011) RNA Binding Targets Aminoacyl-tRNA Synthetases to Translating Ribosomes. Journal of Biological Chemistry 286: 20688-20700.
35. Popenko VI, Ivanova JL, Cherny NE, Filonenko VV, Beresten SF, et al. (1994) Compartmentalization of certain components of the protein synthesis apparatus in mammalian cells. Eur J Cell Biol 65: 60-69.
36. Stapulionis R, Deutscher MP (1995) A channeled tRNA cycle during mammalian protein synthesis. Proc Natl Acad Sci U S A 92: 7158-7161.
37. Hermesh O, Jansen R-P (2013) Take the (RN)A-train: Localization of mRNA to the endoplasmic reticulum. Biochimica et Biophysica Acta (BBA) - Molecular Cell Research 1833: 2519-2525.
38. Choo KH, Ranganathan S (2008) Flanking signal and mature peptide residues influence signal peptide cleavage. BMC Bioinformatics 9: S15.
39. Targoff IN (1990) Autoantibodies to aminoacyl-transfer RNA synthetases for isoleucine and glycine. Two additional synthetases are antigenic in myositis. Journal of Immunology (Baltimore, Md: 1950) 144: 1737-1743.

40. Targoff IN, Trieu EP, Plotz PH, Miller FW (1992) Antibodies to glycyl-transfer RNA synthetase in patients with myositis and interstitial lung disease. Arthritis Rheum 35: 821-830.
41. Hervé C, Mickleburgh I, Hesketh J (2004) Zipcodes and postage stamps: mRNA localisation signals and their trans-acting binding proteins. Briefings in functional genomics & proteomics 3: 240–256.
42. Weis BL, Schleiff E, Zerges W (2013) Protein targeting to subcellular organelles via MRNA localization. Biochim Biophys Acta 1833: 260-273.
43. Stephens SB, Nicchitta CV (2009) mRNA Translation on the Endoplasmic Reticulum: Kinetic Advantages to Protein Synthesis on the ER
. In: Zimmermann R, editor. Protein Transport into the Endoplasmic Reticulum: Landes Bioscience.
44. Will S, Joshi T, Hofacker IL, Stadler PF, Backofen R (2012) LocARNA-P: accurate boundary prediction and improved detection of structural RNAs. RNA 18: 900–914.
45. Jossinet F, Ludwig TE, Westhof E (2010) Assemble: an interactive graphical tool to analyze and build RNA architectures at the 2D and 3D levels. Bioinformatics 26: 2057–2059.

SUPPLEMENTARY FIGURES

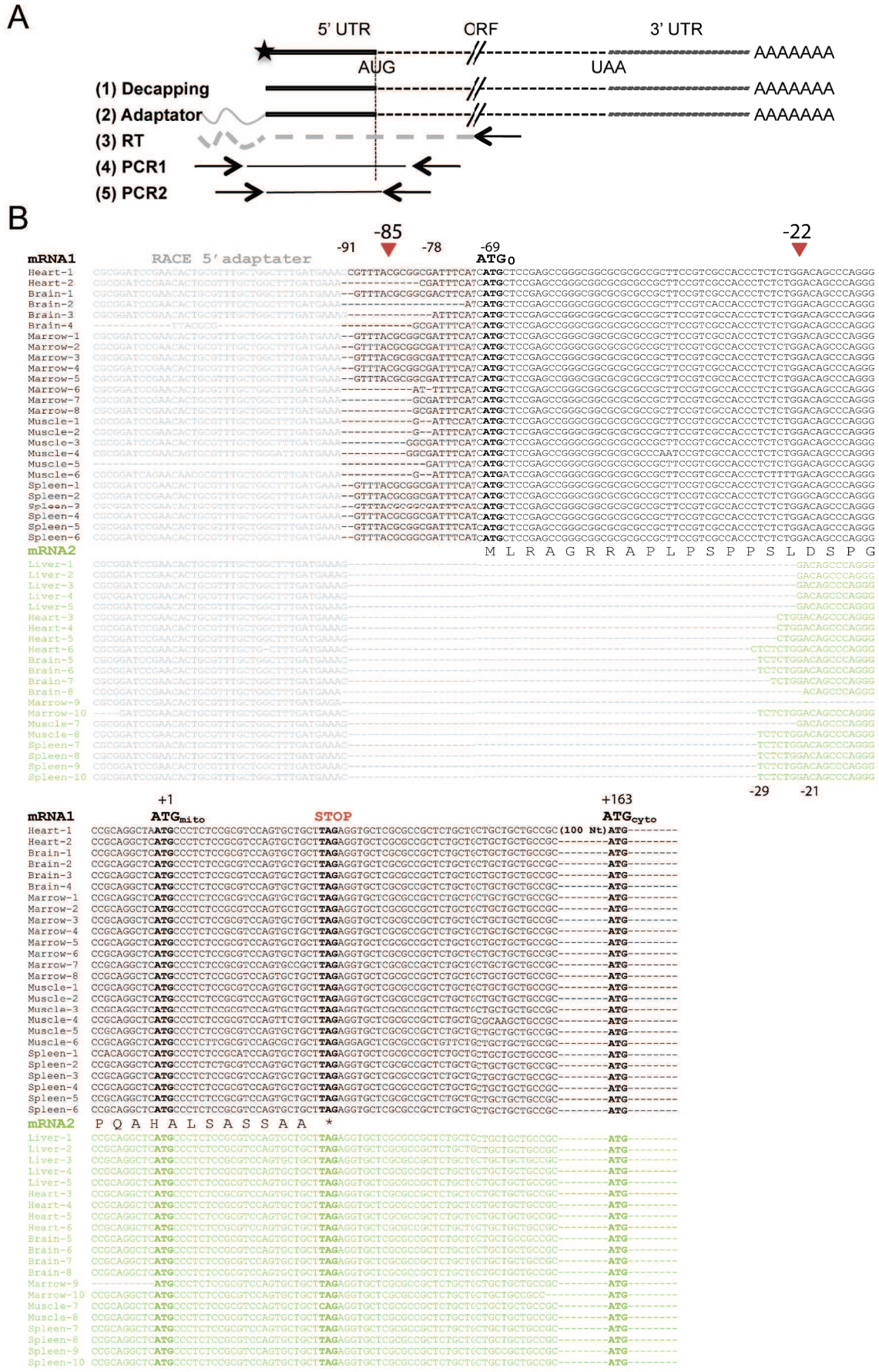

SUPPLEMENTARY FIGURE 1: Sequences of human GRS mRNA isoforms identified by RACE-PCR. (A) 5'-RLM RACE PCR principle: UTRs and ORF are indicated. In 5'-RLM-RACE experiments, mRNA is first (1) decapped, (2) ligated to a 5'-adapter, and (3) reverse transcribed using a specific primer. The resulting cDNA is then amplified by two successive PCR reactions (4 and 5) with primers complementary to the adapter and designed intentionally to hybridize after the AUG codon of interest. (B) Sequencing results of the 5'-RLM RACE PCR experiment on total RNA extracted from 6 different human tissues (heart, brain, bone marrow, muscle, spleen and liver). Sequences were ordered according to the tissue source and the length of the 5'-UTR (mRNA1 or mRNA2). The RACE 5'-adapter sequence is indicated in grey, the three ATGs and the stop codon are in bold and the amino acid sequence of the short peptide encoded by the uORF is shown below.

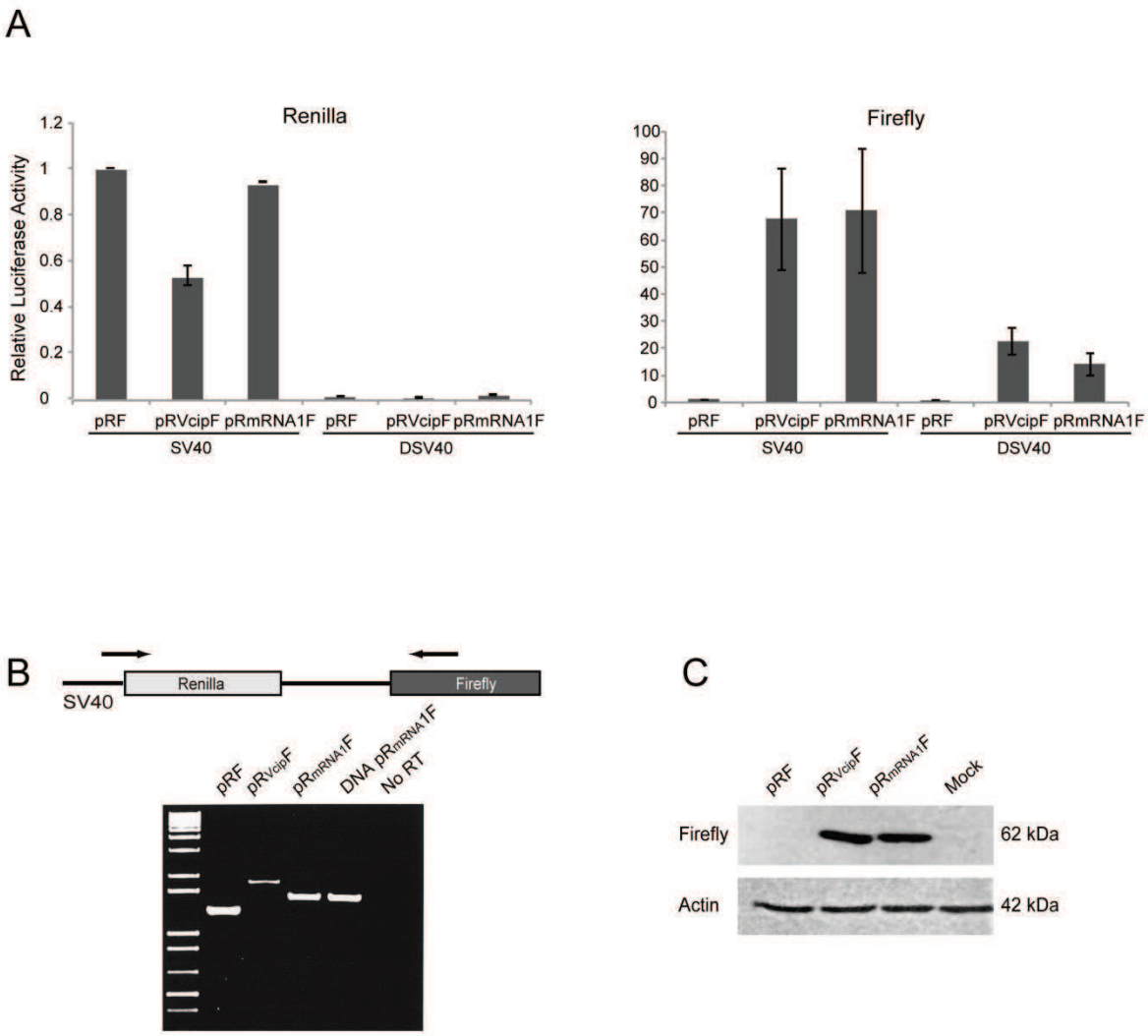

SUPPLEMENTARY FIGURE 2: Control experiments to rule out second cistron expression from the bicistronic reporter pRF. (A) Ruling out cryptic promoters: Absence of a cryptic promoter was eliminated by transfection of promoterless reporters (ΔSV40). In the absence of the SV40 promoter, no mRNA is generated and expression of the renilla and firefly luciferases was drastically reduced. (B) Eliminating splicing eventualities: The schematic representation of pRF indicates the positions of the primers used for the RT-PCR analysis (arrows). RT-PCR analysis was performed on total RNA extracted from transfected COS-7 cells (with the three reporter constructs: pRF, $pR_{Vcip}F$ and $pR_{mRNA1}F$). Two controls were achieved: (i) a direct PCR amplification (no RT) was done on $pR_{mRNA1}F$ transfected cells to rule out the presence of residual DNA in the RNA preparation, and (ii) the $pR_{mRNA1}F$ vector DNA was used as a positive control to verify the size of the amplified product. (C) Ruling out ribosome readthrough: Western blot analysis shows that the firefly luciferase is translated as such (62 kDa) from both $pR_{Vcip}F$ and $pR_{mRNA1}F$ constructs. ß-actin (42 kDa) detection was used as loading control.

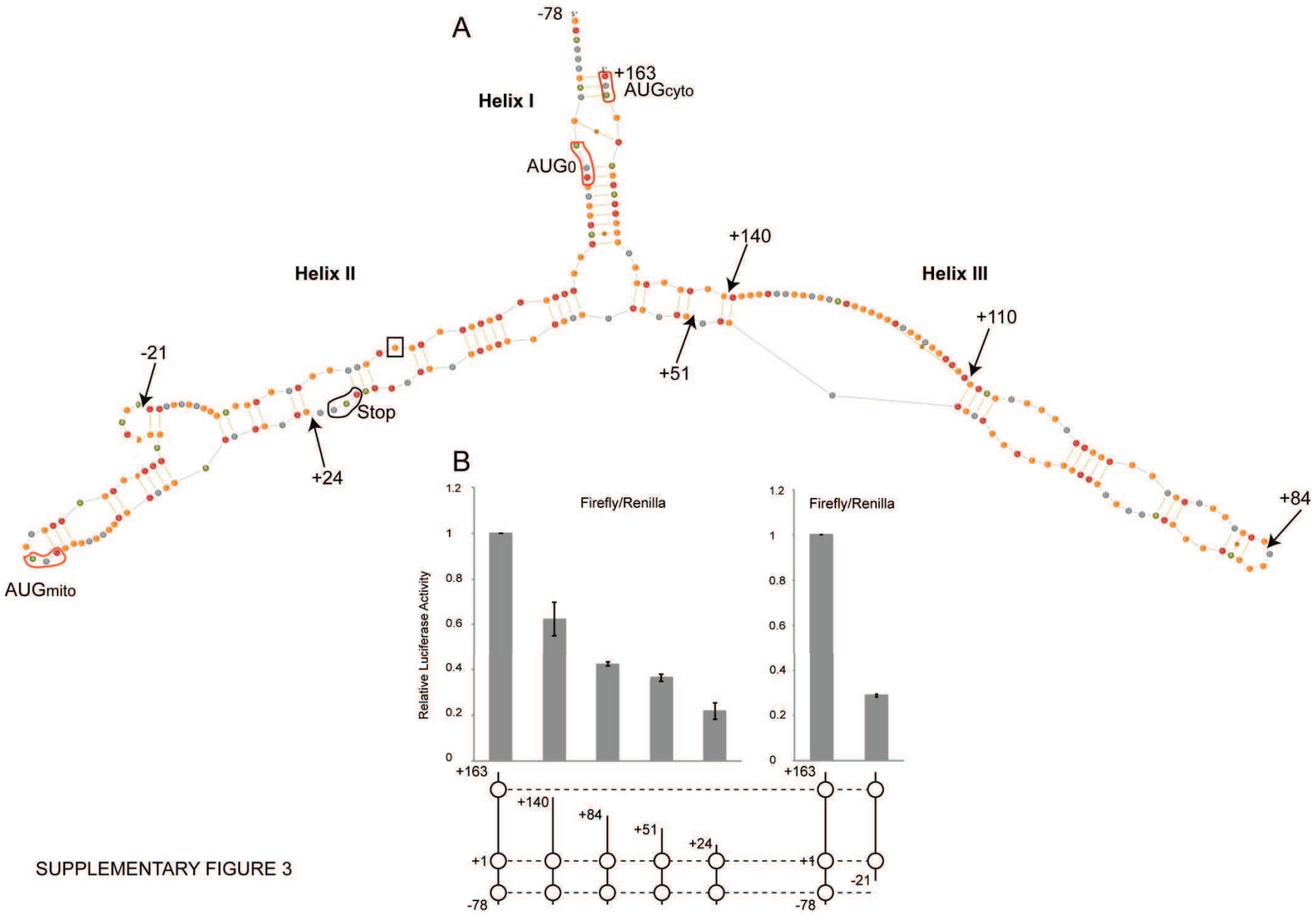

SUPPLEMENTARY FIGURE 3

SUPPLEMENTARY FIGURE 3: Alignment-based secondary structure of mRNA1 IRES. This model was built using LocARNA [44] and Assemble [45] Programs. (A) The 3 AUG initiator codons are circled in red, the uORF stop codon in black, and the frameshift deletion is squared. The sites for progressive shortening of mRNA1 are indicated by arrows. (B) Short versions of the mRNA1 IRES sequence were cloned in pRF and their respective luciferase activities were measured. Graphic representations of $pR_{mRNA1}F$, $pR_{mRNA1}F$ deletants and $pR_{mRNA2}F$ activities are relative to the pRF negative control. Error bars were calculated from 3 independent experiments.

II. HUMAN GRS EXPRESSION AND FUNCTION IN NEURONS

Worldwide, several teams are studying GRS in hereditary peripheral neuropathies. These studies have been published between 2003 and today and concern various aspects, going from *in vitro* structural and functional studies to the design of animal models (reviewed in Motley *et al.,* 2010; Wallen and Antonellis 2013). Most of the work has been done in order to characterize GRS pathogenic mutants. All data collected by our colleagues on GRS mutations and their possible implications in CMT2D or dSMA-V are focused on GRS canonical function. Because different mutations have different effects on GRS aminoacylation activity, localization and dimerization (Antonellis *et al.,* 2006; Nangle *et al.,* 2007; Xie *et al.,* 2007; He *et al.,* 2011), it was proposed that all these alterations are important for an alternative neuron-specific function of GRS.

During the first 3 years of my PhD, I studied the molecular mechanisms that control GRS expression. This allowed us to understand how GRS accumulates differentially in the cytosol and the mitochondria, but also to observe that, at least in our hands, the formation of GRS granules observed by Antonnellis' group was less obvious (Antonellis *et al.,* 2006). This led us to postulate, like other groups, the existence of an alternative function where the formation of GRS granules depends on the presence of specific neuronal proteins. We based our working hypothesis on the fact that glycine (the GRS substrate) is part of a complex and still enigmatic network of secretory vesicles in inhibitory neurons (Gasnier, 2000). We thus decided to investigate the putative functions of GRS in glycine loading into these neuronal synaptic vesicles.

1. Mitochondrial and Cytoslic GRS expression in neurons

First, we characterized the expression of GRS from mRNA1 and mRNA2 in differentiated SH-SY5Y human neuroblastoma cells. In these neuronal cells (Figure 30 A), similar to our previous study in COS-7 cells *(see Article-Figure 2 A)*, the GRS expression level was lower when translated from mRNA1 than from mRNA2. Nevertheless, both mRNA isoforms were able to generate GRS that localizes in the cell body but also in the neuronal projections as previously described (Antonellis *et al.,* 2006; Nangle *et al.,* 2007) (Figure 30 B). Because of the particular cellular shape (thick and thus difficult to observe, even by confocal microscopy) of the differentiated SH-SY5Y compared to the flat and large COS-7 cells, it was impossible to accurately differentiate the mitochondrial from the cytosolic enzyme. Moreover, GRS distribution seemed more or less homogenous in the cell. Based on this finding, the question

we wanted to answer next was how and why some of the previous studies described clearcut GRS accumulation in granular neuronal structures (Antonellis *et al.,* 2006; Stum *et al.,* 2011)…and not us?

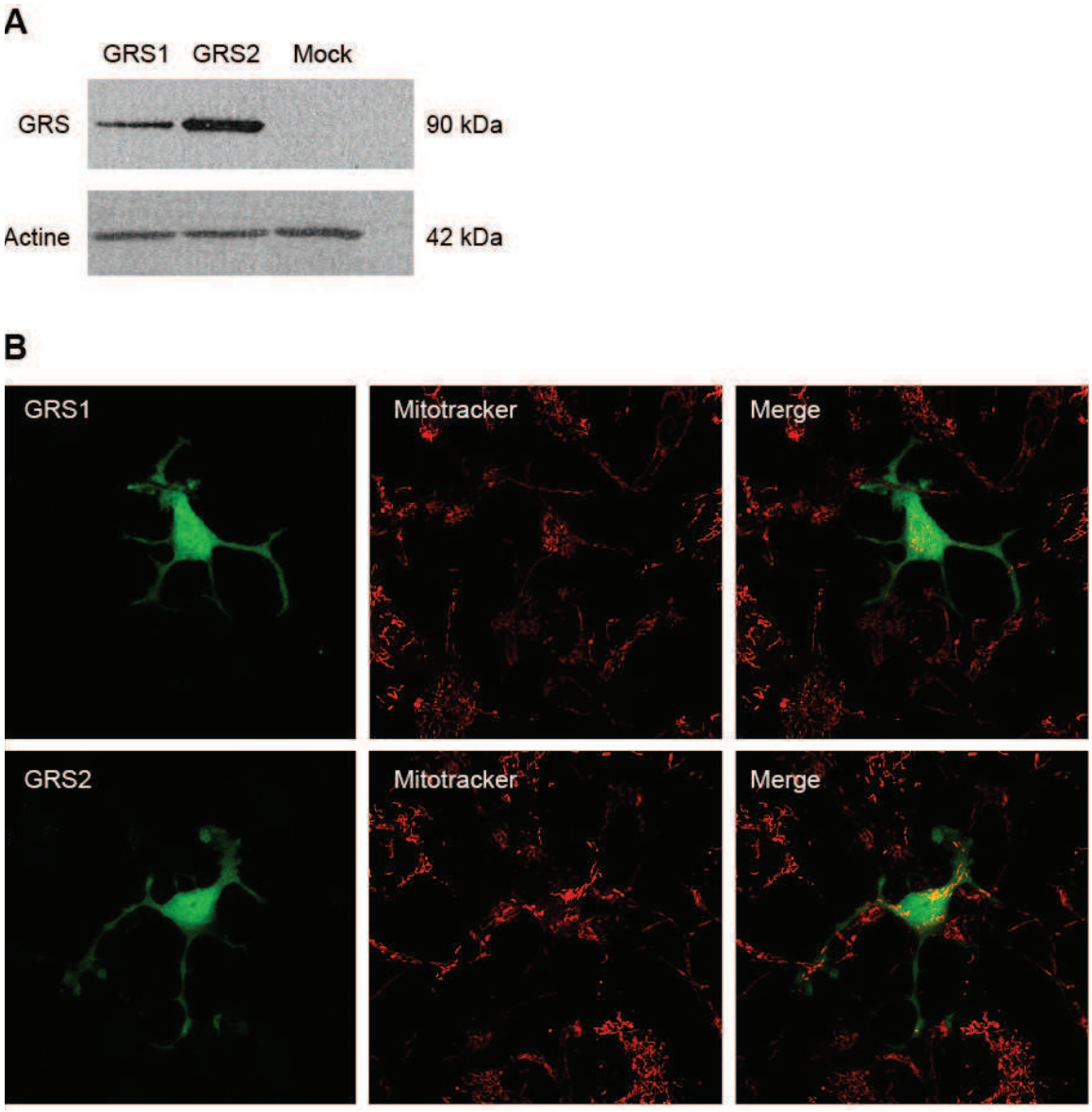

Figure 30. GRS expression in neurons

pcDNA3.1-mRNA1 and pcDNA3.1-mRNA2 constructs were transiently transfected in differentiated SH-SY5Y neuroblastoma cells. GRS was fused to a V5 epitope at its C-terminus, allowing protein detection *via* an anti-V5-tag antibody. **(A)** Western blot analysis: Anti-V5 HRP conjugated antibody detects the cytosolic GRS (≈ 90 kDa), and anti-actin antibody, the 42 kDa β-actin. **(B)** Mitochondrial and cytosolic GRS were detected by immunofluorescence, using an anti-V5 antibody coupled to FITC (green) and mitochondria were stained with Mitotracker Orange CMTMRos (red). Merged images show a specific localization of GRS detectable in the cytoplasm of the cell body and neurite projections for both mRNA1 and mRNA2.

2. GRS accumulates in granules

When overexpressing mRNA1 and mRNA2 (in pcDNA3.1 expression vectors) in differentiated SH-SY5Y neuroblasts, we noticed that GRS localization was not concentrated in granules as observed by Antonellis and collaborators (Antonellis *et al.,* 2006). On the contrary, we observed a diffused expression like Nangle and collaborators (Nangle *et al.,* 2007). However, the main difference between both studies lies in the approach of GRS detection and the cell types used. Indeed, the granular structures observed by Antonellis were detected with an antibody directed against the endogenous GRS in (i) peripheral nerve axons *in vivo*, (ii) SH-SY5Y differentiated cells and (iii) 40 % of GRS transfected mouse MN1 motoneurons. Yet, in the study performed by Nangle and collaborators, WT GRS and mutants fused to a V5-tag were overexpressed in differentiated N2a mouse neuroblasts. Based on these data, we decided to abandon V5-tagged GRS overexpression and to perform our experiments by seeking endogenous GRS granules with GRS-specific antibodies, in order to avoid off-target results due to the C terminal V5 epitope. Moreover, we are aware that experimental conditions may vary considerably from one laboratory to another, so we chose to test different conditions, by adding $CaCl_2$ and KCl, known to induce neuronal activation.

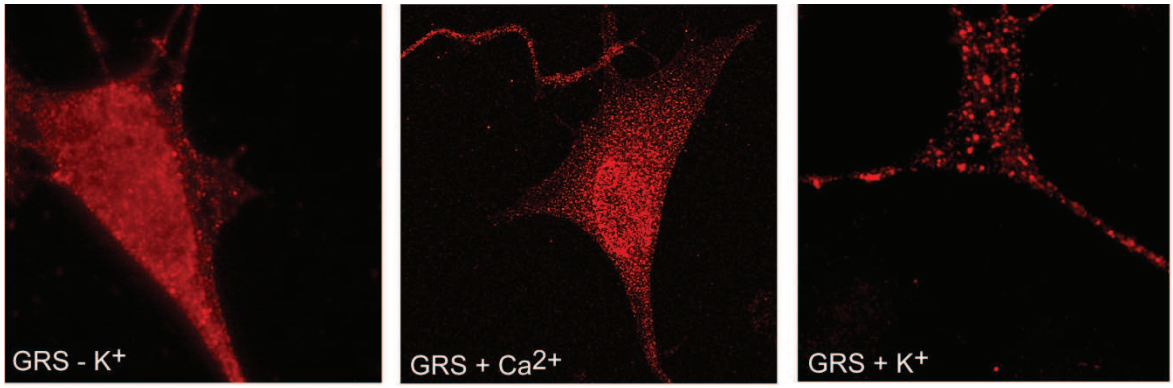

Figure 31. GRS granule formation in neurons
Differentiated SH-SY5Y cells were **(A)** left untreated or **(B)** treated with 5 mM Ca^{2+} for 15 minutes or **(C)** with 30 mM KCl for 10 minutes. Endogenous GRS was detected by specific monoclonal rabbit anti GRS antibody (red).

2.1. K+/Ca2+ dependent granules formation

In our hands, when detected in differentiated SH-SY5Y cells, endogenous GRS was localized in small puncta dispersed in the cell body and the neuronal projections (Figure 30 A). When we treated cells with 5 mM $CaCl_2$, we didn't observe significant changes, yet puncta seemed more regular (Figure 30 B). Surprisingly, in the presence of 30 mM KCl, we detected the

expected granules (Figure 30 C). Addition of calcium and potassium in differentiated neuron cultures leads to Ca^{2+} channel opening and thus induces synaptic vesicle release. The potassium-induced granular localization of GRS led us to the following hypothesis: in neuronal cells such as the SH-SY5Y cell line, GRS could be localized in proximity of synaptic vesicles, and could be potentially involved in synaptic transmission.

2.2. GRS and synaptic vesicles colocalization

Once we identified physiological conditions that lead to the formation of GRS granules in neuronal cells (which corroborate the results obtained by Antonellis) we sought to explore the nature of these granules and their potential role in nerve signal transduction. Therefore, we performed a colocalization experiment with endogenous GRS and the presynaptic vesicle marker synaptophysin (Figure 32). The superimposition of the two signals was not perfect, but let us sense a proximity between GRS granules and synaptophysin. Interestingly, this vicinity appeared to be clearer in neuronal projections than in the cellular body.

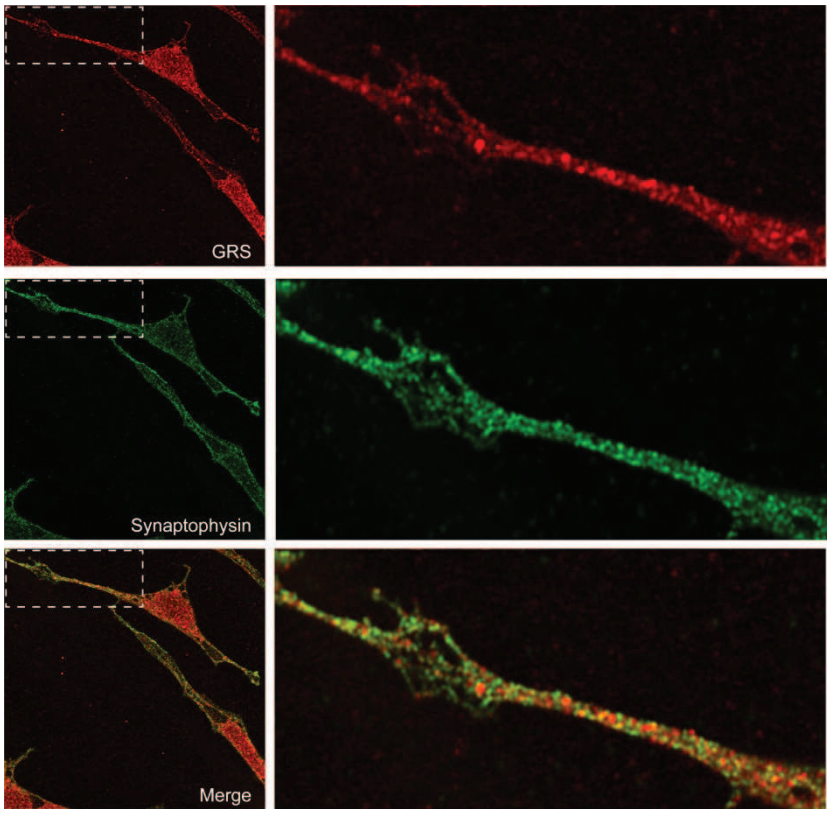

Figure 32. GRS and synaptic vesicle colocalization

GRS granules (red) localize in close proximity with the synaptic vesicle protein synaptophysin (green) in differentiated SH-SY5Y cells. Merged images show a partial superimposition of GRS granules with synaptic vesicles, increased in neuronal projections. The right panel is a magnified presentation of the boxed regions.

3. A possible role of GRS in Glycinergic transmission

Our results showing that GRS granules partially colocalize with synaptic vesicles (synaptophysin) led us to question granule formation in peripheral nerve axons and to propose a new working hypothesis: by binding the Vesicular Inhibitory Amino Acid Transporter (VIAAT), specifically expressed in glycinergic neurons, GRS would control glycine accumulation in synaptic vesicles. The last part of my project was thus focused on GRS's possible involvement in glycinergic transmission.

3.1. Glycinergic/GABA inhibitory transmission and the synaptic vesicle transporter VIAAT

Glycine and GABA are the major fast inhibitory neurotransmitters. Both amino acids share the same transporter VIAAT, a transmembrane protein in charge of entering glycine and GABA into synaptic vesicles (Dumoulin *et al.,* 1999). But, the mechanism of selection between GABA and glycine is poorly understood (Aubrey *et al.,* 2007) (Figure 33 A).

Two observations described in the literature prompted us to think that there is a missing element present in vertebrates and absent in other eukaryotic organisms. Some of them (plants, protozoans, insects and nematodes) do not perform glycinergic transmission that would require vesicle loading with glycine:

First, in vertebrates, VIAAT has a much lower affinity for glycine than for GABA, a situation that makes glycine accumulation in synaptic vesicles difficult to explain (McIntire *et al.,* 1997).

Second, the nematode *C. elegans* VIAAT homolog, UNC-47, is able to load glycine in vesicular structures when expressed in human pancreatic cells (BON cells). Since glycinergic neurotransmission is not present in *C. elegans*, it was surprising that UNC-47 could still recognize and transport glycine.

We propose that this missing element could be GRS, which is significantly different between vertebrates and other eukaryotic organisms that do not perform glycinergic transmission. Thus, we speculated that, in glycinergic neurons, VIAAT and GRS would collaborate to bind glycine (thanks to the GRS active site) to allow glycine loading in synaptic vesicles (thanks to VIAAT) (Figure 33 B).

3.2. VIAAT specifically relocalizes GRS

In order to test our hypothesis, we co-transfected human cytosolic GRS and rat VIAAT (kind gift of Dr Bruno Gasnier) in COS-7 cells. Indeed, Dumoulin and collaborators have shown that overexpression of VIAAT in COS-7 kidney cells induces VIAAT accumulation in

intracellular vesicular structures able to load glycine inside. (Dumoulin *et al.,* 1999; Sagné *et al.,* 1997) (Figure 34).

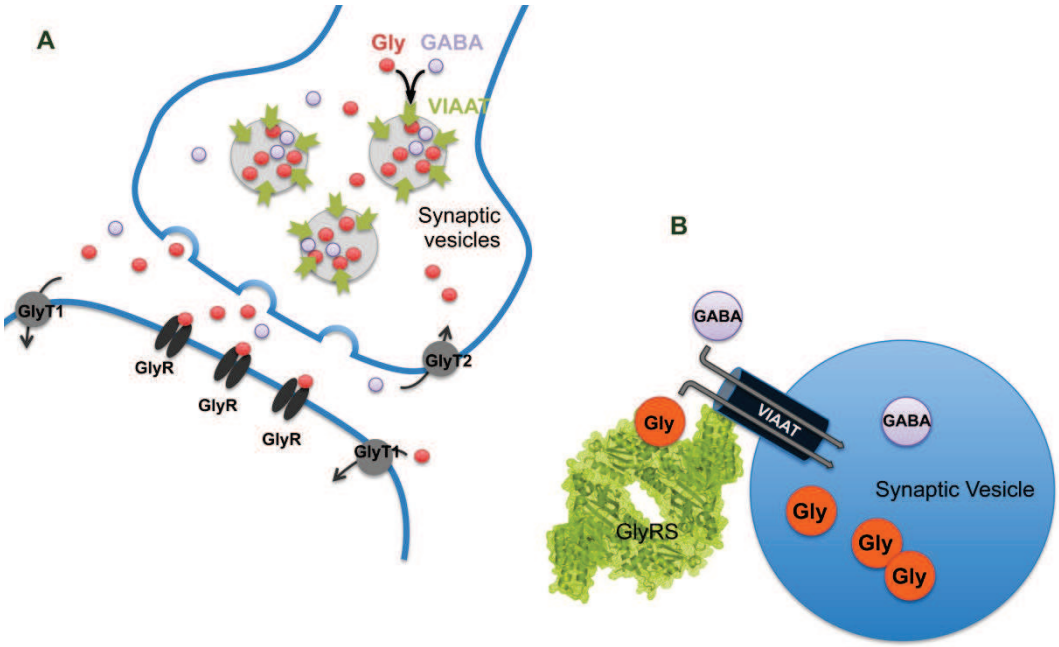

Figure 33. Our working hypothesis: GRS is involved in glycinergic transmission
(A) Organization of the inhibitory neuron synaptic junction: In the pre-synaptic neuron, synaptic vesicles are loaded with glycine (red) and GABA (light purple) by their shared transporter VIAAT (green). The GlyT2 transporter (grey) is responsible for glycine reuptake and neuron refilling. In post-synpatic neurons, glycine receptors (GlyR) conduct glycinergic neurotransmission and GlyT1 transporters manage glycine clearance from the synaptic cleft. **(B)** Loading synaptic vesicles with glycine: According to our hypothesis, GRS (green) would interact with VIAAT (dark blue) to channel and promote efficient glycine loading into the synaptic vesicle.

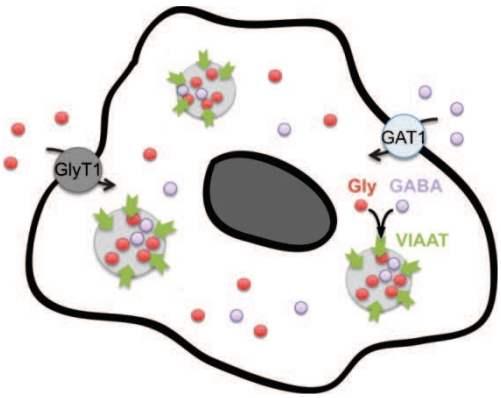

Figure 34. COS-7 mimic of synaptic filling with glycine and GABA
Transfected glycine and GABA transporters GlyT1 and GAT1 are in charge of glycine and GABA uptake in COS-7 cells. When co-transfected with VIAAT, glycine and GABA are both loaded in artificial vesicle structures, mimicking synaptic vesicle loading (according to Sagné *et al.,* 1997).

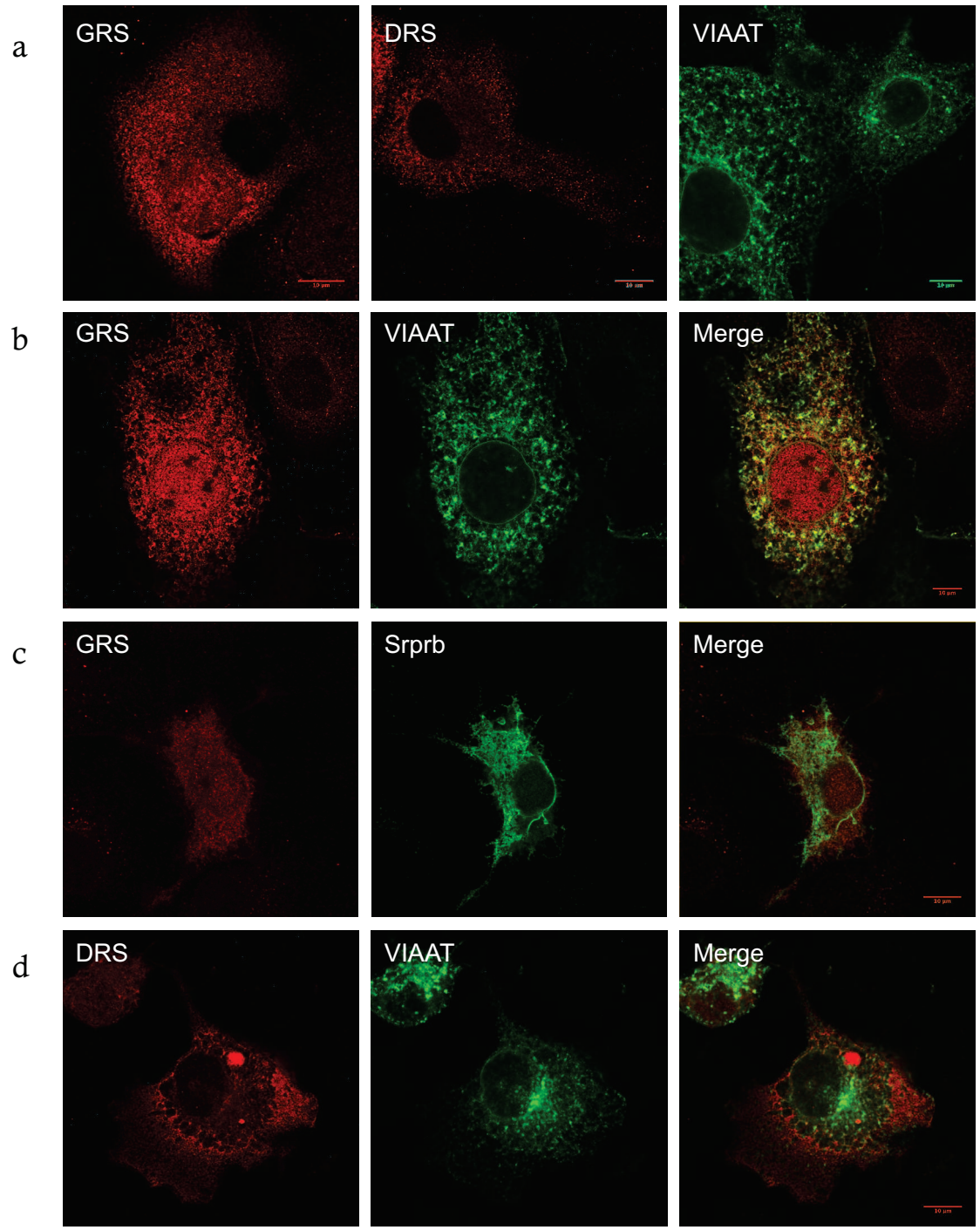

Figure 35. GRS and VIAAT colocalization

GRS was expressed alone, with VIAAT or with the B subunit of the signal recognition particle receptor (Srprb) in COS-7 cells. Likewise, VIAAT was transfected alone or co-transfected with the human aspartyl-tRNA synthetase (DRS). Transfected GRS was detected *via* an anti-V5 tag antibody, whereas other proteins were detected *via* specific antibodies. When expressed alone, GRS and DRS display diffuse localization, while VIAAT is distributed in vesicular structures (Dumoulin *et al.,* 1999) (a).

Based on these previous experiments, we decided to co-express GRS with VIAAT in COS-7 cells (a cellular model that we know behaves adequately in transfection and microscopy experiments), in order to see if GRS forms granules and if these granules in turn colocalize with VIAAT. We observed a radical change in the GRS localization profile from diffuse (Figure 35, a and b) to granule-like structures that partially colocalize with VIAAT. In control experiments, if we replace VIAAT by the B subunit of the signal recognition particle receptor (Srprb) (a protein also expressed in the endoplasmic reticulum) or GRS by another aminoacyl-tRNA synthetase (aspartyl-tRNA synthetase: DRS), we do not observe any colocalization (Figure 35 c and d), suggesting that the partial colocalisation of VIAAT and GRS is specific to those two proteins.

3.3. GRS mutants and VIAAT co-expression and colocalization

Subsequently, we wanted to test the specificity of this colocalization by identifying the GRS domain involved in its interaction with VIAAT. We performed a multiple sequence alignment and chose domains that are significantly different between vertebrates and other eukaryotic organisms that do not perform glycinergic transmission (e.g. plants, protozoans, and especially insects and nematodes). These invertebrates do not have functional glycine receptors and instead use only GABA, or sometimes glutamate, to mediate inhibitory neurotransmission (Chalphin and Saha, 2010). The human GRS domains that we deleted are indicated in Figure 36 and correspond to the N-terminal WHEP domain, insertions 2 and 3 in the catalytic domain and the C-terminal peptide. We decided to exclude the active site from our deletion program, because it is already involved in glycine and ATP binding. Since glycinergic neurotransmission is not present in the nematode *C. elegans*, we also cloned the GRS gene from *C. elegans*. We imagined that this protein would be the best negative control in our colocalization experiments with VIAAT.

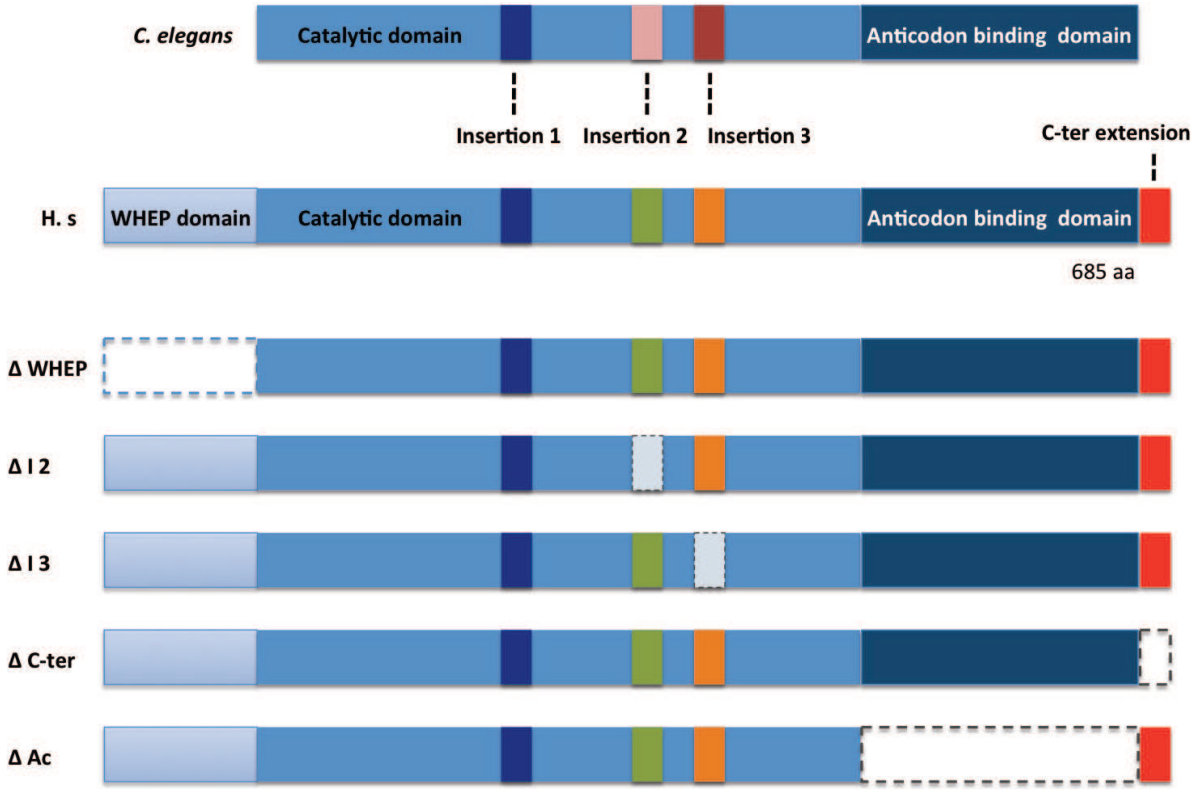

Figure 36. Comparison of domain organizations of *C. elegans* and human GRSs and design of human GRS deletants

Based on sequence comparisons between both GRSs, several variants of the human GRS were designed, missing the WHEP domain (light blue), Insertions 2 (I2) (green) or 3 (I3) (orange), the anticodon domain (Ac) (dark blue) or the C-terminal peptide (C-ter) (red). Insertion 1 in the catalytic domain does not vary significantly between these enzymes and was not tested.

So far, we could only assess the localization of three mutants: those lacking either the WHEP domain, Insertion 2 or Insertion 3 in the catalytic domain. In each case, we obtained a perfect colocalization between the mutated GRSs and VIAAT (Figure 37). Thus, none of these domains (WHEP, I2 or I3) are involved in colocalization between GRS and VIAAT. Moreover, it appears that the deletions we performed induced structural changes in protein folding that make the GRS interaction domain more accessible to VIAAT.

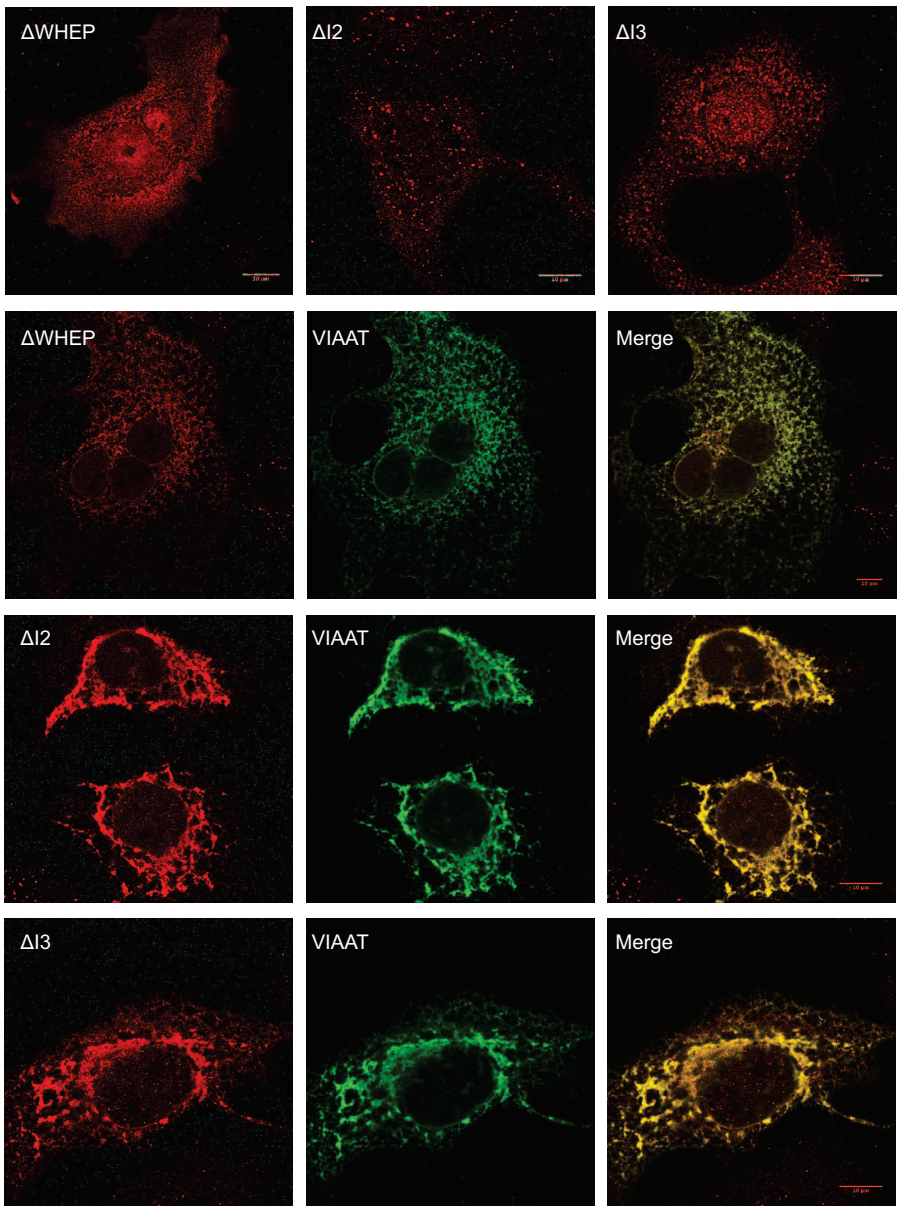

Figure 37. GRS mutants and VIAAT colocalization
GRS mutants lacking the WHEP domain, Insertion 2 or Insertion 3 were transfected alone or with VIAAT in COS-7 cells. Transfected GRS mutants were detected *via* an anti-V5 tag antibody. When transfected alone, GRS mutants are more or less diffuse in the cytoplasm, whereas all of them colocalize with VIAAT.

Although our results show that human GRS colocalizes with VIAAT, we still have to test the *C. elegans* GRS as well as the two mutants lacking the anticodon domain and the C-terminal region. All these proteins should also be tested without the C-terminal V5-tag. This is especially relevant since the major difference between the Antonellis and Schimmel laboratories when looking for GRS granules was the absence or the presence of such a tag at the C-terminus of the protein (Antonellis *et al.,* 2006; Nangle *et al.,* 2007).

3.4. Conclusions

In this study, we showed that both mRNA1 and mRNA2 are translated in differentiated SH-SY5Y neuroblasts and the produced GRS localizes in both the cell body and neuronal projections. Like in COS-7 cells, we obtained better GRS expression from mRNA2 than from mRNA1, but here, due to technical limitations (SH-SY5Y sensitivity to digitonin treatment), we couldn't distinguish the mitochondrial from the cytoplasmic or the ER-bound enzymes. Moreover, we didn't observe any particular granular distribution as previously observed by Antonellis and collaborators (Antonellis *et al.,* 2006). Interestingly, when we shifted our localization study from V5-tagged GRS to endogenous GRS in differentiated SH-SY5Y neuroblasts, we could identify GRS accumulation in small granules. By doing so, we avoided interference due to the C-terminal V5-tag that we initially inserted for exogenous GRS detection. Surprisingly, when neurons were further treated with KCl, GRS accumulated in even bigger granules, which were more distinct in the neuronal projections when compared to the cell body. KCl treatment induces neuronal membrane depolarization and Ca^{2+} release, which in turn causes synaptic vesicle formation. For this reason, we tested the possible distribution of these GRS granules along with synaptic vesicles. We found that at least some of these granules were clearly colocalizing with the pre-synaptic vesicle marker synaptophysin.

Taking into consideration this particular GRS distribution in neurons and the results from other laboratories showing that CMT mutations didn't affect aminoacylation or dimerization of GRS (Antonellis *et al.,* 2006, Nangle *et al.,* 2007), it appears more and more likely that GRS has specific neuronal function(s). Together, observations showing that (i) GRS granular formation could be induced upon neuronal membrane depolarization, (ii) GRS colocalizes with synaptic vesicles, and (iii) glycine is both the GRS substrate and a major inhibitory neurotransmitter; led us to propose that GRS would play a role in glycinergic transmission.

Glycinergic along with GABAnergic neurons conduct inhibitory transmission in the central and peripheral nervous system. GABA and glycine neurotransmission could be triggered either by mixed GABA-glycine axon terminals, or purely glycine and purely GABA axon terminals. Glycinergic synapses are mainly located in the spinal cord, the brain stem and the retina (Gasnier, 2000) where they regulate a wide range of motor and sensory functions. Both neurotransmitters share the same vesicular inhibitory amino acid transporter (VIAAT) that loads GABA and glycine into synaptic vesicles. While the exact mechanism of glycine and GABA selectivity has not been determined, VIAAT exhibits higher affinity for GABA and it was proposed that competition for VIAAT loading is triggered by changes in the intracellular concentration of both neurotransmitters. Indeed, presynaptic GABA content depends on the

plasma membrane GABA transporter, GAT1 and the glutamate decarboxylase enzyme GAD65, whereas presynaptic glycine concentrations depend on the plasma membrane glycine transporter, GlyT2 (Aubrey *et al.,* 2007). Interestingly, the protein GAD65 associates with VIAAT on the synaptic vesicle and promotes GABA loading, thus providing a kinetic advantage over glycine for vesicular uptake. It was proposed that the VIAAT active site and the GAD65 catalytic site are tightly coupled to provide efficient transfer of GABA from its site of synthesis to the site of transport (Jin *et al.,* 2003). As synaptic glycine is mostly uptaken from the extracellular medium, one can imagine GRS as a good candidate to bind both VIAAT and its natural substrate glycine and channel glycine loading in the synaptic vesicle. Moreover, during evolution, glycinergic neurotransmission appeared within vertebrates (Chalphin and Saha, 2010), while in invertebrates, inhibitory neurotransmission is mediated by GABA or glutamate only. Thus, we think that GRS collaborates with VIAAT for efficient charging of glycine in synaptic vesicles and that the 12 amino acid GRS C-terminal extension could be the missing link between vertebrates and invertebrates that appeared co-evolutionary with glycinergic transmission.

In neurons, translation of dendritically localized mRNAs is thought to play a role in synaptic plasticity. Some dendritically-localized proteins (i.e. the α subunit of calcium–calmodulin-dependent kinase II, dendrin, microtubule-associated protein 2, activity-regulated cytoskeletal protein neurogranin) are translated from an mRNA containing an IRES and could be expressed in both cap–independent and cap-dependent manners (Pinkstaff *et al.,* 2001). In the case of GRS, the IRES structure we identified in mRNA1 could potentially increase the GRS concentration in neurons, not only to sustain local translation, but also to participate in vesicle loading with glycine.

III. STRUCTURAL STUDIES OF GRS MRNA 5'-UTRS

As already mentioned in *Introduction Ch.I*, protein expression is regulated at the posttranscriptional level before translation. Once the mRNA is synthesized in the nucleus, it already carries information about where, when and how to be translated. This information is primarily encoded by the RNA structure. Different RNA structural motifs allow each mRNA to be recognized by a large array of regulatory proteins, thus determining half-life, stability, particular localization, and recognition by the translation (ribosomal) machinery (Knapinska *et al.,* 2005; Hervé *et al.,* 2004).

In the results we obtained previously concerning the particular regulation of the human mitochondrial and cytosolic GRSs expression, the presence of two mRNAs with multiple initiation codons and an IRES, prompted us to determine the 5'-UTR structure of both mRNA isoforms (mRNA1 and mRNA2).

Several approaches are generally used to determine the structure of a given RNA. The theoretical determination is based on comparative analysis of homologous RNA sequences from different species and calculation of the most stable structure using the thermodynamic parameters of base pairing (Pace *et al.,* 1999). However, more accurate models can be achieved only by experimental approaches such as X-ray crystallography, nuclear magnetic resonance spectroscopy (NMR) or chemical and enzymatic probing. Chemical and enzymatic probing has been used over the last 35 years to precisely characterize the secondary structure of numerous RNAs from the tRNAs to complex viral genomes (Weeks *et al.,* 2010). Several reagents are used to probe RNA folding. Certain organic molecules like DMS, CMTC, kethoxal or metal ions can modify accessible unpaired groups of specific nucleotides and thus indicate which nucleotides are engaged in interactions and which are free. RNA molecules can be also treated with RNases T1, S1 and T2 to assign single stranded regions and with RNase V1 to assign double stranded domains. In order to obtain insight into the initiation codon disposition in the secondary structure of the IRES containing mRNA1 and the shorter mRNA2 or the presence of other regulatory structures, we chose three approaches: lead chemical probing, enzymatic probing, and SHAPE.

1. In solution RNA probing of GRS mRNA1 and mRNA2 5'-UTRs

We selected several fragments of different lengths containing the 5'-UTR of both mRNA1 and mRNA2 isoforms (from 100 to 1275 nt). RNA fragments were obtained by *in vitro* transcription, purified and kept in native conditions during the whole process. We first approached the problem by direct labelling on the 5' extremity of the molecules with [γ ^{32}P]-

ATP. Unfortunately, the RNA structures were so compact that the 5' extremity remained inaccessible and we could not obtain enough radiolabelled molecules, even in denaturating conditions.

As alternative approach, we chose the reverse transcription method where RNAs are first statistically modified by aformentioned chemicals or digested by RNases, and then reverse transcribed into cDNA using a specific radiolabeled oligodesoxyribonucleotide. The reverse transcriptase is stopped when it runs into modified nucleotides or RNA breaks. Sequencing reactions and controls are run in parallel, in order to determine the exact position of each modified/cut nucleotide and control the integrity of the probed RNA molecule *(see Material & Methods-Figure 44)*.

We first used lead (Pb^{2+}) to probe mRNA1 and mRNA2 5'-fragments, a treatment that reveals highly flexible non-paired regions in the folded RNA (Figure 38 A, B and C). We then performed RNase T1, S1 and V1 digestions (Figure 38 C). Unfortunately both RNA molecules were so structured that the reverse transcriptase stopped repetitively, presumably not because of the treatment but because of its inability to unwind the RNA structure. Indeed, as seen on Figure 38, control and sequencing experiments displayed strong stops, indicating that reverse transcriptase could not proceed steadily along the molecule. Moreover, the background signal was so elevated that putative signals due to chemical or enzymatic treatments couldn't be detected.

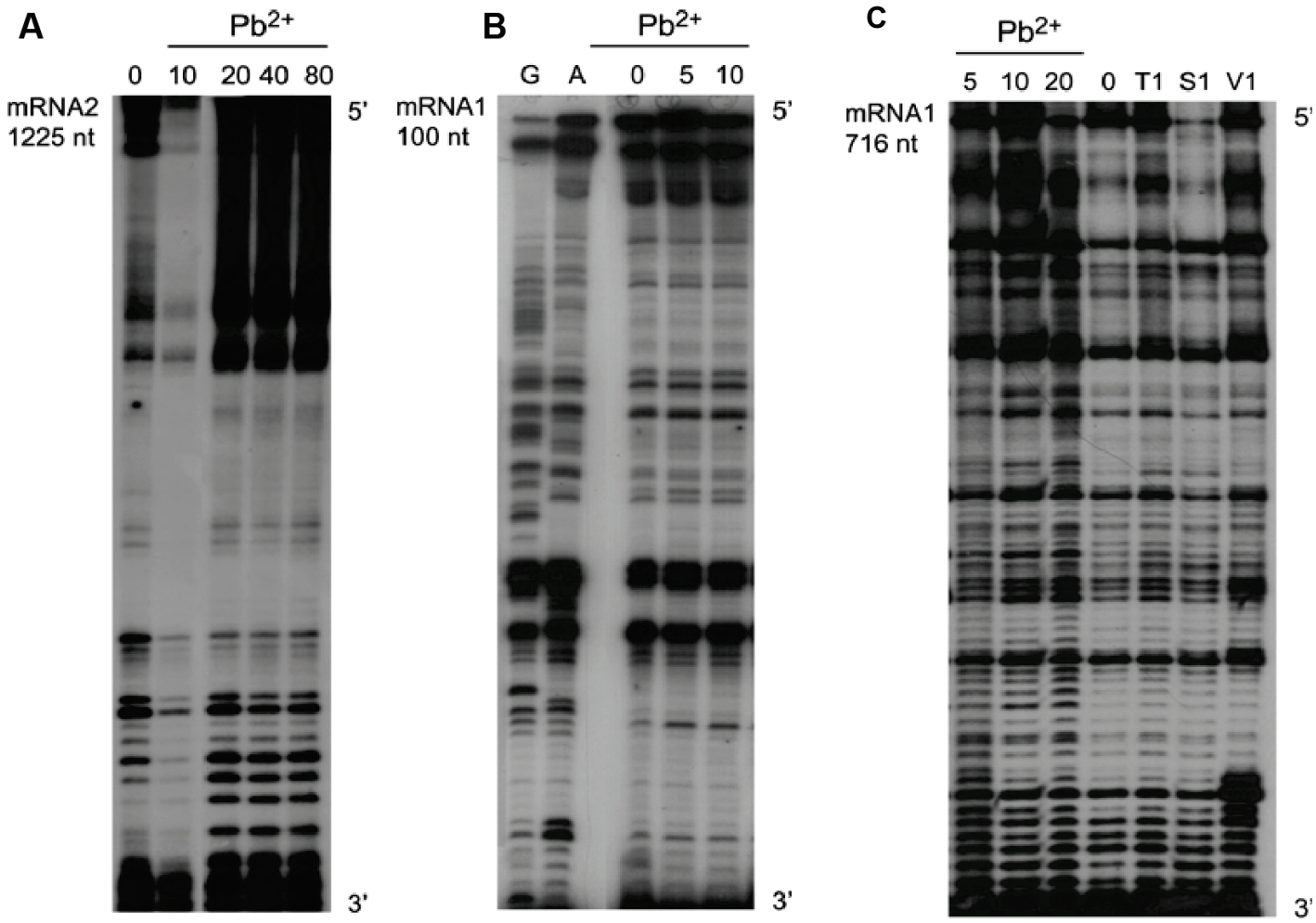

Figure 38. Determination of mRNA1 and mRNA2 5'-UTR structure by chemical and enzymatic probing

Representative autoradiographs corresponding to several probing experiments: **(A)** 1275 nt sequence of mRNA2 and **(B)** the first 100 nt sequence of mRNA1 including only part of the IRES structure were probed with increasing concentration of Pb^{2+}. Reverse transcription was performed with oligonucleotides hybridizing the region downstream AUG_{cyto} and AUG_{mito}, respectively. **(C)** A 716 nt sequence of mRNA1 including the complete 5'-UTR and a part of the coding region was also probed with increasing concentration of Pb^{2+} (lane 1-3) and with T1, S1 and V1 RNases (lane 5-7). Reverse transcription was performed with an oligonucleotide hybridizing the region downstream of AUG_{cyto}. Controls are indicated as (0) and sequencing experiments as G and A.

2. SHAPE (Selective 2'-hydroxyl acylation analyzed by primer extension)

Even though these results were disappointing, we didn't give up the struggle and followed a new strategy: we chose the SHAPE technique, which is supposed to be more sensitive than conventional chemical probing. We tested only mRNA1 containing the IRES structure and used the 716 nt fragment, that covers the whole 5'-UTR. The 1M7 (1-methyl-7-nitroisatoic anhydride) SHAPE reagent reacts with the 2'-hydroxyl group of flexible (exposed) nucleotides to form a 2'-O-adduct *(see Material & Methods-Figure 44)*. Reverse transcription is then performed to detect the exact position of the SHAPE reactive nucleotides. The main differences from the classical techniques described above are that (i) the specific oligonucleotide hybridizing the RNA sequence is labelled with a highly sensitive fluorophore and (ii) the extension reaction is monitored in real-time. Usually the 1M7 reagent is used at a concentration between 4 mM and 8 mM. In our experiments we tested a range from 4 mM to 150 mM (Figure 39 A and B), knowing that at the highest concentration the reaction mixture precipitated. Once again, it was impossible to analyze the results because there was no difference between the 1M7 treated and non treated RNA (Figure 39 blue and green spectra). Again, many strong stops were present throughout the sequence. We tried several conditions, varying different parameters in the extension reaction presented in *Material & Methods-Table 5*. Neither extension at high temperature (60 °C), nor addition of 10% DMSO in conjunction with the AMV reverse transcriptase, nor the usage of Superscript III (another highly processive reverse transcriptase) allowed progression through the strong stop artifacts caused by the highly structured 5'-UTR of mRNA1.

A

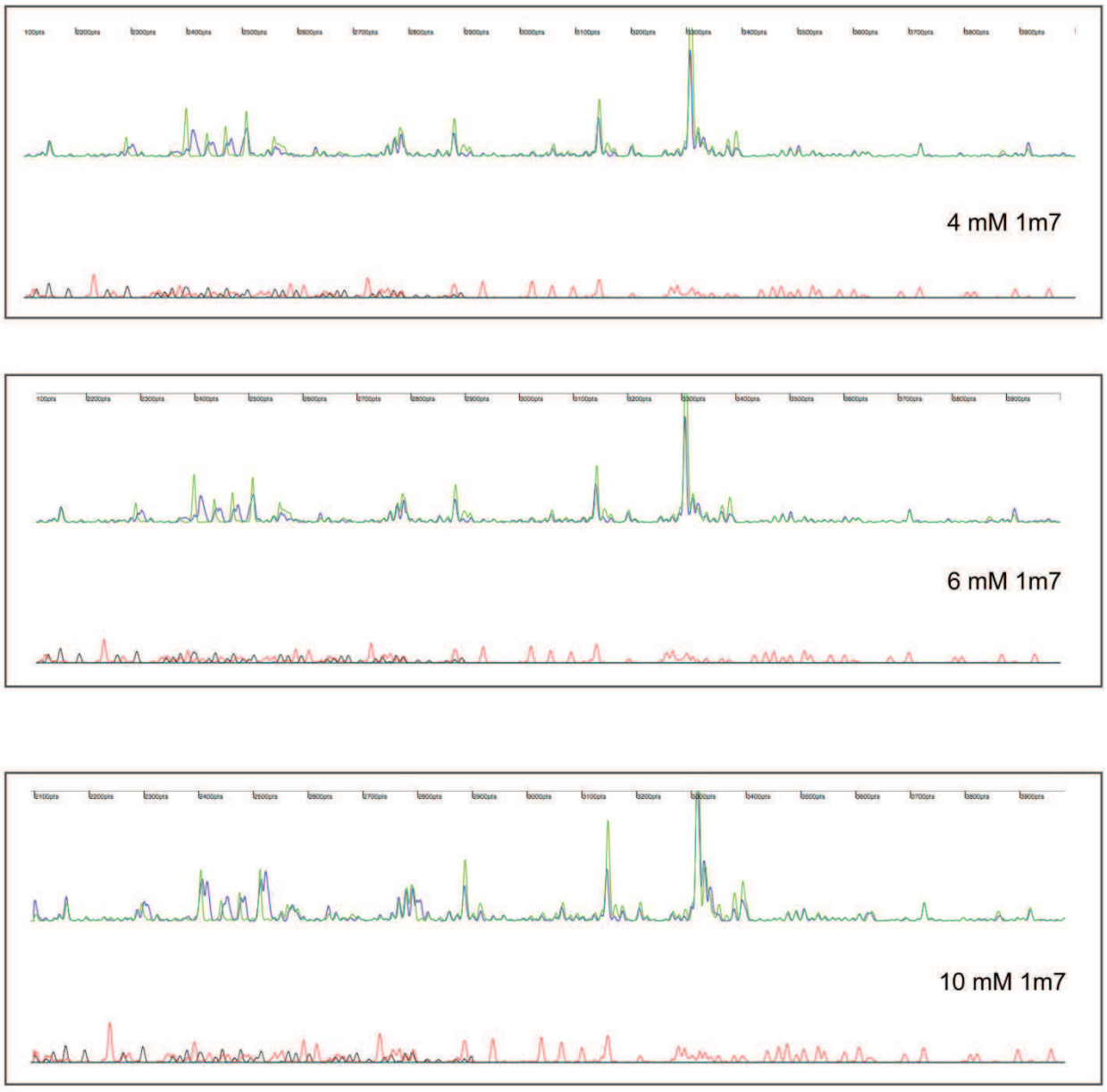

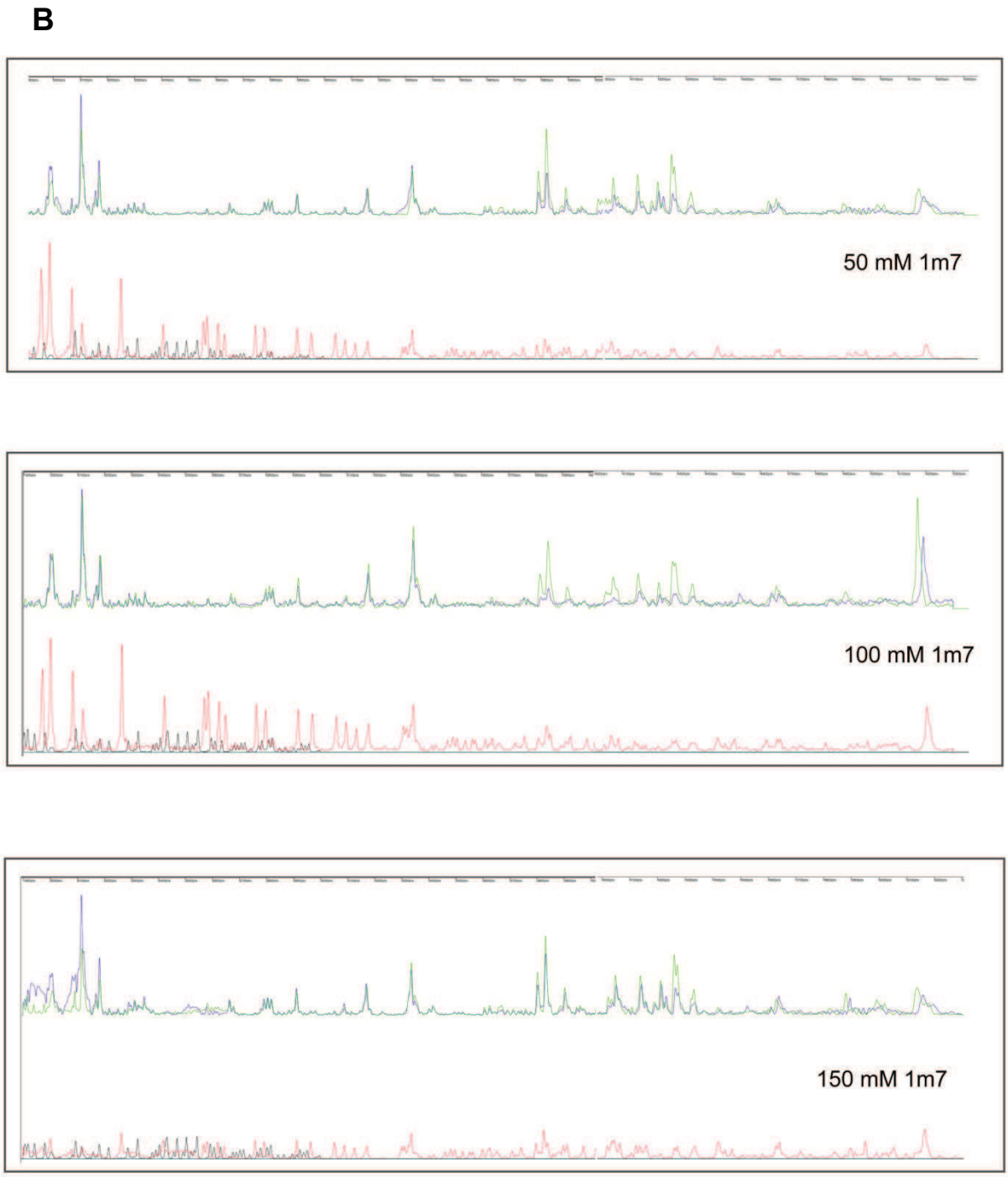

Figure 39. Electropherograms corresponding to the study of mRNA1 5'-UTR structure by SHAPE

The first 716 nt of mRNA1 including the 5'-UTR and a part of the coding region were treated with 4, 6 and 10 **(A)** or 50, 100 and 150 mM **(B)** 1M7 reagent. Reverse transcription was performed with an oligonucleotide targeting a region downstream of the AUG_{cyto}. Extension was performed with AMV RT for **(A)** 30 minutes at 42 °C without DMSO or **(B)** 2 minutes at 42 °C and 30 minutes at 55 °C without DMSO. Electropherograms corresponding to (i) the 1M7 treated RNAs are presented in blue, (ii) non-treated RNAs in green, (iii) G sequencing reactions in black and (iv) A sequencing reactions in red.

3. Conclusions

In this study, we tried to determine the 5'-UTR structure of GRS mRNA1 and mRNA2, using classical chemical and enzymatic probing, as well as the SHAPE technique. We faced several technical difficulties due to the apparently highly structured regions of the GRS mRNAs, especially in the 5'-UTR containing the IRES sequence. We couldn't use direct mRNA labelling and all the reverse transcription conditions that we tested were not sufficient to unfold this structure and allow correct reverse transcription. Even if our attempts to determine the structure of this 5'-UTR were unsuccessful, it wasn't really surprising. Until now, there are only few experimentally solved structures of cellular IRES, while most of them are *in silico* predictions. A few groups have succeeded in determining the highly structured IRES region of some cellular IRES (Bonnal *et al.,* 2003; Le Quesne *et al.,* 2001; Yaman *et al.,* 2003; Martineau *et al.,* 2004). There are also other examples of such structural studies (Mitchell *et al.,* 2003; Jopling *et al.,* 2004), yet these are based on data that are much less convincing. In these particular cases, numerous reverse transcription strong stops appeared in both the treated and non-treated RNAs, exactly like in our study.

The common feature of all of these IRES is their high GC% content (between 65% and 75%) and the apparent presence of strong structures. A study (Baird *et al.,* 2007) compared the existing IRES structures in order to find common structural organization in cellular IRESs like in viral IRES (Beales *et al.,* 2003) but without any success. It seems that small motifs recruiting ITAF (IRES trans-acting factor) proteins are more important than the presence of a specific structure.

In our case, structural characterization of the GRS IRES will be essential to unravel the complex mechanism that regulates its expression and potentially its particular localization. We thus used an *in silico* approach to build a structural model of this IRES (see article: Elaborate uORF/IRES features control expression and localization of human glycyl-tRNA synthetase), which shows the possible localization of all three initiation codons (AUG_0, AUG_{mito} and AUG_{cyto}) as well as the uORF stop codon. Considering the stable fold of the GRS IRES, we think that a crystallization approach could work and may allow us to finally determine its structure.

Expression of all multifunctional and regulatory proteins is tightly regulated in the cell. Anarchic expression of such proteins could provoke disruptions in cellular homeostasis and induce damages raging from cellular death to tumorigenesis. To maintain controlled expression of thousands of proteins, cells have developed several strategies, from transcription regulation to post translational modifications. At the mRNA level, regulations include generation of different splice variants and association with various protein factors that influence stability and translation efficiency. Moreover, translation can be specific to tissue type, stage of development, cellular conditions or cellular compartments.

AaRSs belong to a family of ubiquitously expressed housekeeping proteins with key roles in translation. AaRSs are also multifunctional proteins characterized by a myriad of important non-canonical functions in different cellular compartments (cytosol, nucleus, nucleolus, extracellular) (reviewed in Pang *et al.,* 2014). These alternative functions range from transcription and translation regulation, to modulation of inflammatory responses, angiogenesis and tumorigenesis. Some aaRS are also hijacked by viruses to ensure efficient viral reproduction in the host cell (e.g. HIV and poliovirus).

One can imagine that a simple misregulation in expression of an aaRScould lead to a cellular disaster. Indeed, this is exactly what happens when aaRSs are mutated or not correctly expressed: they provoke cancer development or neurodegenerative pathologies (reviewed in Yao and Fox, 2013). To ensure a correct switch from aminoacylation to alternative functions, aaRSs employ various strategies: while some aaRSs acting as cytokines are generated by mRNA alternative splicing or proteolytic cleavage, others are translocated from one cellular compartment to another. Often the switch is a phosphorylation signal, which allows the release of the modified aaRS from the multisynthetase complex and facilitates its subsequent interaction with other proteins.

GRS is an example of an aaRS with moonlighting functions: i) It is involved in Ap4A synthesis (Guo *et al.,* 2009), it acts ii) as a proapoptotic factor in tumorigenesis (Park *et al.,* 2012), and iii) as an ITAF in poliovirus mRNA translation initiation (Andreev *et al.,* 2012), and iv) it was identified as an autoantigenic factor in antisynthetase syndrome (Targoff *et al.,* 1990). Finally, the most studied non-canonical function of GRS is still to be discovered and causes axonal degeneration in CMT2D and dSMA-V diseases (Antonellis *et al.,* 2003). Whereas all other synthetases (except KRS) are encoded by two distinct genes (one for the cytosol and one for the mitochondria), both cytosolic and mitochondrial GRSs are generated from the same gene.

Despite the diversity of cellular pathways involving human GRS, nothing was known about the regulatory mechanisms that could explain its efficient and controlled expression in

different cellular compartments and different cell types (e.g. macrophages and neurons) where GRS canonical and alternative functions take place. During my thesis, I answered a simple general question: How is GRS expression regulated at the post-transcriptional level? I deciphered a regulatory molecular mechanism that sheds light on the complexity of GRS control and the coordinate execution of all its functions. Based on these results, I aimed to bring some clues about GRS expression and GRS alternative functions to light, especially in neurons.

I. REGULATION OF GRS EXPRESSION

In the firstr part of our study we uncovered two mRNAs (mRNA1 and mRNA2) potentially coding for both cytosolic and mitochondrial GRS in six different tissues (liver, spinal cord, brain, skeletal muscle, heart and spleen). *In vitro* translation, immunolocalization and expression from bicistronic vectors in COS-7 cells, allowed us to uncover a particular mechanism regulating the expression and localization of GRS in the cytosol, the mitochondria and at the endoplasmic reticulum (ER), consistent with the complex role of GRS in the cell. mRNA1 was found in all tissues except liver, while mRNA2 was ubiquitously expressed. mRNA1 is longer than mRNA2 and displays a complex 5'-UTR containing 3 initiation codons: i) AUG_0, intiating translation of a uORF expressed thanks to an IRES structure; ii) AUG_{mito}, intiating translation of the mitochondrial GRS; and iii) ATG_{cyto}, initiating translation of the cytosolic GRS. mRNA2 is shorter and does not contain AUG_0 or the IRES element. We showed that mRNA2 efficiently expresses the cytosolic and the mitochondrial GRSs, while mRNA1 mostly expresses the cytosolic enzyme. We propose that mRNA2 is constitutively expressed to synthetize both mitochondrial and cytosolic enzymes for aminoacylation. In contrast, in mRNA1, uORF translation hinders the synthesis of mitochondrial GRS and guarantees efficient translation of the cytosolic enzyme. Strikingly, mRNA1 is able to generate cytosolic GRS in a cap-independent manner (IRES), and this cytosolic GRS co-localizes with ER-bound ribosomes. Such localization has also been observed for free cytosolic FRS and aaRSs from the multisynthetase complex (David *et al.,* 2011).

1. Determination of the IRES structure

To understand how the GRS IRES is recognized by the initiation complex, we plan to crystallize the mRNA1 5'-UTR. Taking into account its high GC content and highly structured regions, which impeded our efforts to determine this structure with classical probing and SHAPE techniques, we think that this IRES domain is stable enough *in vitro* to crystallize. We will produce mRNA1 5'-UTR *in vitro* transcripts and purify them under non-denaturating conditions, in order to keep the native folding of this RNA fragment unchanged. This structure should give us information not only about the IRES and the positions of the initiation codons, but also about the presence of a putative zip-code element targeting GRS to the ER ribosomes.

2. ER localization

ER-localized translation is a complex process leading to the synthesis of secreted or membrane proteins but also of cytosolic proteins (reviewed in Gerst, 2008). Figure 40 summarizes the different mechanisms that have been identified until now to target mRNA translation to the ER. Three scenarios can apply to mRNA1 GRS synthesis: (i) mRNA1 is located to the ER before translation initiation, thanks to its IRES structure or part of this structure, (ii) mRNA1 is co-translationally targeted to the ER *via* the translated uORF peptide that could be recognized as a SRP signal, (iii) translation of the uORF creates a new structural feature in the untranslated 3'-domain of the mRNA, which directs mRNA1 to the ER.

However, several observations led us to favour options (ii) and/or (iii) for ER localization of mRNA1: Indeed, the uORF needs to be translated (mutants c and f *(see Article-Figure 3)* do not seem to localize at ER-bound ribosomes but they still need to be tested in the presence of digitonin); the sequence of the uORF peptide seems to be important (the frameshift mutant g localizes in mitochondria); the targeting mechanism is a "general" mechanism that does not involve tissue-specific effectors, since our experiments were done in COS-7 cells. Thus, in order to decipher this mechanism, we will first work on a process involving the cytosolic ribonucleoprotein particle (SRP) system.

Co-translational transport of secretory and membrane proteins depends on the well-known SRP and its membrane bound receptor (SR) (Figure 41 A). Newly synthesized proteins destined for secretion or membrane insertion carry a hydrophobic signal sequence at their N-termini. SRP interacts with this hydrophobic signal sequence as soon as it emerges from the ribosomal polypeptide exit tunnel (1). Peptide elongation is then retarded upon binding of SRP to the ribosome nascent chain complex (RNC). Subsequently, the SRP-RNC complex is targeted to the endoplasmic reticulum membrane by the interaction with the SR (2). GTP binding to SRP and SR has been shown to be a prerequisite for formation of the SRP-SR complex.

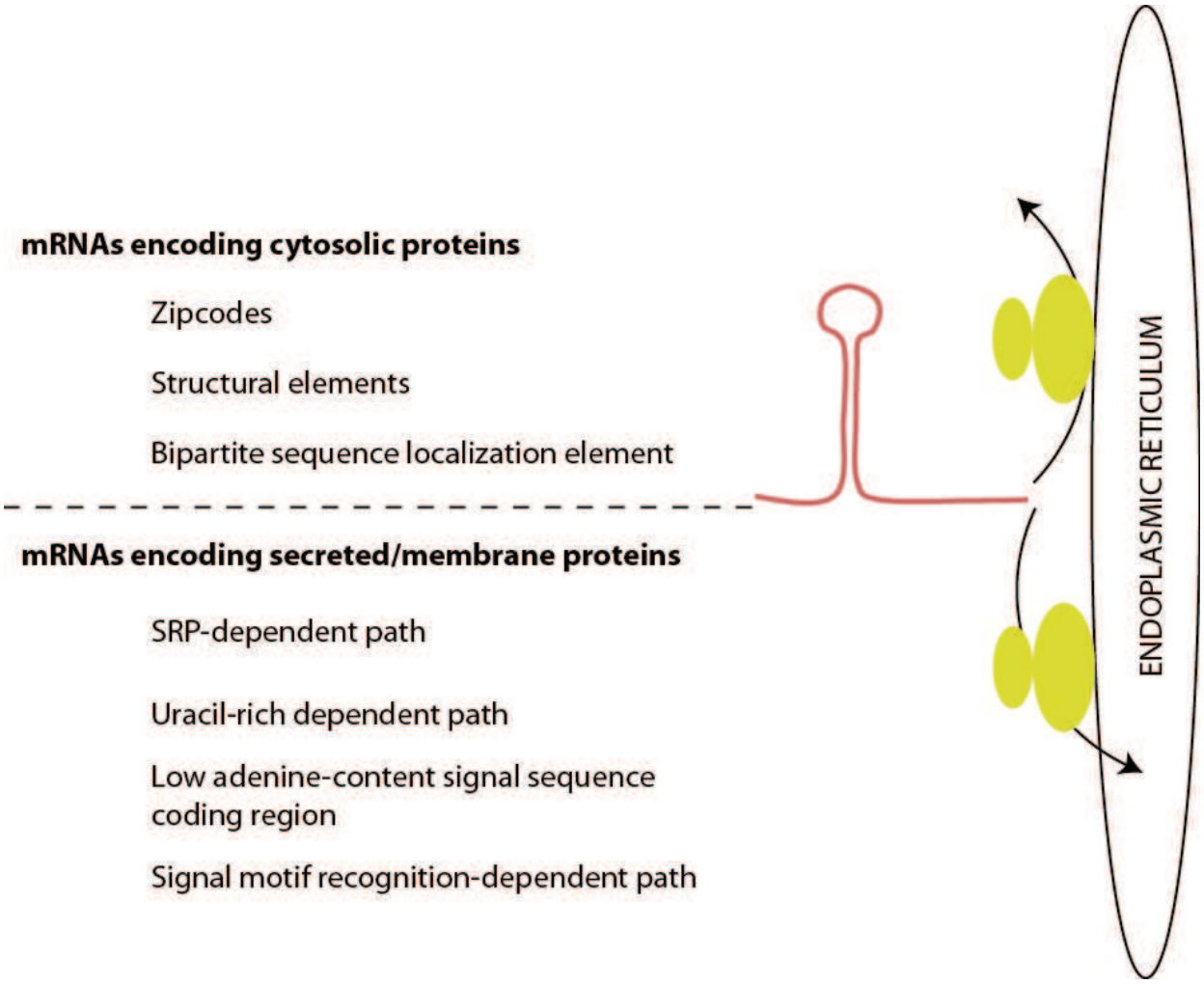

Figure 40. Two mRNA populations are delivered to the ER

These two populations corresponds to (i) mRNAs encoding secreted or membrane proteins that contain either signal sequences or transmembrane domains. The nascent proteins are translocated to the ER upon synthesis and (ii) mRNAs encoding cytosolic proteins that lack these elements and typically encode soluble, cytosolic proteins. Secreted or transmembrane proteins are directed to the ER by four mechanisms, the first being the classical signal recognition particle (SRP)-dependent path, that involves translation and signal peptide recognition by the SRP system. Alternatively, secreted and transmembrane proteins can be delivered in a translation-independent manner *via* three potential routes: A uracil-rich-dependent path, a low adenine-content signal sequence coding region path for mRNAs bearing signal sequences and a sequence motif recognition-dependent path that involves zip codes. The pathway for cytosolic protein delivery depends upon at least three types of cis-elements embedded within the mRNA: Zip codes, structural elements, and bipartite sequence localization elements. These cis-elements are probably all recognized by specific RNA binding proteins (RBPs) that, together with the transport machinery, target mRNAs to the ER. Yellow structures represent ribosomes present on or in close juxtaposition to the ER. Black arrows indicate either protein insertion into the ER or translation of cytosolic proteins. (adapted from Kraut-Cohen and Gerst, 2010).

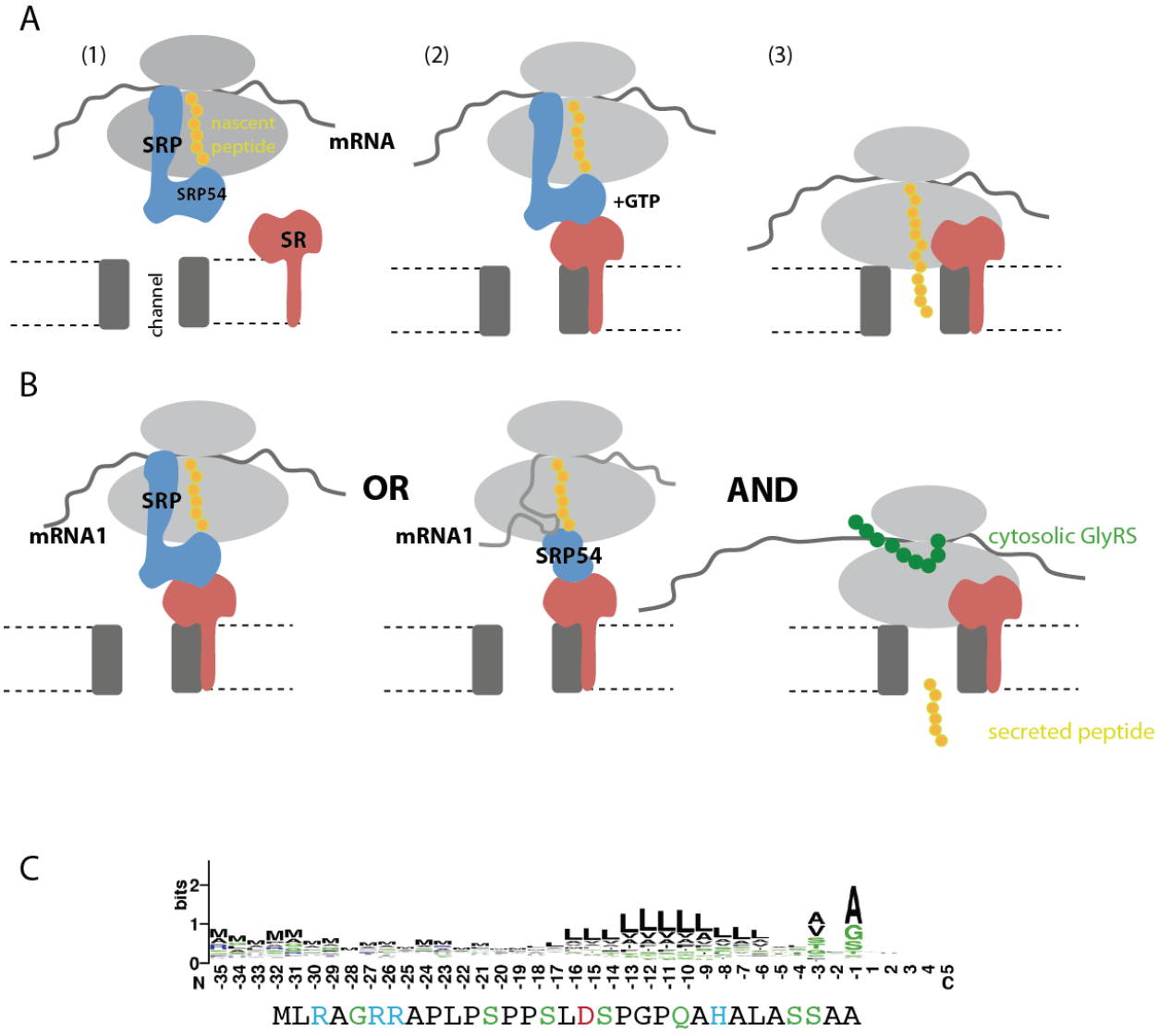

Figure 41. SRP cycle and our hypothesis involving SRP in mRNA1 ER-localization
(A) Overview of co-translational targeting of proteins directed for secretion or membrane insertion. **(B)** Two scenarios for mRNA1 ER localization involving SRP components are depicted. For details, see the main text. **(C)** Comparison between the consensus sequence of eukaryotic signal peptides and the sequence of the mRNA1 uORF peptide. The amino-acid residues are grouped and coloured based on the R group of their side-chain. Red denotes polar acidic amino-acid residues (D, E); Blue denotes polar basic amino-acid residues (K, R, H); Green denotes polar uncharged amino-acid residues (C, G, N, Q, S, T, Y); Black denotes non-polar hydrophobic amino-acid residues (A, F, I, L, M, P, V, W) (Adapted from Choo and Ranganathan, 2008).

The RNC is then transferred to the protein-conducting channel in the ER membrane (3) after which as a result of GTP hydrolysis, the SRP-SR complex dissociates and the ribosome resumes translation.

In the case of GRS mRNA1, it is reasonable to propose that the sequence of the uORF peptide (Figure 41 C) is hydrophobic enough so that it can be recognized by the SRP and thus target translation to the ER. The implication of the uORF peptide in this mechanism is supported by the fact that when introducing a frameshift mutation in the coding sequence, the hydrophobicity of the synthesized N-terminus changes; this is the case with mutant g, where the N-terminal sequence contains more charged amino acids than the uORF peptide: MLRAGRRARFRRHPLWTAQGRRLMPSPRPVP. If it is sufficient to hinder SRP54 interaction, then the downstream mitochondrial targeting signal can relocalize GRS into the mitochondria.

Alternatively, we can also imagine a minimal SRP complex. Indeed, in higher eukaryotes, the SRP consists of 6 proteins (SRP9, SRP14, SRP19, SRP54, SRP68 and SRP72) assembled onto the 300 nucleotides onto the 7S RNA. However, the universally conserved SRP core, comprises only protein SRP54 bound to helix 8 of the 7S RNA. This protein combines the two key functions of the SRP: signal sequence binding and GTP-dependent SR interaction. Because uORF translation unfolds the IRES structure of mRNA1, it could lead to the emergence of new structural motives at the 5'-end of the mRNA. Interestingly, we found a sequence upstream of the stop codon of the uORF that potentially forms a short RNA helix and mimics the SRP54 binding motif of helix 8. SRP54 could then recognize this RNA mimic in combination with the uORF peptide and target the ribosome to the ER (Figure 41 B). Moreover, the presence of the uORF stop codon would be sufficient to stop translation (and replace the SRP in delaying peptide synthesis). The presence of this stop codon could also explain why the resulting GRS is found in the cytosol and is not secreted or membrane bound (Figure 41 B).

To test this hypothesis, first, we will design new mutants (Figure 42) by introducing other frameshift mutations (2) and confirm that the peptide sequence is indeed important for GRS localization (frameshifts allow changes in the aa sequence without disturbing the IRES structure). We could also insert the mRNA1 5'-UTR upstream of a reporter gene (1) such as DsRed (Discosoma red fluorescent protein) or GFP (green fluorescent protein) to evaluate its ability to relocalize the protein to the ER. Another option is to remove the uORF stop codon and determine if the fused peptide can then lead to the secretion of GRS. Interestingly, in high throughput analysis of global mapping of translation initiation sites in mammalian HEK cells (Human Embryonic Kidney) (Lee *et al.,* 2012b), GRS translation initiation was detected

at AUG_0, consistent with our findings, but also at a non-AUG initiation codon (CTG) located 46 nucleotides downstream of AUG_{mito} (3). In this circumstance, the cytosolic GRS would thus be fused to a 37 amino acids N-terminal peptide. Strikingly this 37 amino acid peptide (LLLLPPRLLARPSLLLRRSLSAASCAPISLPAAASRS) is very hydrophobic and could also be a target signal for the SRP54 and the SRP machinery. This observation, together with our data on GRS translation on ER-bound ribosomes could explain how GRS is secreted by macrophages (cytokine activity) or is responsible for anti-GRS syndrome. We would like to convert the CUG start site to a conventional AUG to ensure controlled and efficient expression and see if the resulting GRS is indeed located to the ER and further secreted.

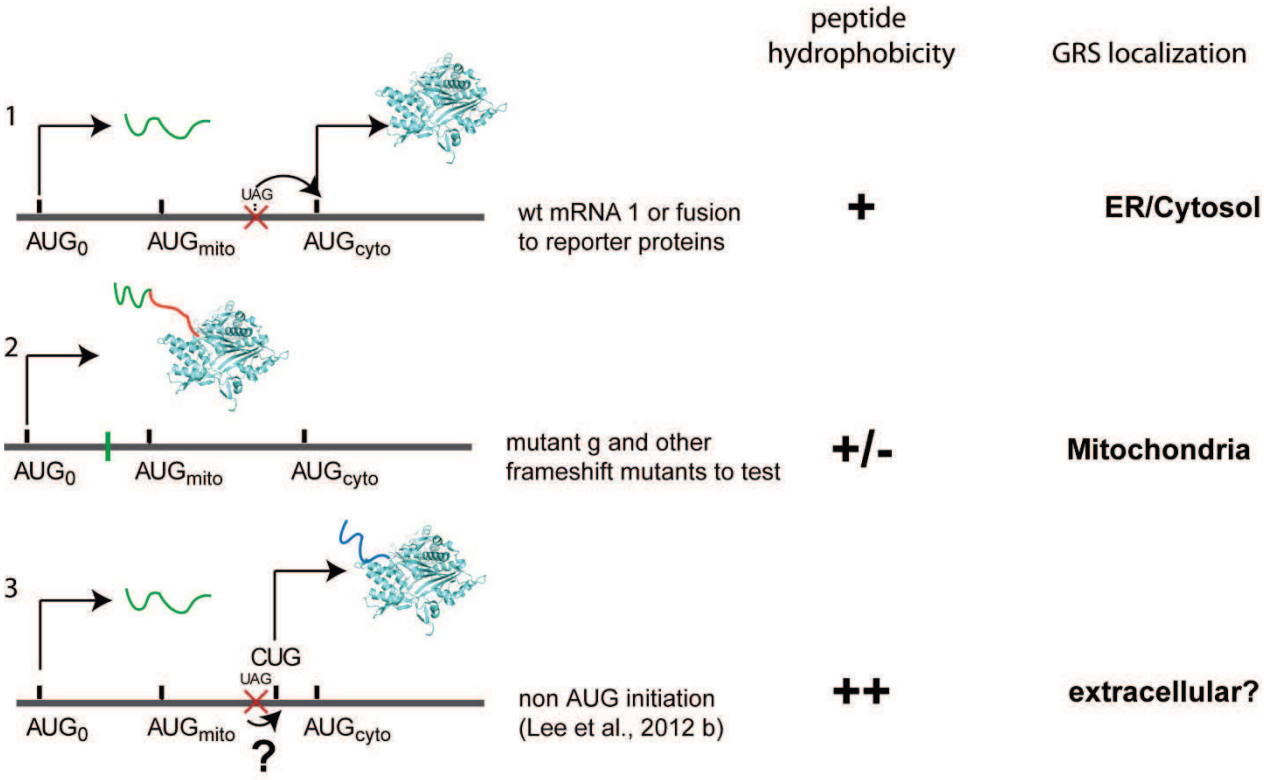

Figure 42. Is the uORF of mRNA1 responsible for GRS localization?
(1) wt mRNA1 IRES localizes GRS translation at the ER and leads to the synthesis of a cytosolic GRS; (2) mutant mRNA1 sequences should help us to determine if the uORF peptide is involved in GRS targeting to the ER. (3) Based on other's data, the localization of GRS synthesis at the ER site could also lead to GRS secretion, if GRS translation initiation/reinitiation takes place at the CUG codon. In this case, does the IRES structure control initiation?

3. GRS dependent expression and localization in neurons

So far, GRS mRNA1 IRES was tested in COS-7 cells. We looked at various stress conditions, such as starvation, glucose deprivation, hypoxia, etc…that could affect GRS expression. Currently, we don't know if mRNA1 IRES is present to ensure constant expression of cytosolic GRS in all tissues, or if it responds to particular cellular conditions or stress in specific tissues only. Usually IRES activity depends on the presence of different ITAFs. These factors are often tissue-specific and are expressed under precise cellular conditions. For example, IRES mediated expression of Apaf-1 (Mitchell *et al.,* 2003), of N-myc (Jopling and Willis, 2001), and of five other dendritically localized proteins (Pinkstaff *et al.,* 2001) are enhanced in neuronal cells. Because GRS is particularly important in neurons, mRNA1 IRES could be involved in its neuron-specific expression upon specific neuronal signal.

Neurons are highly polarized cells with dendrites and axons extending at long distance from the cell body to form synapses that mediate neuronal transmission. Establishment and maintenance of neuronal polarity start during neuronal differentiation and are dependent on the integrity and spatial organization of the ER. It is thus important to confirm (or not) that GRS colocalizes with ER-bound ribosomes in neurons. Our first attempt was not successful because SH-SY5Y neuroblasts are quite sensitive to any treatment and detach easily from microscope slides. However we will improve our experimental conditions or change the neuronal cell type we use. If GRS is associated to the ER, this could explain how it is targeted to distal axons. In order to test mRNA1 IRES activity in neurons, we want to use the constructs that we designed for our COS-7 experiments to transfect SH-SY5Y neuroblasts (differentiated or not), mouse motoneurons, and primary spinal neurons. We will also test different cell stress conditions as well as $KCl/CaCl_2$ treatments (known to induce synaptic activity) on these transfected neurons. Ultimately, we would like to identify neuronal ITAFs that would bind and regulate mRNA1 GRS expression. This could be achieved by transfecting a biotinylated mRNA1 into COS-7 cells and in neurons. The pulled-down proteins could then be identified by mass spectrometry.

II. GLYCYNERGIC TRANSMISSION: COULD GRS BE INVOLVED?

In the second part of our study we looked for a putative alternative function for GRS in neurons. In our hands, GRS granules were observed only with endogenous GRS and especially when treating neuronal cells with KCl, which activates synaptic vesicle exocytosis. We further showed that some of these GRS granules co-localized partially with the synaptic vesicle protein synaptophysin. These observations, with previous studies suggesting a specific non-canonical function of GRS in neurons, led us to the following hypothesis: Since glycine, the natural substrate of GRS, is also a major inhibitory neurotransmitter, could GRS be involved in glycinergic inhibitory neurotransmission?

Glycinergic neurons in the spinal cord are small inhibitory interneurons that inhibit the long spinal sensory and moto- neurons (Figure 43). When glycine is released from the axon of these interneurons, it binds glycine receptors (GlyR) on the dendrites and soma of the connected sensory and moto- neurons, thus blocking further excitation. Therefore, in the absence of glycinergic inputs, motoneurons are more excitable and are presumed to fire excessively and without coordination, resulting in severe muscle spasms (Zeilhofer *et al.,* 2012). Also, loss of glycinergic synaptic transmission induces neuropathic pain.

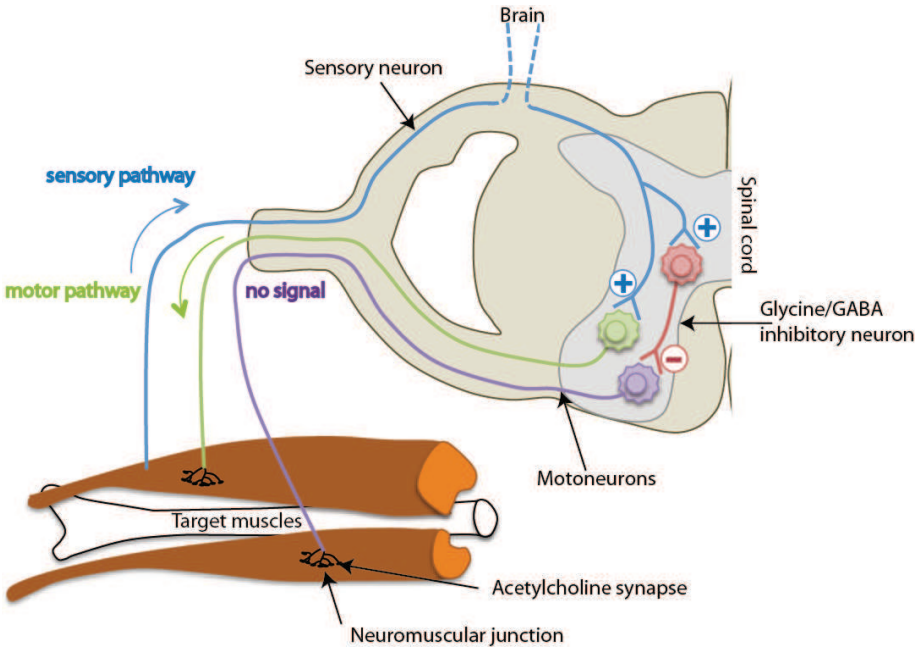

Figure 43. Spinal cord neurons interplay

Activated motoneuron (green) induces muscle contraction. Sensory neurons (blue) convey information to the brain to activate Glycine/GABA inhibitory neurons (red). Glycine/GABA transmission inhibits motoneurons (purple) to prevent contraction of the opposing muscle (*via* the acetylcholine synapse on the neuromuscular junction). Activation and inhibition are indicated with + and – signs respectively.

Interestingly in a mouse model (with mutated GlyT2 transporters), where glycinergic transmission is disturbed, alterations in the maturation of neuromuscular junctions were observed (Bogdanik *et al.,* 2012). Likwise, *Gars*$^{Nmf249/+}$ and *GRS*$^{C201R/+}$ CMT mouse models exhibit such defects in neuromuscular junctions that precede progressive degeneration (Seburn *et al.,* 2006; Achilli *et al.,* 2009; Motley *et al.,* 2011, Sleigh *et al.,* 2014). They include incorrect synaptic elimination and defects in the maturation of acetylcholine receptors. Besides, a transgenic mouse, overexpressing the WT GRS, was crossed either with *Gars*$^{Nmf249/+}$ or *GRS*$^{C201R/+}$ mice. Despite WT GRS overexpression, these mice still exhibited motor and sensory axon loss as well as neuromuscular junction impairments leading to the conclusion that GRS associated peripheral neuropathy is not due to GRS loss-of-function (Motley *et al.,* 2011). We noticed that the transgene used in these experiments contained only 47 nucleotides upstream of the AUG_{mito} and did not include AUG_0 or the entire IRES structure that we identified. It is thus possible that overexpressed WT GRS was not correctly localized and could not make up for the *Gars*$^{Nmf249/+}$ or *GRS*$^{C201R/+}$ mutations. Thus, it remains unclear if GRS CMT causing mutations are leading to gain- or loss-of-function in neuronal cells. The path that we chose to develop next is to clearly consider a loss-of function for GRS mutants inducing CMT2D.

Glycinergic neurotransmission includes several key membrane receptors: GlyT1 and GlyT2, *(see Results & Discussion Ch.II-3.1 Figure 33)*, which allow glycine entry into neuronal cells, VIAAT which loads synaptic vesicles with glycine and GlyR, the glycine receptor present in the post-synaptic membrane. All of them are specific for glycine, except VIAAT, which recognizes both glycine and GABA (the second major inhibitory neurotransmitter). Glycinergic neurons are mainly located in the spinal cord, brainstem and retina, while GABAnergic neurons are found preferentially in the brain. However, several neurons are characterized by mixed Glycine/GABA neurotransmission. VIAAT exhibits higher affinity to GABA (compared to glycine) and associates to GAD65 (glutamate decarboxylase) to further increase the transport of newly synthesized GABA into synaptic vesicles. We proposed a similar mechanism, where GRS would bind VIAAT and help glycine transport into synaptic vesicles.

We have shown that the cytosolic V5-tagged GRS colocalizes with VIAAT in a vesicular network structure (in COS-7 cells). In order to test which region of GRS interacts with VIAAT, we designed and examined several mutants *(see Results & Discussion Ch.II-3.3 Figure 36)*. The design was based on multiple sequence alignments of eukaryotic GRSs where we identified and removed structural domains highly conserved only in vertebrates. We showed

that deletion of the WHEP domain as well as insertions II and III (in the catalytic domain) do not impede GRS co-localization with VIAAT. Moreover, these mutants show a better co-localization profile than WT GRS-V5, suggesting that a relaxed structure of GRS (induced by deletions) actually improves its interaction with VIAAT. In fact, we think that the V5-tag, present at the C-terminus of WT GRS, impairs its interaction with VIAAT. Several observations appears to support this idea:

- In our and other's experiments, C-terminal V5-tagged GRS shows a diffuse distribution in the soma and neurite projections when expressed in differentiated or non differentiated SH-SY5Y human neuroblasts but do not show any granule formation.
- Invertebrates lack glycinergic transmission (inhibitory synapses are essentially GABA or glutamatergic) and invertebrates' GRSs lack 12 amino acids at their C-terminus compared to vertebrate's GRSs.
- In Human Embryonic Kidney (HEK) cells, *C. elegans* VIAAT can still load glycine into vesicular structures (Aubrey *et al*., 2007).

Is there a correlation between the presence of this short C-terminal domain (conserved only in vertebrate GRSs) VIAAT interaction, and glycinergic neurotransmission?

To answer this question, we have to test other GRS variants for their capacity to colocalize with VIAAT, especially the *C. elegans* GRS (which is our invertebrate model), the human GRS lacking its 12 C-terminal amino acids, and CMT mutants. Because we suppose that GRS interacts with VIAAT *via* its C-terminus, we will remove the V5-tag in all these constructs.

Antonellis and collaborators have shown that GRS granules do not colocalize with the Golgi apparatus in differentiated neurons (Antonellis *et al.,* 2006), however colocalization with the ER was not tested. Because ER, along with the cytoskeleton, is a major element of protein trafficking in axons in both central and peripheral neurons and contributes to all aspects of neuronal function including local trafficking of neuronal receptors (glycine, GABA and glutamate receptors), neurotransmitter release and synaptic plasticity, we want to evaluate if GRS mRNA1 and/or $KCl/CaCl_2$ treatments can improve GRS co-localization with VIAAT. Finally, to confirm that GRS interacts with VIAAT to channel glycine in synaptic vesicles, we will need to perform co-immunoprecipitation assays and determine the influence of GRS on the capacity of VIAAT to bind and transport glycine.

If GRS indeed interacts with VIAAT and takes part in glycinergic neurotransmission, then GRS CMT causing mutations could interfere with this function and explain at least partially its involvement in neurodegeneration. One can imagine that this perturbation could (i) lead

to defects in the maturation of neuromuscular junctions at early stages of development but also (ii) impair motoneuron inhibition (*via* spinal cord interneurons: Figure 43), which in turn would induce nerve degeneration, coherent with the CMT pathology.

In this part I will describe the techniques I used to determine the structure of the 5'UTR of mRNA1 and mRNA2 and to characterize the expression of GRS in neurons. First we tried to assess the secondary structure of both 5'UTRs using the classical techniques of chemical and enzymatic probing, as well as the new SHAPE method, unfortunately without success. Therefore an *in silico* prediction model of the 5'UTR of mRNA1 containing the IRES site was elaborated by Fabrice Jossinet.

The methods concerning GRS expression and GRS regulation in COS-7 (cap-independent translation initiation, mitochondrial and cytoplasmic GRS synthesis) and the co-localization of GRS with the endoplasmic reticulum bound ribosomes are detailed in our article **"Elaborate uORF/IRES features control expression and localization of human moonlighting glycyl-tRNA synthetase"**.

I. STRUCTURE DETERMINATION OF 5' UTRS

1. Principle

We used in-solution RNA probing to determine the structure of the 5'-UTR of GRS mRNA isoforms. Secondary structures of RNA are characterized by base-pairing interactions between nucleotides leading to the formation of double stranded regions, loops and bulges. In solution probing methods are based on the recognition of paired and non-paired nucleotides (double or single stranded, or engaged in tertiary structure) by different chemicals or enzymes. Usually, a combination of both enzymatic and chemical probing is used to determine the secondary structure of a given RNA molecule (Jaeger *et al.,* 1993). For example lead (Pb^{2+}) reveals flexible regions, DMS (dimethyl sulfate) modifies specifically N1 of adenines or N3 of cytosines, and CMCT (1-cyclohexyl-(2-morpholinoethyl) carbodiimide metho-p-toluene sulphonate) targets N1 of guanines or N3 of uridines when these positions are not engaged in Watson-Crick interactions. Endonucleases T1, S1 and T2 recognize single stranded regions and RNAse V1 cuts double stranded domains. Chemical probes present the advantage of being small and able to access nucleotides in constricted regions more easily compared to enzymes. Incidentally, most of them are also toxic and difficult to manipulate.

Treatments must be performed in order to introduce at most one modification or one enzymatic digestion per RNA molecule (statistical modification of RNA). Next, probed nucleotides are revealed by reverse transcription (Figure 44) and differential nucleotide accessibilities allow the construction of a model.

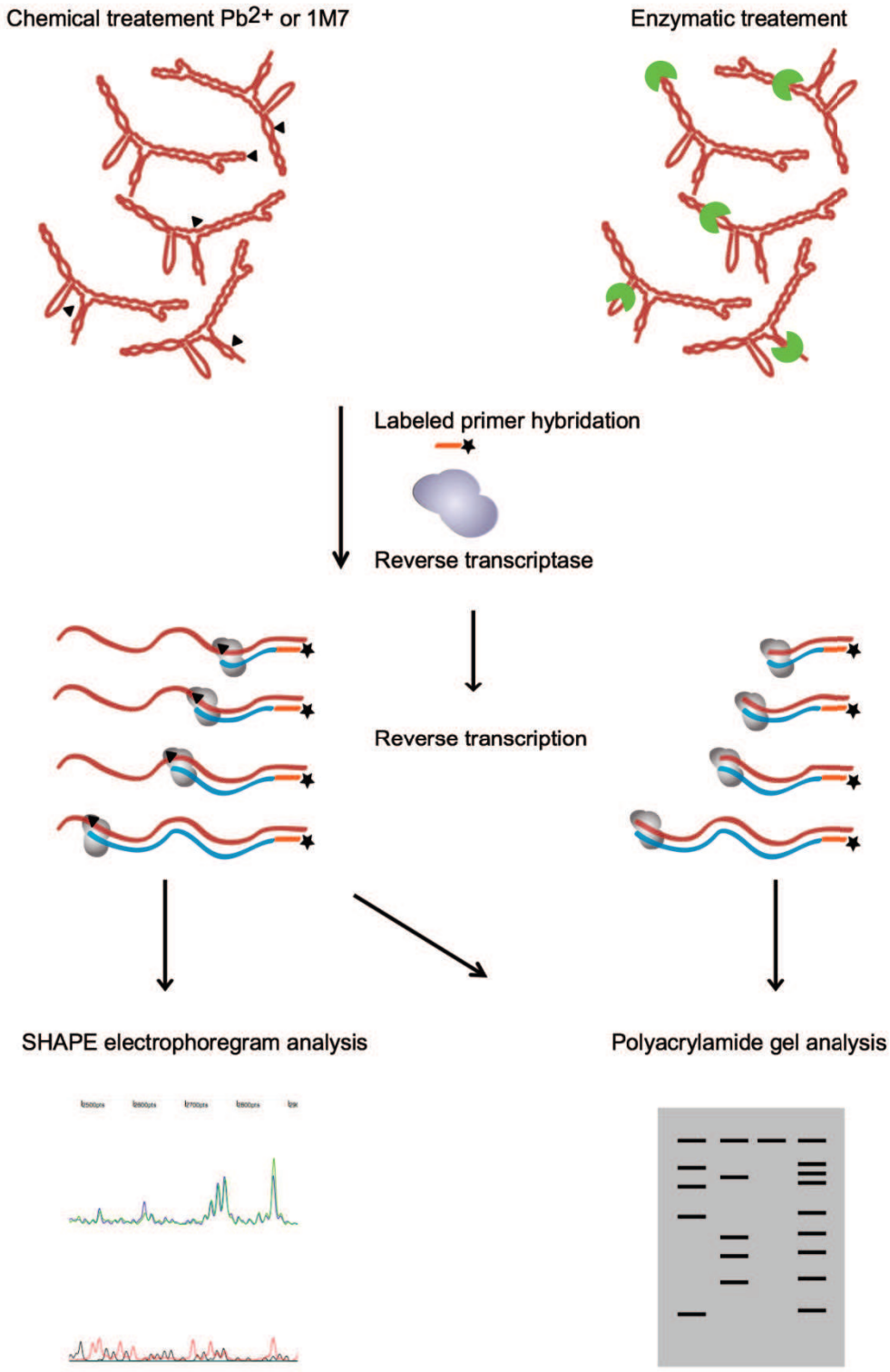

Figure 44. Principles of RNA secondary structure determination in solution
First the RNA of interest in its native fold (in red) is treated either (i) with a chemical compound: Pb^{2+} for the classical probing or 1M7 (1-methyl-7-nitroisatoic anhydride) for the SHAPE method (indicated with ▲) or (ii) with an RNase (T1, S1, T2, V1) (in green). Treated RNA is then hybridized with a specific radiolabeled oligonucleotide (orange). Reverse transcriptase (grey) is added to generate a complementary cDNA and the resulting cDNA is analyzed either on a polyacrylamide denaturating gel or on a capillary electrophoresis sequencer (SHAPE experiment).

2. RNA sample preparation for probing experiments

We used two different mRNA1 and one mRNA2 fragments to perform our probing and SHAPE experiments (Figure 45). The mRNA1 fragments were 100 nt and 716 nt long respectively, while mRNA2 was 1275 nt long.

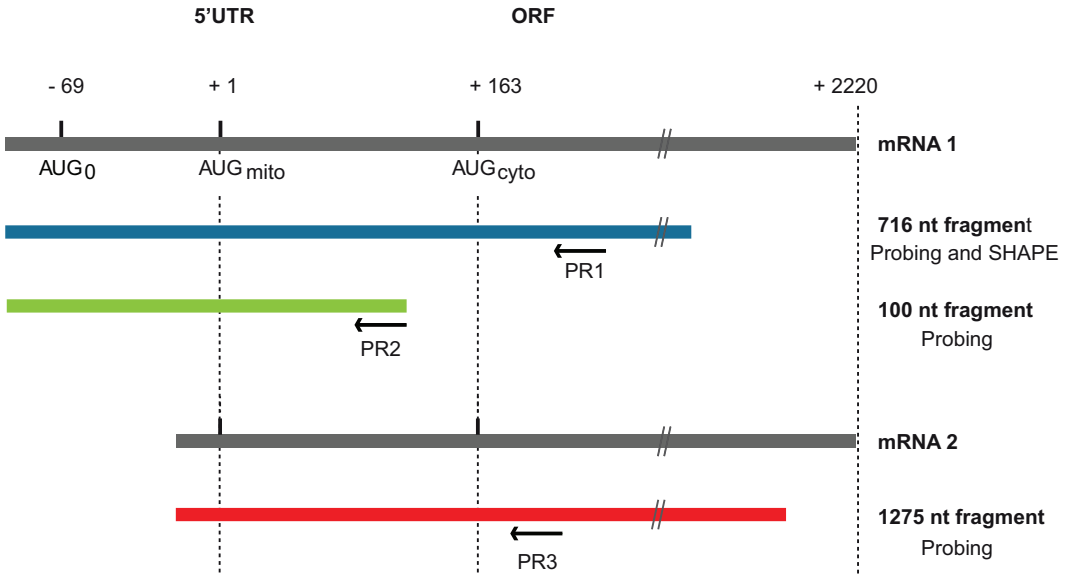

Figure 45. Schematic representation of RNA molecules used in probing and SHAPE experiments

Full-length mRNA1 and mRNA2 (grey) are presented with their corresponding initiation codons AUG_0, AUG_{mito} and AUG_{cyto}. RNA fragments that were used are indicated with different colours: the 1275 nt long mRNA2 fragment (red) and the 100 nt long mRNA1 fragment (green) were used only in classic probing experiments, while the 716 nt long mRNA1 fragment (blue) was used in both classic probing and SHAPE experiments. Specific primers (PR1, PR2 and PR3) were designed to perform primer extension.

Linerized DNA matrix (50 µg), containing the T7 promoter sequence upstream of the mRNA region of interest, was incubated in 500 µL of transcription mixture containing 40 mM Tris-HCl pH 8.1 (at 37 °C), 22 mM $MgCl_2$, 5 mM DTT, 4 mM ATP, 4 mM CTP, 4 mM GTP, 4mM UTP, 5 mM GMP, 1 mM spermidine and 6 µg T7 RNA polymerase for 2 hours at 37 °C. Then, 1300 units of DNase I were added for 20 minutes at 37 °C and the reaction was stopped by phenol extraction. RNA was purified first on Illustra NAP-5 columns (GE Healthcare) to remove the non-incorporated nucleotides. RNA pellets obtained by ethanol precipitation were resuspended in 300 µL H_2O and further purified on a Superdex 200 10/300 GL gel filtration column (GE Healthcare) in the presence of 150 mM KCl, 50 mM HEPES-KOH pH 7.4 to remove the DNA matrix and abortive transcription products.

3. Lead chemical probing

Probing reactions (10 µL) were carried out in presence of 1 pmol of purified RNA transcripts in 50 mM Tris acetate pH 7.5, 50 mM potassium acetate, 5 mM magnesium acetate and 5 to 80 mM Pb^{2+} acetate ($[CH_3COO]_2Pb.3H_2O$). The reaction was incubated for 6 min at 25 °C and stopped by adding 5.8 mM EDTA and 1 µg *E. coli* tRNA. Modified RNAs were ethanol precipitated in the presence of 1 µg of glycogen.

4. Enzymatic probing

S1, T1 and V1 endonucleases were used for RNA digestion. One pmol of RNA was incubated either with $3.15x10^{-3}$ units of S1 (in the presence of 1 mM $ZnCl_2$), $9.11x10^{-3}$ units of T1, or 0.1 units of V1 in 25 mM Tris-HCl pH 7.5, 1 mM $MgCl_2$ and 50 mM NaCl. The reaction was incubated for 10 min at 25 °C and stopped by phenol extraction followed by ethanol precipitation in the presence of 1 µg of glycogen.

5. Primer extension and sequencing reaction

Modified or digested nucleotides are revealed by reverse transcription: the reverse transcriptase extends RNA until it encounters a modification or the end of the digested fragment.

5.1. Desoxyoligoribonucleotide labeling

Oligonucleotides are first radiolabelled and then hybridized to the targeted RNA to initiate the reverse transcription. We used three different primers (Figure 45): PR1 5'-GCTTTGTCTACGTCTACTTGGGG-3', PR2 5'-GTTGTAAAACGACGGCCAGTG-3' and PR3 5'-AGCCTCAGAGGTGCCA-3', for hybridizing mRNA1 716 nt, mRNA1 100 nt and mRNA2 1275 nt fragments, respectively. Oligonucleotides were first purified on a denaturating (8 M Urea) 12% polyacrylamide gel, electroeluted and precipitated. Then, 200 pmol of oligonucleotide were subjected to 5'-phosphorylation in 50 mM Tris-HCl (pH 7.6 at 25 °C), 10 mM $MgCl_2$, 5 mM DTT, 1 mM spermidine, 15 µCi ATP-γ ^{32}P (3000Ci/mmol) and 1 unit T4 polynucleotide kinase, for 30 minutes at 37 °C. Non incorporated ATP-γ ^{32}P was removed on Illustra NAP-5 columns, and purified radiolabelled oligonucleotides were precipitated. Their specific activity was measured on a scintillation counter (LS6500, Beckman Coulter).

5.2. Reverse transcription and sequencing

Reverse transcription was performed with the Avian Myeloblastosis Virus Reverse Transcriptase (AMV RT) at 42 °C for 30 minutes. RNA previously subjected to Pb^{2+}, RNase treatments, or the non-treated controls were resuspended in 8 µL H_2O with 100 000 cpm of radiolabeled oligonucleotide, incubated for 2 minutes at 90 °C and cooled for 2 minutes on ice. Two µL of 5X reverse transcription buffer (250 mM Tris-HCl pH 8.5, 30 mM $MgCl_2$ and 200 mM KCl) were added and the reaction was further incubated for 15 minutes at 25 °C. Reverse transcription was then initiated by the addition of 1 unit of AMV RT and 4,5 µL mix containing 0,93 mM of each dNTP, 50 mM Tris-HCl pH 8.5, 6 mM $MgCl_2$ and 40 mM KCl. Primer extension was stopped by ethanol precipitation. The pellet was resuspended directly in denaturing loading dye (90% formamide, 10 mM EDTA pH 8, 0.025% xylene cyanol, and 0.025% bromophenol blue) and loaded onto a denaturing 10% polyacrylamide (19/1) gel. Radioactive bands corresponding to amplified fragments were revealed on an autoradiogram (Kodak) and further analyzed.

5.3. Control experiments

In all probing experiments, 2 different controls are essential to assign (i) nucleotide sequence and (ii) the quality of the probed RNA molecule:

- (i) The sequencing reaction uses non-modified RNA which is reverse transcribed in the presence of dideoxynucleotides triphosphates (ddNTP). This approach is based on the Sanger sequencing method, where statistical incorporation of ddNTP stops the elongation reaction. Four sequencing reactions are performed in the presence of the four dNTPs (dATP, dTTP, dGTP and dCTP) and only one ddNTP per reaction (ddATP, ddTTP, ddGTP or ddCTP). As ddNTPs lack the 3'-OH group of dNTPs, further incorporation of dNTPs is blocked, thus revealing the position of each nucleotide. For example, if we want to assess the position of G nucleotides, the sequencing reaction would be performed in the presence of 1.5 mM dATP, 1.5 mM dTTP, 1.5 mM dGTP, 0.25 mM dCTP and 50 µM ddCTP.
- (ii) A non-modified RNA is reverse transcribed to check the quality of the transcript. Reverse transcription of high quality RNA should generate a unique band with a high molecular weight. However, additional bands of lower molecular weicht can be observed due to structured regions in the RNA molecule, which are difficult to unfold by the reverse transcriptase.

6. SHAPE (Selective 2'-Hydroxyl acylation Analyzed by Primer Extension)

SHAPE technology is an automated method used to examine long RNA structures. It is based on chemical probing using compounds that react with the 2-OH of flexible and accessible nucleotides. Then the 2-O-adduct is detected by reverse transcription. The 716 nt fragment of mRNA1 was synthesized and purified as described above. Five different concentrations (4, 6, 10, 50, 100, and 150 mM) of 1M7 (1-methyl-7-nitroisatoic anhydride) (resuspended in anhydrous DMSO) or DMSO as a control were incubated with 1 pmol of target RNA and 2 µg *E. coli* tRNA for 5 minutes at 25 °C. The 1M7 reagent is highly reactive and quickly oxidizes, therefore the reaction self quenches and then is ethanol precipitated. Primer extension was performed as in classical probing. Different conditions of reverse transcription were tested and are summarized in (Table 5). Four primer extensions experiments were run in parallel. They were performed under the same conditions except for fluorophores (VIC, FAM, NED, PET) were used to label the PR1 primer. These reverse transcription reactions allowed us to distinguish between the control RNA, the modified RNA and the two sequencing reactions (T and C). After precipitation, the resulting cDNAs were resuspended in formamide, run on capillary electrophoresis sequencer (3130xL Genetic Analyzer, Applied Biosystems) and electropherograms were analyzed using the SHAPEfinder software (Vasa *et al.,* 2008). Extension reaction with control RNA and the four primers were included for the calibration of the mobility shift.

Table 5. Different reverse transcription conditions

RNA (pmol)	0,5X TE / H_2O	Reverse Transcriptase	Elongation T°	DMSO	Result
1	H_2O	AMV	30 min 42°C	0	+/-
1	H_2O	AMV	1min 42°C, 25 min 50°C, 5 min 60°C	0	+/-
1	H_2O	AMV	2 min 42°C, 30 min 55°C	0	+/-
1	H_2O	AMV	2 min 42°C, 30 min 55°C	10	+/-
1	H_2O	AMV	2 min 42°C, 30 min 60°C	0 +10% glycerol	-
1	TE	AMV	2min 42°C, 30 min 55°C	0	-
1	TE	AMV	2min 42°C, 30 min 55°C	10	-
1	H_2O	Superscript II	2 min 42°C, 30 min 55°C	0	+/-

Several reverse transcription experimental conditions were tested. In all of them, 1 pmol of RNA, with or without 1M7 treatment was subjected to reverse transcription using an AMV or

Superscript III reverse transcriptase. Different extension times were tested in the presence or in the absence of 10% DMSO. To evaluate the success of these reverse transcription reactions we took into account the number of strong stops detected in the non treated RNA sample. The number of strong stops is inversely proportional to the reverse transcriptase processivity.

II. GRS expression in neurons

In order to characterize GRS expression in neurons, we used human SH-SY5Y neuroblasts. In this neuronal cell line, we performed GRS immunolocalization studies upon KCl stimulation as well as co-localization experiments with synaptophysin (major synaptic vesicle protein).

1. SH-SY5Y differentiation, transfection and expression

Human SH-SY5Y neuroblastoma cells were differentiated with retinoic acid: cells were plated at a concentration of $1x10^5$ per well (6 well plate) on glass coverslips treated with 10 µg entactin–collagen IV–laminin attachment matrix (Millipore). All-trans retinoic acid (10 µM) (Sigma) was then added to the culture medium for six days and the medium was changed every 48 h. Cells were then transfected with 200 ng pcDNA3.1-mRNA1, pcDNA3.1-mRNA2 or the pcDNA3.1-mRNA-ORF (cytosolic GRS ORF without any 5'-UTR) using 6 µL Dreamfect gold reagent (OZ Biosciences), following the manufacturer's instructions. GRS was detected using a 1:5000 dilution of mouse monoclonal anti-V5-tag-Hrp conjugated antibody (Life Technologies) in 1X TBS-Tween 20 (0.5%), and 3% non-fat dry milk for western blot and a 1:500 dilution of mouse monoclonal anti V5-tag FITC conjugated antibody (Life Technologies) in 1X PBS and 3% BSA for immunolocalization studies.

2. K^+/Ca^{2+} treatments and immunostaining

Differentiated SH-SY5Y were treated with 30 mM KCl for 10 minutes or 5mM $CaCl_2$ for 15 minutes and directly fixed with 4% paraformaldehyde (PFA) for 20 minutes, washed with 1X PBS, permeabilized 5 minutes with ice cold methanol and washed again with PBS. Cells were then incubated in 1X PBS and 3% BSA for 30 minutes. Endogenous GRS was detected with rabbit polyclonal anti-GRS (Abcam: ab42905) at a 1:500 dilution and synaptophysin was detected with mouse monoclonal anti-synaptophysin (Abcam: ab8049) at a 1:10 dilution. Primary antibodies were diluted in 1X PBS containing 3% BSA and incubated over night at 4 °C. After three washes in 1X PBS, SH-SY5Y cells were incubated with 1:300 anti-rabbit TRITC antibody (Sigma-Aldrich) and 1:1000 anti-mouse FITC (Molecular Probes) for one hour, washed again and mounted on microscopic slides with anti-fading solution. Cells were finally visualized with a confocal laser scanning microscope (Zeiss LSM 780 Confocal system). The resulting images were analyzed and merged using the ImageJ Software (Schneider *et al.,* 2012).

III. GRS and VIAAT colocalizations

Facing difficulties in manipulating neurons (fixation/permeabilization/imaging), we went back to COS-7 cells to characterize the potential interaction between GRS and the vesicular transporter VIAAT (Vesicular Inhibitory Amino Acid Transporter). It had been demonstrated previously, that when transiently overexpressed in COS-7 cells, VIAAT localizes in particular vesicular structures, which mimic glycine loading vesicles in glycinergic neurons (Dumoulin *et al.,* 1999). We thus used the same system to co-express the human cytosolic GRS and VIAAT.

1. Plasmid constructions

The pcDNA3.1 plasmid containing the rat VIAAT coding sequence was a kind gift from Dr Bruno Gasnier. The cytosolic GRS ORF sequence was amplified by PCR from pcDNA3.1-mRNA1 and cloned again into pcDNA3.1. Then, GRS mutants were generated by PCR using this construct as a template (Table 6). Deletions were obtained by amplifying the entire vector with primers introducing a unique *BamH*I restriction site. Internaly deleted regions were replaced by a Gly-Ser-Gly-Ser amino acid sequence to reduce as much as possible interferences from misfolding of the recombinant mutant proteins. All constructs maintained the V5-tag at the C-terminus of GRS. Finally, the *C. elegans* GRS coding sequence was obtained by RT-PCR and cloned into pcDNA3.1 between *Kpn*I and *Xba*I, in fusion with a C-terminal V5-tag. The total RNA used to perform RT-PCR was extracted from N2 roundworms (*C. elegans*) using Tri-reagent (Sigma-Aldrich) following the manufacturer's instructions.

Five mutants, lacking different parts of GRS, were generated: the ΔWHEP mutant does not contain the N-terminal WHEP domain (helix-turn-helix domain also present in WRS, HRS and EPRS); ΔI2 and ΔI3 lack insertions 2 or 3, respectively, from the catalytic domain; ΔAC lacks the anticodon binding domain and ΔC-ter lacks only the last 12 amino acids, which are not present in the *C. elegans* GRS sequence.

2. Transfection and immunostaining

Twenty-four hours prior to transfection, $1.3x10^5$ COS-7 cells were plated on glass coverslips in 6-well plates. pcDNA3.1-mRNA-ORF (100 ng WT or mutant) were transfected alone or with 1 μg of pcDNA3.1-VIAAT in the presence of pBluescript SK+ DNA (qs 3 μg) and 3.6 μL Nanofectin (GE healthcare). Twenty four hours after transfection, cells were washed with 1X PBS, fixed and permeabilized in ice cold methanol for 5 minutes, washed again with 1X

PBS, and blocked for 30 minutes in 1X PBS containing 3% BSA at room temperature. Then, cells were incubated with primary antibodies: a 1:500 dilution of mouse monoclonal anti V5-tag (Life Technologies) and 1:1000 of rabbit anti-VIAAT specific antibodies (kind gift from Bruno Gasnier) for 2 hours at 37 °C in 1X PBS/3% BSA. Cells were washed 3 times in 1X PBS and were incubated with secondary antibodies: a 1:500 dilution of anti mouse-TRITC conjugated and a 1:500 dilution of anti rabbit-FITC conjugated for 40 minutes at 37 °C. Immunostained COS-7 were washed in 1X PBS, counterstained with DAPI, mounted with anti-fading solution, and visualized under confocal laser scanning microscope (Zeiss LSM 780 Confocal system (Carl Zeiss, Göttingen, Germany). The resulting images were analyzed using the ImageJ Software (Schneider *et al.,* 2012).

Table 6. Construction of GlyRS domain mutants

	Deletion	Matrix	PCR primers (5'-3')
WT GRS		pCDNA3.1-mRNA1	GAAGGTACCATGGACGGCGCGGGGGC (FW)
			TTAATTTCTAGACTACGTAGAATCGAGACCGA (RV)
Δ WHEP	Δ D2-D62	pCDNA3.1GRS-ORF	CTAGCATGGATATTGTAGACCGAGCAAAAATGGAAGATACCCTGAAGAGGAGGTTTTTCTATGATCA (FW)
			AGCTTGATCATACAAAAACCTCCTCTTCAGGGTATCTTCCATTTTTGCTCGGACTACAATATCCATG (RV)
Δ I2	Δ D307-N348	pCDNA3.1GRS-ORF	AATAAGGATCCGGCAGCAACACAGTATTAGGCTATTTCATTGGCCGCATCTACCTCTACCTCACG (FW)
			TTATTGGATCCGCTGCCGCTGCCTTTCTCACTGGGATCTACAAAGTGCTCAATTTCTGCCATTGTG (RV)
Δ I3	Δ A421-V504	pCDNA3.1GRS-ORF	AATAAGGATCCGGCAGCAAGAGATTCCAGAAAACACTATATGTGGAAGAAGTTGTTCCGAATGTAATTG (FW)
			TTATTGGATCCGCTGCCGCTGCCGCTGCCTCGTGCATGACAGGAGAGGTCATAACAGG (RV)
Δ AC	Δ S552-I685	pCDNA3.1GRS-ORF	CGAGCTCGGATCCGATCAGGTAAGCCTATCCCTAACCCTCTCCTCGGTCTCGATTCTACGTAGT (FW)
			TTATTGGATCCGAAGAATGTTCTCTGTTCATCTCCTTCTCGTACATGG (RV)
Δ C-ter	Δ673-I685	pCDNA3.1GRS-ORF	CGAGCTCGGATCCGATCAGGTAAGCCTATCCCTAACCCTCTCCTCGGTCTCGATTCTACGTAGT (FW)
			AATTAAGGATCCCCAGAGGATACCTGGCCTCCACATCAGC (RV)
C.elegans GRS		C.elegans RNA	AAATTGGTACCATGGCTACTCCGGAAATTGAAGCGAAACTCGCCCCTCTTCGTGC (FW)
			AATTTTCTAGATTATTCAGTTGCGCTCGCTTCGAATTTTGGATATTTGGCCTGAGC (RV)

A

Achilli, Francesca, Virginie Bros-Facer, Hazel P. Williams, Gareth T. Banks, Mona AlQatari, Ruth Chia, Valter Tucci, et al. "An ENU-Induced Mutation in Mouse Glycyl-tRNA Synthetase (GARS) Causes Peripheral Sensory and Motor Phenotypes Creating a Model of Charcot-Marie-Tooth Type 2D Peripheral Neuropathy." *Disease Models & Mechanisms* 2, no. 7–8 (August 2009): 359–73. doi:10.1242/dmm.002527.

Ainger, Kevin, Daniela Avossa, Amy S. Diana, Christopher Barry, Elisa Barbarese, and John H. Carson. "Transport and Localization Elements in Myelin Basic Protein mRNA." *The Journal of Cell Biology* 138, no. 5 (1997): 1077–87.

Akiri, G., D. Nahari, Y. Finkelstein, S. Y. Le, O. Elroy-Stein, and B. Z. Levi. "Regulation of Vascular Endothelial Growth Factor (VEGF) Expression Is Mediated by Internal Initiation of Translation and Alternative Initiation of Transcription." *Oncogene* 17, no. 2 (July 16, 1998): 227–36. doi:10.1038/sj.onc.1202019.

Allam, Heba, and Naushad Ali. "Initiation Factor eIF2-Independent Mode of c-Src mRNA Translation Occurs via an Internal Ribosome Entry Site." *Journal of Biological Chemistry* 285, no. 8 (February 19, 2010): 5713–25. doi:10.1074/jbc.M109.029462.

Andreev, D. E., J. Hirnet, I. M. Terenin, S. E. Dmitriev, M. Niepmann, and I. N. Shatsky. "Glycyl-tRNA Synthetase Specifically Binds to the Poliovirus IRES to Activate Translation Initiation." *Nucleic Acids Research* 40, no. 12 (July 1, 2012): 5602–14. doi:10.1093/nar/gks182.

Antonellis, Anthony, Rachel E. Ellsworth, Nyamkhishig Sambuughin, Imke Puls, Annette Abel, Shih-Queen Lee-Lin, Albena Jordanova, et al. "Glycyl tRNA Synthetase Mutations in Charcot-Marie-Tooth Disease Type 2D and Distal Spinal Muscular Atrophy Type V." *The American Journal of Human Genetics* 72, no. 5 (2003): 1293–99.

Antonellis, Anthony, Shih-Queen Lee-Lin, Amy Wasterlain, Paul Leo, Martha Quezado, Lev G. Goldfarb, Kyungjae Myung, Shawn Burgess, Kenneth H. Fischbeck, and Eric D. Green. "Functional Analyses of Glycyl-tRNA Synthetase Mutations Suggest a Key Role for tRNA-Charging Enzymes in Peripheral Axons." *The Journal of Neuroscience: The Official Journal of the Society for Neuroscience* 26, no. 41 (October 11, 2006): 10397–406. doi:10.1523/JNEUROSCI.1671-06.2006.

Araujo, Patricia R., Kihoon Yoon, Daijin Ko, Andrew D. Smith, Mei Qiao, Uthra Suresh, Suzanne C. Burns, and Luiz O. F. Penalva. "Before It Gets Started: Regulating Translation at the 5′ UTR." *International Journal of Genomics* 2012 (May 28, 2012): e475731. doi:10.1155/2012/475731.

Arcondéguy, Tania, Eric Lacazette, Stefania Millevoi, Hervé Prats, and Christian Touriol. "VEGF-A mRNA Processing, Stability and Translation: A Paradigm for Intricate Regulation of Gene Expression at the Post-Transcriptional Level." *Nucleic Acids Research*, July 12, 2013, gkt539. doi:10.1093/nar/gkt539.

Arif, Abul, Jie Jia, Robyn A. Moodt, Paul E. DiCorleto, and Paul L. Fox. "Phosphorylation of Glutamyl-Prolyl tRNA Synthetase by Cyclin-Dependent Kinase 5 Dictates Transcript-Selective Translational Control." *Proceedings of the National Academy of Sciences of the United States of America* 108, no. 4 (January 25, 2011): 1415–20. doi:10.1073/pnas.1011275108.

Arnez, John G., and Jean Cavarelli. "Structures of RNA-Binding Proteins." *Quarterly Reviews of Biophysics* 30, no. 03 (1997): 195–240. doi:10.1017/S0033583597003351.

Aubrey, Karin R., Francesco M. Rossi, Raquel Ruivo, Silvia Alboni, Gian Carlo Bellenchi, Anne Le Goff, Bruno Gasnier, and Stéphane Supplisson. "The Transporters GlyT2 and VIAAT

Cooperate to Determine the Vesicular Glycinergic Phenotype." *The Journal of Neuroscience* 27, no. 23 (June 6, 2007): 6273–81. doi:10.1523/JNEUROSCI.1024-07.2007.

B

Baird, Stephen D., Stephen M. Lewis, Marcel Turcotte, and Martin Holcik. "A Search for Structurally Similar Cellular Internal Ribosome Entry Sites." *Nucleic Acids Research* 35, no. 14 (July 1, 2007): 4664–77. doi:10.1093/nar/gkm483.

Balvay, Laurent, Ricardo Soto Rifo, Emiliano P. Ricci, Didier Decimo, and Théophile Ohlmann. "Structural and Functional Diversity of Viral IRESes." *Biochimica Et Biophysica Acta* 1789, no. 9–10 (October 2009): 542–57. doi:10.1016/j.bbagrm.2009.07.005.

Barker, Andrew, Michael R. Epis, Corrine J. Porter, Benjamin R. Hopkins, Matthew C. J. Wilce, Jackie A. Wilce, Keith M. Giles, and Peter J. Leedman. "Sequence Requirements for RNA Binding by HuR and AUF1." *Journal of Biochemistry* 151, no. 4 (April 1, 2012): 423–37. doi:10.1093/jb/mvs010.

Bastide, Amandine, Zeineb Karaa, Stephanie Bornes, Corinne Hieblot, Eric Lacazette, Herve Prats, and Christian Touriol. "An Upstream Open Reading Frame within an IRES Controls Expression of a Specific VEGF-A Isoform." *Nucleic Acids Research* 36, no. 7 (April 2008): 2434–45. doi:10.1093/nar/gkn093.

Beales, Lucy P., Andreas Holzenburg, and David J. Rowlands. "Viral Internal Ribosome Entry Site Structures Segregate into Two Distinct Morphologies." *Journal of Virology* 77, no. 11 (June 1, 2003): 6574–79. doi:10.1128/JVI.77.11.6574-6579.2003.

Beretta, L., A. C. Gingras, Y. V. Svitkin, M. N. Hall, and N. Sonenberg. "Rapamycin Blocks the Phosphorylation of 4E-BP1 and Inhibits Cap-Dependent Initiation of Translation." *The EMBO Journal* 15, no. 3 (February 1, 1996): 658–64.

Betteridge, Z., H. Gunawardena, J. North, J. Slinn, and N. McHugh. "Anti-Synthetase Syndrome: A New Autoantibody to Phenylalanyl Transfer RNA Synthetase (anti-Zo) Associated with Polymyositis and Interstitial Pneumonia." *Rheumatology (Oxford, England)* 46, no. 6 (June 2007): 1005–8. doi:10.1093/rheumatology/kem045.

Bogdanik, Laurent P., Harold D. Chapman, Kathy E. Miers, David V. Serreze, and Robert W. Burgess. "A MusD Retrotransposon Insertion in the Mouse Slc6a5 Gene Causes Alterations in Neuromuscular Junction Maturation and Behavioral Phenotypes." *PLoS ONE* 7, no. 1 (January 17, 2012): e30217. doi:10.1371/journal.pone.0030217.

Bonnal, Sophie, Frédéric Pileur, Cécile Orsini, Fabienne Parker, Françoise Pujol, Anne-Catherine Prats, and Stéphan Vagner. "Heterogeneous Nuclear Ribonucleoprotein A1 Is a Novel Internal Ribosome Entry Site Trans-Acting Factor That Modulates Alternative Initiation of Translation of the Fibroblast Growth Factor 2 mRNA." *The Journal of Biological Chemistry* 280, no. 6 (February 11, 2005): 4144–53. doi:10.1074/jbc.M411492200.

Bonnal, Sophie, Céline Schaeffer, Laurent Créancier, Simone Clamens, Hervé Moine, Anne-Catherine Prats, and Stéphan Vagner. "A Single Internal Ribosome Entry Site Containing a G Quartet RNA Structure Drives Fibroblast Growth Factor 2 Gene Expression at Four Alternative Translation Initiation Codons." *The Journal of Biological Chemistry* 278, no. 41 (October 10, 2003): 39330–36. doi:10.1074/jbc.M305580200.

Bunn, C. C., R. M. Bernstein, and M. B. Mathews. "Autoantibodies against Alanyl-tRNA Synthetase and tRNAAla Coexist and Are Associated with Myositis." *The Journal of Experimental Medicine* 163, no. 5 (May 1, 1986): 1281–91.

C

Cader, Muhammed Z., Jingshan Ren, Paul A. James, Louise E. Bird, Kevin Talbot, and David K. Stammers. "Crystal Structure of Human Wildtype and S581L-Mutant Glycyl-tRNA Synthetase, an Enzyme Underlying Distal Spinal Muscular Atrophy." *FEBS Letters* 581, no. 16 (juin 2007): 2959–64. doi:10.1016/j.febslet.2007.05.046.

Calvo, Sarah E., David J. Pagliarini, and Vamsi K. Mootha. "Upstream Open Reading Frames Cause Widespread Reduction of Protein Expression and Are Polymorphic among Humans." *Proceedings of the National Academy of Sciences* 106, no. 18 (2009): 7507–12.

Casciola-Rosen, Livia, Felipe Andrade, Danielle Ulanet, Wes Bang Wong, and Antony Rosen. "Cleavage by Granzyme B Is Strongly Predictive of Autoantigen Status Implications for Initiation of Autoimmunity." *The Journal of Experimental Medicine* 190, no. 6 (September 20, 1999): 815–26. doi:10.1084/jem.190.6.815.

Chalphin, Alexander V., Margaret S. Saha, Alexander V. Chalphin, and Margaret S. Saha. "The Specification of Glycinergic Neurons and the Role of Glycinergic Transmission in Development." *Frontiers in Molecular Neuroscience* 3 (2010): 11. doi:10.3389/fnmol.2010.00011.

Chang, K.-J. "Translation Initiation from a Naturally Occurring Non-AUG Codon in Saccharomyces Cerevisiae." *Journal of Biological Chemistry* 279, no. 14 (February 9, 2004): 13778–85. doi:10.1074/jbc.M311269200.

Chappell, Stephen A., Gerald M. Edelman, and Vincent P. Mauro. "A 9-Nt Segment of a Cellular mRNA Can Function as an Internal Ribosome Entry Site (IRES) and When Present in Linked Multiple Copies Greatly Enhances IRES Activity." *Proceedings of the National Academy of Sciences* 97, no. 4 (February 15, 2000): 1536–41. doi:10.1073/pnas.97.4.1536.

Chen, Ching-Yi, Roberto Gherzi, Jens S. Andersen, Guido Gaietta, Karsten Jürchott, Hans-Dieter Royer, Matthias Mann, and Michael Karin. "Nucleolin and YB-1 Are Required for JNK-Mediated Interleukin-2 mRNA Stabilization during T-Cell Activation." *Genes & Development* 14, no. 10 (2000): 1236–48.

Chen, Shun-Jia, Grace Lin, Kuang-Jung Chang, Lu-Shu Yeh, and Chien-Chia Wang. "Translational Efficiency of a Non-AUG Initiation Codon Is Significantly Affected by Its Sequence Context in Yeast." *Journal of Biological Chemistry* 283, no. 6 (February 8, 2008): 3173–80. doi:10.1074/jbc.M706968200.

Chihara, Takahiro, David Luginbuhl, and Liqun Luo. "Cytoplasmic and Mitochondrial Protein Translation in Axonal and Dendritic Terminal Arborization." *Nature Neuroscience* 10, no. 7 (July 2007): 828–37. doi:10.1038/nn1910.

Choo, Khar H., and Shoba Ranganathan. "Flanking Signal and Mature Peptide Residues Influence Signal Peptide Cleavage." *BMC Bioinformatics* 9, no. Suppl 12 (December 12, 2008): S15. doi:10.1186/1471-2105-9-S12-S15.

Cobbold, Laura C., Keith A. Spriggs, Stephen J. Haines, Helen C. Dobbyn, Christopher Hayes, Cornelia H. de Moor, Kathryn S. Lilley, Martin Bushell, and Anne E. Willis. "Identification of Internal Ribosome Entry Segment (IRES)-Trans-Acting Factors for the Myc Family of IRESs." *Molecular and Cellular Biology* 28, no. 1 (January 2008): 40–49. doi:10.1128/MCB.01298-07.

Coldwell, M. J., S. A. Mitchell, M. Stoneley, M. MacFarlane, and A. E. Willis. "Initiation of Apaf-1 Translation by Internal Ribosome Entry." *Oncogene* 19, no. 7 (February 17, 2000): 899–905. doi:10.1038/sj.onc.1203407.

Corral-Debrinski, M., C. Blugeon, and C. Jacq. "In Yeast, the 3' Untranslated Region or the Presequence of ATM1 Is Required for the Exclusive Localization of Its mRNA to the Vicinity of Mitochondria." *Molecular and Cellular Biology* 20, no. 21 (November 1, 2000): 7881–92. doi:10.1128/MCB.20.21.7881-7892.2000.

Crino, P. B., and J. Eberwine. "Molecular Characterization of the Dendritic Growth Cone: Regulated mRNA Transport and Local Protein Synthesis." *Neuron* 17, no. 6 (December 1996): 1173–87.

Cusack, S., C. Berthet-Colominas, M. Härtlein, N. Nassar, and R. Leberman. "A Second Class of Synthetase Structure Revealed by X-Ray Analysis of Escherichia Coli Seryl-tRNA Synthetase at 2.5 A." *Nature* 347, no. 6290 (September 20, 1990): 249–55. doi:10.1038/347249a0.

D

David, Alexandre, Nir Netzer, Michael Brad Strader, Suman R. Das, Cai Yun Chen, James Gibbs, Philippe Pierre, Jack R. Bennink, and Jonathan W. Yewdell. "RNA Binding Targets Aminoacyl-tRNA Synthetases to Translating Ribosomes." *Journal of Biological Chemistry* 286, no. 23 (June 10, 2011): 20688–700. doi:10.1074/jbc.M110.209452.

Davuluri, R. V., Y. Suzuki, S. Sugano, and M. Q. Zhang. "CART Classification of Human 5' UTR Sequences." *Genome Research* 10, no. 11 (November 2000): 1807–16.

Dobbyn, H. C., K. Hill, T. L. Hamilton, K. A. Spriggs, B. M. Pickering, M. J. Coldwell, C. H. de Moor, M. Bushell, and A. E. Willis. "Regulation of BAG-1 IRES-Mediated Translation Following Chemotoxic Stress." *Oncogene* 27, no. 8 (February 14, 2008): 1167–74. doi:10.1038/sj.onc.1210723.

Dumoulin, Andréa, Philippe Rostaing, Cécile Bedet, Sabine Lévi, Marie-Françoise Isambert, Jean-Pierre Henry, Antoine Triller, and Bruno Gasnier. "Presence of the Vesicular Inhibitory Amino Acid Transporter in GABAergic and Glycinergic Synaptic Terminal Boutons." *Journal of Cell Science* 112, no. 6 (1999): 811–23.

E

Eriani, Gilbert, Marc Delarue, Olivier Poch, Jean Gangloff, and Dino Moras. "Partition of tRNA Synthetases into Two Classes Based on Mutually Exclusive Sets of Sequence Motifs." *Nature* 347, no. 6289 (September 13, 1990): 203–6. doi:10.1038/347203a0.

Ermanoska, Biljana, William W. Motley, Ricardo Leitão-Gonçalves, Bob Asselbergh, LaTasha H. Lee, Peter De Rijk, Kristel Sleegers, et al. "CMT-Associated Mutations in Glycyl- and Tyrosyl-tRNA Synthetases Exhibit Similar Pattern of Toxicity and Share Common Genetic Modifiers in Drosophila." *Neurobiology of Disease* 68 (August 2014): 180–89. doi:10.1016/j.nbd.2014.04.020.

F

Fernandez, J., I. Yaman, R. Mishra, W. C. Merrick, M. D. Snider, W. H. Lamers, and M. Hatzoglou. "Internal Ribosome Entry Site-Mediated Translation of a Mammalian mRNA Is Regulated by Amino Acid Availability." *The Journal of Biological Chemistry* 276, no. 15 (April 13, 2001): 12285–91. doi:10.1074/jbc.M009714200.

Fernandez, James, Ibrahim Yaman, Charles Huang, Haiyan Liu, Alex B. Lopez, Anton A. Komar, Mark G. Caprara, et al. "Ribosome Stalling Regulates IRES-Mediated Translation in Eukaryotes, a Parallel to Prokaryotic Attenuation." *Molecular Cell* 17, no. 3 (février 2005): 405–16. doi:10.1016/j.molcel.2004.12.024.

Fersht, A. R., and M. M. Kaethner. "Enzyme Hyperspecificity. Rejection of Threonine by the Valyl-tRNA Synthetase by Misacylation and Hydrolytic Editing." *Biochemistry* 15, no. 15 (July 27, 1976): 3342–46.

Fox, Jennifer T., William K. Shin, Marie A. Caudill, and Patrick J. Stover. "A UV-Responsive Internal Ribosome Entry Site Enhances Serine Hydroxymethyltransferase 1 Expression for DNA Damage Repair." *Journal of Biological Chemistry* 284, no. 45 (November 6, 2009): 31097–108. doi:10.1074/jbc.M109.015800.

Froelich, Clifford A., and Eric A. First. "Dominant Intermediate Charcot-Marie-Tooth Disorder Is Not Due to a Catalytic Defect in Tyrosyl-tRNA Synthetase." *Biochemistry* 50, no. 33 (août 2011): 7132–45. doi:10.1021/bi200989h.

Frugier, Magali, Michael Ryckelynck, and Richard Giege. "tRNA-Balanced Expression of a Eukaryal Aminoacyl-tRNA Synthetase by an mRNA-Mediated Pathway." *EMBO Reports* 6, no. 9 (September 2005): 860–65. doi:10.1038/sj.embor.7400481.

G

Gasnier, Bruno. "The Loading of Neurotransmitters into Synaptic Vesicles." *Biochimie* 82, no. 4 (avril 2000): 327–37. doi:10.1016/S0300-9084(00)00221-2.

Gerst, Jeffrey E. "Message on the Web: mRNA and ER Co-Trafficking." *Trends in Cell Biology* 18, no. 2 (February 2008): 68–76. doi:10.1016/j.tcb.2007.11.005.

Giegé, Richard, Marie Sissler, and Catherine Florentz. "Universal Rules and Idiosyncratic Features in tRNA Identity." *Nucleic Acids Research* 26, no. 22 (November 1, 1998): 5017–35. doi:10.1093/nar/26.22.5017.

Gingras, A. C., Y. Svitkin, G. J. Belsham, A. Pause, and N. Sonenberg. "Activation of the Translational Suppressor 4E-BP1 Following Infection with Encephalomyocarditis Virus and Poliovirus." *Proceedings of the National Academy of Sciences of the United States of America* 93, no. 11 (May 28, 1996): 5578–83.

Goerlich, O., R. Foeckler, and E. Holler. "Mechanism of Synthesis of adenosine(5')tetraphospho(5')adenosine (AppppA) by Aminoacyl-tRNA Synthetases." *European Journal of Biochemistry / FEBS* 126, no. 1 (August 1982): 135–42.

Gonzalez, Michael, Heather McLaughlin, Henry Houlden, Min Guo, Liu Yo-Tsen, Marios Hadjivassilious, Fiorella Speziani, et al. "Exome Sequencing Identifies a Significant Variant in Methionyl-tRNA Synthetase (MARS) in a Family with Late-Onset CMT2." *Journal of Neurology, Neurosurgery, and Psychiatry* 84, no. 11 (November 2013): 1247–49. doi:10.1136/jnnp-2013-305049.

Greenberg, Y., M. King, W. B. Kiosses, K. Ewalt, X. Yang, P. Schimmel, J. S. Reader, and E. Tzima. "The Novel Fragment of Tyrosyl tRNA Synthetase, Mini-TyrRS, Is Secreted to Induce an Angiogenic Response in Endothelial Cells." *The FASEB Journal* 22, no. 5 (May 1, 2008): 1597–1605. doi:10.1096/fj.07-9973com.

Guo, F., J. Gabor, S. Cen, K. Hu, A.J. Mouland, and L. Kleiman. "Inhibition of Cellular HIV-1 Protease Activity by Lysyl-tRNA Synthetase." *Journal of Biological Chemistry* 280, no. 28 (2005): 26018–23. doi:10.1074/jbc.M502454200.

Guo, Min, and Paul Schimmel. "Essential Nontranslational Functions of tRNA Synthetases." *Nature Chemical Biology* 9, no. 3 (February 15, 2013): 145–53. doi:10.1038/nchembio.1158.

Guo, R.-T., Y. E. Chong, M. Guo, and X.-L. Yang. "Crystal Structures and Biochemical Analyses Suggest a Unique Mechanism and Role for Human Glycyl-tRNA Synthetase in Ap4A Homeostasis." *Journal of Biological Chemistry* 284, no. 42 (October 16, 2009): 28968–76. doi:10.1074/jbc.M109.030692.

H

Han, Jung Min, Seung Jae Jeong, Min Chul Park, Gyuyoup Kim, Nam Hoon Kwon, Hoi Kyoung Kim, Sang Hoon Ha, Sung Ho Ryu, and Sunghoon Kim. "Leucyl-tRNA Synthetase Is an Intracellular Leucine Sensor for the mTORC1-Signaling Pathway." *Cell* 149, no. 2 (avril 2012): 410–24. doi:10.1016/j.cell.2012.02.044.

Harding, Heather P., Yuhong Zhang, Huiquing Zeng, Isabel Novoa, Phoebe D. Lu, Marcella Calfon, Navid Sadri, et al. "An Integrated Stress Response Regulates Amino Acid Metabolism and Resistance to Oxidative Stress." *Molecular Cell* 11, no. 3 (March 2003): 619–33.

He, Weiwei, Hui-Min Zhang, Yeeting E. Chong, Min Guo, Alan G. Marshall, and Xiang-Lei Yang. "Dispersed Disease-Causing Neomorphic Mutations on a Single Protein Promote the Same Localized Conformational Opening." *Proceedings of the National Academy of Sciences of the United States of America* 108, no. 30 (July 26, 2011): 12307–12. doi:10.1073/pnas.1104293108.

Hervé, Chabanon, Ian Mickleburgh, and John Hesketh. "Zipcodes and Postage Stamps: mRNA Localisation Signals and Their Trans-Acting Binding Proteins." *Briefings in Functional Genomics & Proteomics* 3, no. 3 (2004): 240–56.

Hill, J. R., and D. R. Morris. "Cell-Specific Translation of S-Adenosylmethionine Decarboxylase mRNA. Regulation by the 5' Transcript Leader." *The Journal of Biological Chemistry* 267, no. 30 (October 25, 1992): 21886–93.

Hinnebusch, A. G. "Molecular Mechanism of Scanning and Start Codon Selection in Eukaryotes." *Microbiology and Molecular Biology Reviews* 75, no. 3 (September 1, 2011): 434–67. doi:10.1128/MMBR.00008-11.

Hirakata, M., A. Suwa, S. Nagai, M. A. Kron, E. P. Trieu, T. Mimori, M. Akizuki, and I. N. Targoff. "Anti-KS: Identification of Autoantibodies to Asparaginyl-Transfer RNA Synthetase Associated with Interstitial Lung Disease." *Journal of Immunology (Baltimore, Md.: 1950)* 162, no. 4 (February 15, 1999): 2315–20.

Howard, O. M. Zack, Hui Fang Dong, De Yang, Nina Raben, Kanneboyina Nagaraju, Antony Rosen, Livia Casciola-Rosen, et al. "Histidyl-tRNA Synthetase and Asparaginyl-tRNA Synthetase, Autoantigens in Myositis, Activate Chemokine Receptors on T Lymphocytes and Immature Dendritic Cells." *The Journal of Experimental Medicine* 196, no. 6 (September 16, 2002): 781–91.

Huez, I., S. Bornes, D. Bresson, L. Créancier, and H. Prats. "New Vascular Endothelial Growth Factor Isoform Generated by Internal Ribosome Entry Site-Driven CUG Translation Initiation." *Molecular Endocrinology (Baltimore, Md.)* 15, no. 12 (December 2001): 2197–2210. doi:10.1210/mend.15.12.0738.

Huez, Isabelle, Laurent Creancier, Sylvie Audigier, Marie-Claire Gensac, Anne-Catherine Prats, and Herve Prats. "Two Independent Internal Ribosome Entry Sites Are Involved in Translation Initiation of Vascular Endothelial Growth Factor mRNA." *Molecular and Cellular Biology* 18, no. 11 (November 1998): 6178–90.

Hughes, Thomas A. "Regulation of Gene Expression by Alternative Untranslated Regions." *Trends in Genetics* 22, no. 3 (March 2006): 119–22. doi:10.1016/j.tig.2006.01.001.

I

Iacono, Michele, Flavio Mignone, and Graziano Pesole. "uAUG and uORFs in Human and Rodent 5′untranslated mRNAs." *Gene* 349 (April 2005): 97–105. doi:10.1016/j.gene.2004.11.041.

Iakova, Polina, Guo-Li Wang, Lubov Timchenko, Marek Michalak, Olivia M Pereira-Smith, James R Smith, and Nikolai A Timchenko. "Competition of CUGBP1 and Calreticulin for the Regulation of p21 Translation Determines Cell Fate." *The EMBO Journal* 23, no. 2 (January 28, 2004): 406–17. doi:10.1038/sj.emboj.7600052.

Ibba, M, and D Soll. "Aminoacyl-tRNA Synthesis." *Annual Review of Biochemistry* 69 (2000): 617–50. doi:10.1146/annurev.biochem.69.1.617.

J

Jackson, Richard J., Christopher U. T. Hellen, and Tatyana V. Pestova. "The Mechanism of Eukaryotic Translation Initiation and Principles of Its Regulation." *Nature Reviews Molecular Cell Biology* 11, no. 2 (février 2010): 113–27. doi:10.1038/nrm2838.

Jaeger, J A, J SantaLucia, and I Tinoco. "Determination of RNA Structure and Thermodynamics." *Annual Review of Biochemistry* 62, no. 1 (1993): 255–85. doi:10.1146/annurev.bi.62.070193.001351.

Jang, S. K., H. G. Kräusslich, M. J. Nicklin, G. M. Duke, A. C. Palmenberg, and E. Wimmer. "A Segment of the 5' Nontranslated Region of Encephalomyocarditis Virus RNA Directs Internal Entry of Ribosomes during in Vitro Translation." *Journal of Virology* 62, no. 8 (August 1, 1988): 2636–43.

Jenkins, Robert H., Rasha Bennagi, John Martin, Aled O. Phillips, James E. Redman, and Donald J. Fraser. "A Conserved Stem Loop Motif in the 5′Untranslated Region Regulates Transforming Growth Factor-β1 Translation." Edited by Y. Adam Yuan. *PLoS ONE* 5, no. 8 (August 26, 2010): e12283. doi:10.1371/journal.pone.0012283.

Jeong, E. J., G. S. Hwang, K. H. Kim, M. J. Kim, S. Kim, and K. S. Kim. "Structural Analysis of Multifunctional Peptide Motifs in Human Bifunctional tRNA Synthetase: Identification of RNA-Binding Residues and Functional Implications for Tandem Repeats." *Biochemistry* 39, no. 51 (December 26, 2000): 15775–82.

Jia, Jie, Abul Arif, Partho S. Ray, and Paul L. Fox. "WHEP Domains Direct Noncanonical Function of Glutamyl-Prolyl tRNA Synthetase in Translational Control of Gene Expression." *Molecular Cell* 29, no. 6 (March 28, 2008): 679–90. doi:10.1016/j.molcel.2008.01.010.

Jiang, M., J. Mak, A. Ladha, E. Cohen, M. Klein, B. Rovinski, and L. Kleiman. "Identification of tRNAs Incorporated into Wild-Type and Mutant Human Immunodeficiency Virus Type 1." *Journal of Virology* 67, no. 6 (1993): 3246–53.

Jin, Hong, Heng Wu, Gregory Osterhaus, Jianning Wei, Kathleen Davis, Di Sha, Eric Floor, Che-Chang Hsu, Richard D. Kopke, and Jang-Yen Wu. "Demonstration of Functional Coupling between Γ-Aminobutyric Acid (GABA) Synthesis and Vesicular GABA Transport into Synaptic Vesicles." *Proceedings of the National Academy of Sciences* 100, no. 7 (April 1, 2003): 4293–98. doi:10.1073/pnas.0730698100.

Johannes, G., and P. Sarnow. "Cap-Independent Polysomal Association of Natural mRNAs Encoding c-Myc, BiP, and eIF4G Conferred by Internal Ribosome Entry Sites." *RNA (New York, N.Y.)* 4, no. 12 (December 1998): 1500–1513.

Jones, C.P., J. Saadatmand, L. Kleiman, and K. Musier-Forsyth. "Molecular Mimicry of Human tRNALys Anti-Codon Domain by HIV-1 RNA Genome Facilitates tRNA Primer Annealing." *RNA* 19, no. 2 (2013): 219–29. doi:10.1261/rna.036681.112.

Jopling, C. L., and A. E. Willis. "N-Myc Translation Is Initiated via an Internal Ribosome Entry Segment That Displays Enhanced Activity in Neuronal Cells." *Oncogene* 20, no. 21 (May 10, 2001): 2664–70. doi:10.1038/sj.onc.1204404.

Jopling, Catherine L., Keith A. Spriggs, Sally A. Mitchell, Mark Stoneley, and Anne E. Willis. "L-Myc Protein Synthesis Is Initiated by Internal Ribosome Entry." *RNA (New York, N.Y.)* 10, no. 2 (February 2004): 287–98.

Jordanova, Albena, Joy Irobi, Florian P. Thomas, Patrick Van Dijck, Kris Meerschaert, Maarten Dewil, Ines Dierick, et al. "Disrupted Function and Axonal Distribution of Mutant Tyrosyl-tRNA Synthetase in Dominant Intermediate Charcot-Marie-Tooth Neuropathy." *Nature Genetics* 38, no. 2 (février 2006): 197–202. doi:10.1038/ng1727.

Jousse, C., A. Bruhat, V. Carraro, F. Urano, M. Ferrara, D. Ron, and P. Fafournoux. "Inhibition of CHOP Translation by a Peptide Encoded by an Open Reading Frame Localized in the Chop 5'UTR." *Nucleic Acids Research* 29, no. 21 (November 1, 2001): 4341–51.

K

Kapasi, Purvi, Sujan Chaudhuri, Keyur Vyas, Diane Baus, Anton A. Komar, Paul L. Fox, William C. Merrick, and Barsanjit Mazumder. "L13a Blocks 48S Assembly: Role of a General Initiation Factor in mRNA-Specific Translational Control." *Molecular Cell* 25, no. 1 (January 12, 2007): 113–26. doi:10.1016/j.molcel.2006.11.028.

Kiebler, Michael A., and Luc DesGroseillers. "Molecular Insights into mRNA Transport and Local Translation in the Mammalian Nervous System." *Neuron* 25, no. 1 (2000): 19–28.

Kim, S. J., K. Park, D. Koeller, K. Y. Kim, L. M. Wakefield, M. B. Sporn, and A. B. Roberts. "Post-Transcriptional Regulation of the Human Transforming Growth Factor-Beta 1 Gene." *The Journal of Biological Chemistry* 267, no. 19 (July 5, 1992): 13702–7.

Kim, Sunghoon, Sungyong You, and Daehee Hwang. "Aminoacyl-tRNA Synthetases and Tumorigenesis: More than Housekeeping." *Nature Reviews Cancer* 11, no. 10 (September 23, 2011): 708–18. doi:10.1038/nrc3124.

Kim, Y. K., B. Hahm, and S. K. Jang. "Polypyrimidine Tract-Binding Protein Inhibits Translation of Bip mRNA." *Journal of Molecular Biology* 304, no. 2 (November 24, 2000): 119–33. doi:10.1006/jmbi.2000.4179.

Kleiman, Lawrence, Christopher P. Jones, and Karin Musier-Forsyth. "Formation of the tRNALys Packaging Complex in HIV-1." *FEBS Letters*, Transfer RNA, 584, no. 2 (January 21, 2010): 359–65. doi:10.1016/j.febslet.2009.11.038.

Klishin, A., N. Lozovaya, J. Pintor, M. T. Miras-Portugal, and O. Krishtal. "Possible Functional Role of Diadenosine Polyphosphates: Negative Feedback for Excitation in Hippocampus." *Neuroscience* 58, no. 2 (January 1994): 235–36.

Knapinska, Anna M., Patricia Irizarry-Barreto, Sri Adusumalli, Ioannis Androulakis, and Gary Brewer. "Molecular Mechanisms Regulating mRNA Stability: Physiological and Pathological Significance." *Current Genomics* 6, no. 6 (2005): 471–86.

Ko, Y. G., E. Y. Kim, T. Kim, H. Park, H. S. Park, E. J. Choi, and S. Kim. "Glutamine-Dependent Antiapoptotic Interaction of Human Glutaminyl-tRNA Synthetase with Apoptosis Signal-Regulating Kinase 1." *The Journal of Biological Chemistry* 276, no. 8 (February 23, 2001): 6030–36. doi:10.1074/jbc.M006189200.

Ko, Young-Gyu, Young-Sun Kang, Eun-Kyoung Kim, Sang Gyu Park, and Sunghoon Kim. "Nucleolar Localization of Human Methionyl–Trna Synthetase and Its Role in Ribosomal RNA Synthesis." *The Journal of Cell Biology* 149, no. 3 (May 1, 2000): 567–74. doi:10.1083/jcb.149.3.567.

Komar, Anton A., and Maria Hatzoglou. "Cellular IRES-Mediated Translation: The War of ITAFs in Pathophysiological States." *Cell Cycle* 10, no. 2 (January 15, 2011): 229–40. doi:10.4161/cc.10.2.14472.

Komar, Anton A., and Maria Hatzoglou. "Internal Ribosome Entry Sites in Cellular mRNAs: Mystery of Their Existence." *Journal of Biological Chemistry* 280, no. 25 (June 24, 2005): 23425–28. doi:10.1074/jbc.R400041200.

Kozak, M. "At Least Six Nucleotides Preceding the AUG Initiator Codon Enhance Translation in Mammalian Cells." *Journal of Molecular Biology* 196, no. 4 (August 20, 1987): 947–50.

Kraut-Cohen, Judith, and Jeffrey E. Gerst. "Addressing mRNAs to the ER: Cis Sequences Act Up!" *Trends in Biochemical Sciences* 35, no. 8 (août 2010): 459–69. doi:10.1016/j.tibs.2010.02.006.

Kushner, J. P., D. Boll, J. Quagliana, and S. Dickman. "Elevated Methionine-tRNA Synthetase Activity in Human Colon Cancer." *Proceedings of the Society for Experimental Biology and Medicine. Society for Experimental Biology and Medicine (New York, N.Y.)* 153, no. 2 (November 1976): 273–76.

L

Lal, Ashish, Krystyna Mazan-Mamczarz, Tomoko Kawai, Xiaoling Yang, Jennifer L Martindale, and Myriam Gorospe. "Concurrent versus Individual Binding of HuR and AUF1 to Common Labile Target mRNAs." *The EMBO Journal* 23, no. 15 (August 4, 2004): 3092–3102. doi:10.1038/sj.emboj.7600305.

Lang, Kenneth J. D., Andreas Kappel, and Gregory J. Goodall. "Hypoxia-Inducible Factor-1alpha mRNA Contains an Internal Ribosome Entry Site That Allows Efficient Translation during Normoxia and Hypoxia." *Molecular Biology of the Cell* 13, no. 5 (May 2002): 1792–1801. doi:10.1091/mbc.02-02-0017.

Latour, Philippe, Christel Thauvin-Robinet, Chantal Baudelet-Méry, Pierre Soichot, Veronica Cusin, Laurence Faivre, Marie-Claire Locatelli, et al. "A Major Determinant for Binding and Aminoacylation of tRNAAla in Cytoplasmic Alanyl-tRNA Synthetase Is Mutated in Dominant Axonal Charcot-Marie-Tooth Disease." *The American Journal of Human Genetics* 86, no. 1 (January 8, 2010): 77–82. doi:10.1016/j.ajhg.2009.12.005.

Law, G. L., A. Raney, C. Heusner, and D. R. Morris. "Polyamine Regulation of Ribosome Pausing at the Upstream Open Reading Frame of S-Adenosylmethionine Decarboxylase." *The Journal of Biological Chemistry* 276, no. 41 (October 12, 2001): 38036–43. doi:10.1074/jbc.M105944200.

Le Quesne, J. P., M. Stoneley, G. A. Fraser, and A. E. Willis. "Derivation of a Structural Model for the c-Myc IRES." *Journal of Molecular Biology* 310, no. 1 (June 29, 2001): 111–26. doi:10.1006/jmbi.2001.4745.

Lee, Hye Jin, Jin Park, Khriezanou Nakhro, Jin Mo Park, Yoon-Mi Hur, Byung-Ok Choi, and Ki Wha Chung. "Two Novel Mutations of GARS in Korean Families with Distal Hereditary Motor Neuropathy Type V." *Journal of the Peripheral Nervous System* 17, no. 4 (2012): 418–21.

Lee, Sooncheol, Botao Liu, Soohyun Lee, Sheng-Xiong Huang, Ben Shen, and Shu-Bing Qian. "Global Mapping of Translation Initiation Sites in Mammalian Cells at Single-

Nucleotide Resolution." *Proceedings of the National Academy of Sciences* 109, no. 37 (September 11, 2012): 14728–29. doi:10.1073/pnas.1207846109.

Lee, Yu-Nee, Hovav Nechushtan, Navah Figov, and Ehud Razin. "The Function of Lysyl-tRNA Synthetase and Ap4A as Signaling Regulators of MITF Activity in FcepsilonRI-Activated Mast Cells." *Immunity* 20, no. 2 (February 2004): 145–51.

Lee, Yu-Nee, and Ehud Razin. "Nonconventional Involvement of LysRS in the Molecular Mechanism of USF2 Transcriptional Activity in FcepsilonRI-Activated Mast Cells." *Molecular and Cellular Biology* 25, no. 20 (October 2005): 8904–12. doi:10.1128/MCB.25.20.8904-8912.2005.

Levy, Carmit, and David E. Fisher. "Dual Roles of Lineage Restricted Transcription Factors: The Case of MITF in Melanocytes." *Transcription* 2, no. 1 (February 2011): 19–22. doi:10.4161/trns.2.1.13650.

Lewis, S. M., and M. Holcik. "For IRES Trans-Acting Factors, It Is All about Location." *Oncogene* 27, no. 8 (September 3, 2007): 1033–35. doi:10.1038/sj.onc.1210777.

Lewis, Stephen M., Anne Veyrier, Nicoleta Hosszu Ungureanu, Sophie Bonnal, Stéphan Vagner, and Martin Holcik. "Subcellular Relocalization of a Trans-Acting Factor Regulates XIAP IRES-Dependent Translation." *Molecular Biology of the Cell* 18, no. 4 (April 2007): 1302–11. doi:10.1091/mbc.E06-06-0515.

Loya, A., L. Pnueli, Y. Yosefzon, Y. Wexler, M. Ziv-Ukelson, and Y. Arava. "The 3'-UTR Mediates the Cellular Localization of an mRNA Encoding a Short Plasma Membrane Protein." *RNA* 14, no. 7 (May 29, 2008): 1352–65. doi:10.1261/rna.867208.

Lu, Phoebe D., Heather P. Harding, and David Ron. "Translation Reinitiation at Alternative Open Reading Frames Regulates Gene Expression in an Integrated Stress Response." *The Journal of Cell Biology* 167, no. 1 (October 11, 2004): 27–33. doi:10.1083/jcb.200408003.

M

Mahler, Michael, Frederick W. Miller, and Marvin J. Fritzler. "Idiopathic Inflammatory Myopathies and the Anti-Synthetase Syndrome: A Comprehensive Review." *Autoimmunity Reviews* 13, no. 4–5 (April 2014): 367–71. doi:10.1016/j.autrev.2014.01.022.

Marash, Lea, Noa Liberman, Sivan Henis-Korenblit, Gilad Sivan, Eran Reem, Orna Elroy-Stein, and Adi Kimchi. "DAP5 Promotes Cap-Independent Translation of Bcl-2 and CDK1 to Facilitate Cell Survival during Mitosis." *Molecular Cell* 30, no. 4 (May 23, 2008): 447–59. doi:10.1016/j.molcel.2008.03.018.

Marshall, Lynne, Niall S. Kenneth, and Robert J. White. "Elevated tRNA(iMet) Synthesis Can Drive Cell Proliferation and Oncogenic Transformation." *Cell* 133, no. 1 (April 4, 2008): 78–89. doi:10.1016/j.cell.2008.02.035.

Martin, Franck, Sharief Barends, Sophie Jaeger, Laure Schaeffer, Lydia Prongidi-Fix, and Gilbert Eriani. "Cap-Assisted Internal Initiation of Translation of Histone H4." *Molecular Cell* 41, no. 2 (January 21, 2011): 197–209. doi:10.1016/j.molcel.2010.12.019.

Martineau, Yvan, Christine Le Bec, Laurent Monbrun, Valérie Allo, Ing-Ming Chiu, Olivier Danos, Hervé Moine, Hervé Prats, and Anne-Catherine Prats. "Internal Ribosome Entry Site Structural Motifs Conserved among Mammalian Fibroblast Growth Factor 1 Alternatively Spliced mRNAs." *Molecular and Cellular Biology* 24, no. 17 (September 2004): 7622–35. doi:10.1128/MCB.24.17.7622-7635.2004.

Mathews, M. B., and R. M. Bernstein. "Myositis Autoantibody Inhibits Histidyl-tRNA Synthetase: A Model for Autoimmunity." *Nature* 304, no. 5922 (July 14, 1983): 177–79.

Mathews, M. B., M. Reichlin, G. R. Hughes, and R. M. Bernstein. "Anti-Threonyl-tRNA Synthetase, a Second Myositis-Related Autoantibody." *The Journal of Experimental Medicine* 160, no. 2 (August 1, 1984): 420–34.

Mazumder, B., and P. L. Fox. "Delayed Translational Silencing of Ceruloplasmin Transcript in Gamma Interferon-Activated U937 Monocytic Cells: Role of the 3' Untranslated Region." *Molecular and Cellular Biology* 19, no. 10 (October 1999): 6898–6905.

Mazumder, Barsanjit, Prabha Sampath, Vasudevan Seshadri, Ratan K. Maitra, Paul E. DiCorleto, and Paul L. Fox. "Regulated Release of L13a from the 60S Ribosomal Subunit as a Mechanism of Transcript-Specific Translational Control." *Cell* 115, no. 2 (October 17, 2003): 187–98.

McIntire, Steven L., Richard J. Reimer, Kim Schuske, Robert H. Edwards, and Erik M. Jorgensen. "Identification and Characterization of the Vesicular GABA Transporter." *Nature* 389, no. 6653 (October 23, 1997): 870–76. doi:10.1038/39908.

McLaughlin, Heather M., Reiko Sakaguchi, William Giblin, NISC Comparative Sequencing Program, Thomas E. Wilson, Leslie Biesecker, James R. Lupski, et al. "A Recurrent Loss-of-Function Alanyl-tRNA Synthetase (AARS) Mutation in Patients with Charcot-Marie-Tooth Disease Type 2N (CMT2N)." *Human Mutation* 33, no. 1 (January 2012): 244–53. doi:10.1002/humu.21635.

McLaughlin, Heather M., Reiko Sakaguchi, Cuiping Liu, Takao Igarashi, Davut Pehlivan, Kristine Chu, Ram Iyer, et al. "Compound Heterozygosity for Loss-of-Function Lysyl-tRNA Synthetase Mutations in a Patient with Peripheral Neuropathy." *The American Journal of Human Genetics* 87, no. 4 (October 8, 2010): 560–66. doi:10.1016/j.ajhg.2010.09.008.

Meier, V. S., R. Böhni, and D. Schümperli. "Nucleotide Sequence of Two Mouse Histone H4 Genes." *Nucleic Acids Research* 17, no. 2 (January 25, 1989): 795.

Miller, Richard J. "Presynaptic Receptors." *Annual Review of Pharmacology and Toxicology* 38, no. 1 (1998): 201–27. doi:10.1146/annurev.pharmtox.38.1.201.

Miras-Portugal, M. T., J. Pintor, and J. Gualix. "Ca 2+ Signalling in Brain Synaptosomes Activated by Dinucleotides." *Journal of Membrane Biology* 194, no. 1 (June 1, 2003): 1–10. doi:10.1007/s00232-003-2024-x.

Mitchell, S. A., E. C. Brown, M. J. Coldwell, R. J. Jackson, and A. E. Willis. "Protein Factor Requirements of the Apaf-1 Internal Ribosome Entry Segment: Roles of Polypyrimidine Tract Binding Protein and Upstream of N-Ras." *Molecular and Cellular Biology* 21, no. 10 (May 2001): 3364–74. doi:10.1128/MCB.21.10.3364-3374.2001.

Mitchell, Sally A., Keith A. Spriggs, Mark J. Coldwell, Richard J. Jackson, and Anne E. Willis. "The Apaf-1 Internal Ribosome Entry Segment Attains the Correct Structural Conformation for Function via Interactions with PTB and Unr." *Molecular Cell* 11, no. 3 (2003): 757–71.

Motley, William W., Kevin L. Seburn, Mir Hussain Nawaz, Kathy E. Miers, Jun Cheng, Anthony Antonellis, Eric D. Green, et al. "Charcot-Marie-Tooth-Linked Mutant GARS Is Toxic to Peripheral Neurons Independent of Wild-Type GARS Levels." *PLoS Genetics* 7, no. 12 (December 2011): e1002399. doi:10.1371/journal.pgen.1002399.

Motley, William W., Kevin Talbot, and Kenneth H. Fischbeck. "GARS Axonopathy: Not Every Neuron's Cup of tRNA." *Trends in Neurosciences* 33, no. 2 (February 2010): 59–66. doi:10.1016/j.tins.2009.11.001.

Motzik, Alex, Hovav Nechushtan, Shen Yun Foo, and Ehud Razin. "Non-Canonical Roles of Lysyl-tRNA Synthetase in Health and Disease." *Trends in Molecular Medicine* 19, no. 12 (décembre 2013): 726–31. doi:10.1016/j.molmed.2013.07.011.

Mukhopadhyay, Rupak, Partho Sarothi Ray, Abul Arif, Anna K. Brady, Michael Kinter, and Paul L. Fox. "DAPK-ZIPK-L13a Axis Constitutes a Negative-Feedback Module Regulating Inflammatory Gene Expression." *Molecular Cell* 32, no. 3 (November 7, 2008): 371–82. doi:10.1016/j.molcel.2008.09.019.

Mun, Joohee, Yong-Hak Kim, Jonghan Yu, Jinhee Bae, Dong-Young Noh, Myeong-Hee Yu, and Cheolju Lee. "A Proteomic Approach Based on Multiple Parallel Separation for the Unambiguous Identification of an Antibody Cognate Antigen." *ELECTROPHORESIS* 31, no. 20 (October 2010): 3428–36. doi:10.1002/elps.201000136.

N

Nanbru, C., I. Lafon, S. Audigier, M. C. Gensac, S. Vagner, G. Huez, and A. C. Prats. "Alternative Translation of the Proto-Oncogene c-Myc by an Internal Ribosome Entry Site." *The Journal of Biological Chemistry* 272, no. 51 (December 19, 1997): 32061–66.

Nangle, Leslie A., Wei Zhang, Wei Xie, Xiang-Lei Yang, and Paul Schimmel. "Charcot-Marie-Tooth Disease-Associated Mutant tRNA Synthetases Linked to Altered Dimer Interface and Neurite Distribution Defect." *Proceedings of the National Academy of Sciences of the United States of America* 104, no. 27 (July 3, 2007): 11239–44. doi:10.1073/pnas.0705055104.

Naveau, Marie, Christine Lazennec-Schurdevin, Michel Panvert, Yves Mechulam, and Emmanuelle Schmitt. "tRNA Binding Properties of Eukaryotic Translation Initiation Factor 2 from Encephalitozoon Cuniculi." *Biochemistry* 49, no. 40 (October 12, 2010): 8680–88. doi:10.1021/bi1009166.

O

Ofir-Birin, Yifat, Pengfei Fang, Steven P. Bennett, Hui-Min Zhang, Jing Wang, Inbal Rachmin, Ryan Shapiro, et al. "Structural Switch of Lysyl-tRNA Synthetase between Translation and Transcription." *Molecular Cell* 49, no. 1 (January 10, 2013): 30–42. doi:10.1016/j.molcel.2012.10.010.

Otani, Atsushi, Bonnie M. Slike, Michael I. Dorrell, John Hood, Karen Kinder, Karla L. Ewalt, David Cheresh, Paul Schimmel, and Martin Friedlander. "A Fragment of Human TrpRS as a Potent Antagonist of Ocular Angiogenesis." *Proceedings of the National Academy of Sciences of the United States of America* 99, no. 1 (January 8, 2002): 178–83. doi:10.1073/pnas.012601899.

Oyama, Masaaki, Chiharu Itagaki, Hiroko Hata, Yutaka Suzuki, Tomonori Izumi, Tohru Natsume, Toshiaki Isobe, and Sumio Sugano. "Analysis of Small Human Proteins Reveals the Translation of Upstream Open Reading Frames of mRNAs." *Genome Research* 14, no. 10b (October 15, 2004): 2048–52. doi:10.1101/gr.2384604.

Oyama, Masaaki, Hiroko Kozuka-Hata, Yutaka Suzuki, Kentaro Semba, Tadashi Yamamoto, and Sumio Sugano. "Diversity of Translation Start Sites May Define Increased Complexity of the Human Short ORFeome." *Molecular & Cellular Proteomics: MCP* 6, no. 6 (June 2007): 1000–1006. doi:10.1074/mcp.M600297-MCP200.

P

Pace, Norman R., Brian C. Thomas, and Carl R. Woese. "Probing RNA Structure, Function, and History by Comparative Analysis." *COLD SPRING HARBOR MONOGRAPH SERIES* 37 (1999): 113–42.

Palam, Lakshmi Reddy, Thomas D. Baird, and Ronald C. Wek. "Phosphorylation of eIF2 Facilitates Ribosomal Bypass of an Inhibitory Upstream ORF to Enhance CHOP Translation." *Journal of Biological Chemistry* 286, no. 13 (April 1, 2011): 10939–49. doi:10.1074/jbc.M110.216093.

Pang, Yan Ling Joy, Kiranmai Poruri, and Susan A. Martinis. "tRNA Synthetase: tRNA Aminoacylation and beyond: Aminoacyl-tRNA Synthetases." *Wiley Interdisciplinary Reviews: RNA* 5, no. 4 (July 2014): 461–80. doi:10.1002/wrna.1224.

Pareyson, Davide, and Chiara Marchesi. "Diagnosis, Natural History, and Management of Charcot-Marie-Tooth Disease." *Lancet Neurology* 8, no. 7 (July 2009): 654–67. doi:10.1016/S1474-4422(09)70110-3.

Pareyson, Davide, Mary M. Reilly, Angelo Schenone, Gian Maria Fabrizi, Tiziana Cavallaro, Lucio Santoro, Giuseppe Vita, et al. "Ascorbic Acid in Charcot-Marie-Tooth Disease Type 1A (CMT-TRIAAL and CMT-TRAUK): A Double-Blind Randomised Trial." *Lancet Neurology* 10, no. 4 (April 2011): 320–28. doi:10.1016/S1474-4422(11)70025-4.

Park, M. C., T. Kang, D. Jin, J. M. Han, S. B. Kim, Y. J. Park, K. Cho, et al. "Secreted Human Glycyl-tRNA Synthetase Implicated in Defense against ERK-Activated Tumorigenesis." *Proceedings of the National Academy of Sciences* 109, no. 11 (March 13, 2012): E640–E647. doi:10.1073/pnas.1200194109.

Park, Sang Gyu, Hye Jin Kim, You Hong Min, Eung-Chil Choi, Young Kee Shin, Bum-Joon Park, Sang Won Lee, and Sunghoon Kim. "Human Lysyl-tRNA Synthetase Is Secreted to Trigger Proinflammatory Response." *Proceedings of the National Academy of Sciences of the United States of America* 102, no. 18 (May 3, 2005): 6356–61. doi:10.1073/pnas.0500226102.

Park, Sang Gyu, Paul Schimmel, and Sunghoon Kim. "Aminoacyl tRNA Synthetases and Their Connections to Disease." *Proceedings of the National Academy of Sciences* 105, no. 32 (August 12, 2008): 11043–49. doi:10.1073/pnas.0802862105.

Park, Sang Wook, Sung Soo Kim, Nam Jin Yoo, and Sug Hyung Lee. "Frameshift Mutation of MARS Gene Encoding an Aminoacyl-tRNA Synthetase in Gastric and Colorectal Carcinomas with Microsatellite Instability." *Gut and Liver* 4, no. 3 (September 2010): 430–31. doi:10.5009/gnl.2010.4.3.430.

Pelletier, J., and N. Sonenberg. "Internal Initiation of Translation of Eukaryotic mRNA Directed by a Sequence Derived from Poliovirus RNA." *Nature* 334, no. 6180 (July 28, 1988): 320–25. doi:10.1038/334320a0.

Pinkstaff, J. K., S. A. Chappell, V. P. Mauro, G. M. Edelman, and L. A. Krushel. "Internal Initiation of Translation of Five Dendritically Localized Neuronal mRNAs." *Proceedings of the National Academy of Sciences of the United States of America* 98, no. 5 (February 27, 2001): 2770–75. doi:10.1073/pnas.051623398.

Q

Qin, Xiangjing, Zhitai Hao, Qingnan Tian, Zhemin Zhang, Chun Zhou, and Wei Xie. "Cocrystal Structures of Glycyl-tRNA Synthetase in Complex with tRNA Suggest Multiple Conformational States in Glycylation." *The Journal of Biological Chemistry* 289, no. 29 (July 18, 2014): 20359–69. doi:10.1074/jbc.M114.557249.

R

Ray, Partho Sarothi, and Paul L. Fox. "A Post-Transcriptional Pathway Represses Monocyte VEGF-A Expression and Angiogenic Activity." *The EMBO Journal* 26, no. 14 (July 25, 2007): 3360–72. doi:10.1038/sj.emboj.7601774.

Ray, Partho Sarothi, Richa Grover, and Saumitra Das. "Two Internal Ribosome Entry Sites Mediate the Translation of p53 Isoforms." *EMBO Reports* 7, no. 4 (April 2006): 404–10. doi:10.1038/sj.embor.7400623.

Riley, Alura, Lindsay E. Jordan, and Martin Holcik. "Distinct 5' UTRs Regulate XIAP Expression under Normal Growth Conditions and during Cellular Stress." *Nucleic Acids Research* 38, no. 14 (August 2010): 4665–74. doi:10.1093/nar/gkq241.

Rodova, M., V. Ankilova, and M. G. Safro. "Human Phenylalanyl-tRNA Synthetase: Cloning, Characterization of the Deduced Amino Acid Sequences in Terms of the Structural Domains and Coordinately Regulated Expression of the Alpha and Beta Subunits in Chronic Myeloid Leukemia Cells." *Biochemical and Biophysical Research Communications* 255, no. 3 (February 24, 1999): 765–73. doi:10.1006/bbrc.1999.0141.

Rossor, Alexander M., James M. Polke, Henry Houlden, and Mary M. Reilly. "Clinical Implications of Genetic Advances in Charcot-Marie-Tooth Disease." *Nature Reviews. Neurology* 9, no. 10 (October 2013): 562–71. doi:10.1038/nrneurol.2013.179.

Ruan, H., L. M. Shantz, A. E. Pegg, and D. R. Morris. "The Upstream Open Reading Frame of the mRNA Encoding S-Adenosylmethionine Decarboxylase Is a Polyamine-Responsive Translational Control Element." *The Journal of Biological Chemistry* 271, no. 47 (November 22, 1996): 29576–82.

Rudinger-Thirion, Joëlle, Alain Lescure, Caroline Paulus, and Magali Frugier. "Misfolded Human tRNA Isodecoder Binds and Neutralizes a 3′ UTR-Embedded Alu Element." *Proceedings of the National Academy of Sciences* 108, no. 40 (October 4, 2011): E794–E802. doi:10.1073/pnas.1103698108.

Ryckelynck, Michaël, Richard Giegé, and Magali Frugier. "tRNAs and tRNA Mimics as Cornerstones of Aminoacyl-tRNA Synthetase Regulations." *Biochimie*, Facets of the RNA world, 87, no. 9–10 (September 2005): 835–45. doi:10.1016/j.biochi.2005.02.014.

S

Sagné, Corinne, Salah El Mestikawy, Marie-Françoise Isambert, Michel Hamon, Jean-Pierre Henry, Bruno Giros, and Bruno Gasnier. "Cloning of a Functional Vesicular GABA and Glycine Transporter by Screening of Genome Databases." *FEBS Letters* 417, no. 2 (November 10, 1997): 177–83. doi:10.1016/S0014-5793(97)01279-9.

Sajish, Mathew, Quansheng Zhou, Shuji Kishi, Delgado M. Valdez, Mili Kapoor, Min Guo, Sunhee Lee, Sunghoon Kim, Xiang-Lei Yang, and Paul Schimmel. "Trp-tRNA Synthetase Bridges DNA-PKcs to PARP-1 to Link IFN-γ and p53 Signaling." *Nature Chemical Biology* 8, no. 6 (June 2012): 547–54. doi:10.1038/nchembio.937.

Sampath, Prabha, Barsanjit Mazumder, Vasudevan Seshadri, and Paul L. Fox. "Transcript-Selective Translational Silencing by Gamma Interferon Is Directed by a Novel Structural Element in the Ceruloplasmin mRNA 3' Untranslated Region." *Molecular and Cellular Biology* 23, no. 5 (March 2003): 1509–19.

Schepens, Bert, Sandrine A. Tinton, Yanik Bruynooghe, Rudi Beyaert, and Sigrid Cornelis. "The Polypyrimidine Tract-Binding Protein Stimulates HIF-1alpha IRES-Mediated Translation during Hypoxia." *Nucleic Acids Research* 33, no. 21 (2005): 6884–94. doi:10.1093/nar/gki1000.

Schmidt, Eric, and Paul Schimmel. "Mutational Isolation of a Sieve for Editing in a Transfer RNA Synthetase." *Science* 264, no. 5156 (1994): 265–67.

Schneider, Caroline A., Wayne S. Rasband, and Kevin W. Eliceiri. "NIH Image to ImageJ: 25 Years of Image Analysis." *Nature Methods* 9, no. 7 (July 2012): 671–75.

Schray, Beate, and Rolf Knippers. "Binding of Human Glutaminyl-tRNA Synthetase to a Specific Site of Its mRNA." *Nucleic Acids Research* 19, no. 19 (1991): 5307–12.

Schüler, Martin, Sean R. Connell, Aurelie Lescoute, Jan Giesebrecht, Marylena Dabrowski, Birgit Schroeer, Thorsten Mielke, Pawel A. Penczek, Eric Westhof, and Christian M. T. Spahn. "Structure of the Ribosome-Bound Cricket Paralysis Virus IRES RNA." *Nature Structural & Molecular Biology* 13, no. 12 (December 2006): 1092–96. doi:10.1038/nsmb1177.

Seburn, Kevin L., Leslie A. Nangle, Gregory A. Cox, Paul Schimmel, and Robert W. Burgess. "An Active Dominant Mutation of Glycyl-tRNA Synthetase Causes Neuropathy in a Charcot-Marie-Tooth 2D Mouse Model." *Neuron* 51, no. 6 (September 21, 2006): 715–26. doi:10.1016/j.neuron.2006.08.027.

Segev, Nava, and Nissim Hay. "Hijacking Leucyl-tRNA Synthetase for Amino Acid-Dependent Regulation of TORC1." *Molecular Cell* 46, no. 1 (April 13, 2012): 4–6. doi:10.1016/j.molcel.2012.03.028.

Seo, Ah Jung, Youn Ho Shin, Seo Jin Lee, Doyeun Kim, Byung Sun Park, Sunghoon Kim, Kyu Ha Choi, et al. "A Novel Adenoviral Vector-Mediated Mouse Model of Charcot-Marie-Tooth Type 2D (CMT2D)." *Journal of Molecular Histology* 45, no. 2 (April 2014): 121–28. doi:10.1007/s10735-013-9537-0.

Siskind, Carly E., Seema Panchal, Corrine O. Smith, Shawna M. E. Feely, Joline C. Dalton, Alice B. Schindler, and Karen M. Krajewski. "A Review of Genetic Counseling for Charcot Marie Tooth Disease (CMT)." *Journal of Genetic Counseling* 22, no. 4 (August 2013): 422–36. doi:10.1007/s10897-013-9584-4.

Slavoff, Sarah A., Andrew J. Mitchell, Adam G. Schwaid, Moran N. Cabili, Jiao Ma, Joshua Z. Levin, Amir D. Karger, Bogdan A. Budnik, John L. Rinn, and Alan Saghatelian. "Peptidomic Discovery of Short Open Reading Frame–encoded Peptides in Human Cells." *Nature Chemical Biology* 9, no. 1 (January 2013): 59–64. doi:10.1038/nchembio.1120.

Sleigh, J. N., S. J. Grice, R. W. Burgess, K. Talbot, and M. Z. Cader. "Neuromuscular Junction Maturation Defects Precede Impaired Lower Motor Neuron Connectivity in Charcot-Marie-Tooth Type 2D Mice." *Human Molecular Genetics* 23, no. 10 (May 15, 2014): 2639–50. doi:10.1093/hmg/ddt659.

Somers, Joanna, Tuija Pöyry, and Anne E. Willis. "A Perspective on Mammalian Upstream Open Reading Frame Function." *The International Journal of Biochemistry & Cell Biology* 45, no. 8 (August 2013): 1690–1700. doi:10.1016/j.biocel.2013.04.020.

Sonenberg, Nahum, and Alan G. Hinnebusch. "Regulation of Translation Initiation in Eukaryotes: Mechanisms and Biological Targets." *Cell* 136, no. 4 (février 2009): 731–45. doi:10.1016/j.cell.2009.01.042.

Song, Lin, and Rocky S. Tuan. "MicroRNAs and Cell Differentiation in Mammalian Development." *Birth Defects Research Part C: Embryo Today: Reviews* 78, no. 2 (June 2006): 140–49. doi:10.1002/bdrc.20070.

Spriggs, K. A., M. Bushell, S. A. Mitchell, and A. E. Willis. "Internal Ribosome Entry Segment-Mediated Translation during Apoptosis: The Role of IRES-Trans-Acting Factors." *Cell Death & Differentiation* 12, no. 6 (2005): 585–91. doi:10.1038/sj.cdd.4401642.

Spriggs, Keith A., Laura C. Cobbold, Catherine L. Jopling, Rebecca E. Cooper, Lindsay A. Wilson, Mark Stoneley, Mark J. Coldwell, et al. "Canonical Initiation Factor Requirements of the Myc Family of Internal Ribosome Entry Segments." *Molecular and Cellular Biology* 29, no. 6 (March 2009): 1565–74. doi:10.1128/MCB.01283-08.

Stein, I., A. Itin, P. Einat, R. Skaliter, Z. Grossman, and E. Keshet. "Translation of Vascular Endothelial Growth Factor mRNA by Internal Ribosome Entry: Implications for Translation under Hypoxia." *Molecular and Cellular Biology* 18, no. 6 (June 1998): 3112–19.

Stoneley, M. "C-Myc 5′ Untranslated Region Contains an Internal Ribosome Entry Segment." *, Published Online: 21 January 1998; | doi:10.1038/sj.onc.1201763* 16, no. 3 (January 21, 1998). doi:10.1038/sj.onc.1201763.

Storkebaum, Erik, Ricardo Leitao-Goncalves, Tanja Godenschwege, Leslie Nangle, Monica Mejia, Inge Bosmans, Tinne Ooms, et al. "Dominant Mutations in the Tyrosyl-tRNA Synthetase Gene Recapitulate in Drosophila Features of Human Charcot-Marie-Tooth Neuropathy." *Proceedings of the National Academy of Sciences of the United States of America* 106, no. 28 (July 14, 2009): 11782–87. doi:10.1073/pnas.0905339106.

Stum, Morgane, Heather M. McLaughlin, Erica L. Kleinbrink, Kathy E. Miers, Susan L. Ackerman, Kevin L. Seburn, Anthony Antonellis, and Robert W. Burgess. "An Assessment of Mechanisms Underlying Peripheral Axonal Degeneration Caused by Aminoacyl-tRNA Synthetase Mutations." *Molecular and Cellular Neuroscience* 46, no. 2 (février 2011): 432–43. doi:10.1016/j.mcn.2010.11.006.

Subramanian, Murugan, Florence Rage, Ricardos Tabet, Eric Flatter, Jean-Louis Mandel, and Hervé Moine. "G–quadruplex RNA Structure as a Signal for Neurite mRNA Targeting." *EMBO Reports* 12, no. 7 (May 13, 2011): 697–704. doi:10.1038/embor.2011.76.

T

Targoff, I. N. "Autoantibodies to Aminoacyl-Transfer RNA Synthetases for Isoleucine and Glycine. Two Additional Synthetases Are Antigenic in Myositis." *Journal of Immunology (Baltimore, Md.: 1950)* 144, no. 5 (March 1, 1990): 1737–43.

Targoff, I. N., E. P. Trieu, P. H. Plotz, and F. W. Miller. "Antibodies to Glycyl-Transfer RNA Synthetase in Patients with Myositis and Interstitial Lung Disease." *Arthritis and Rheumatism* 35, no. 7 (July 1992): 821–30.

Targoff, Ira N. "Myositis Specific Autoantibodies." *Current Rheumatology Reports* 8, no. 3 (June 2006): 196–203.

Teerink, H., H. O. Voorma, and A. A. Thomas. "The Human Insulin-like Growth Factor II Leader 1 Contains an Internal Ribosomal Entry Site." *Biochimica Et Biophysica Acta* 1264, no. 3 (December 27, 1995): 403–8.

Touriol, Christian, Stéphanie Bornes, Sophie Bonnal, Sylvie Audigier, Hervé Prats, Anne-Catherine Prats, and Stéphan Vagner. "Generation of Protein Isoform Diversity by Alternative Initiation of Translation at Non-AUG Codons." *Biology of the Cell* 95, no. 3–4 (mai 2003): 169–78. doi:10.1016/S0248-4900(03)00033-9.

Tzima, Ellie, and Paul Schimmel. "Inhibition of Tumor Angiogenesis by a Natural Fragment of a tRNA Synthetase." *Trends in Biochemical Sciences*, SPECIAL ISSUE: CELEBRATING 30 YEARS OF TiBS, 31, no. 1 (January 2006): 7–10. doi:10.1016/j.tibs.2005.11.002.

U

Ubeda, M., M. Schmitt-Ney, J. Ferrer, and J. F. Habener. "CHOP/GADD153 and Methionyl-tRNA Synthetase (MetRS) Genes Overlap in a Conserved Region That Controls mRNA Stability." *Biochemical and Biophysical Research Communications* 262, no. 1 (August 19, 1999): 31–38. doi:10.1006/bbrc.1999.1140.

V

Vagner, S., M. C. Gensac, A. Maret, F. Bayard, F. Amalric, H. Prats, and A. C. Prats. "Alternative Translation of Human Fibroblast Growth Factor 2 mRNA Occurs by Internal Entry of Ribosomes." *Molecular and Cellular Biology* 15, no. 1 (January 1995): 35–44.

Vasa, Suzy M., Nicolas Guex, Kevin A. Wilkinson, Kevin M. Weeks, and Morgan C. Giddings. "ShapeFinder: A Software System for High-Throughput Quantitative Analysis of Nucleic Acid Reactivity Information Resolved by Capillary Electrophoresis." *RNA (New York, N.Y.)* 14, no. 10 (October 2008): 1979–90. doi:10.1261/rna.1166808.

Vester, Aimée, Gisselle Velez-Ruiz, Heather M. McLaughlin, NISC Comparative Sequencing Program, James R. Lupski, Kevin Talbot, Jeffery M. Vance, et al. "A Loss-of-Function Variant in the Human Histidyl-tRNA Synthetase (HARS) Gene Is Neurotoxic In Vivo." *Human Mutation* 34, no. 1 (January 1, 2013): 191–99. doi:10.1002/humu.22210.

Vyas, Keyur, Sujan Chaudhuri, Douglas W. Leaman, Anton A. Komar, Alla Musiyenko, Sailen Barik, and Barsanjit Mazumder. "Genome-Wide Polysome Profiling Reveals an Inflammation-Responsive Posttranscriptional Operon in Gamma Interferon-Activated Monocytes." *Molecular and Cellular Biology* 29, no. 2 (January 2009): 458–70. doi:10.1128/MCB.00824-08.

W

Wakasugi, K., and P. Schimmel. "Two Distinct Cytokines Released from a Human Aminoacyl-tRNA Synthetase." *Science (New York, N.Y.)* 284, no. 5411 (April 2, 1999): 147–51.

Wakasugi, Keisuke, Bonnie M. Slike, John Hood, Atsushi Otani, Karla L. Ewalt, Martin Friedlander, David A. Cheresh, and Paul Schimmel. "A Human Aminoacyl-tRNA Synthetase as a Regulator of Angiogenesis." *Proceedings of the National Academy of Sciences* 99, no. 1 (January 8, 2002): 173–77. doi:10.1073/pnas.012602099.

Wallen, Rachel C, and Anthony Antonellis. "To Charge or Not to Charge: Mechanistic Insights into Neuropathy-Associated tRNA Synthetase Mutations." *Current Opinion in Genetics & Development*, Molecular and genetic bases of disease, 23, no. 3 (juin 2013): 302–9. doi:10.1016/j.gde.2013.02.002.

Weeks, Kevin M. "Advances in RNA Secondary and Tertiary Structure Analysis by Chemical Probing." *Current Opinion in Structural Biology* 20, no. 3 (June 2010): 295–304. doi:10.1016/j.sbi.2010.04.001.

Wolf, Yuri I., L. Aravind, Nick V. Grishin, and Eugene V. Koonin. "Evolution of Aminoacyl-tRNA Synthetases—Analysis of Unique Domain Architectures and Phylogenetic Trees Reveals a Complex History of Horizontal Gene Transfer Events." *Genome Research* 9, no. 8 (August 1, 1999): 689–710. doi:10.1101/gr.9.8.689.

Won Lee, Sang, Young Sun Kang, and Sunghoon Kim. "Multifunctional Proteins in Tumorigenesis: Aminoacyl-tRNA Synthetases and Translational Components." *Current Proteomics* 3, no. 4 (December 1, 2006): 233–47. doi:10.2174/157016406780655577.

X

Xie, Wei, Leslie A. Nangle, Wei Zhang, Paul Schimmel, and Xiang-Lei Yang. "Long-Range Structural Effects of a Charcot-Marie-Tooth Disease-Causing Mutation in Human Glycyl-tRNA Synthetase." *Proceedings of the National Academy of Sciences of the United States of America* 104, no. 24 (June 12, 2007): 9976–81. doi:10.1073/pnas.0703908104.

Y

Yaman, Ibrahim, James Fernandez, Haiyan Liu, Mark Caprara, Anton A. Komar, Antonis E. Koromilas, Lingyin Zhou, et al. "The Zipper Model of Translational Control: A Small Upstream ORF Is the Switch That Controls Structural Remodeling of an mRNA Leader." *Cell* 113, no. 4 (May 16, 2003): 519–31.

Yang, D.-Q., M.-J. Halaby, and Y. Zhang. "The Identification of an Internal Ribosomal Entry Site in the 5′-Untranslated Region of p53 mRNA Provides a Novel Mechanism for the Regulation of Its Translation Following DNA Damage." *Oncogene* 25, no. 33 (avril 2006): 4613–19. doi:10.1038/sj.onc.1209483.

Yannay-Cohen, Nurit, Irit Carmi-Levy, Gillian Kay, Christopher Maolin Yang, Jung Min Han, D. Michael Kemeny, Sunghoon Kim, Hovav Nechushtan, and Ehud Razin. "LysRS Serves as a Key Signaling Molecule in the Immune Response by Regulating Gene Expression." *Molecular Cell* 34, no. 5 (juin 2009): 603–11. doi:10.1016/j.molcel.2009.05.019.

Yannay-Cohen, Nurit, and Ehud Razin. "Translation and Transcription: The Dual Functionality of LysRS in Mast Cells." *Molecules and Cells* 22, no. 2 (October 31, 2006): 127–32.

Yao, Peng, and Paul L. Fox. "Aminoacyl-tRNA Synthetases in Medicine and Disease: tRNA Synthetases and Disease." *EMBO Molecular Medicine* 5, no. 3 (March 2013): 332–43. doi:10.1002/emmm.201100626.

Z

Zeilhofer, Hanns Ulrich, Hendrik Wildner, and Gonzalo E. Yevenes. "Fast Synaptic Inhibition in Spinal Sensory Processing and Pain Control." *Physiological Reviews* 92, no. 1 (January 2012): 193–235. doi:10.1152/physrev.00043.2010.

Jana Alexandrova

Tissue-specific expression of the human Glycyl-tRNA synthetase: connection with the Charcot-Marie-Tooth disease

Human Glycyl-tRNA synthetase (GRS) is a housekeeping enzyme with a key role in protein synthesis, both in the cytosol and the mitochondria. In human, mutations in GRS cause the Charcot-Marie-Tooth (CMT) peripheral neuropathy. Though GRS activity is required in all cells, the CMT-associated mutations affect only the peripheral nervous system, suggesting an additional non canonical role.

To understand how GRS is involved in CMT pathology, we first elucidated the original post-transcriptional regulatory mechanism that controls the expression of both the mitochondrial and the cytosolic GRS from a single gene. We identified two mRNA isoforms: one coding for both enzymes; and a longer one containing a functional IRES and an uORF encoding only the cytosolic GRS, evidence that expression and localization of human GRS are tightly controlled. Furthermore, we found a particular Ca^{2+} dependant distribution of GRS in neurons, giving us a first clue about a potential non-canonical role in neurons.

La glycyl-ARNt synthétase humaine (GRS) est une enzyme clé dans la traduction des protéines dans le cytosol et la mitochondrie. Chez l'Homme, des mutations de la GRS conduisent à la neuropathie périphérique Charcot-Marie-Tooth (CMT). Bien que l'activité de la GRS soit ubiquitaire, les mutations associées à la CMT n'affectent que les nerfs périphériques, suggérant un rôle supplémentaire de la GRS dans les neurones.

Pour comprendre ce rôle, nous avons d'abord élucidé le mécanisme particulièrement complexe qui contrôle l'expression de la GRS mitochondriale et cytosolique à partir du même gène. Nous avons identifié deux ARNm : un codant pour les deux enzymes ; et un autre plus long qui contient une IRES fonctionnelle et un uORF. Cet ARNm complexe, ne génère que la GRS cytosolique et montre que son expression et localisation sont étroitement contrôlées. De plus, nous avons montré une distribution particulière de la GRS dans des neurones, qui est un premier indice sur un rôle non canonique.

Expression tissu-spécifique de la Glycyl-ARNt synthétase humaine : connexion avec la maladie de Charcot-Marie-Tooth

La Glycyl-ARNt synthétase humaine (GlyRS) est une aminoacyl-ARNt synthétase (aaRS). Les aaRS, enzymes clés dans la traduction des protéines, catalysent l'attachement de l'acide aminé sur leurs ARN de transfert homologues (1). Outre leur fonction essentielle dans l'aminoacylation, au cours des deux dernières décennies, on a observé que les aaRS sont des protéines multifonctionnelles impliquées dans des processus biologiques divers tel que la réponse immunitaire, l'apoptose, la voie de mTOR, ainsi que la régulation transcriptionnelle ou traductionelle de certains gènes (2). Certaines de ces synthétases sont aussi associées à différentes maladies comme le cancer, des maladies autoimmunes et neuronales (3).

Chez les eucaryotes, la réaction d'aminoacylation a lieu non seulement dans le cytoplasme mais également dans d'autres compartiments cellulaires comme la mitochondrie. Contrairement aux ARNt qui sont codés par le génome mitochondrial, toutes les aaRSs destinées à la traduction dans cette organelle sont codées par le génome nucléaire, synthétisées dans le cytosol puis importées dans la mitochondrie. Dans la majorité des cas, les aaRS mitochondriales sont codées par des gènes distincts de ceux qui codent pour les enzymes cytosoliques. La GlyRS est une exception (4), elle fait partie des deux seuls systèmes humains (avec la LysRS) où un gène unique est à l'origine des deux enzymes : la GlyRS cytosolique et la GlyRS mitochondriale. Dans ce cas particulier, la stratégie utilisée par la cellule est une initiation de la traduction à partir de deux AUG différents sur le même ARN messager. Ce phénomène conduit donc à la synthèse de deux protéines avec une séquence identique, sauf que la GlyRS mitochondriale est fusionnée à une extension N-terminale comportant le signal d'adressage vers la mitochondrie.

Mon travail de thèse comporte deux parties. D'une part, il s'est focalisé sur la compréhension globale de l'expression des GlyRS humaines ; ainsi j'ai étudié l'organisation de l'ARNm, afin de comprendre les mécanismes moléculaires impliqués dans la régulation de l'initiation de la traduction des formes cytosolique et mitochondriale. D'autre part, je me suis intéressée à la localisation subcellulaire et l'accumulation tissue-spécifique (dans le système nerveux) de la GlyRS. Cette étude a permis d'obtenir des résultats originaux qui pourraient élucider certaines des fonctions alternatives associées à la GlyRS et mieux comprendre son implication dans la maladie de Charcot-Marie-Tooth.

I. Régulation de l'expression de la GlyRS humaine

Chaque étape de l'expression d'un gène, à partir de la chromatine jusqu'à la protéine fonctionnelle, est régulée avec précision pour éviter un dysfonctionnement cellulaire. Ainsi, la présence de régions non traduites (UTRs) alternatives pour un ARNm donné est une source importante de régulation. Entre 15 et 21% des gènes contiennent des 5 'ou 3' UTR alternatives, générées soit par des promoteurs de transcription alternatifs (5'UTR), épissage (5 'et 3' UTR), ou des sites de polyadénylation alternatives (3 'UTR). Cette diversité donne la possibilité d'exprimer différent protéines à des stades de développement différents, des tissus, des conditions physiologiques, ou des compartiments cellulaires différents. Vu la complexité la GlyRS : deux protéines avec des localisations différentes, exprimées à partir d'un seul gène, avec des fonctions secondaires et implications dans diverses maladies, nous voulions explorer l'existence d'ARN messagers de la GlyRS avec des UTRs alternatives. J'ai utilisé la technique de la RACE PCR (Rapid Amplification of cDNA Ends) sur différents tissus humains, cerveau, moelle épinière, muscle, cœur, ratte et foie pour rechercher de façon exhaustive les différents isoformes de l'ARNm codant pour les GlyRS. Contrairement à ce qui avait été publié précédemment (5), j'ai identifié deux isoformes, qui diffèrent par leurs tailles (et leurs séquences) au niveau de extrémité 5' de l'ARNm.

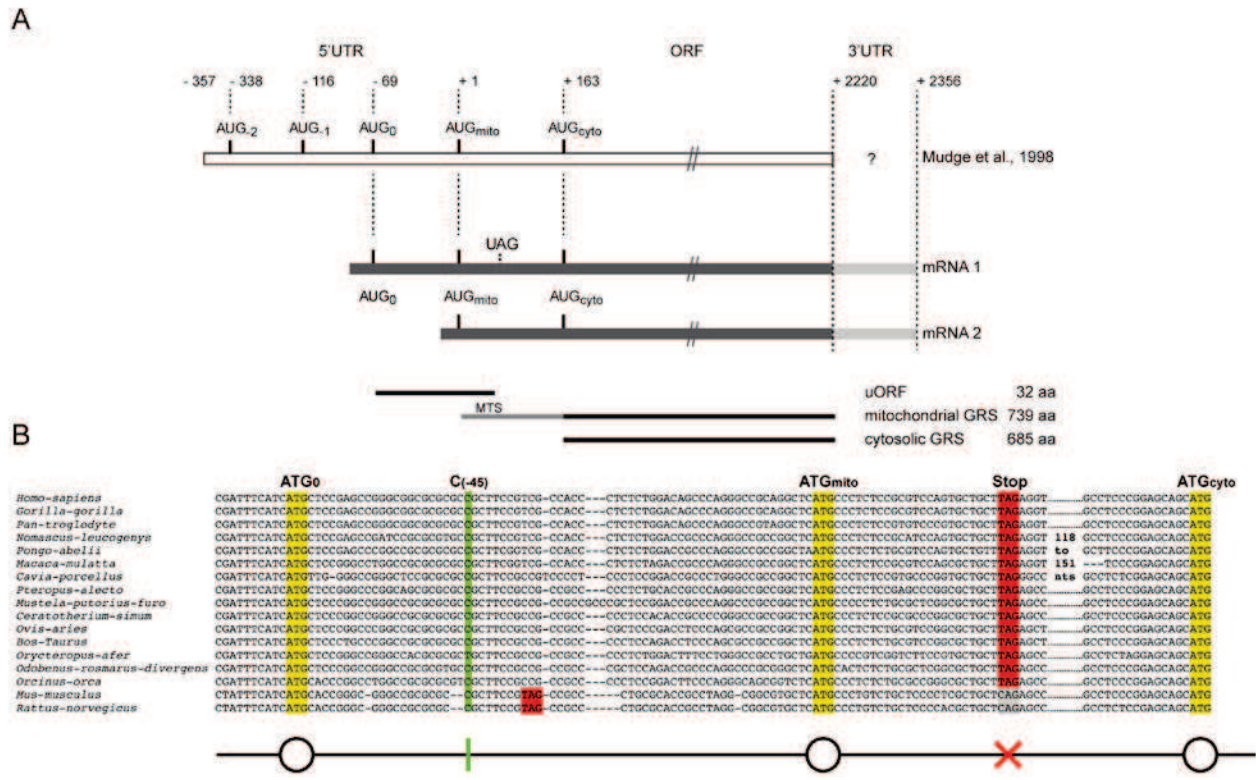

Figure 1. Description des ARNm de la GlyRS humaine identifiés par RACE PCR

(A) L'ARNm long (mRNA2) présente une extrémité 5' avec trois codons d'initiation potentiels : (1) AUG_0, (2) AUG_{mito} et (3) l' AUG_{cyto} initiant potentiellement la synthèse d'un peptide de 32 acides aminés, de la GlyRS mitochondriale avec son signal de localisation (MTS) et de la GlyRS cytosolique, respectivement. L'ARNm court (mRNA1) présente une extrémité 5' ne contenant pas l'AUG_0 et codant pour les GlyRS cytosolique et mitochondriale. **(B)** L'ARNm long avec ses trois codons d'initiation est présent uniquement chez les mammifères et son organisation est très bien conservé.

Le messager le plus court (mRNA1) est retrouvé dans tous les tissus. Comme chez tous les autres eucaryotes la séquence en 5' contient deux codons initiateurs et comme attendu, elle permet la synthèse de la GlyRS mitochondriale et de la GlyRS cytosolique. Ainsi les deux codons initiateurs ont été appelés AUG_{mito} (traduction de l'enzyme mitochondriale caractérisée par le signal de localisation en N-terminal) et AUG_{cyto} (traduction de l'enzyme cytosolique).

Le messager le plus long (mRNA2) lui est retrouvé dans tous les tissus, sauf dans le foie. Il contient un troisième codon d'initiation en amont des AUG mito et cyto. Ce codon, AUG_0 délimite une uORF (upstream Open Reading Frame) et permettrait ainsi la synthèse d'un peptide de 32 acides aminés (que nous n'avons pas pu mettre en évidence). Cette organisation particulière de l'extrémité 5' de l'ARN messager avec les trois codons AUG et le uORF est très bien conservée uniquement chez les mammifères. De façon remarquable, cet ARNm long, code préférentiellement pour la GlyRS cytosolique.

Grace à des expériences d'immunolocalisation et de traduction *in vitro* d'une série de mutants (où les 3 AUG ont été mutés individuellement ou par paires), j'ai ainsi confirmé l'identité des codons d'initiation AUG_{mito} et AUG_{cyto} dans l'ARNm long (Figure 2).

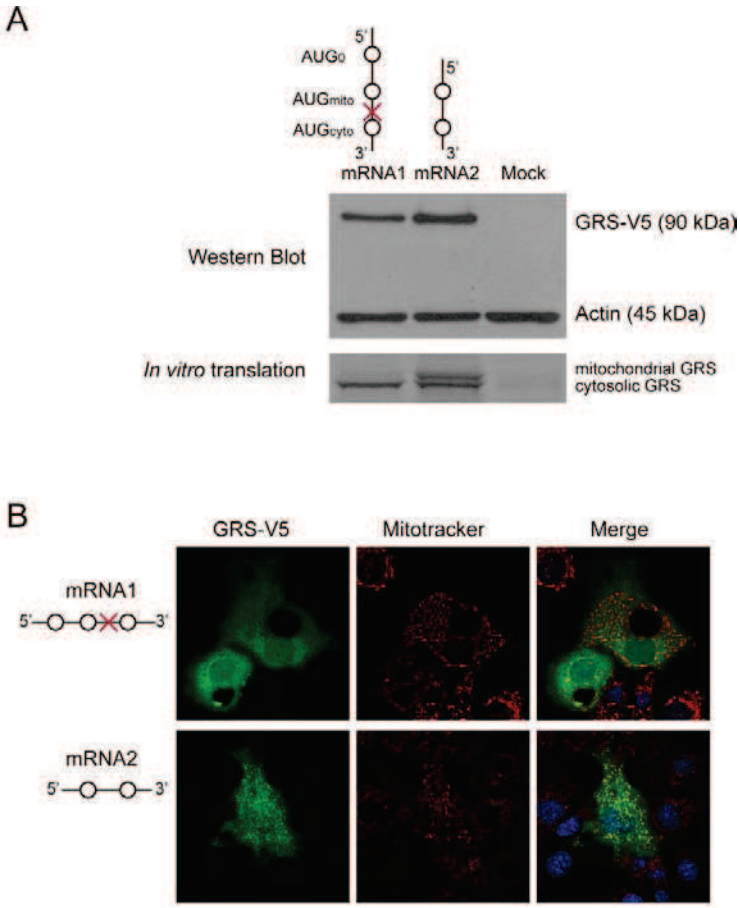

Figure 2. Traduction des deux isoformes de l'ARNm de la GlyRS *in vivo* et *in vitro*. (A) Western blot analyse de cellules transfectées avec pcDNA3.1 codant pour mRNA1 ou mRNA2, fusionnés à un épitope V5 à leur extrémité 3'. La GlyRS-V5 ainsi traduite est détectée par des anticorps anti-V5. La détection de la ß-actine à 42 kDa (anticorps anti-actine) est utilisée comme contrôle. La traduction *in vitro* radioactive des GlyRSs à partir des mRNA1 and mRNA2 a été réalisée dans des extraits de germe de blé. **(B)** La GlyRS-V5 est détectée par immunofluorescence, via des anticorps anti-V5 conjugués FITC (vert). Les mitochondries sont marquées avec le Mitotracker Orange CMTMRos (rouge) et les noyaux avec du DAPI (bleu).

De plus, l'introduction d'un nucléotide supplémentaire, induisant un décalage du cadre de lecture, m'a également permis de montrer sans ambiguïté que, malgré sa proximité avec l'extrémité 5' de l'ARN (environ une quinzaine de nucléotides), le ribosome initie efficacement la traduction à l'AUG_0 (Figure 3). Ces résultats d'une part indiquent que la synthèse du peptide est possible et d'autre part expliquent l'absence de synthèse de la GlyRS mitochondriale à partir de l'ARNm long. En effet, la séquence de la uORF englobe l'AUG_{mito} et la synthèse du peptide, en empêchant la reconnaissance de ce codon initiateur, inhibe la synthèse de la GlyRS mitochondriale. En revanche, le codon stop de la uORF étant situé entre

l'AUG_{mito} et l'AUG_{cyto} (Figure 1), l'initiation de la traduction de la GlyRS cytosolique n'est pas perturbée.

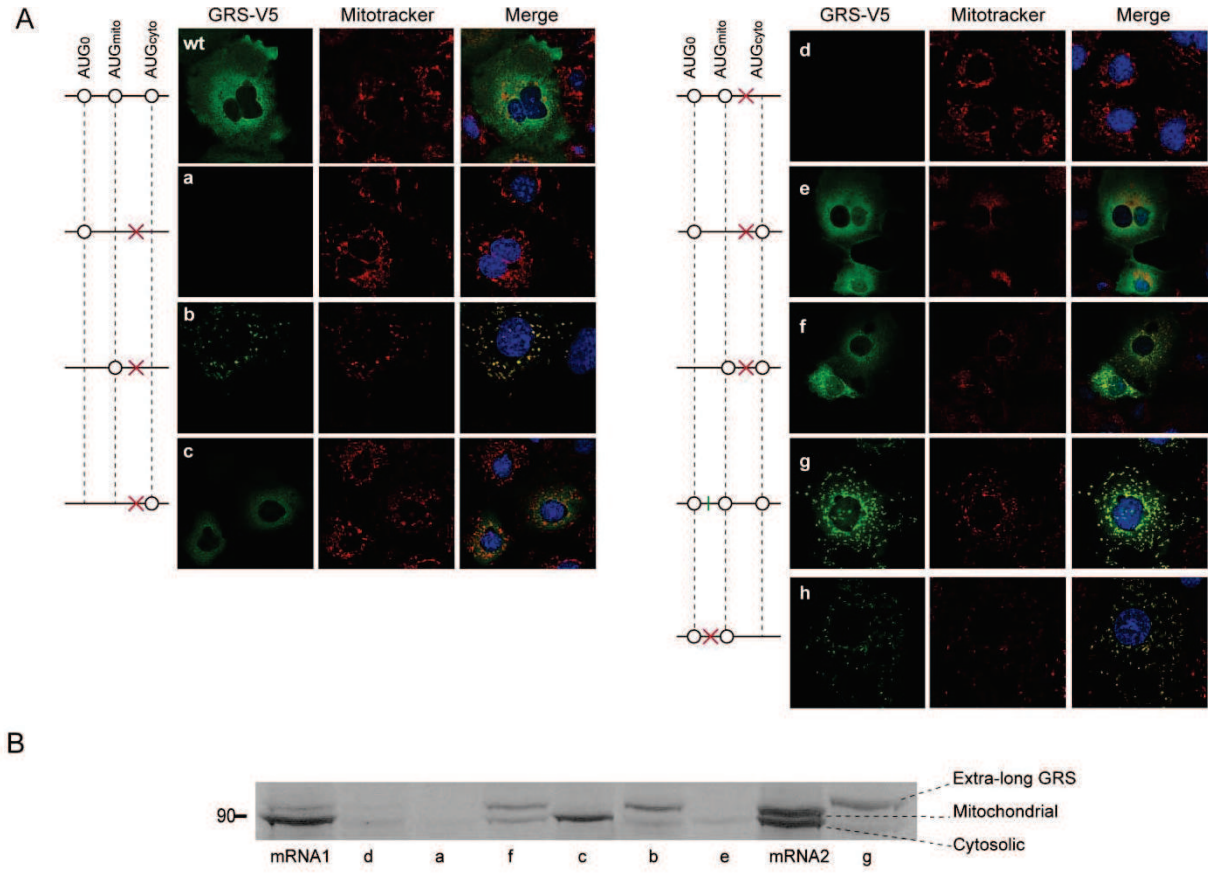

Figure 3. Immunolocalisation de la GlyRS exprimée à partir de mRNA1 muté. (A) Six mutants (a à h) ont été générés, où les différents codons AUG ont été testé pour l'initiation de la traduction. Le marquage de la GlyRS-V5, les mitochondries et le noyau ont été réalisés comme indiqué dans la légende de la Figure 2. **(B)** Les mêmes mutants ont été utilisés dans l'expérience de traduction *in vitro* (extraits de réticulocytes de lapin) en présence de méthionine ^{35}S.

Une étude plus approfondie de l'initiation de la traduction à partir de l'ARNm long a permis la mise en évidence d'un site interne d'entré du ribosome (IRES) fonctionnel, permettant d'exprimer la GlyRS de manière cap indépendante. Cet IRES est extrêmement fort, même plus fort que certains IRES virales. Fonctionnellement, cet IRES est actif dans des conditions normales dans la cellule (Figure 4) ainsi que dans des conditions de stress tel que stress de réticulum, manque de nutriments, de glucose, inhibition de la voie de mTOR ou hypoxie, mais je n'ai pas pu identifier une condition particulière où il serait plus fortement induit.

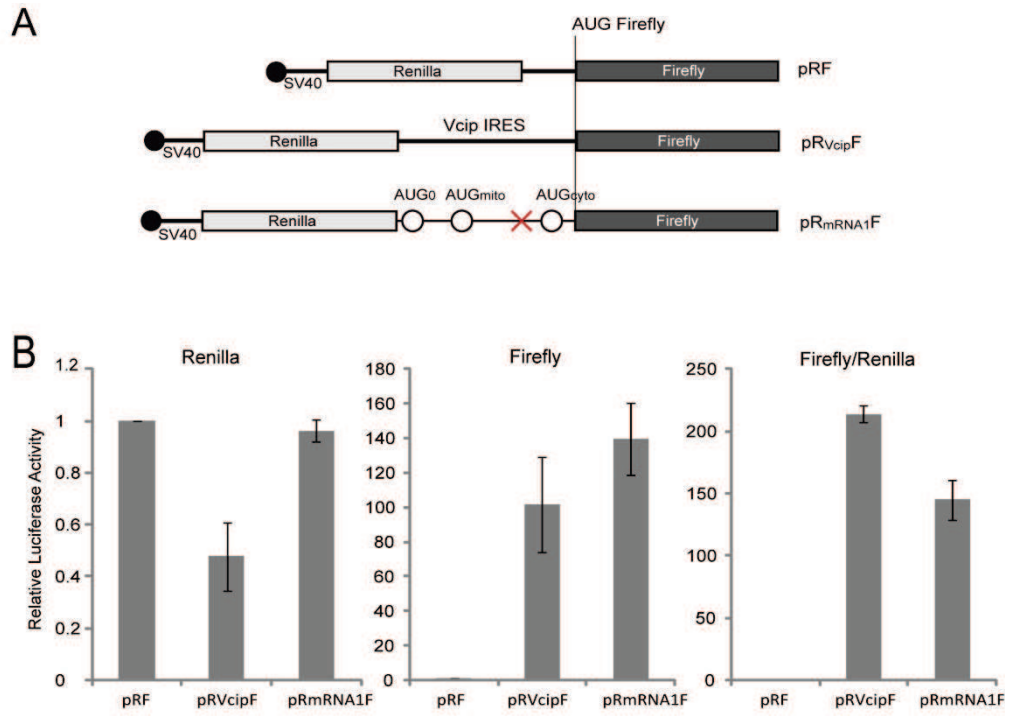

Figure 4. Comparaison des éléments IRES de mRNA1 et Vcip pour leur capacité d'initier la traduction. (A) Représentation schématique des constructions biscistroniques pRF: les séquences correspondantes à l'IRES de Vcip et mRNA1 5'-end (contenant les trois codons AUG) ont été insérées dans la région intercistronique entre les ORFs de la renilla et la firefly luciférase ($pR_{Vcip}F$ et $pR_{mRNA1}F$). La coiffe attachée à l'extrémité 5' de l'ARN messager bicistronique est indiquée avec un cercle noir. **(B)** pRF, $pR_{Vcip}F$ et $pR_{mRNA1}F$ ont été transfectés dans des cellules COS-7 et les activités de la renilla (initiation cap dépendante) et la firefly (initiation IRES-dépendante) luciférases ont été mesurées. Les activités luciférase de $pR_{Vcip}F$ et $pR_{mRNA1}F$ sont représentées relatives à l'activité pRF. Les bars d'erreur ont été calculés à partir de trois expériences indépendantes.

Afin de donner une image plus précise des 5'UTRs de l'ARN messager court et long de la GlyRS et de la disposition des AUG initiateurs, j'ai essayé de déterminer la structure de cette région en utilisant les techniques de cartographie en solution et de SHAPE (selective 2'-hydroxyl acylation analyzed by primer extension). Malheureusement la séquence très riche en GC (74%) s'organise dans une structure très stable qui ne permet ni un marquage direct de l'ARN ni une extension efficace par la reverse transcriptase. Malgré les nombreuses conditions testées, je n'ai pas pu établir la structure de la région 5'. Ce résultat rejoint ce qui a été observé jusqu'à présent sur les IRES cellulaires, où très peu de choses sont connues puisque que la majorité des structures proposées sont essentiellement le résultat de prédictions *in sillico*.

Compte tenu de l'implication de la GlyRS dans de nombreuses fonctions alternatives, ainsi que dans la maladie de Charcot-Marie-Tooth, on suppose que cet IRES peut jouer un rôle important dans l'expression tissu-spécifique de la synthétase, en particulier dans les tissus neuronaux.

II. Localisations et une fonction alternative possible

La GlyRS est un parfait exemple d'une enzyme multifonctionnelle. Outre sa fonction essentielle dans la synthèse protéique, elle joue un rôle protecteur dans la tumorigenèse, elle synthétise aussi l'Ap4A (molécule de signalisation intra et extracellulaire) et stimule l'initiation de la traduction du génome du Poliovirus en se fixant sur son IRES (6, 7, 8). De plus, chez l'Homme, il a été montré que des mutations de la GlyRS provoquent des phénotypes cliniques associés à la pathologie de Charcot-Marie-Tooth de type 2D (CMT-2D) et à une forme sévère infantile d'atrophie musculaire spinale de type V (SMA-V). Bien que l'activité d'aminoacylation de la GlyRS soit indispensable dans toutes les cellules, les mutations associées à la CMT-2D n'affectent que le système nerveux périphérique. De plus, la GlyRS est observée sous forme de granules (de nature inconnue) dans ces axones. L'ensemble de ces observations suggèrent l'importance de sa localisation dans la pathogenèse de la CMT et qu'elle joue un rôle clé dans le maintien des axones du système nerveux périphérique. Cependant, le lien existant entre une synthèse protéique déficiente, la pathologie et la spécificité tissulaire n'est pas établi à ce jour. Ainsi, la détermination du rôle de ces granules mais surtout du mécanisme qui contrôle leur formation dans les neurones est essentielle dans la compréhension des pathologies SMA-V et CMT-2D.

Je me suis donc intéressée à l'expression et à l'accumulation tissue-spécifique de la GlyRS ainsi qu'à l'existence d'une fonction alternative pour cette enzyme dans le système nerveux. Des expériences d'immunolocalisation dans des neuroblastes différentiés SH-SY5Y ont permis de montrer que la GlyRS exprimée à partir de l'ARNm court et l'ARNm long est localisée dans le core du neurone mais aussi dans les projections neuronales (Figure 5).

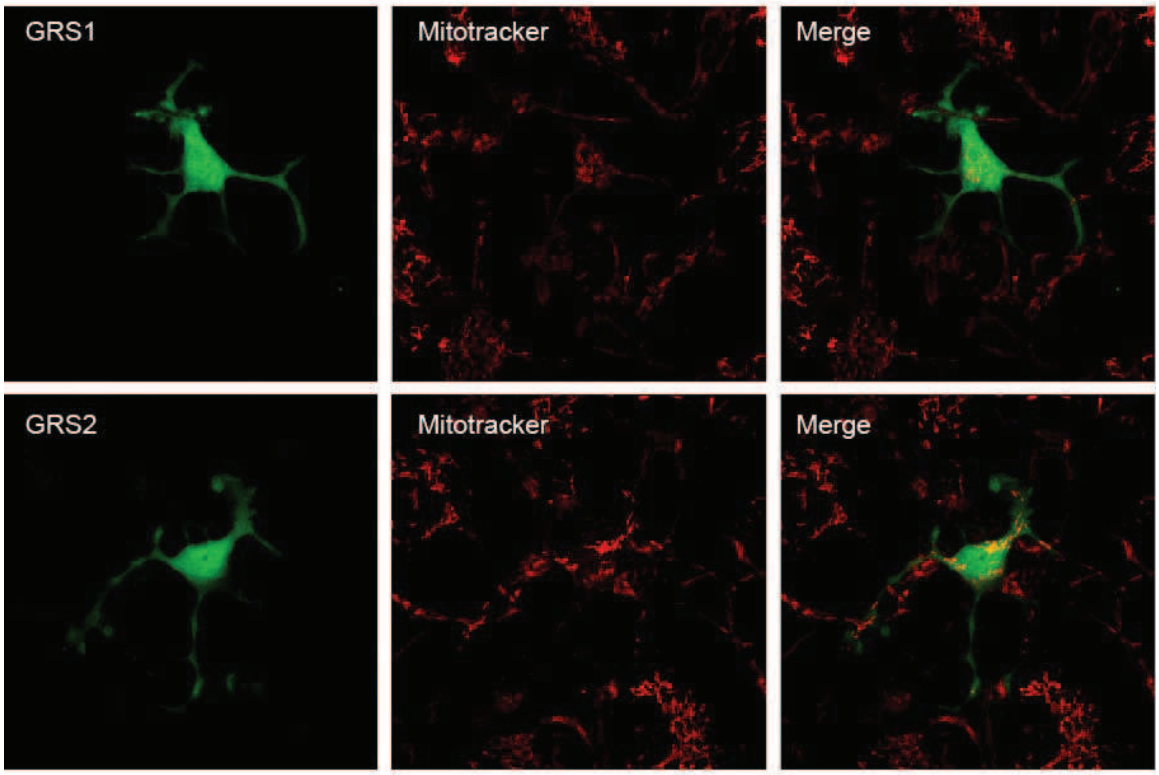

Figure 5. Expression de la GlyRS dans des neurones

Les constructions pcDNA3.1-mRNA1 et pcDNA3.1-mRNA2 ont été exprimées de manière transitoire dans des neuroblastes différentiées SH-SY5Y. La GlyRS est fusionnée à un épitope V5 à son extrémité C-terminale, permettant ainsi une détection par des anticorps anti-V5. **(A)** Analyse par Western blot: des anticorps anti-V5 conjugués HRP permettent de détecter la GlyRS cytosolique (≈ 90 kDa), et des anticorps anti-actine, la β-actine de 42 kDa. **(B)** Les GlyRS mitochondriale et cytosolique ont été détectées par immunofluorescence, en utilisant des anticorps anti-V5 couplés au FITC (vert) et les mitochondries ont été marquées avec le Mitotracker Orange CMTMRos (rouge). Les images fusionnées montrent une localisation spécifique de la GlyRS détectable dans le cytoplasme du core neuronal, ainsi que dans les projections de neurites pour mRNA1 et mRNA2.

Nous avons constaté que lorsque les cellules neuronales sont traitées avec 30 mM de KCl ou 5 mM de $CaCl_2$ la GlyRS forme des granules (Figure 6). Ce traitement est généralement utilisé pour induire une exocytose des vésicules synaptiques et ceci nous a conduits à l'hypothèse que la GlyRS pourrait être impliquée dans la signalisation neuronale.

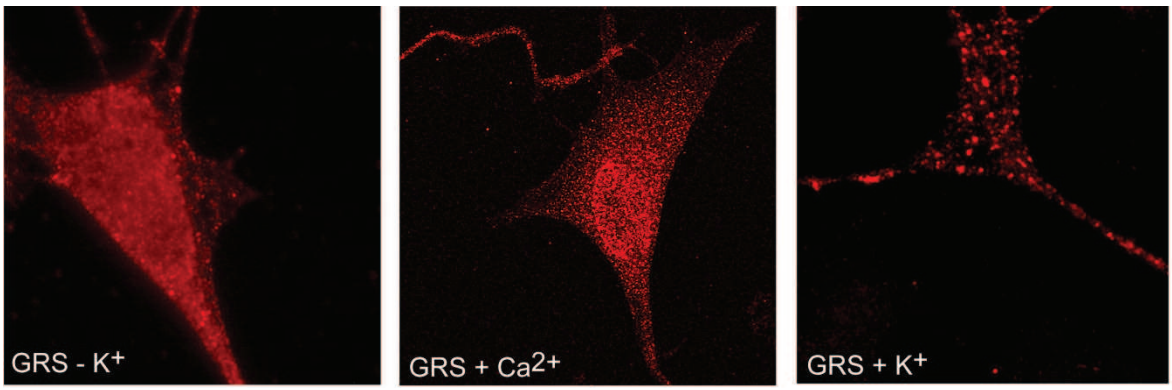

Figure 6. Expression de la GlyRS dans des neurones

Des neuroblastes différenciés SH-SY5Y sont **(A)** pas traités (gauche) ou **(B)** traités avec 5 mM Ca^{2+} pendant 15 minutes ou **(C)** avec 30 mM KCl pendant 10 minutes. La GlyRS endogène est détecté via des anticorps spécifiques (rouge).

En effet, dans le système nerveux des vertébrés, la glycine est non seulement le substrat de la GlyRS, mais c'est aussi un neurotransmetteur inhibiteur, au même titre que le GABA (acide γ-aminobutyrique). Le même transporteur vésiculaire, VIAAT (Vesicular Inhibitory Amino Acid Transporter), permet le remplissage des vésicules neurosynaptiques avec ces deux neurotransmetteurs, mais avec une affinité beaucoup plus faible pour la glycine que pour le GABA. Cependant, le mécanisme qui spécifie le phénotype vésiculaire (Glycine ou GABA) reste incompris.

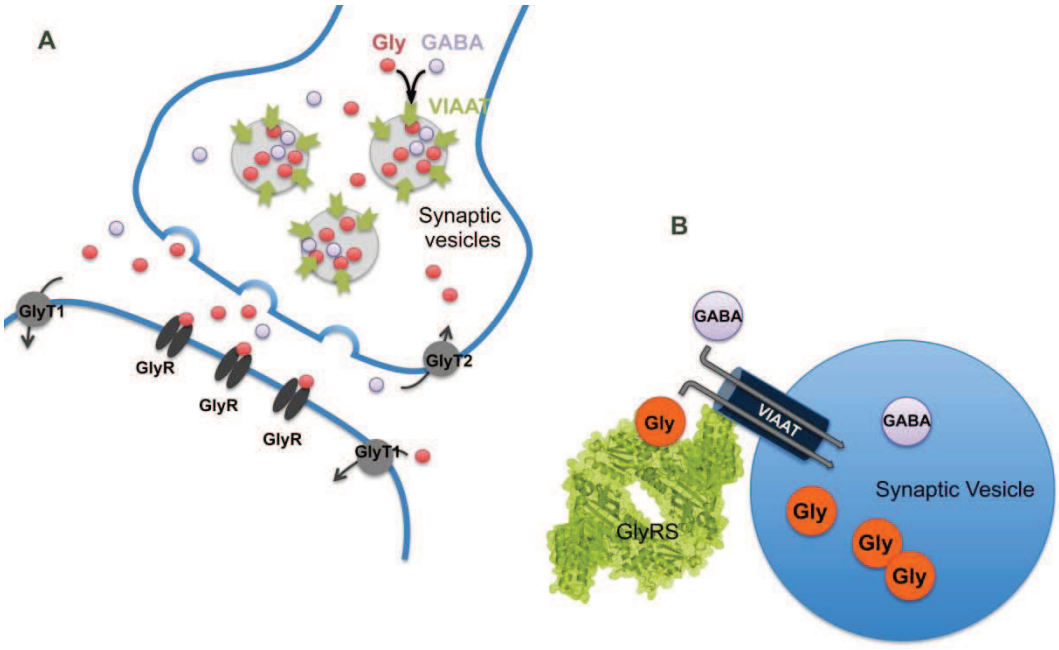

Figure 7. GlyRS et sont rôle potentiel dans la transmission glycinergique

(A) Organisation de la jonction synaptique inhibitrice : Dans le neurone pré-synaptique, les vésicules synaptiques sont remplies avec glycine (rouge) et/ou GABA (violet) via le transporteur commun VIAAT (vert). Le transporteur GlyT2 (gris) est lui responsable de la recapture de la glycine dans le neurone pré-synaptique. Dans le neurone post-synaptique, le récepteur de la glycine (GlyR) conduit la neurotransmission glycinergique **(B)** Remplissage de la vésicule synaptique avec glycine: d'après notre hypothèse, la GlyRS (vert) va interagir avec VIAAT (bleu foncé) affin d'assurer un remplissage plus efficace.

Nous avons alors imaginé une hypothèse de travail, selon laquelle, la coopération entre la GlyRS et VIAAT compenserait ce déficit d'affinité et permettrait l'entrée de glycine dans les vésicules. Dans ce contexte, les mutations dans la GlyRS qui affectent essentiellement le système nerveux périphérique pourraient être expliquées. Mes résultats préliminaires montrent une co-localisation partielle de la GlyRS avec VIAAT. Des délétants de la GlyRS sont actuellement testés afin de démontrer la spécificité de cette co-localisation et de déterminer le ou les domaines de la GlyRS impliqués dans cette interaction. Si ces expériences s'avèrent concluantes, nous pourrons alors analyser l'influence de la GlyRS et de ses mutants pathologiques associées à la CMT-2D sur l'accumulation de glycine dans des vésicules et identifier une éventuelle perte de fonction.

A ce jour le lien entre les mutations de la GlyRS conduisant à la maladie de Charcot-Marie-Tooth, la spécificité tissulaire, la fonction première d'aminoacylation GlyRS et la pathologie restent floues. Nous espérons que les résultats déjà obtenus ainsi que les perspectives de poursuivre le projet en lien avec la transmission glycinergique vont contribuer à mieux comprendre le mécanisme moléculaire de la CMT- 2D.

Références

1. Ibba M, Soll D (2000) Aminoacyl-tRNA synthesis. *Annu Rev Biochem* 69:617–650.
2. Paul M, Schimmel P (2013) Essential nontranslational functions of tRNA synthetases. *Nat Chem Biol* 9:145–153.
3. Yao P, Fox PL (2013) Aminoacyl-tRNA synthetases in medicine and disease: tRNA synthetases and disease. *EMBO Mol Med* 5:332–343.
4. Williams J, Osvath S, Khong TF, Pearse M, Power D (1995) Cloning, sequencing and bacterial expression of human glycine tRNA synthetase. *Nucleic Acids Res* 23:1307–1310.
5. Mudge SJ et al. (1998) Complex organisation of the 5′-end of the human glycine tRNA synthetase gene. *Gene* 209:45–50.
6. Guo R-T, Chong YE, Guo M, Yang X-L (2009) Crystal Structures and Biochemical Analyses Suggest a Unique Mechanism and Role for Human Glycyl-tRNA Synthetase in Ap4A Homeostasis. *J Biol Chem* 284:28968–28976.
7. Park MC et al. (2012) Secreted human glycyl-tRNA synthetase implicated in defense against ERK-activated tumorigenesis. *Proc Natl Acad Sci U S A* 109:E640–E647.
8. Andreev DE et al. (2012) Glycyl-tRNA synthetase specifically binds to the poliovirus IRES to activate translation initiation. *Nucleic Acids Res* 40:5602–5614.